Investigating TGFβ signals in cell fate specification in the early mouse embryo

Anna Dorothea Senft

Christ Church

Liz Robertson & Liz Bikoff Laboratory

Sir William Dunn School of Pathology

University of Oxford

A thesis submitted for the degree of Doctor of Philosophy

Trinity Term 2016

To my family and Philipp

who supported me at all times

A B S T R A C T

Investigating TGFβ signals in cell fate specification in the early mouse embryo

Anna Dorothea Senft, Christ Church, submitted for the degree of D. Phil

Trinity Term 2016

TGFβ signalling via Smad transcription factors is essential for axis patterning and subsequent cell fate specification during mammalian embryogenesis. However, the cellular and molecular mechanisms have been difficult to characterise *in vivo* due to early embryonic lethality of mouse mutants and redundant functional activities. Here I show that combined deletion of closely related *Smad2* and *Smad3* in mouse embryonic stem cells impairs induction of lineage specific gene expression during differentiation, while extra-embryonic gene expression is up-regulated. Preliminary data suggest that the underlying mechanism of this differentiation defect reflects the inability of *Smad2/3*$^{-/-}$ cells to establish lineage priming. Collectively, these findings identify novel downstream target genes controlled by *Smad2/3* and an absolute requirement for *Smad2/3* during embryonic differentiation. TGFβ signalling via Smad1 and Smad4 is essential for induction of the transcription factor Blimp1 required for primordial germ cell specification. The direct upstream regulators of Blimp1 are unknown, but T-box factors have recently been suggested to play a role. In a second project, I performed tissue-specific ablation of the T-box transcription factor *Eomes* as well as components of the TGFβ signalling pathway in either the visceral endoderm or the epiblast to examine tissue-specific functions for Blimp1 induction. I show that *Eomes* and *Smad2* functions in the visceral endoderm as well as *Eomes* function in the epiblast are dispensable for Blimp1 induction, but rather are required to restrict Blimp1 induction to posterior epiblast cells. In contrast, epiblast-specific *Smad4* or *Smad1* mutants fail to robustly induce Blimp1 in the epiblast. My preliminary analysis suggests that competence to induce primordial germ cell fate is dependent on the interplay of *Smad2/Eomes* functions in the visceral endoderm and *Smad1/4* functions in the epiblast. Collectively, this thesis provides insight into the transition from pluripotency to cell fate specification in the mammalian embryo that is impossible to obtain from human embryos *in vivo*.

DECLARATION

I declare hat the work presented in this thesis is my own unless otherwise stated.



DPhil Examiners

Dr Dominic Norris

MRC Harwell

Dr Jennifer Nichols

Stem Cell Insitute, University of Cambridge

The present work was funded by the

4-year Wellcome Trust Graduate Programme in

Chromosome and Developmental Biology

ACKNOWLEDGEMENTS

I thank my supervisors Liz Robertson and Liz Bikoff for their guidance, intellectual and technical expertise and support that were vital in developing my projects and inspired my ideas as a scientist and person. Thank you for giving me the freedom to work independently in your lab.

My gratitude goes to members of the Robertson & Bikoff lab, especially to Ita Costello and Arne Mould whose advice, support, inspiration and humour guided me throughout my work. I thank Claire Simon, Andrew Nelson, Mohammed Ahmed, Salah Elias, Jane Rose and Thomas Clague for countless discussions and advise. Special thanks go to Thomas Clague for excellent technical assistance in Western Blotting. I also thank former lab members Marc Morgan, Deborah Bogani, Kim Cheng, Xin Sun and Luke Harland for their help and support. Thank you all for making the lab an entertaining place.

I thank Dominic Norris and Jenny Nichols for taking the time to assess my work. I am grateful to Andy Bassett for stimulating discussions, technical help and advise in setting up the CRISPR-Cas9 system. I thank the animal staff for caring for mice, Nigel Rust for performing flow cytometry and the Dunn School for a supporting environment.

I thank my Wellcome Trust cohort Lars Hanssen, Hamish King, Adam Volanakis and Greta Pintacuda for being an inspiring group of people and the Wellcome Trust for financial support and for opening opportunities during events. I am grateful to Tatyana Nesterova, Neil Brockdorff and members of the Brockdorff lab for a stimulating rotation and to Shankar Srinivas, Rob Klose, Richard Wade-Martins and Stephanie Cragg for their support during my graduate studies in Oxford. I thank my former collegues and friends Phillip Grote and Arica Beisaw, Lars Wittler, Markus Morkel, Matthias Marks, Bernhard Herrmann, Harald Saumweber, Ansgar Klebes, Alexander Glotov, Dirk-Henner Lankenau, Ahmet-Can Berkyurek, Polina Kosillo, Johannes Schmidt, Mridul Agrawal and Philipp Kurbel for listening to my thoughts and for their comments.

1 Introduction

1.1 *Scope of the thesis* 2

1.2 *Overview of the TGFβ signalling pathway* 3

1.2.1 Ligands and receptors 3
1.2.2 Smad effector proteins 5
1.2.3 Smads as transcription factors 5

1.3 *TGFβ signals control cell fate decisions in the early post-implantation mouse embryo* 9

1.3.1 Pre-implantation development 9
1.3.2 Early post-implantation development ~E4.5 - E5.25 9
1.3.3 Naïve, core and primed pluripotency *in vitro* 12
1.3.4 Nodal signalling mediates axis patterning in the mouse embryo from ~E5.0 - E6.25 13
1.3.5 Mechanism of primitive streak induction at ~E6.25 - E6.5 . . . 15
1.3.6 Cell fate specification at gastrulation from ~E6.25 - E7.5 17
1.3.7 From lineage priming to cell fate specification *in vitro* 18
1.3.8 Cooperative functions of Smad2 and Smad3 in the early post-implantation embryo 20
1.3.9 Primordial germ cell specification 23

1.4 *Aims of the thesis* 32

2 Smad2/3 governs the transition of mouse embryonic stem cells from pluripotency to differentiation

2.1 *Preface* 34

2.2 *Generation of Smad2/3$^{-/-}$ and Smad3$^{-/-}$ embryonic stem cells*
CRISPR/Cas9n-mediated *Smad3* ablation in *Smad2$^{-/-}$* or wild type ES cells 35

2.3 *Smad2/3 signals are dispensable for ES cell viability and self-renewal and the expression of pluripotency marker genes*
Characterizing the undifferentiated state 37

2.4 *Dose-dependent Smad2/3 signals are required for growth and differentiation in embryoid bodies and for the differentiation into definitive endoderm in vitro*
Challenging *Smad2$^{-/-}$*, *Smad3$^{-/-}$* and *Smad2/3$^{-/-}$* ES cells to differentiate . . 41

2.5 *Smad2/3$^{-/-}$ EBs lack mesoderm and endoderm marker gene expression and divert to an extra-embryonic-like profile*
Transcriptional profiling of *Smad2$^{-/-}$*, *Smad3$^{-/-}$* and *Smad2/3$^{-/-}$* EBs 45

2.6 *Smad2/3$^{-/-}$ ES cells compromise the initiation of lineage priming in EpiLCs*
Epiblast-like cell differentiation of *Smad2/3$^{-/-}$* ES cells 63

2.7 *Conclusion of project I*
Key findings and immediate future plans for project I 68

3 The role of visceral endoderm- and epiblast-derived Smad signals in inducing the primordial germ cell marker Blimp1

3.1 *Preface* 72

3.2 *Preparations for the screen* 74

3.2.1 Derivation of *Smad1$^{-/-}$* and *Smad1$^{CA/CA}$* mouse strains from the *Smad1^{RobPC}* allele 74
3.2.2 Breeding of mouse lines to allow the conditional ablation of *Eomes, Smad2* as well as *Smad4*, *Smad1* and *Prdm1* in the visceral endoderm and epiblast 74
3.2.3 Blimp1 immunohistochemistry validates Blimp1 expression in primordial germ cells of wild type mouse embryos at E7.5 . . . 77

3.3 *Eomes signals in the epiblast and the VE are dispensable for Blimp1 induction but required to restrict Blimp expression to the posterior epiblast*
The role of Eomes in Blimp1 induction in PGCs 79

3.4 *Deletion of Smad2 from the VE leads to an expanded Blimp1^{+} cell cluster thereby phenocopying Smad2$^{-/-}$ mutants*
The role of Smad2 in the VE for Blimp1 induction 82

3.5 *Smad4 signals in the visceral endoderm are dispensable for Blimp1 induction in the E7.5 epiblast whereas epiblast-derived Smad4 is required to faithfully induce Blimp1*
The role of Smad4 in the VE for Blimp1 induction 84

3.6 *Smad1 in the epiblast, but not the visceral endoderm is required for the induction of Blimp1^{+} epiblast cells at E7.5*
Tissue-specific roles of Smad1 signals for Blimp1 induction 86

3.7 *Prdm1/Blimp1 in the visceral endoderm is dispensable for germ cell specification and embryonic development*
Role of Blimp1 in the VE 89

3.8 *Protocols and reagents established for future experiments* 91

3.8.1 Validation of a published PGCLC differentiation protocol . . 91
3.8.2 Establishing a resource of mutant and reporter ES cell lines for PGCLC differentiation experiments 93
3.8.3 Validation of Stella, p-Smad1/5/8 and Blimp1 antibodies for future experiments 94
3.8.4 Optimization of flow cytometric analysis of *Eomes.GFP* reporter cells from gastrulating embryos 96

3.9 *Conclusion of project II*
Key findings and immediate future plans for project II 99

4 Discussion

4.1 *Summary of findings* 102

4.2 *Discussion of project I* 103

4.2.1 Are Smad2/3 functions dispensable in undifferentiated ES cells? 103
4.2.2 To what extent do cooperative Smad2/3 signals drive embryonic differentiation? 105
4.2.3 Does the extra-embryonic fate represent the default state if embryonic cell fate is blocked? 108
4.2.4 Could Smad2/3 signalling mediate enhancer switching during the acquisition of primed pluripotency? 110
4.2.5 Could Smad2/3 and Smad1 signalling antagonistically regulate *Nanog* expression during the transition from pluripotency to differentiation? 113

4.3 *Discussion of project II* 115

4.3.1 T-box transcription factors in the induction of Blimp1 in primordial germ cell specification 115
4.3.2 What is the role of Nodal signalling in primordial germ cell specification? 116

5 Methods

5.1 *Mice and embryos* 120

5.1.1 Mouse strains and alleles 120
5.1.2 Animal breeding and timed matings 120
5.1.3 Genotyping primers 121
5.1.4 Isolation of blastocysts 123
5.1.5 Isolation of early post-implantation stage embryos 123
5.1.6 Isolation of genital ridges from E12.5 embryos 123

5.2 *Molecular and cell biology* 123

5.2.1 CRISPR/Cas9n 123
5.2.2 RNA and DNA isolation 124
5.2.3 Transcriptional profiling 126
5.2.4 PCR 126
5.2.5 Quantitative RT-PCR and OneStep 127
5.2.6 Southern blotting 129
5.2.7 Flow cytometry 131

5.3 *Protein biochemistry* 131

5.3.1 Antibodies 131
5.3.2 Protein extraction and quantification 132
5.3.3 Western blotting 133
5.3.4 Immunhistochemistry and immunofluorescence staining on paraffin sections 133
5.3.5 Immunfluorescence on ES cells, PGCLCs and embryos 134

5.4 *Tissue culture* 135

5.4.1 Derivation of embryonic stem cells from blastocysts 135
5.4.2 ES cell maintenance 136
5.4.3 ES cell transfection 136
5.4.4 Culture and generation of feeder cells 137
5.4.5 Feeder-depletion of feeder-dependent ES cells 137
5.4.6 Adapting 2i ES cells to serum+LIF conditions 137
5.4.7 Embryoid body differentiation 137
5.4.8 Definitive endoderm differentiation 138
5.4.9 EpiLC differentiation 138
5.4.10 PGCLC differentiation 138
5.4.11 Alkaline phosphatase staining of ES cell colonies 139
5.4.12 Giemsa staining 139

5.5 *Histology* 139

5.5.1 Paraffin embedding and sectioning 139
5.5.2 Whole-mount in situ hybridization 140
5.5.3 Alkaline phosphatase staining of embryos 140

5.6 *Solutions and media used* 140

6 References 143

LIST OF FIGURES

Introduction

1 *The TGFβ signalling pathway* 4

2 *Structural features of Smad proteins* 7

3 *Exit from pluripotency in the early post-implantation mouse embryo* 10

4 *Cell fate specification at gastrulation in the ~E6.5 - E7.5 mouse embryo* 16

5 *Cooperative Smad2/3 signals pattern the early mouse embryo.* 21

6 *Early primordial germ cell development in mice* 24

7 *Compartments of Bmp and Nodal signalling in the ~E6.25 mouse embryo during induction of primordial germ cell precursors* 28

Project I

8 *Validation of Smad2/3$^{-/-}$, Smad3$^{-/-}$, Smad2$^{-/-}$ and wild type ES cell lines* 36

9 *Loss of Smad2/3 signals does not affect ES cell morphology and the expression of pluripotency markers* 39

10 *Smad2/3 expression is non-essential for self-renewal and the ability to form pluripotent ES cell colonies* 41

11 *Loss of Smad2 and Smad2/3 affects embryoid body morphology* 43

12 *Loss of Smad2 and Smad2/3 affects marker gene expression of the primary germ layers during EB and definitive endoderm differentiation* 44

13 *Transcriptional profiling of mutant and wild type EBs during differentiation: Sample clustering and validation of control differentiation* 46

14 *Expression changes of key lineage marker genes in Smad2/3$^{-/-}$, Smad2$^{-/-}$ and Smad2/3$^{-/-}$ EBs during differentiation* 49

15 *Biological function GO term analysis of d3 mis-regulated transcripts for Smad2/3$^{-/-}$, Smad2$^{-/-}$ and Smad3$^{-/-}$ EBs* 60

16 *Venn diagrams of overlapping mis-regulated transcripts at d2 and d3 in Smad2/3$^{-/-}$, Smad2$^{-/-}$ and Smad3$^{-/-}$ EBs* 61

17 *More than a fifth of all EB differentiation-associated transcripts regulated in wild type d3 EBs are significantly and > 2-fold regulated in d3 Smad2/3$^{-/-}$ EBs* . . 64

18 *Expression changes of naïve, core and primed pluripotency marker transcripts in Smad2/3$^{-/-}$, Smad2$^{-/-}$ and Smad2/3$^{-/-}$ EBs during differentiation* 65

19 *EpiLC differentiation of Smad2/3$^{-/-}$ ES cells* 67

Project II

20 *Generation of the null Smad1^{-} and conditional Smad1^{CA} allele from the modified Smad1^{RobPC} allele* 75

21 *Blimp1 immunohistochemistry on sections of E7.5 mouse embryos validates expression in primordial germ cells and the visceral endoderm* 78

22 *Epiblast and visceral endoderm-derived Eomes expression is dispensable for emergence of Blimp1^{+} cells in the epiblast* 80

23 *Visceral endoderm-specific ablation of Smad2 leads to an expansion of Blimp1^{+} cells in the epiblast* 83

24 *Visceral endoderm-derived Smad1 is dispensable for emergence of Blimp1^{+} cells in the epiblast, whereas epiblast-derived Smad1 is essential for robust Blimp1 induction in the posterior epiblast* 85

25 *Visceral endoderm-derived Smad4 is dispensable for emergence of Blimp1^{+} cells in the epiblast, whereas epiblast-derived Smad4 is essential for Blimp1 induction in the posterior epiblast* 87

26 *Examples of the observed thickening and ruffling of visceral endoderm in VE- and epiblast-specific Smad1 mutants at E7.5* 88

27 *Visceral endoderm-derived Prdm1 expression in the VE is dispensable for the emergence of Blimp1^{+} cells in the epiblast* 90

28 *Validation of Blimp1 expression in a published PGCLC differentiation protocol* . . 92

29 *Testing of antibody stainings for Stella, pSmad1/5/8 and Blimp1 in mouse embryos* 96

30 *Flow cytometric analysis of Eomes.GFP^{+} cells from E7.5 embryos* 98

LIST OF TABLES

Introduction

1 *In vitro models for the transition from pluripotency to differentiation* 14

2 *Dose-dependency of Smad2/3 embryonic phenotypes* 22

Project I

3 *Top 20 up- and down-regulated transcript at d3 in wild type EBs* 46

4 *Numbers of mis-regulated transcripts over time* 46

5 *Top 20 down-regulated transcripts at d2* 54

6 *Top 20 down-regulated transcripts at d3* 54

7 *Top 20 up-regulated transcripts at d2* 55

8 *Top 20 up-regulated transcripts at d3* 55

Project II

9 *Mouse lines used for conditional deletions* 77

10 *ES cell lines established to date* 94

Methods

11 *Mouse strains and alleles* 120

12 *Primer sequences used for genotyping* 121

13 *sgRNA primer sequences and CRISPR plasmid genotyping primer* 124

14 *qPCR primer sequences* 127

15 *Antibodies* 131

16 *Solutions and media* 140

S1 *List of exclusive and common transcriptional changes in d3 wild type EBs and d3 EBs in Tripathi et al. 2011* . . . . . disc

S2 *(a) Unbiased lists of significantly ($p \leq 0.05$) and ≥ 2-fold changed transcripts averaged for all clones at each time-point and genotype* . . . . . disc

(b) Unbiased lists of ≥ 2-fold changed transcripts averaged for all clones at each time-point and genotype (no significance restriction) . . . . . disc

S3 *Unbiased full list of log2-fold changes in individual clones of d0, d2 and d3 time-points of each genotype over the averaged corresponding time-point in wild type controls (heatmap)*[1] . . . . . disc

S4 *Unbiased full list of log2-fold changes in individual clones of d0, d2 and d3 time-points of each genotype over the averaged d0 time-point within each genotype (heatmap)*[2] . . . . . disc

S5 *Full list of the genes categorized for each GO term for mis-regulated transcripts in d3 Smad3*$^{-/-}$*, Smad2*$^{-/-}$ *and Smad2/3*$^{-/-}$ *EBs* . . . . . disc

S6 *List of exclusive and common transcriptional changes in d2 and d3 Smad3*$^{-/-}$*, Smad2*$^{-/-}$ *and Smad2/3*$^{-/-}$ *EBs* . . . . . disc

S7 *List of exclusive and common inversely regulated transcriptional changes in d3 wild type and d3 Smad2/3*$^{-/-}$ *EBs* . . . . . disc

[1,2] *Files S3 and S4 include additional profiling data from four Smad2/3*$^{-/-}$ *clones derived from a different parental Smad2*$^{-/-}$ *ES cell line (KT17) that were not included in the analysis in the main body of the thesis.*

-	null allele
2i	2 inhibitors
7AAD	7-aminoactinomycin D
A-P	anterior-posterior
aa	amino acid
Act	activin A
ALK	activin receptor-like kinases
Amhs	anti-müllerian hormones
AP	alkaline phosphatase
ASE	Nodal asymmetric enhancer
ATAC	Assay for Transposase-Accessible Chromatin
AVE	anterior visceral endoderm
axm	axial mesoderm
BAC	bacterial artificial chromosome
Blimp1	B lymphocyte induced maturation protein-1
Bmp	Bone morphogenetic protein
bp	base pairs
BSA	bovine serum albumin
BV	*Blimp1.Venus* BAC transgene (Ohinata et al. 2008)
CA	conditional allele
Cas9n	CRISPR-associated protein 9 nickase
CCE	ES cell line derived from the 129/Sv strain (Robertson et al. 1986)
ch	chorion
ChIP	chromatin immunoprecipitation
cm	cardiac mesoderm
Co-Smad	common Smad
CRISPR	Clustered regularly interspaced short palindromic repeat
cRNA	complementary RNA
d	day
DAPI	4',6-diamidino-2-phenylindole
DE	definitive endoderm
Δ	deletion
Δepi	Conditional ablation using *Sox2.Cre* (Hayahsi et al. 2002a)
ΔVE	Conditional ablation using *Ttr.Cre* (Kwon and Hadjantonakis et al. 2009)
DVE	distal VE
E	embryonic day
EB	embryoid body

EGF	epidermal growth factor
EMT	epithelial-to-mesenchymal transition
emVE	embryonic VE
Eomes	Eomesodermin
EPC	ectoplacental cone
epi	epiblast
EpiLC	epiblast-like cell
EpiSC	epiblast stem cell
ES cell / ESC	embryonic stem cell
ExE / xc	extra-embryonic ectoderm
exm / xm	extra-embryonic mesoderm
exVE	extra-embryonic VE
FACS	Fluorescence-activated cell sorting
fb	forebrain
FCS	fetal calf serum
FD	feeder-dependent
FF	feeder-free
fg	foregut
FGF	fibroblast growth factor
Gdfs	Growth and differentiation factors
GFP	green fluorescent protein
GO	gene ontology
GSK3	glycogensynthase kinase
hb	hindbrain
hESC	human ESC
ICM	inner cell mass
InDel	insertions and deletions
kb	kilo bases
kDA	kilo Dalton
KSR	knockout replacement serum
KT15 and KT17	Smad2$^{-/-}$ cell lines generated by Kim Tremblay
LIF	leukemia inhibitory factor
lpm	lateral plate mesoderm
mb	midbrain
mes / m	mesoderm
MH1	mad homology 1
MH2	mad homology 2
mhg	mid and hindgut
mm10	mus musculus genome assembly 10
n	number
NE	neuroectoderm

p	P value (calculated probability)
p-Smad	phosphorylated Smad
PAM	Protospacer adjacent motif
PBS /PBST	Phosphate-buffered saline (supplemented with Tween-20)
PC	principal component
PCP	prechordal plate
PCR	Polymerase chain reaction
PE	parietal endoderm
PGCLC	primordial germ cell-like cell
PPE	proximal posterior enhancer
pPGC	primordial germ cell precursor
Prdm1	PR domain containing 1
PrE	primitive endoderm
PS	primitive streak
PVE	posterior VE
pxm	paraxial mesoderm
qPCR/ qRT-PCR	quantitative (reverse transcriptase) polymerase chain reaction
R-Smad	recepetor-mediated Smad
RT	room temperature
SCF	stem cell factor
se	surface ectoderm
seq	sequencing
sgRNA	short guide RNA
Smad	Derived from Small body size (Sma) and mothers against decapentaplegic (Mad)
sp	spinal chord
T	Brachyury
TAE	Tris acetate EDTA
TBST	tris-buffered saline supplemented with Tween-20
TE	trophectoderm
TGC	trophoblast giant cell
TGFβ	transforming growth factor beta
TGFβR	TGFb receptor
TS cell	Trophoblast stem cell
µm	micrometer
µM	micromolar
VE	visceral endoderm
WISH	whole-mount in situ hybridization
Wnt	wingless-related integration site
wt	wild type
XENLC	extra-embryonic endoderm-like cell
Yap	yes-associated protein

1

Introduction

1.1 Scope of the thesis

Within 72 hours after implantation the mouse embryo has defined its embryonic axes and undergone initial cell fate specification. These processes are governed largely by transforming growth factor beta (TGFβ) signals. The early embryo also contains specialized tissues required to establish a nutrient supply from the mother. Additionally, primordial germ cells, the progenitors of sperm or oocytes, have been set aside. The mechanisms underlying TGFβ signalling-mediated cell fate specification and the concomitant exit from pluripotency are, however, difficult to examine *in vivo* due to embryonic lethality and redundant and tissue-specific roles of individual factors.

The downstream effectors of the TGFβ signalling pathway are the Smad transcription factors. To characterize further individual and cooperative roles of Smad transcription factors during cell fate specification, I genetically ablated individual and combined Smad function in embryonic stem (ES) cells or in specific tissues in the embryo. The focus of the first part of this thesis is the analysis of cooperative functions of Smad2 and Smad3 in the transition of mouse ES cells from pluripotency to differentiation. The second part of the thesis assesses tissue-specific functions of *Eomes*, *Smad2*, *Smad4*, *Smad1* and *Prdm1* for the induction of the primordial germ cell marker Blimp1 by their ablation in the epiblast and extra-embryonic visceral endoderm.

This thesis does not deal with TGFβ signals other than those listed above and does not cover pre-implantation (before ~E4.5) nor later developmental stages (after ~E7.5), nor does it address the role of the listed factors in the extra-embryonic ectoderm tissue. The experiments have an emphasis on transcriptional effects downstream of Smad2/3 transcription factors (chapter 2), whereas the analysis *in vivo* primarily assesses protein-level changes of the single primordial germ cell marker Blimp1 (chapter 3). Collectively, this thesis will enhance our understanding of the transition from pluripotency to cell fate specification in the mammalian embryo and in ES cells. It will also provide tissue-specific insight into mammalian development that cannot be obtained from human embryos *in vivo*.

1.2 Overview of TGFβ signalling

The TGFβ superfamily of secreted growth factors evolved in metazoans and represents one of the major signalling pathways governing cellular processes ranging from cell differentiation and proliferation to morphogenesis and tissue homeostasis (Huminiecki et al. 2009, Massagué et al. 2012). Their malfunction has been associated with human disease (reviewed in Massagueé et al. 2012). In this thesis I focus on the role of Smad effector proteins within the TGFβ pathway and their role in the early post-implantation mouse embryo and in differentiating ES cells.

1.2.1 Ligands and receptors

TGFβ ligands can be grouped into two branches; the Tgfβ/Nodal/Activin, and bone morphogenetic proteins (Bmps)/ growth and differentiation factors (Gdfs)/anti-müllerian hormones (Amhs) classes which reflect differences in subsequent Smad-signalling (Shi and Massagué 2003). There are twelve different TGFβ receptors in mammals: seven type I receptors (Alk1-7) and five type II receptors (TgfβR-II, ActR-IIA, ActR-IIB, BmpR-II and AmhR-II) (Moustakas and Heldin 2009). The binding of extra-cellular dimeric ligands leads to the formation of heterotetrameric complexes of type I and type II receptors, which show serine/threonine kinase activity (reviewed by Wrana et al. 2008) (Fig 1). Specific receptor combinations can bind different ligands, and one ligand can bind to more than one receptor (for an overview of important combinations see Moustakas and Heldin 2009). Heterotetramerisation allows type II receptors to phosphorylate and thereby activate type I receptors, which in turn recruit the primary intracellular effector proteins of the pathway, receptor-mediated Smad proteins (R-Smads, from the *Drosophila melanogaster* protein Mad for mothers against decapentaplegic and the *Caenorabditis elegans* protein Sma for small body size). In the mouse embryo, the pool of secreted Nodal ligand has been shown to depend on tissue-specific enhancers, including the Wnt- and Notch-dependent enhancers as well as auto-regulatory Smad2/3-dependent enhancers (Norris et al. 1999 and 2002, Adachi et al. 1999, Vincent et al. 2004, Saijoh et al. 2005, Papanayotou et al. 2014).

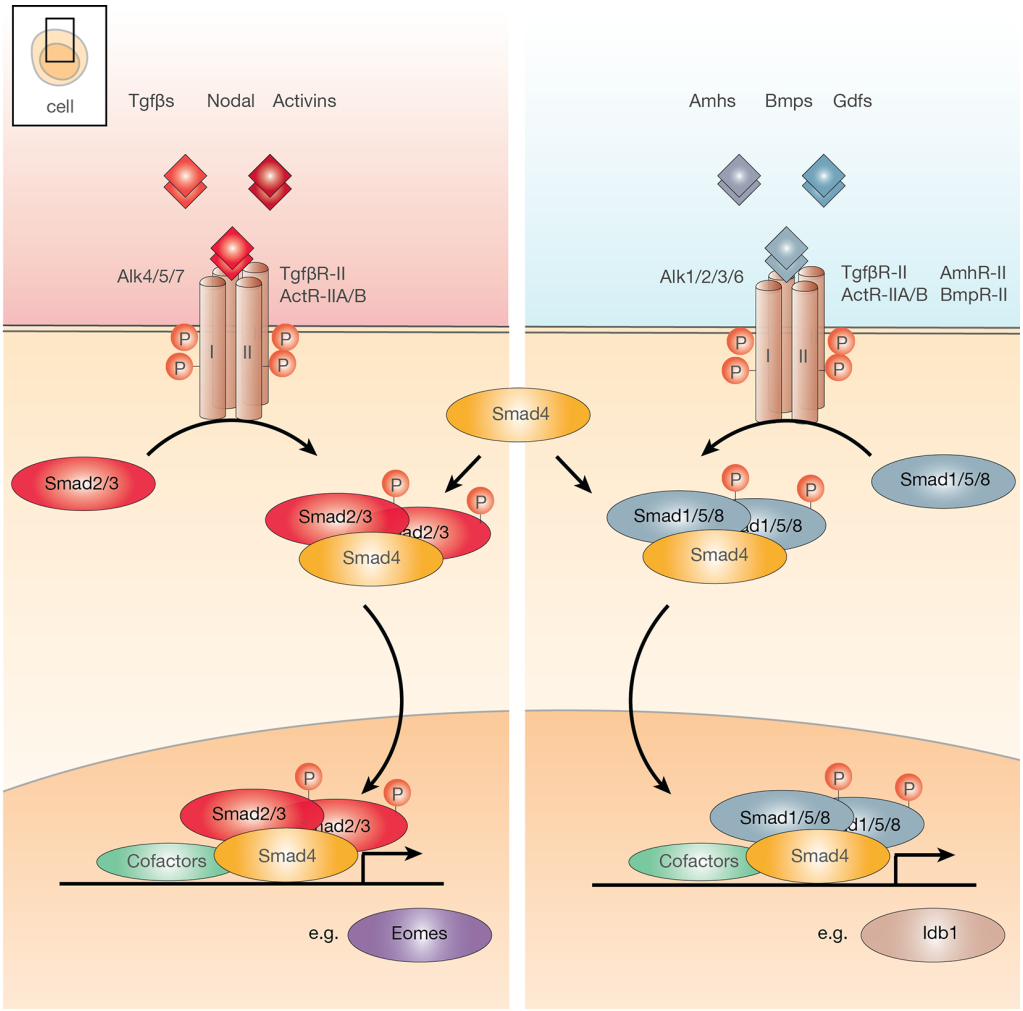


Figure 1 The TGFβ signalling pathway.

Schematic representation of the TGFβ pathway. Ligand dimers (such as Nodal, Tgfβs or Activins) bind to two pairs of serine threonine kinase type I and type II receptors. In this complex, type II receptors phosphorylate type I receptors, which in turn phosphorylate R-Smads (dependent on the ligand Smad2/3 or Smad1/5/8, respectively). Two phosphorylated R-Smads (homo or heterodimers) complex with one co-Smad (Smad4) to translocate to the nucleus. On the chromatin level the heterotrimer partners with lineage-specific transcription factors (such as FoxH1) and cofactors (such as the chromatin modifier and Smad4 regulator Trim33) to modulate target gene expression in a context-dependent manner. The T-Box transcription factor *Eomes* and *Idb1* (also known as *Id1*) are representative direct target genes of the Nodal and Bmp pathways (Lopez-Rovira et al. 2002, Kim et al. 2011).

Furthermore, ligand availability can be influenced by antagonists like Lefty1/2, Follistatin (Fst) or Cerberus 1 (Cer1) (Chen et al. 2004, Fainsod et al. 1997, Piccolo et al. 1999), maturation of ligands by proprotein convertases like Pace4 and Furin (Constam and Robertson 1999, Le Good et al. 2005) as well as cofactors including Cripto and Cryptic (Ding et al. 1998, Gaio et al., 1999, Chu and Shen 2010).

1.2.2 Smad effector proteins

Activated type I receptors phosphoylate two serine residues at the C-terminal end of the R-Smads, which then associate with the common Smad (co-Smad). It is assumed that transcriptionally active Smad complexes consist of heterotrimers (two phosphorylated (p-) R-Smads and one co-Smad) (Chacko et al. 2001, Qin et al. 2001, Massagué et al. 2005), but data has also suggested signal transduction via heterodimers (Inman and Hill 2002). R-Smad/co-Smad oligomers translocate to the nucleus and modulate gene expression by direct or indirect DNA binding with cofactors in a context-dependent manner (Massagué 2012) (Fig 1). Intriguingly, co-Smad-independent signalling has been documented during early mouse development among other systems (Chu et al. 2004).

There are eight Smad proteins in mammals: five R-Smads (Smad2/3 and Smad1/5/8), one co-Smad (Smad4) as well as two inhibitory Smads (Smad6/7) (Fig 2). Smad2/3 are phosphorylated by Alk4/5/7 type I receptors activated by Tgfβ/Nodal/Activin ligands, whereas Smad1/5/8 R-Smads are phosphorylated by Alk1/2/3/6 type I receptors activated by Bmps/Gdfs/Amhs ligands (Miyazawa et al. 2002, Derynck and Zhang 2003, Shi and Massagué 2003, Lebrun et al. 1999). Type II receptors for Smad2/3 include TgfβR-II and ActR-IIA/B. Smad1/5/8 use the type II receptors BmpR-II, ActR-IIA/B and TgfβR-II and AmhR-II (Moustakas and Heldin 2009). Individual Smad proteins are highly conserved in all metazoans (Schmierer and Hill 2007, Macias and Massagué 2015). Closely related R-Smads share cooperative and highly dose-dependent functional activities during mouse post-implantation development and in mouse ES cells (see section 1.3).

1.2.3 Smads as transcription factors

R-Smads and the co-Smad all possess conserved structural domains: a N-terminal mad homology 1 (MH1) domain, a C-terminal MH2 domain and the intervening linker region (Fig 2a). The MH1 domain mediates DNA binding. Crystal structures of Smad1, Smad3

and Smad4 bound to DNA have been documented (Shi et al. 1998, Baburajendran et al. 2010, 2011). The Smad MH1 domain recognizes the Smad binding element (SBE) 5'-CAGAT-3' (Fig 2b) and the amino acid (aa) sequence of the binding site is identical for Smad1/3/5 (Shi et al. 1998, reviewed in Shi and Massagué 2003). Importantly, DNA-binding by Smad2 has not been reported to date. Smad2 exists in two isoforms distinguished by a ~30 aa insert in the long isoform (encoded by exon 3, Dennler et al. 1999, Yagi et al. 1999) that sterically blocks DNA binding *in vitro* (Shi et al. 1998) (Fig 2b). Intriguingly, the strongly expressed long Smad2 isoform is dispensable for embryonic development (Dunn et al. 2005).

The linker region serves as an entry point for regulatory inputs e.g. through phosphorylation by cyclin-dependent kinases CDK8/9, mitogen-activated protein (MAP) kinases and glycogen synthase kinase GSK3 that can in turn lead to recruitment of cofactors such as yes-associated protein (YAP) or leads to protein degradation (Alarcón et al. 2009, Kretzschmar et al. 1999, Fuentealba et al. 2007, Gao et al. 2009). Through these interactions TGFβ signalling outputs are linked with other signalling pathways such as fibroblast growth factor (FGF), wingless-related integration site (Wnt) and Hippo signalling (reviewed in Attisano and Wrana 2013 and Massagué 2012).

The MH2 domain is primarily responsible for protein-protein interactions including interactions with receptors and the nuclear pore complex to mediate nucleocytoplasmatic shuttling (Massagué 2012). Deletion of the nuclear export signal responsible for Smad4 nuclear shuttling, however, does not disturb embryonic development (Biondi et al. 2007). The MH2 domain also mediates interactions with co-factors such as lineage-specific transcription factors and proteins that modify chromatin structure (Massagué 2012). Monoubiquitinylation/deubiquitination of the MH2 domain of Smad4 by Trim33 (also known as Tif1γ or Ectodermin) and FAM/Usp9x, respectively, leads to the de- and reassembly of Smad transcriptional complexes and can thus influence responsiveness to TGFβ signalling (Agricolo et al. 2011, Dupont et al. 2009). Trim33 also binds p-Smad2/3 and there is competition between Trim33 and Smad4 for Smad2/3 binding (He et al. 2006). Trim33 can directly bind H3K9me3 and H3K18ac histone modifications resulting

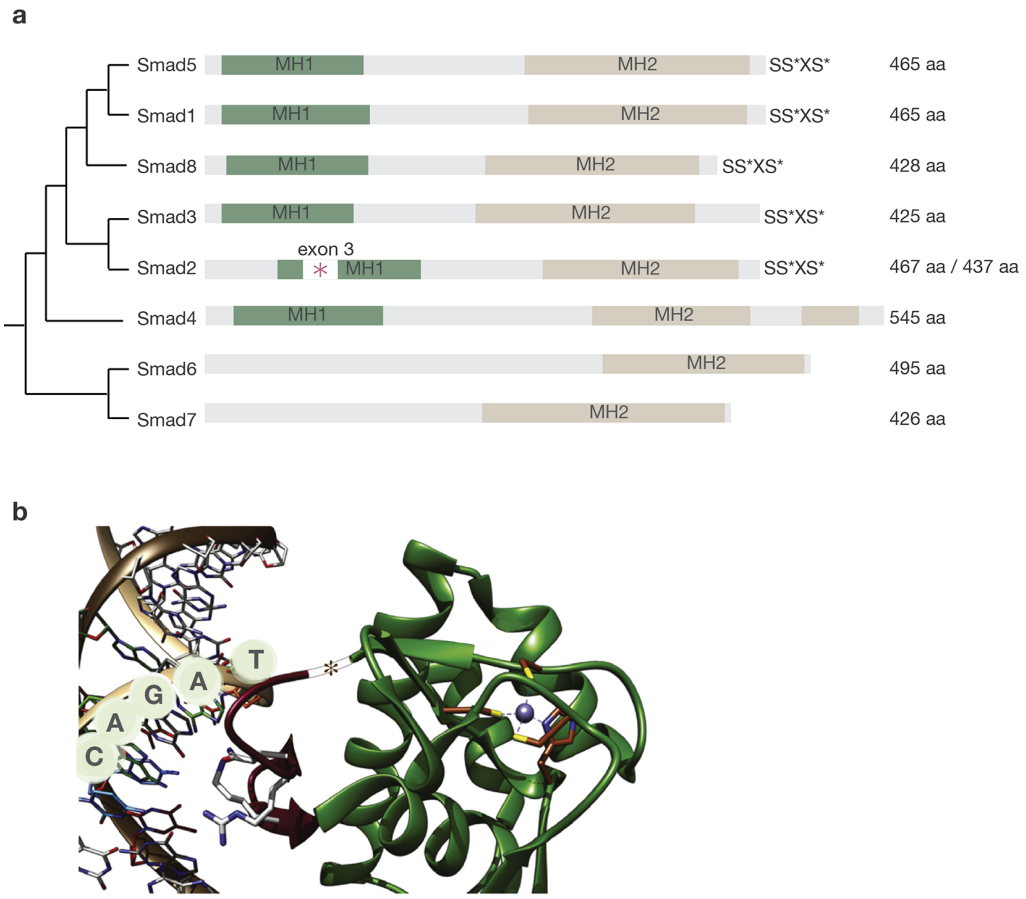


Figure 2 Structural features of Smad proteins.

(**a**) Schematic representation of evolutionary similarity among Smad proteins in mice. (**b**) Structure of the the Smad MH1 domain (green) with residues (dark brown) that recognize the Smad binding element (SBE) with the sequence 5'-CAGAT-3'. MH1 domain is shown for Smad3, but is almost identical between Smads (see also Fig 5 for Smad2/3 alignment). The position of the short 30 aa insert present in the long isoform of Smad2 and encoded by exon 3 (marked with an asterisk, see also (a)) is thought to abolish DNA binding. The SSXS motif acts as the phosphorylation site for receptors. Individual figures were modified from Kaivo-oja et al. 2006 and Macias and Massagué 2015.

in the displacement of the chromatin-compacting factor heterochromatin binding protein 1γ (HP1γ) thereby increasing accessibility of genes for transcriptional activation (Xi et al. 2011). Trim33 has been shown to modulate TGFβ signalling outputs in the early mouse embryo in a Smad4-dependent manner (Morsut et al. 2010, see also section 1.3). p-Smad2/3-Trim33 complexes were shown to bind upstream regulatory regions of the mesoderm and endodermal *Gsc* and *Mixl1* genes in ES cells (Xi et al. 2011). Furthermore, interaction with Smad4 and the transcription factor FoxH1 is required for *Gsc* and *Mixl1* activation (Chen et al. 1997, Labbé et al. 1998, Hart et al. 2005). Smad interaction with the T-box transcription factor Eomes and the pluripotency factors Oct4 and Nanog has

also been observed (Vallier et al. 2009, Teo et al. 2011, Mullen et al. 2011). Thus, specificity is thought to be achieved through a context-dependent interaction of Smad proteins with transcription factors and functional modulators, which affect the Smads themselves or the chromatin landscape (reviewed in Massagué 2012 and Hill 2016).

Smad complexes can act as activators or repressors depending on context (Massagué et al. 2012). Transcriptional profiling experiments in mouse and human ES cells have revealed Smad-dependent positive and negative expression changes upon differentiation (Costello et al. 2009, Guzman-Ayala et al. 2009, Redshaw et al. 2013, Mullen et al. 2011, Gomes Fernandes et al. 2016). Furthermore, ChIP-seq studies have identified genome-wide Smad binding sites and overlapping binding with transcriptional cofactors such as Eomes, Foxh1, Oct4, MyoD, Gata4, Otx2 and Brachyury (Kim et al. 2011, Mullen et al. 2011, Teo et al. 2011, Tsankov et al. 2015, Faial et al. 2015). For example, Smad2/3 forms a complex with Oct4 and NuRD to repress mesendoderm genes in hESC, whereas complexes with FoxH1 activate mesendodermal genes upon hESC differentiation (Beyer et al. 2013).

Thus, in human ES cells Smad3 co-binds the genome with the pluripotency factor Oct4 leading to activation of Nanog, Lefty1/2 and Smad7 expression (Mullen et al. 2011). In differentiated cells such as mesenchymal progenitors, Smad3 co-occupies the genome with lineage-specific transcription factors such as myoblast determination protein 1 (Myod1) (Mullen et al. 2011). Recent studies have shown that the capacity of ES cells to differentiate is dependent on the level of Oct4 expression and its relocalization on the genome during lineage priming and differentiation (Karwacki-Neisius et al. 2013, Radzisheuskaya et al. 2013, Buecker et al. 2014). It remains to be discovered how Smad signals such as Smad2/3 are involved in the transition from pluripotency to differentiation. Even though individual targets and Smad binding have been validated and identified in the early mouse embryo (Yoon et al. 2011, 2015, Brown et al. 2011, Teo et al. 2011, Vallier et al. 2009, Norris et al. 2002, Papanayotou et al. 2014, Hoodless et al. 2001, Simon et al. 2017), a comprehensive picture of transcriptional targets and chromatin binding of Smad proteins in tissues of the early mouse embryo is lacking.

1.3 TGFβ signals control cell fate specification in the early post-implantation mouse embryo

The gestation period in mouse is ~21 days. This section focuses on TGFβ signals controlling cell fate decisions in the early post-implantation mouse embryo between embryonic day (E) 4.5 - 7.5.

1.3.1 Pre-implantation development

TGFβ signals are expressed at pre-implantation stages. Initial cell fate decisions prior to implantation occur during the segregation of the epithelial extra-embryonic trophectoderm (TE) from precursors of the inner cell mass (ICM) in the compacted morula and slightly later when the primitive endoderm (PrE) and epiblast (Epi) lineages diverge within the ICM of the blastocyst at ~E4.5 (Fig 3). These events are not overtly affected in TGFβ signalling mutants (reviewed in Papanayotou and Colligon, 2014). Instead, the first and second cell fate decisions are primarily governed by Hippo (Hirate et al. 2013 and 2015, Maître et al. 2016, Nishioka et al. 2009), and FGF signalling, respectively (Chazaud et al. 2006). The tissues of the E4.5 blastocyst can be distinguished by the mutually exclusive expression of *Cdx2* in the TE, *Nanog* in the epiblast (epi) and *Gata6* in the PrE (Nishioka et al. 2008, Nichols et al. 1998, Chazaud et al. 2006).

1.3.2 Early post-implantation development ~E4.5 - E5.25

Shortly after implantation, the mural TE not in contact with the epiblast gives rise to invasive primary trophoblast giant cells (TGCs) that undergo endoreduplication and promote attachment of the embryo to the uterus (Roberts et al. 2011). Fgf4 secreted from the epiblast leads to activation of Fgf receptor 2 (Fgfr2) and differentiation of polar TE to trophoblast stem (TS) cells that form the ectoplacental cone (EPC) and the extra-embryonic ectoderm (ExE) that will later contribute to the spongiotrophoblast and the chorion and labyrinth layer of the embryonic part of the placenta, respectively (Roberts et al. 2011, see Figure 3). Fgfr2 in the ExE activates *Cdx2*, which activates the T-box factor

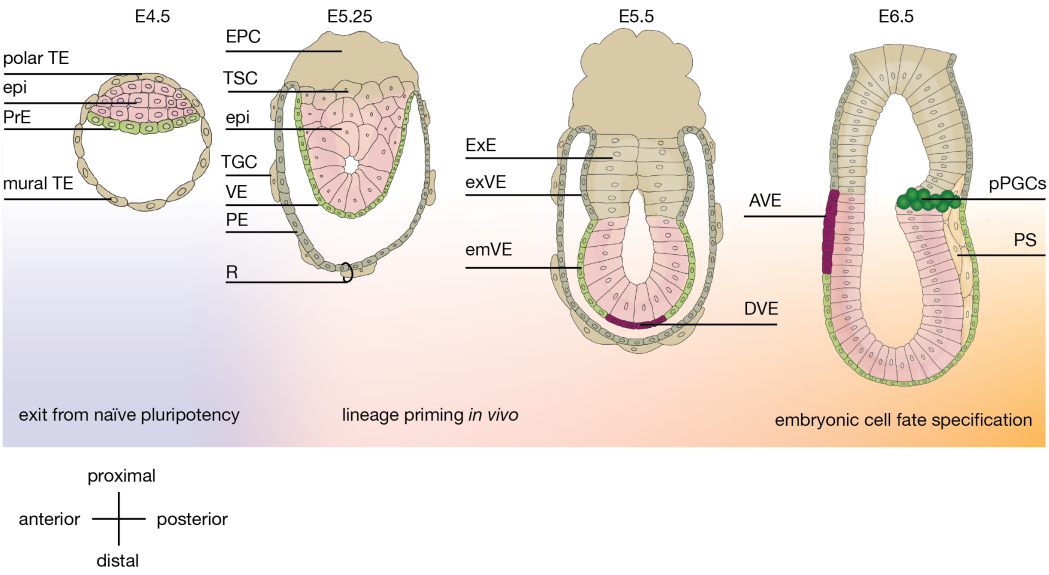


Figure 3 Exit from pluripotency in the early post-implantation mouse embryo.

Schematic depiction of the tissues of the early post-implantation embryo from E4.5 to E6.5 with the pluripotency status of the inner cell mass and later epiblast indicated below. For simplicity, EPC and Reichert's membrane are not shown at E6.5. E: embryonic day, epi: epiblast, PrE: primitive endoderm, TE: trophectoderm, EPC: ectoplacental cone, TSC: trophoblast stem cell, TGC: trophoblast giant cell, VE: visceral endoderm, PE: parietal endoderm, R: Reichert's membrane, ExE: extra-embryonic ectoderm, emVE/ExVE: embryonic/extra-embryonic VE, DVE: distal VE, AVE: anterior VE, pPGCs: precursors of primordial germ cells, PS: primitive streak. Embryos are not drawn to scale. Embryo drawings were partially adapted from Arnold and Robertson 2009 and Tang et al. 2016.

Eomes in the ExE. *Eomes* mutants can implant, but are unable to maintain TS cells (Russ et al. 2000, Strumpf et al. 2005).

The PrE differentiates into the parietal endoderm (PE) that secretes extra-cellular-matrix (also known as Reichert's membrane) and shields the embryo from the maternal environment (Robertson 2014). PrE in proximity to the epiblast will differentiate into the embryonic visceral endoderm (emVE) that later contributes to the yolk sac and gut endoderm (Kwon et al. 2008, see also Fig 6). PrE overlying the ExE forms extra-embryonic VE (exVE). Within these extra-embryonic tissues the epiblast resides. At E4.5 it consists of ~25 cells that will give rise to the embryo proper and this small population of cells will undergo extensive growth, elongation and cavitation to form the early post-implantation E5.25 epiblast or 'egg cylinder' of about ~100 - 120 cells (Snow 1977,

reviewed in Robertson, 2014) (Fig 3). Cavitation and formation of the proamniotic cavity involve the epithelialization of epiblast cells (Coucouvanis and Martin 1995).

Pluripotency is defined as the capability of cells to give rise to cells from all three embryonic germ layers including primordial germ cells. The pre-implantation ICM/epiblast can contribute readily to form germ-line chimeras and contribute to all embryonic lineages, while the post-implantation epiblast cannot (Gardner 1968, Gardner and Cockroft 1998, Rossant et al. 2008). Egg cylinder stage cells however, retain the ability to form teratocarcinomas containing tissues of the three germ layers (Solter et al. 1970, Stevens 1970) and can also be induced to form primordial germ cells (PGCs, i.e. precursors of egg and sperm cells) *ex vivo* (Ohinata et al. 2009). These experiments demonstrate that the ~E4.5 - E5.25 embryo transitions between two distinct pluripotent states. In this thesis, pluripotency in the pre-implantation ICM/epi is referred to as naïve. The post-implantation pluripotent epiblast up to E6.5 is defined as primed. The primed epiblast is in the state of lineage priming, in which it is no longer able to contribute to the blastocyst. Embryonic cell fate specification refers to differentiation events in the epiblast at gastrulation starting at ~E6.5 (Fig 3).

Naïve and primed pluripotent states in the embryo are highly transient and the exit from pluripotency to lineage priming is a continuous process. On the transcriptional level, naïve and primed pluripotency *in vivo* can be marked by the exclusive expression of *Zfp42/Rex1* and *Fgf5*, respectively, among others, even though these genes have no obvious functional role in the transition *in vivo* (Hébert et al. 1991 and 1994, Rogers et al. 1991, Pelton et al. 2002, Masui et al. 2008). Naïve and primed states exhibit continued expression of *Oct4* among others (Schöler et al. 1990, Pelton et al. 2002). Different states of pluripotency can be modelled in pluripotent embryonic stem (ES) cells *in vitro*.

1.3.3 Naïve, core and primed pluripotency in vitro

1.3.3.1 Embryonic Stem Cells

Pluripotent ES cells can be obtained from the ICM of mouse blastocysts, cultured almost indefinitely, and introduced back into blastocysts to produce chimeras (Evans and Kaufman 1981, Martin 1981, Bradley et al. 1984, Robertson et al. 1986). Traditionally, ES cells have been cultured in serum-containing medium either under co-culture with mouse embryonic fibroblasts or the addition of recombinant leukemia inhibitory factor (LIF) (Robertson 1987, Smith et al. 1988, Nichols 1990). Culture of ES cells in serum-free medium containing the GSK3 inhibitor CHIR99021 and the MEK inhibitor PD0325901 ('2i') as well as LIF has established a more homogenous ES cell population than under serum conditions as for example assessed by *Nanog* expression (Chambers et al. 2007, Ying et al. 2008 reviewed in Nichols and Smith 2009). Pluripotency *in vitro* relies on factors such as LIF, which are only required in the maintenance of diapaused blastocysts in the mouse embryo but not for general development (reviewed in Nichols and Smith 2012). Genome-wide transcriptional profiling experiments have demonstrated close resemblance of 2i+LIF ES cells with preimplantation epiblast *in vivo* (Boroviak et al. 2014). Transcriptional profiling of ES cells grown in serum+LIF and 2i+LIF confirmed the closer relation of 2i+LIF cells to the blastocyst as well as the more homogenous expression of pluripotency markers under 2i conditions, but emphasized that serum, in contrast to 2i, led to a more homogenous expression of cell-cycle related transcripts and questioned the view of a globally more homogenous state of the 2i+LIF culture (Marks et al. 2012, Kolodziejczyk et al. 2015). In this thesis, I will refer to pluripotent states of ES cells cultured in serum+LIF or in 2i+LIF as core or naïve pluripotency, respectively (see also Table 1).

1.3.3.2 Epiblast-like Cells

Naïve ES cells can be differentiated into a transient primed state of pluripotency as epiblast-like cells (EpiLCs) after culture in Activin A and basic FGF (bFGF)-containing

medium for two days (Hayashi et al. 2011). EpiLCs express a unique signature of primed markers including *Fgf5* and *Fgf15*, *Wnt3*, *Dnmt3b*, *Dnmt3l* and *Otx2*, while they down-regulate markers expressed in naïve ES cells including *Klf2*, *Klf4*, *Essrb*, *Zfp42/Rex1* as well as *Prdm14*, *Tbx3* and *Tcl1* (Hayashi et al. 2011, Buecker et al. 2014). While *Oct4* transcript levels remained unchanged in comparison to ES cells, *Sox2* and *Nanog* transcript and protein levels decreased upon EpiLC differentiation (Hayashi et al. 2011). Similar to naïve and core pluripotency markers *in vivo* only a fraction of primed pluripotency markers show functional relevance during the transition from pluripotency to differentiation *in vivo* (reviewed in Nichols and Smith 2012). EpiLC contribute with high efficiency to the primordial germ cell fate *in vitro* (Hayashi et al. 2011, Buecker et al. 2014). Transcriptome and chromatin accessibility analysis of EpiLCs and naïve ES cells revealed global switches of Oct4 binding at enhancers. Switching of Oct4 could also be induced by overexpression of the transcription factor Otx2, an Oct4 co-factor, in EpiLCs (Buecker et al. 2014).

In the early mouse embryo the acquisition of primed pluripotency occurs concomitantly with complex axis patterning processes that finally lead to induction of embryonic cell fate specification at gastrulation. In the following section, I will first introduce the further development of the mouse embryo and then touch upon ES cell-based *in vitro* models that can partially recapitulate later states of lineage priming and embryonic cell fate specification.

1.3.4 Nodal signalling mediates axis patterning in the mouse embryo from ~E5.0 - E6.25

TGFβ signals are involved in the early differentiation of the epiblast, the VE and the TE. In this thesis, I primarily focus on the involvement of TGFβ signals in the VE and the epiblast (for reviews on the involvement of TGFβ signalling in extra-embryonic ectoderm development, see Simmons and Cross, 2005, Constam 2014 and Arnold and Robertson 2009). At E5.0 - E5.5, Nodal signalling from the epiblast induces Smad2 phosphorylation in the VE. Proximal ExE-derived inhibitory Bmp4 signals restrict Smad2-mediated induction of the distal VE (DVE) to the most distal cells of the VE (reviewed in Takaoka

Table 1 *In vitro* models for the transition from pluripotency to differentiation.

Model system	3D	Culture	Source	Pluripotency	References
ES cells	no	serum + LIF (or fibroblasts)	ICM	core	Evans and Kaufman 1981 Martin 1981 Smith et al. 1988
		2i + LIF	ICM	naive	Ying et al. 2008
EpiLCs	no	Activin A + bFGF (2 days)	2i ES	primed	Hayashi et al. 2011
PGCLCs	yes	BMP4 + LIF	EpiLCs	PGCs	Hayashi et al. 2011
EpiSCs	no	Activin A + bFGF	~ E5.5 epiblast or 2i ES	primed	Tesar et al. 2007 Brons et al. 2007 Guo et al. 2009
EBs	yes	serum - LIF	ES	differentiated	Martin 1981 Wiles and Keller, 1991
		Activin A + EGF	ES	DE	Morrison et al. 2008

and Hamada, 2012) (Fig 3). The DVE can be identified by localized expression of the Nodal antagonists *Lefty1*, *Cer1* and the transcription factor *Hex* (Brennan et al. 2001, Mesnard et al. 2006, Thomas and Beddington 1998). The emergence of the DVE sets up a proximal-distal gradient of Nodal signalling and thereby establishes the proximal-distal axis of the embryo.

Mutant embryos that completely lack *Nodal*, *Smad4* or lack *Nodal* in the epiblast cavitate, but display a thickened VE and fail to induce the DVE (Conlon et al. 1991, 1994, Brennan et al. 2001, Lu and Robertson 2004, Sirard et al. 1998, Chu et al. 2004). *Smad2/3* mutants arrest earlier and do not cavitate (Dunn et al. 2004). Inhibition of Nodal signalling in E5.5 mouse embryos with follistatin (Fst) leads to a decrease in p-Smad2 in the DVE and the loss of DVE markers suggesting that Smad2 is also involved in DVE formation (Yamamoto et al. 2009). Yamamoto et al. showed that p-Smad1 is excluded from the region of DVE formation and propose an antagonistic model of p-Smad1 and p-Smad2 function in DVE formation.

Recruitment of additional cells to the DVE leads to formation of the anterior VE (AVE) at E5.5 that migrates proximally up to the embryonic-extra-embryonic interface and acts as a signalling centre to specify the anterior side of the underlying epiblast (reviewed in Stower and Srinivas, 2014). The AVE thereby establishes the anterior-posterior axis.

Smad2$^{-/-}$, *Lhx1*$^{-/-}$*; Foxa2*$^{-/-}$ as well as VE-specific *Eomes* mutants (*EomesΔVE*) fail to induce the AVE, whereas mutants of *Bmp8b* and the negative Smad4 regulator *Trim33* expand the AVE (Waldrip et al. 1998, Perea-Gomez et al. 1999, Dufort et al. 1998, Nowotschin et al. 2013, Morsut et al. 2010, Ohinata et al. 2009).

1.3.5 Mechanism of primitive streak induction at ~E6.25-E6.5

The emergence of the primitive streak (PS) becomes visible as proximal-posterior epiblast cells delaminate into the space between epiblast and VE at E6.25 - E6.5 and serves as hallmark to define the onset of mesoderm formation and thus gastrulation (reviewed in Tam and Loebel, 2007). Overt streak formation requires posterior epiblast cells to undergo an epithelial-to-mesenchymal transition (EMT) that leads to emergence of mesenchymal cells that constitute mesodermal lineages. As gastrulation procedes, the streak extends distally and the endoderm migrates from the streak intermingled with mesoderm cells (reviewed in Arnold and Robertson 2009).

Nodal signalling in the epiblast combined with antagonists from the AVE is essential for the induction and positioning of the PS in the posterior epiblast (Brennan et al. 2001, Perea-Gomez et al. 2002). This sets up an A-P gradient of Nodal signalling activity in the epiblast with the highest levels inducing PS formation at the proximal-posterior region of the epiblast. The AVE expresses Nodal, Bmp and Wnt antagonists including *Lefty1*, *Cer1* and *Dkk1* (Meno et al 1998, Belo et al. 1997, Miura et al. 2010). The AVE is also involved in the formation of rostral neuroectoderm (Rhinn et al. 1998, reviewed in Beddington and Robertson 1998, 1999), even though neuroectoderm can form in the absence of *Nodal* (Camus et al. 2006). Deletion of global *Nodal*, *Bmp4*, *Wnt3* as well as *Smad4* or *Smad2/3* abolishes primitive streak formation (Conlon et al. 1994, Liu et al. 1999, Winnier et al. 1995, Sirard et al. 1998, Dunn et al. 2004). *Nodal* and *Wnt3* (but not *Bmp4*) are also expressed in the VE, but specific ablation of either factor in the VE or the auto-regulatory Nodal asymmetric enhancer (ASE) that drives *Nodal* expression in the VE has less pronounced effects than their deletion in the epiblast, suggesting a primary

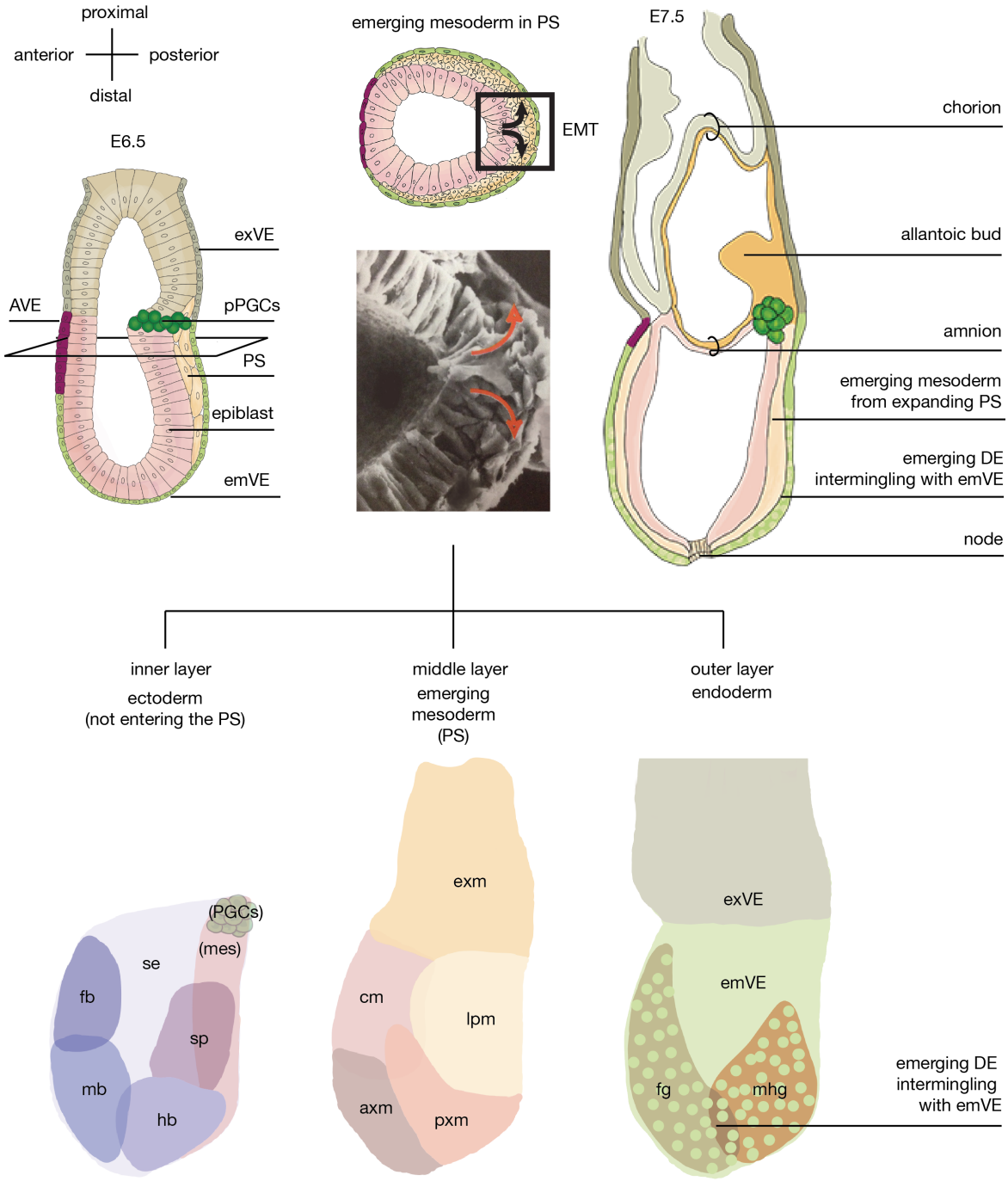


Figure 4 Cell fate specification at gastrulation in the ~E6.5 - E7.5 mouse embryo.

Schematic representation of cell fate specification during mouse gastrulation from E6.5 to E7.5. During gastrulation the epiblast increases in size: while the epiblast comprises ~660 cells at E6.5, it comprises ~15 000 cells by E7.5 (Snow 1977). Graphics were modified from Tam and Gad, 2004, Arnold and Robertson, 2009, Tang et al. 2016 and Pereira et al. 2011. E: embryonic day, AVE: anterior visceral endoderm, emVE/exVE: embryonic or extra-embryonic VE, pPGCs: primordial germ cell precursors, PS: primitive streak, EMT: epithelial-to-mesenchymal transition, DE: definitive endoderm, mes: mesoderm, sp: spinal chord, hb: hindbrain, mb: midbrain, fb: forebrain, se: surface ectoderm, exm: extra-embryonic mesoderm, lpm: lateral plate mesoderm, pxm: paraxial mesoderm, axm: axial mesoderm, cm: cardiac mesoderm, mhg: mid- and hindgut, fg: foregut. Embryos are not drawn to scale.

requirement of Nodal and Wnt3 ligands in the epiblast (Barrow et al. 2007, Tortelote et al. 2013, Yoon et al. 2015, Lu and Robertson 2004, Varlet et al. 1997, Kumar et al. 2015, Norris et al. 2002). A complex of p-Smad2 and FoxH1 binds to the Nodal ASE to mediate Nodal auto-induction in the distal epiblast (Norris et al. 2002, Norris and Robertson, 1999, Kim et al. 2011).

1.3.6 Cell fate specification at gastrulation from ~E6.25 – E7.5

The process of gastrulation converts the single layer of epiblast cells into a three-layered structure comprising a middle layer of mesoderm surrounded by an outer endoderm layer as well as an inner ectoderm layer (Fig 4). These primary germ layers are the progenitors of all cell types of the adult (reviewed in Arnold and Robertson, 2009, Tam and Loebel 2007). Graded Nodal and Bmp signals pattern mesodermal and endodermal cells as they emerge from the streak and while it expands with the growing embryo along the proximal-distal axis and towards the anterior (reviewed in Tam and Loebel, 2007). Posterior streak derivatives are exposed to highest Bmp signalling, whereas most anterior streak derivatives are exposed to highest Nodal signalling. Intriguingly, a few cells in the most proximal posterior epiblast are exposed to highest doses of Bmp signalling and become restricted from entering the PS and undergoing EMT. These cells are the precursors of primordial germ cells (pPGCs), the cells that will give rise exclusively to germ cells, the precursors of oocytes or sperm cells (see section 1.3.8). Epiblast cells that do not become pPGCs, will undergo EMT and thus enter the PS.

Fate mapping experiments have demonstrated that timing and position of cells within the streak determines their subsequent fate (Lawson et al. 1991). This study showed that the first mesoderm population that emerges constitutes extra-embryonic mesoderm (exm) which migrates proximally and displaces the ExE (Fig 4). Exm contacting the VE will differentiate into blood islands and yolk sac vasculature, whereas the remaining exm will form the allantois to connect the foetal circulatory system with the ExE-derived chorion to allow development of the foetal part of the placenta (Fig 4). Mesoderm emerging

further distally as the PS extends towards the distal tip of the embryo gives rise to the cardiac, lateral plate and paraxial mesodermal subtypes (cm, lpm, pxm). Distal streak derivatives will form the definitive endodermal (DE) lineage which will intercalate into the overlying VE to develop the primitive gut tube that becomes regionalized to form foregut (fg) and mid- and hindgut (mhg), from which the endodermal parts of liver, pancreas, stomach and intestine are derived (Kwon et al. 2008). Cells that egress from the distal-anterior tip of the PS will form axial mesoderm and the anatomically distinct structure of the node. Left-right asymmetry within the developing embryo is established by the node and this structure also gives rise to the notochord which secretes Shh signals required for patterning the distal-ventral axis of the overlying neuroectoderm (reviewed in Ribes and Briscoe 2009). The ectoderm (the precursor lineage of surface ectoderm and neuroectoderm) emerges from epiblast cells that do not enter the streak (Li et al. 2013a). To study the transition from lineage priming to embryonic cell fate specification *in vitro*, ES-cell based models can be applied to simulate the events of gastrulation.

1.3.7 From lineage priming to cell fate specification in vitro

1.3.7.1 Epiblast Stem Cells

Cells of the early post-implantation E5.5-E6.5 epiblast can be isolated as pluripotent epiblast stem cells (EpiSCs) that can be maintained in culture medium containing Activin A and bFGF (Tesar et al. 2007, Brons et al. 2007). Similarly, EpiSCs can be induced from ES cells with Activin A and bFGF (Guo et al. 2009). Transcriptional profiling of EpiSCs suggests that EpiSCs resemble the late gastrulating mouse embryo as profiles resemble the anterior PS of E7.5 embryos and can be enhanced upon Wnt stimulation (Kojima et al. 2014, Tsakiridis et al. 2014). In agreement with this observation, EpiSCs can differentiate into derivatives of the three germ layers *in vitro*, but are unable to contribute to chimeras (Tesar et al. 2007, Brons et al. 2007, Han et al. 2010). Analysis of transcriptomes of EpiSCs in comparison to EpiLCs revealed expression of somatic differentiation genes including *Hoxa1*, *Hoxb1-b3*, *Snai1*, *Id3*, and *Fgf8* in EpiSCs that were not expressed in EpiLCs (Kurimoto et al. 2015, Factor et al. 2014). In contrast to

EpiLCs, EpiSCs also express early differentiation markers such as the mesodermal markers *T* and *Wnt8a* or the endoderm markers *Gata4*, *Gata6* and *Sox17* (Hayashi et al. 2011, Buecker et al. 2014). In contrast to EpiLCs, EpiSCs contribute only very poorly to the primordial germ cell fate *in vitro* but EpiSC derivation and contribution to the germ cell fate can be enhanced by inhibition of Wnt signalling (Hayashi and Surani, 2009, Sugimoto et al. 2015, Sumi et al. 2013). Comparison of transcriptome, histone ChIP- and DNase-seq profiles of naïve ES cells and EpiSCs identified a limited number of EpiSC-specific transcripts including *Fgf5*, *Cer1*, and *Lefty1* (Factor et al. 2014). EpiSC-specific transcripts comprised only 6% of all expressed transcripts (Factor et al. 2014). Strikingly, genes expressed in both states differed in their enhancer activation. Naïve ES cells bear predominantly active proximal enhancers, while distal enhancers remain dormant. Conversely, in EpiSC proximal enhancers were inactive and more distal enhancers became dominant and were subsequently used during differentiation (Factor et al. 2014). Together with the analysis of enhancer switches in EpiLCs (Buecker et al. 2014, see section 1.3.4.2) this demonstrates that the transition from pluripotency to lineage priming and subsequent differentiation is marked by chromatin architectural re-arrangements.

1.3.7.2 Embryoid bodies

Removal of feeder cells or LIF from ES cells grown in serum-containing medium triggers undirected differentiation of ES cells to multicellular aggregates called embryoid bodies (EBs) (Martin 1981). To some extent, EBs recapitulate cell fate specification in the post-implantation mouse embryo. EBs can form derivatives of extra-embryonic endoderm and the three epiblast-derived germ layers and after two to three days in culture start to express ectodermal, mesodermal, and endodermal marker transcripts (Doetschmann et al. 1985, Costello et al. 2011). Serum in the culture medium biases EBs towards a mesoderm/endodermal fate (Wiles and Keller, 1991), while serum-free culture biases EBs towards neural fates (Wiles and Johannson 1999). Day 4-5 EBs form a central cavity and epithelialize similar to E4.5 - 5.0 embryos, consisting of an inner ectodermal layer and an outer layer of endoderm enclosing the cavity (Coucouvanis and Martin, 1999). EBs have thus been used to study the induction of differentiation genes for tissues of the germ

layers and extra-embryonic endoderm as well as the secretion of extra-cellular matrix (Costello et al. 2009, 2011). Treatment with recombinant signalling molecules can enrich cell populations of particular germ layers: treatment of EBs with Activin A and epidermal growth factor (EGF) does, for example, enrich endodermal cell populations (Morrison et al. 2008, Costello et al. 2011) (see also Table 1).

In the following two subsections, I will describe the roles of Smad2 and Smad3 during cell fate specification at gastrulation as well as the known and unknowns about the role of Bmp and Nodal signalling in the specification of precursors of the primordial germ cell (PGC) lineage. These two sections provide the rationale for the experiments undertaken in chapters 2 and 3 of this thesis.

1.3.8 Cooperative functions of Smad2 and Smad3 in the early post-implantation embryo

Smad2 and *Smad3* are thought to have originated from gene duplication events during chordate evolution (Dehal et al. 2002). The short isoform of mouse Smad2 shares 90% of its amino acid sequence with Smad3, with most divergence in the linker region (Fig 5a). *Smad2* is ubiquitously expressed in the early mouse embryo (Waldrip et al. 1998, Tremblay et al. 2000, Dunn et al. 2004). In contrast, *Smad3* is expressed at lower levels and confined to the ExE, the embryonic and extra-embryonic mesoderm and the definitive endoderm (Tremblay et al. 2000, Dunn et al. 2004). Importantly, *Smad3* expression is absent in the VE (Tremblay et al. 2000).

Smad2 mutants fail to specify the AVE and exclusively form extra-embryonic mesoderm which proliferates to form an allantois and blood islands as well as PGCs, but no other recognizable embryonic structures, resulting in early embryonic lethality (Waldrip et al. 1998, see Fig 5b). Chimera experiments suggest that this phenotype is due to Smad2 function in the VE (Waldrip et al. 1998). Smad2 function in the epiblast as well as in ES cells is required for definitive endoderm differentiation (Vincent et al. 2003a, Tremblay et al. 2000, Costello et al. 2011). Rescue experiments in chimeras demonstrated that overexpression of the short isoform of Smad2 (but not the long isoform) restores the contribution of *Smad2*$^{-/-}$ ES cells to endodermal lineages (Dunn et al. 2005). Furthermore,

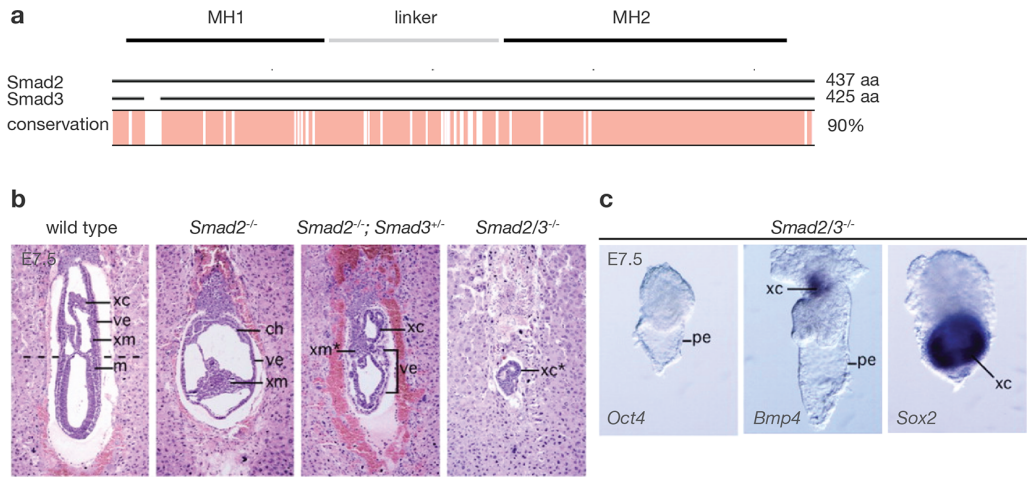


Figure 5 Cooperative Smad2/3 signals pattern the early mouse embryo.

(**a**) Alignment of amino acid sequences of the short isoform of mouse Smad2 and Smad3 proteins with conserved residues shown in rosé. MH1, linker and MH2 regions are shown for the short isoform of Smad2. (**b**) Histological sections of wild type, *Smad2*$^{-/-}$, *Smad2*$^{-/-}$*; Smad3*$^{+/-}$ and *Smad2/3*$^{-/-}$ E7.5 mouse embryos. (**c**) WISH analysis of E7.5 *Smad2*$^{-/-}$*; Smad3*$^{-/-}$ with probes specific for *Oct4*, *Bmp4* and *Sox2*. Images in (b) and (c) were taken from Dunn et al. 2004. Abbreviations: aa: amino acids, MH1/2: mad homology domain 1/2. E: embryonic day, ch: chorion, ve: visceral endoderm, pe: parietal yolk sac endoderm, xc: extra-embryonic ectoderm, m: mesoderm, xm: extra-embryonic mesoderm.

specific ablation of the long isoform of Smad2 furthermore does not disturb embryonic development, suggesting that the short isoform is the primary mediator of Smad2-dependent signalling in the embryo (Dunn et al. 2005).

In striking contrast to these crucial roles of Smad2 in embryogenesis, loss of *Smad3* does not perturb embryonic development and *Smad3*$^{-/-}$ mice are viable and fertile (Datto et al. 1999, Yang et al. 1999, Zhu et al. 1998, Dunn et al. 2004). Double heterozygote *Smad2*$^{+/-}$;*Smad3*$^{+/-}$ mice are also viable and fertile (Dunn et al. 2004). Expression of human *Smad3*, however, fully rescues anterior-posterior patterning and definitive endoderm formation in *Smad2* mutants (and lead to adult viability), suggesting that *Smad2* and *Smad3* are functionally interchangeable (Dunn et al. 2005). Additionally, both Smad2 and Smad3 can activate the Nodal ASE enhancer that drives Nodal expression in the PS and VE (Dunn et al. 2004). Interestingly, the ASE enhancer is also activated in the epiblast of *Smad2* mutants, suggesting that *Smad3* can partially compensate for the loss of *Smad2* (Brennan et al. 2001). In agreement with this model, gradually lowering the dose of

Table 2 Dose-dependency of Smad2/3 embryonic phenotypes.

Smad2	Smad3	embryonic defects	mesoderm	viability	References
+ / +	- / -	no obvious defects	no defects	viable + fertile	Datto et al. 1999
+ / -	+ / -	no obvious defects	no defects	viable + fertile	Dunn et al. 2004
+ / -	- / -	anterior truncations	mild anterior midline defects	lethal	Dunn et al. 2004
Δ epi	+ / +	fail to specify anterior DE and PCP progenitors	no anterior axial mesoderm	lethal	Vincent et al. 2003a
Δ epi	+ / -	fail to specify anterior midline	no axial mesoderm no node	lethal	Vincent et al. 2003a
Δ epi	- / -	severe patterning defects in PS	no anterior and paraxial mesoderm	lethal	Dunn et al. 2004
- / -	+ / +	no DVE/AVE function	only posterior (exm, PGCs)	lethal	Waldrip et al. 1998
- / -	+ / -	no distinct embryonic-extra-embryonic boundary	severely compromised	lethal	Dunn et al. 2004
- / -	- / -	do not cavitate conversion to ExE suggested	none	lethal	Dunn et al. 2004

Abbreviations: DE: definitive endoderm, PCP: prechordal plate, PS: primitive streak, DVE/AVE: distal/anterior visceral endoderm, ExE: extra-embryonic ectoderm, exm: extra-embryonic mesoderm, PGCs: primordial germ cells, Δepi describes the genetic configuration *Sox2.Cre*$^{+/-}$*; Smad2*$^{-/CA}$.

Smad2/3 in the embryo leads to a progressive loss of cell fate specification (see Fig 5 and Table 2). Thus, loss of one copy of *Smad2* in otherwise viable *Smad3*$^{-/-}$ mice leads to failure to develop to term due to mild anterior truncations (Dunn et al. 2004). Smad2 functions in the epiblast are also affected by loss of *Smad3*.

Removal of one *Smad3* allele in epiblast-specific *Smad2* mutants leads to a failure to specify all axial midline tissues, where loss of both *Smad3* alleles in epiblast-specific *Smad2* mutants additionally abolishes formation of paraxial streak derivatives (Vincent et al. 2003a, Dunn et al. 2004). Thus, Nodal-Smad2/3 signalling is crucially required for the specification of mid-streak derivatives and highest levels of Smad2/3 are essential to specify anterior primitive streak derivatives. A summary of the defects observed upon gradual loss of dose-dependent Smad2/3 signalling can be found in Table 2.

Intriguingly, the early defects in global *Smad2* mutants can also be worsened by removal of *Smad3*. *Smad2*$^{-/-}$;*Smad3*$^{+/-}$ mutant embryos lack a distinct boundary between extra-embryonic and embryonic regions and mesoderm formation is - in contrast to abundant extra-embryonic mesoderm formation in *Smad2* mutant embryos - severely compromised (Dunn et al. 2004, see Fig 5b). Complete lack of *Smad2* and *Smad3* completely abolishes mesoderm formation and at E7.5 a small mass of rudimentary epithelial tissue is seen within a normal parietal yolk sac that does not express *Oct4*, whereas the ExE markers *Sox2* and *Bmp4* remain expressed (Dunn et al. 2004, Fig 5c). Due to the difficulty in obtaining *Smad2/3* double mutant embryos and their early arrest their analysis has been limited to the experiments shown in Fig 5b and c. Thus, it is not clear to what extent *Smad2/3* mutants (if at all) develop an epiblast and expression of which genes is ablated, reduced or elevated in the *Smad2*/3 mutant context. Furthermore, the cooperative Smad2 and Smad3 functions in mesoderm and endoderm specification have not been studied on a transcriptional level.

1.3.9 Primordial germ cell specification

1.3.9.1 Emergence of primordial germ cell precursors in the mouse embryo

In the mouse embryo, precursors of PGCs (pPGCs) arise from the posterior epiblast concurrent with the onset of gastrulation (Lawson and Hage, 1994). They can be identified from ~E6.25 onwards by the expression of the PR domain-containing transcription factor Blimp1 (encoded by the *Prdm1* gene), which is the earliest pPGC marker known to date (Vincent et al. 2005, Ohinata et al. 2005) (Fig 6). This posterior location at the embryonic-extra-embryonic interface is critical for the acquisition of the PGC fate, as transplantation of distal epiblast cells to the posterior epiblast at pre- to early streak stages results in PGC formation, whereas transplantation of posterior cells to distal location does not, suggesting that the pPGCs fate is still reversible to a somatic fate and pPGCs are not yet lineage-restricted (Tam and Zhou, 1996). It is, however, possible that clonal analysis (Lawson and Hage, 1994) and transplantation experiments (Tam and

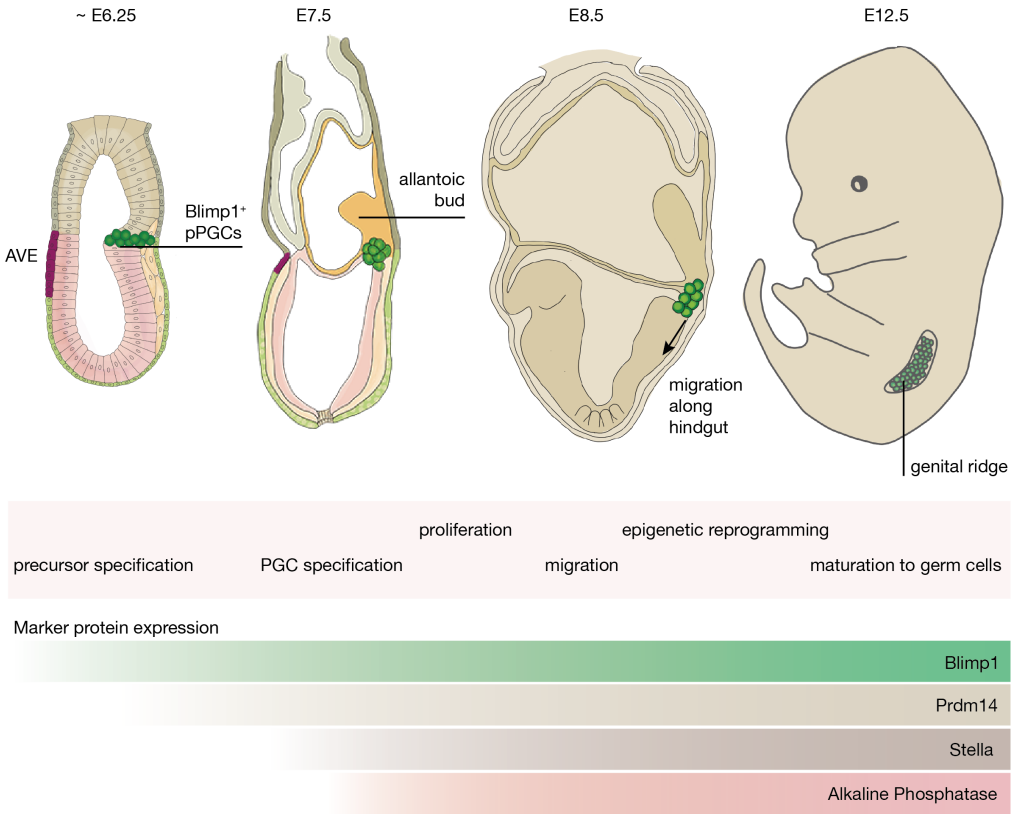


Figure 6 Early primordial germ cell development in mice.

Schematic of primordial germ cell development from ~E6.25 to E12.5. Graphics were modified from Tang et al. 2016 and Pereira et al. 2011. E: embryonic day, AVE: anterior visceral endoderm, pPGCs: primordial germ cell precursors. Embryos are not drawn to scale.

Zhou, 1996) did not label/transplant Blimp1$^+$ cells, as Blimp1 had not been identified as a pPGC marker at the time, making definitive conclusions difficult.

1.3.9.2 Lineage restriction to the PGC fate

Blimp1 function is required for PGC specification, but not for the initial induction of pPGCs, as rare aberrant "PGC-like" cells expressing later PGC markers *Stella* (also known as *Dppa3*) and *Alkaline Phosphatase* (*AP* or *Alpl*) can be detected in *Prdm1*$^{-/-}$ embryos at E8.5 (Vincent et al. 2005, Ohinata et al. 2005). Single cell transcriptional profiling experiments demonstrated that Blimp1 is required for the repression of somatic genes (such as *Hoxb1*) and the re-expression of pluripotency genes (such as *Sox2*) (Ohinata et al. 2005, Yabuta et al. 2006, Kurimoto et al. 2008). PGC fate determination

has thus been suggested to occur around ~E6.75 - E7.25, when pPGCs have expanded to form a cluster of ~40 Blimp1$^+$ cells that co-express the PGC marker *Stella* and have initiated *Hoxb1* repression (Yabuta et al. 2006). Lineage tracing experiments using a *Blimp1.Cre* transgene together with the *ROSA26.EGFP* reporter allele (Mao et al. 2001) showed that Blimp1$^+$ cells contribute almost exclusively to Stella$^+$ PGCs, suggesting they are lineage-restricted, whereas Stella$^+$ Blimp$^-$ cells were observed but attributed to incomplete *Blimp1.Cre* transgene–mediated marker activation (Ohinata et al. 2005, Saitou et al. 2005). Interestingly, Blimp1$^+$; Hoxb1$^+$ cells can still be detected at E7.75 and E8.25 (Yabuta et al. 2006). It remains unclear whether the Blimp1-mediated transcriptional changes in pPGCs and the acquisition of Stella expression truly restrict the PGC fate and prevent somatic fates (reviewed in Mikedis and Downs, 2014).

Blimp1$^+$/Stella$^+$ PGCs subsequently increase their doubling time, continue to reacquire pluripotency marker expression and undergo extensive Blimp1, Prdm14 and AP2γ/Tfap2c-dependent epigenetic reprogramming (Yamaji et al. 2008, Magnúsdóttir et al. 2013, Seki et al. 2005, reviewed in Saitou and Yamaji 2012). PGCs start to migrate into the hindgut epithelium from ~E8.5 onwards and are carried in the dorsal wall of the hindgut until ~E10.5, when they actively migrate from the gut to colonize the developing gonads at E12.5. Interactions between the PGCs and somatic supporting cells promote maturation into sperm and oocytes (reviewed in Molyneaux and Wylie 2004) (Fig 6). Continuity of Blimp1$^+$/Stella$^+$ PGCs from E6.25 to the colonization of the gonads has been inferred from analysis of Blimp1 and Stella and combined reporter mouse strains until Blimp1 and Stella proteins cease to be expressed at ~E13.5 - E15.5 (Ohinata et al. 2008). PGC fate seems to be faithfully established once PGCs initiate migration around ~E8.5, since multiple mouse mutants (e.g. *β1-integrin*, *Lhx1*, *Sox17, Msx1/2, Bax*, and *Kitl*) showing defective PGC migration develop extra-gonadal PGCs that do not re-acquire somatic fates but rather undergo apoptosis or become tumorigenic (Runyan et al. 2006, 2008, Anderson et al. 1999, Tanaka et al. 2010, Hara et al. 2009, Sun et al. 2016).

1.3.9.3 Mechanism of Blimp1$^+$ pPGC induction

a. pPGC induction requires Bmp and Wnt signalling

Induction of Blimp1$^+$ pPGCs occurs in response to Bmp4/Bmp8b signals from the extra-embryonic ectoderm (ExE) and Bmp2 from the VE (Ohinata et al. 2009). Loss of *Bmp4*, *Bmp8b*, *Bmp2* and their downstream signalling components including *Alk2*, *Smad1*, *Smad4* or *Smad5* results in loss or reduction in the number of pPGCs/PGCs (Lawson et al. 1999, Fujiwara et al. 2002, Ying et al. 2000, Ying and Zhao 2001, de Sousa Lopes et al. 2004, Tremblay et al. 2001, Hayashi et al. 2002b, Chu et al. 2004, Chang and Matzuk 2001, Arnold et al. 2006). None of the Bmp signalling-dependent Smads have, however, been shown to directly activate Blimp1 expression. Loss of Bmp signalling also affects allantois development indicating that competence of the proximal posterior epiblast is not restricted to the germ cell fate but also extra-embryonic mesodermal fates (Lawson et al. 1999, de Sousa Lopes et al. 2004, Tremblay et al. 2001, Hayashi et al. 2002b, Ying et al. 2000).

In addition to Bmp signals, Wnt signals are essential to achieve competence for pPGC formation, since loss of *Wnt3*, which is expressed in the emerging mesoderm of the primitive streak, or its downstream effector β-catenin leads to a failure in induction of Blimp1$^+$ epiblast cells (Ohinata et al. 2009). ChIP-seq for the Tcf1 transcription factor that mediates activation of β-catenin-induced transcription failed to identify binding in proximity to *Prdm1* in *in vitro* differentiated primordial germ cell-like cells (see below, Aramaki et al. 2013).

b. The role of Nodal signalling in pPGC induction

In the epiblast, Nodal signalling maintains *Bmp4* expression in the ExE, which in turn induces Wnt3 signals in the epiblast (Ben-Haim et al. 2006). Wnt3 subsequently reinforces *Nodal* expression in the epiblast via the Lef/Tcf-dependent proximal posterior epiblast (PPE) enhancer (Ben-Haim et al. 2006, Norris and Robertson 1999) (see Fig 7b).

The Nodal co-receptor Cripto is also regulated by Wnt3 via β-catenin (Morkel et al. 2003), but *Wnt3* mutants (in contrast to β-catenin mutants) have residual *Cripto* mRNA in the epiblast (Ben-Haim et al. 2006), and thus Cripto is not the only determinant responsible for the failure to maintain Nodal in *Wnt3*$^{-/-}$ embryos. Interestingly, the Nodal-Bmp4-Wnt3 feedback loop involves un-processed pro-Nodal, as mutation of the SPC motif of Nodal required for proprotein conversion by Furin and Pace4 does not affect the initiation of PS formation (Beck et al. 2002). Furthermore, this feedback loop is independent of Smad2 (Brennan et al. 2001). Additionally, *Nodal* mutants show reduced expression of *Oct4* which is also required for the specification of PGCs (Mesnard et al. 2006, Kurimoto et al. 2008, Okamura et al. 2008). Efficient differentiation of primordial germ cell like cells *in vitro* depends on Activin A stimulation to induce EpiLCs competent for germ cell fate induction (Hayashi et al. 2011, see below). Treatment of E6.0 epiblasts with BMP4 and LIF *ex vivo* had no effect on Blimp1 expression upon addition of recombinant Nodal, its inhibitor Lefty1 (Meno et al. 1998) or the ALK5/6/7 inhibitor SB431542 (Inman et al. 2002). Thus, sustained Nodal activity is dispensable for Blimp1 induction (Ohinata et al. 2009).

pPGCs are one of the earliest embryonic cell fates to be allocated and it has been suggested that pPGCs, in contrast to cells of the somatic lineages, do not undergo EMT at gastrulation, but do later during their migration (Kurimoto et al. 2008). E-Cadherin remains expressed in PGCs, whereas it is down-regulated in somatic neighbours, and blocking E-Cadherin with an antibody negatively affects PGC formation (Okamura et al. 2003). Interestingly, E-Cadherin is not down regulated in epiblast-specific *Eomes* mutants (Arnold et al. 2008). The role of Nodal signalling (and the downstream target Eomes) in pPGC specification has, however, not been assessed. Moreover, the molecular determinants that confer competence to induce Blimp1^{+} pPGCs remain elusive.

It is known that restriction of the PS and pPGC formation to the posterior epiblast is mediated by Nodal/Wnt antagonists secreted from the AVE and depends on Nodal signalling in the epiblast and Smad2/Eomes activity in the VE (Brennan et al. 2001,

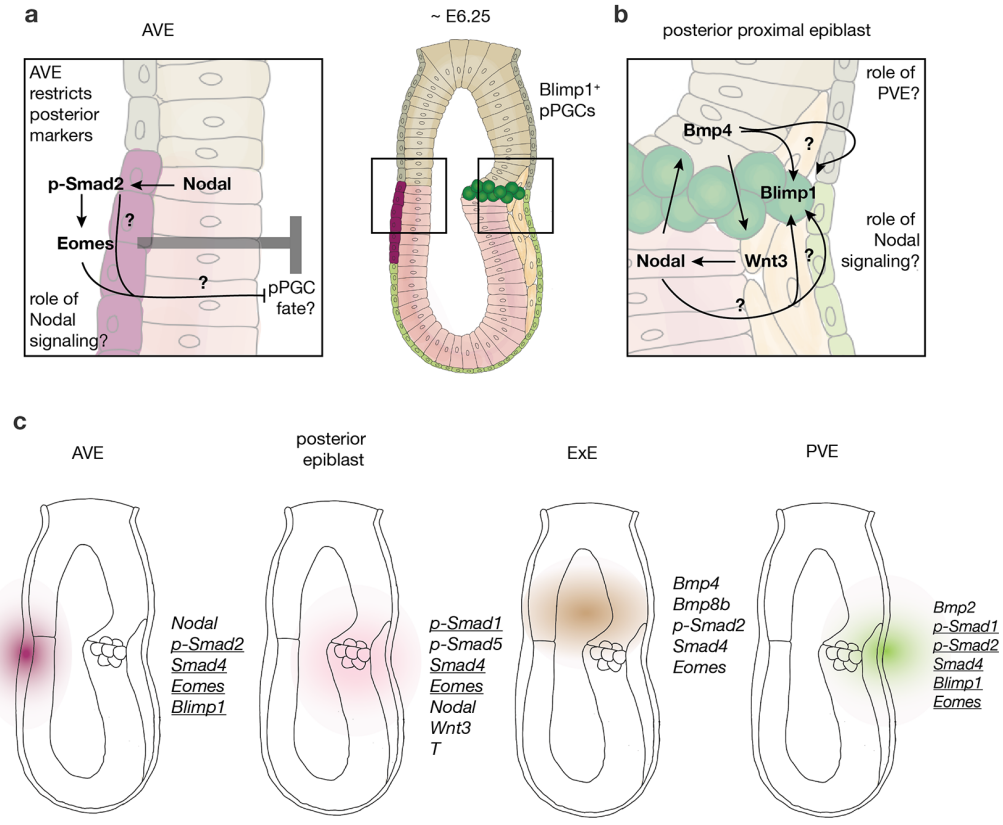


Figure 7 Compartments of Bmp and Nodal signalling in the ~ E6.25 mouse embryo during induction of primordial germ cell precursors.

(**a** and **b**) Schematic depiction of the anterior and posterior region of the embryonic-extra-embryonic interface of epiblast, extra-embryonic ectoderm and visceral endoderm. Important genes expressed in the respective tissues and their known and unknown (?) relations to each other are indicated. (**c**). Signalling centres potentially involved in establishing competence for the germ cell fate. Selected Bmp and Nodal signals that are expressed in the respective region at ~ E6.25 are shown (inferred primarily from WISH data). Note that expression of factors is not exclusive to the shown centres as several factors (e.g. Nodal, p-Smad2, Smad4) show ubiquitous expression throughout the epiblast and visceral endoderm prior to gastrulation. Tissue-specific roles of underlined factors in the visceral endoderm and/or epiblast will be studied in this thesis. Graphics were modified from Tang et al. 2016. E: embryonic day, AVE: anterior visceral endoderm, pPGCs: primordial germ cell precursors, PVE: posterior visceral endoderm. Embryos are not drawn to scale.

Nowotschin et al. 2013, Ohinata et al. 2009) (see Fig 7a). *Smad2*$^{-/-}$ mutant embryos display an expanded primitive streak and an increase in the number of Blimp1^{+} pPGCs (Waldrip et al. 1998, Ohinata et al. 2009). *Nodal*$^{-/-}$ and *Smad2*$^{-/-}$;*Smad3*$^{-/-}$ mutants have not been studied with respect to PGC formation (Brennan et al. 2001, Dunn et al. 2004). Collectively, the existing data fail to answer whether Nodal signalling is solely required to restrict pPGC formation or is also actively required for the induction of pPGCs.

c. Does Bmp/Smad signalling in the VE regulate primordial germ cell specification?

Whereas Bmp4 and Bmp8b are not expressed in the VE and act from the ExE (Lawson et al. 1999, Fujiwara et al. 2001, Ying et al. 2000), Bmp2 is exclusively expressed in the VE (see Fig 7c). Loss of Bmp2 reduces PGC numbers and *Bmp2*$^{+/-}$;*Bmp4*$^{+/-}$ (but not *Bmp2*$^{+/-}$;*Bmp8b*$^{+/-}$) embryos exhibit fewer PGC than *Bmp4*$^{+/-}$ embryos suggesting an involvement of the VE in Bmp signal transduction (Ying and Zhao, 2001). Loss of Bmp8b has been shown to expand the AVE, thereby impacting competence of epiblast cells to induce Blimp1 (Ohinata et al. 2009). Loss of the type I Bmp receptor Alk2, which is expressed in the VE at the onset of gastrulation (Roelen et al. 1994, Gu et al. 1999) results in the absence of PGCs (de Sousa Lopes et al. 2004). Expression of constitutively active Alk2 in the VE by the same authors was sufficient to rescue PGC formation in *Bmp4*$^{-/-}$ embryos, suggesting that Alk2, like Bmp2, acts in the VE.

p-Smad1/5/8 is also activated in the VE during gastrulation, and a Bmp-responsive-element isolated from the *Id1* promoter (Monteiro et al. 2004) drives reporter allele expression specifically in the extra-embryonic VE (de Sousa Lopes et al. 2004). Loss of *Smad1* results in a strong reduction or absence of PGCs (Tremblay et al. 2001, Hayashi et al 2002b). The mutant *Smad1* phenotype could not be rescued in chimeras comprised of wildtype ES cells and mutant extra-embryonic tissues, suggesting essential Smad1 activities reside in the VE (Tremblay et al. 2001). Smad4 mutants arrest prior to PGC formation (Sirard et al. 1998). Epiblast-specific *Smad4* mutants lack PGCs, but initiate gastrulation and all mesoderm progenitors are specified. However, the embryos fail to specify anterior primitive streak progenitors (Chu et al. 2004). VE-specific *Smad4* ablation, and the less severe phenotype of epiblast-specific *Smad4* mutants in comparison to *Smad4* mutants, demonstrate essential roles of VE-derived Smad4 for cell fate specification (Sirard et al. 1998, Chu et al. 2004, Li et al. 2010). PGC specification has, however, not been assessed in VE-specific mutants (Li et al. 2010).

In addition to its expression in pPGCs, Blimp1 is also expressed in the VE prior to gastrulation (Vincent et al. 2005, Ohinata et al. 2005). Chimera experiments show that

Blimp1 in extra-embryonic tissues cannot rescue the PGC maintenance defect (Ohinata et al. 2005), but a role for VE-derived Blimp1 for PGC maintenance has not been genetically excluded and its requirement in later stages of embryonic development has also not been studied. Reconstitution experiments *ex vivo* suggest an involvement of ExE and VE in the induction of Blimp1 (de Sousa Lopes et al. 2007). Thus, epiblasts stripped of VE induce Blimp1 when stimulated with high doses of Bmp4 and LIF (Ohinata et al. 2009). The role of the VE is largely overlooked in studies focussing on PGCLC induction *in vitro,* which centres on induction of the PGC fate from an epiblast-like state (see below, Hayashi et al. 2011). Thus, the involvement of VE-derived Bmp signals in pPGC induction remains controversial.

d. Primordial Germ Cell-like cells

High doses of recombinant human BMP4 can induce primordial germ cell-like (PGCLCs) from EpiLCs (Hayashi et al. 2011) (see section 1.3.4.2). After two days, 40 % of cells start expressing the primordial germ cell marker *Prdm1* as assessed using the *Prdm1.Venus* transgene (Hayashi et al. 2011, Ohinata et al. 2008). The co-expression of the later PGC marker *Stella* with *Prdm1* can be detected in a small proportion (~7%) of day 4 PGC-LCs (Hayashi et al. 2011). Addition of SCF, BMP8b, and EGF to cultures exposed to BMP4 and LIF enhanced the number of Blimp1$^+$; Stella$^+$ cells that form to ~13 % at day 4 and two days later, these Blimp1$^+$; Stella$^+$ PGCLCs also exhibit alkaline phosphatase staining (Hayashi et al. 2011). Sorted Prdm1.Venus$^+$ day 2 and Prdm1.Venus$^+$;Stella$^+$ day 4 and day 5 PGCLCs up regulated key PGC markers such as *Prdm1*, *Prdm14*, *Tcfap2c/AP2y* and *Stella* (Hayashi et al. 2011). PGCLCs can produce viable gametes and offspring, when male PGC-LCs are transplanted into seminiferous tubules of neonatal *W/W^v* mice (lacking endogenous germ cells), or when female PGCLC/gonadal stem cell aggregates are transplanted as reconstituted ovaries under the ovarian bursa of nude mice (Hayashi et al. 2011, Hayashi et. al 2012). Similar to BMP4 and LIF, overexpression of a combination of *Prdm1*, *Tcfap2c/AP2y* and *Prdm14* or overexpression of *Nanog* alone can also induce the PGCLC fate (Nakaki et al. 2013, Murakami et al. 2016).

e. Upstream regulators of Blimp1 expression in PGCLCs

Recently, the T-box factor Brachyury/T, expression of which depends on Wnt signals (Arnold et al. 2000), was shown to bind to a T-box site at the *Prdm1* locus in PGCLCs *in vitro* and to reinforce Blimp1 and later PGC marker gene expression (Aramaki et al. 2013). However, T does not induce initial Blimp1 expression in PGCLCs or *in vivo* and it has therefore been suggested that the T-box site can be bound by alternative T-box transcription factors such as Eomes, which is also expressed in pPGCs (Aramaki et al. 2013, Kurimoto et al. 2008). Intriguingly, overexpression of Eomes in *Wnt3*$^{-/-}$ EpiLCs that are unable to induce Blimp1 upon Bmp4 and LIF stimulation led to Blimp1 induction (Aramaki et al. 2013).

The pluripotency factor Nanog is also expressed in the posterior epiblast and when overexpressed in EpiLCs binds to the putative T-dependent Blimp1 enhancer leads to activation of PGC markers including *Prdm1*. However, the order of induction of *Prdm1* and *Prdm14* was reverted compared to Bmp4 and LIF induction of PGCLCs or PGCs *in vivo* (Murakami et al. 2016, Yamaji et al. 2008). Nanog induced a Blimp1-dependent PGCLC fate, as *Prdm1*$^{-/-}$ EpiLCs that overexpressed Nanog resulted in similar abnormalities as they are observed in *Prdm1*$^{-/-}$ PGCs *in vivo* (Ohinata et al. 2005). However, *Nanog* ablation in PGCLCs did not impair initial Blimp1 induction (Murakami et al. 2016). The functional role of Nanog and the putative Blimp1 enhancer in regulating Blimp1 induction *in vivo* have not been assessed.

1.4 Aims of the thesis

This study was initiated to dissect cooperative Smad2 and Smad3 functions during cell fate specification (project I, chapter 2). A second project examined tissue-specific contributions of Nodal- and Bmp-dependent signals in the induction of Blimp1$^+$ pPGCs (project II, chapter 3). The following questions constitute the focus of this thesis:

Project I

1. Does combined loss of Smad2/3 function in ES cells have an impact on cell viability, self-renewal and pluripotency marker expression?
2. Can *Smad2/3*$^{-/-}$ ES cells initiate cell fate specification during differentiation in embryoid bodies?
3. How does loss of Smad3, Smad2 or the combined loss of Smad2/3 function affect gene expression profiles during differentiation?
4. Can *Smad2/3*$^{-/-}$ ES cells initiate lineage priming in EpiLCs?

Project II

1. Is *Eomes* expression in the VE or in the epiblast required to induce Blimp1$^+$ pPGCs?
2. Does specific ablation of *Smad2* expression in the VE phenocopy the expansion of Blimp1$^+$ pPGCs observed in global Smad2 loss of function mutants?
3. Does ablation of *Smad4* expression in the VE affect the induction of Blimp1$^+$ pPGCs?
4. Is *Smad1* expression in the VE required to induce Blimp1$^+$ pPGCs?
5. Does *Prdm1* expression in the VE have a role in the induction of Blimp1$^+$ pPGCs and/or in later development?

2

Smad2/3 governs the transition of mouse embryonic stem cells from pluripotency to differentiation

2.1 Preface

TGFβ signalling via Smad2/3 is essential for cell fate specification in the mouse embryo (see chapter 1). The mechanistic dissection of the underlying defects in early embryonic lethal Smad2/3 double-mutant embryos *in vivo* has been limited in the past (Dunn et al. 2004). Additionally, functional redundancy of Smad2 and Smad3 on the level of transcriptional outputs of individual and combined factors has not been characterized.

In this chapter, I describe an experimental system that allows the dissection of transcriptional changes underlying graded Smad2/3 activities guiding the differentiation of mouse ES cells. I show that combined deletion of *Smad2* and *Smad3* in ES cells (section 2.2) does not overtly compromise the undifferentiated state as assessed by pluripotency marker expression and colony formation (section 2.3). Combined loss of Smad2 and Smad3 does, however, affect the differentiation into embryoid bodies (section 2.4). Transcriptional profiling reveals that *Smad2/3*$^{-/-}$ embryoid bodies acquire a unique expression profile characterized by impaired induction of mesoderm and endoderm lineage specific genes and acquisition of a more extra-embryonic-like state (section 2.5). Parallel profiling of *Smad2* or *Smad3* mutant ES cells during embryoid body differentiation shows only partial overlap of gene expression changes apparent in the compound mutant ES cells and emphasises dose-dependency of Smad2/3 signalling. Preliminary data suggest that the underlying mechanism of the differentiation defect could lie in the inability of *Smad2/3*$^{-/-}$ cells to adopt an epiblast-like state that is competent to initiate lineage priming (section 2.6).

Collectively, my results have identified novel downstream targets of Smad2/3 signals and an absolute requirement for Smad2/3 during the differentiation of embryonic lineages. Future experiments aim to identify chromatin accessibility changes governing possible Smad2/3-dependent lineage priming and will be discussed in the conclusion in section 2.7 and in chapter 4.

2.2 Generation of *Smad2/3*$^{-/-}$ and *Smad3*$^{-/-}$ embryonic stem cells

To study cooperative Smad2/3 functions, we aimed to analyse ES cells in which Smad2, Smad3 or combined Smad2/3 protein expression had been genetically ablated. Control wild type and *Smad2*$^{-/-}$ ES cell lines harbouring the *Smad2*^{Robm1} null allele were available. *Smad2*^{Robm1} removes Smad2 protein expression and leads to an early lethal gastrulation defect in embryos and a definitive endoderm specification defect in both the embryo and differentiating ES cells (Waldrip et al. 1998, Tremblay et al. 2000, Costello et al. 2011). To obtain *Smad2*$^{-/-}$;*Smad3*$^{-/-}$ ES cells (hereafter referred to as *Smad2/3*$^{-/-}$) and isogenic *Smad3*$^{-/-}$ ES cells we sought to ablate Smad3 protein expression in *Smad2*$^{-/-}$ as well as in wild type ES cells.

I searched for validated *Smad3* null alleles to delete a genomic region that has been previously been shown to ablate Smad3 protein function. The *Smad3*^{tm1Xfw} allele (Datto et al. 1999) replaces the genomic region surrounding exon 1 (~3kb) with a neomycin cassette and ablates Smad3 protein expression (Datto et al. 1999). I therefore decided to delete this region by CRISPR/Cas9-mediated deletion. To reduce off-target effects I used Cas9 nickase (Cas9n) (Ran et al. 2013). Two sets of paired short guide RNAs (sgRNAs) targeting the genomic regions flanking the first exon of *Smad3* (spanning ~3kb) produced multiple lines harbouring the expected deletion (Figure 8).[1]

I screened for the deletion and genomic integrity of the locus by Southern blotting of individually targeted *Smad2*$^{-/-}$ or wild type clones (data not shown). PCR across the deletion region in clones with the predicted deletion size together with subsequent sequencing confirmed the lack of a ~3kb fragment with slight variation across different clones and alleles due to insertion and deletions (InDels) induced by non-homologous end joining (Fig 8b and data not shown). In addition to newly generated *Smad3*$^{-/-}$ and *Smad2/3*$^{-/-}$ lines I also confirmed the genotypes of all *Smad2*$^{-/-}$ and wild type lines that will

[1] I tested multiple Cas9wt and Cas9n deletion strategies (single cut as well as larger deletion) and optimized transfection conditions to select for optimal cutting/deletion efficiencies, which resulted in usage of the described strategy (data not shown, see chapter 5 for details on the final strategy used).

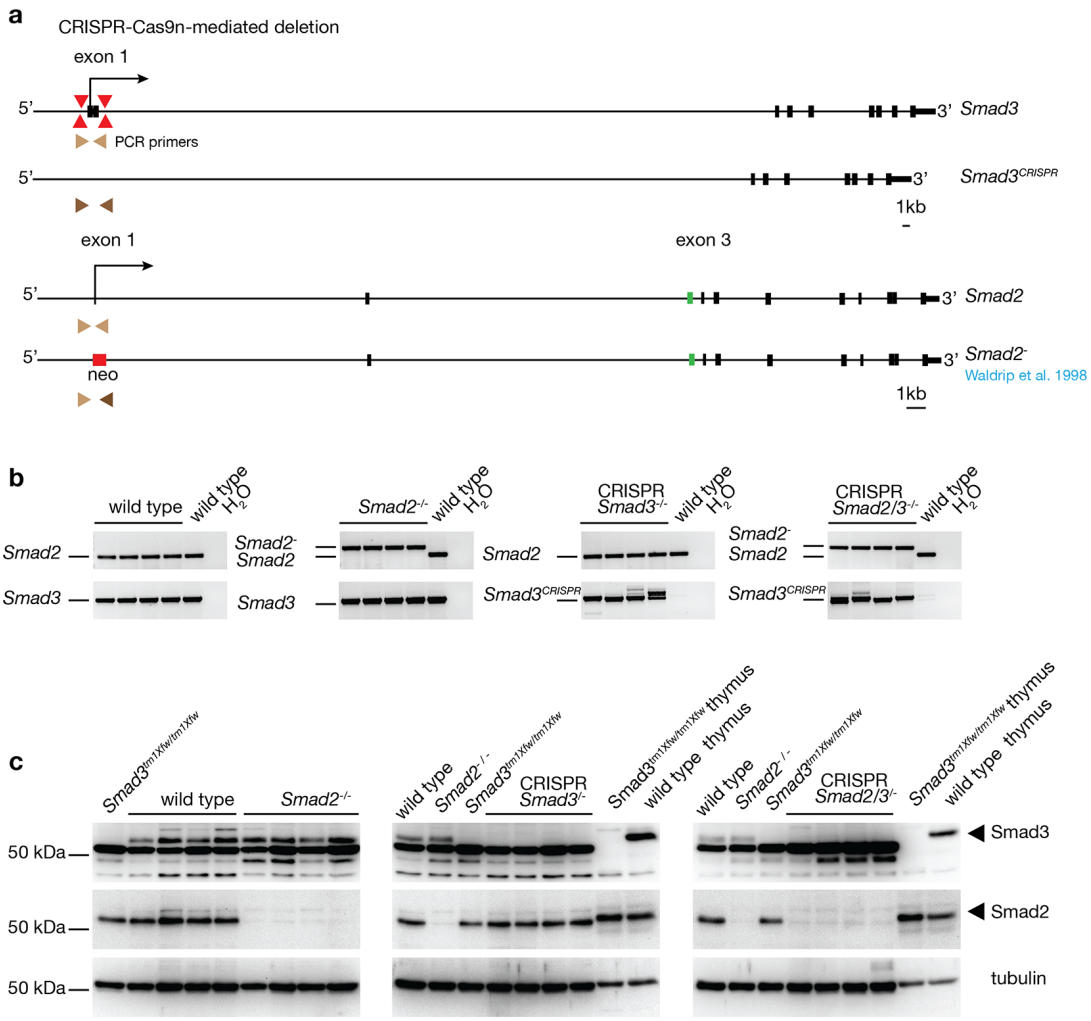


Figure 8 Validation of *Smad2/3*$^{-/-}$, *Smad3*$^{-/-}$, *Smad2*$^{-/-}$ and wild type ES cell lines.

(**a**) *Smad3* deletion strategy with two sets of sgRNAs (red triangles) targeting CRISPR-Cas9n to the genomic region flanking exon 1 to induce deletion of the fragment by two double-nicks. This strategy was used to obtain *Smad2/3*$^{-/-}$ and *Smad3*$^{-/-}$ ES cell lines by targeting *Smad2*$^{-/-}$ and wild type ES cells. The offset of 5' and 3' double-nicks were 1 bp and 8 bp, respectively. The wild type *Smad3* as well as wild type and null *Smad2* and *Smad2*$^{-}$ alleles (Waldrip et al. 1998) are also shown. Smad2 protein exists in two isoforms distinguished by the presence or absence of exon 3 (marked in green). Arrows indicate genotyping primers of the respective allele shown in b (**b**) PCR genotyping of the cell lines used in this study (see chapter 5 for primer sequences). For *Smad2/3*$^{-/-}$ and *Smad3*$^{-/-}$ ES cell lines primers flanking the 5' and 3' double-nick sites were used to confirm the deletion in homozygous clones identified via Southern blotting (data not shown). (**c**) Western blot of *Smad2/3*$^{-/-}$ and *Smad3*$^{-/-}$ as well as *Smad2*$^{-/-}$ and wild type ES cell lines used in this chapter with antibodies specific to Smad3, Smad2 (both isoforms) and tubulin. Note that prominent bands in Smad3 blots represent unspecific background that is present to varying degree in all ES cell samples. The recognition site of the Smad3 antibody lies in the region most divergent between the highly homologous Smad2 and Smad3 proteins and is - on the genomic level - unaffected by the used deletion strategy.

be used in this chapter. All lines were confirmed to be male (presence of X and Y chromosome) by PCR (data not shown). To confirm loss of Smad3 protein in CRISPR-Cas9n-edited clones, we performed Western blotting using a monoclonal Smad3 peptide antibody recognizing 100 amino acids including parts of the linker and MH2 domain of human Smad3 (Fig 8c). To compare my CRISPR/Cas9n-edited *Smad3* allele to the *Smad3*^{tm1Xfw} allele we derived ES cells from *Smad3*$^{tm1Xfw/tm1Xfw}$ blastocysts (Datto et al. 1999). We also isolated adult thymus tissue from *Smad3*$^{tm1Xfw/tm1Xfw}$ mice and wildtype littermates, as adult thymus expresses Smad2 and Smad3 (Datto et al. 1999, Rosendahl et al. 2003). We also validated all wild type and *Smad2*$^{-/-}$ ES cell lines used in this chapter for the presence and absence of Smad2/3 protein, respectively.

Figure 8c shows the complete lack of Smad3 protein in *Smad2/3*$^{-/-}$ and *Smad3*$^{-/-}$ lines comparable to the conventional *Smad3*$^{tm1Xfw/tm1Xfw}$ cells and thymus from *Smad3*$^{tm1Xfw/tm1Xfw}$ mice, whereas wild type and *Smad2*$^{-/-}$ cells and wild type thymus tissue expressed high levels of Smad3 protein. Loss of Smad2 protein function as seen in the parental *Smad2*$^{-/-}$ line was confirmed in all clones of *Smad2/3*$^{-/-}$ and *Smad2*$^{-/-}$cells investigated. We did not detect effects of Smad3 or Smad2 protein loss on Smad2 or Smad3 protein levels respectively. We confirmed our CRISPR deletion strategy using an alternative polyclonal Smad3 peptide antibody (data not shown, see chapter 5).

Confident to have achieved faithful ablation of Smad2/3 and single Smad3 protein expression in ES cells, I proceeded with the characterization of *Smad2/3*$^{-/-}$ in comparison to *Smad3*$^{-/-}$ and established *Smad2*$^{-/-}$ lines (Tremblay et al. 2000).

2.3 Smad2/3 signals are dispensable for ES cell viability and self-renewal and the expression of pluripotency marker genes

Nodal and Bmp signalling are active in ES cells and the inner cell mass of the mouse embryo (reviewed in Papanayotou and Colligon, 2014). Controlled levels of expression are crucial for the maintenance of the undifferentiated state, as *Nodal* overexpression drives ES cells towards mesodermal and endodermal fate while neural fate markers are

decreased (Pfendler et al. 2005). Analysis of ES cells that lack Nodal or had been subjected to pharmacological inhibition of Alk4/5/7 receptors using SB431523 (Inman et al. 2002), however, suggested that Nodal signalling is dispensable for ES cell maintenance (Conlon et al. 1991, James et al. 2005). In human ES cells, Nodal signalling is essential for ES cell maintenance (reviewed in Pauklin and Vallier 2015). Analysis of *Smad4*$^{-/-}$ ES cells showed moderate gene expression changes in the undifferentiated state. *Gdf1*, *Tgfb2*, *Lefty2* as well as Bmp-dependent *Idb1/2/3* transcripts and the extra-cellular matrix marker *Mmp14* in addition to gastrulation marker including *T*, *Fgf8*, *Sp5* were slightly down-regulated. By contrast, early ICM markers *Zscan4* and *Tbx3* and VE marker transcripts *Dpp4, H19* and *Gata6* were slightly up-regulated (Costello et al. 2009). Bmp signalling has been reported to stimulate self-renewal in ES cells and Smad1, Oct4, Sox2 and Nanog binding sites in ES cells have been shown to partially overlap (Ying et al. 2003, Chen et al. 2008). However, combined loss of *Smad1/5* in ES cells fails to affect ES cell maintenance or self-renewal in mice suggesting limited roles of Bmp signalling in ES cells (Gomes Fernandes et al. 2016). As *Smad2/3*$^{-/-}$ embryos arrest earlier than Nodal mutants and p-Smad2 is detected in Nodal mutants (Dunn et al. 2004, Yamamoto et al. 2009), it is not clear if loss of Smad2/3 has effects on the undifferentiated state in ES cells.

I therefore sought to assess whether undifferentiated ES cells were affected by loss of Smad2/3. *Smad2/3*$^{-/-}$ ES cells were indistinguishable from wild type and *Smad2*$^{-/-}$ or *Smad3*$^{-/-}$ cells by visual inspection, irrespective of whether they were cultured in serum+LIF or 2i+LIF conditions (Fig 9a). This, together with the ability to culture mutant cells without noticeable cell death for multiple passages, suggested that ES cell viability and the potential for self-renewal were unaffected.

To investigate a possible phenotype at a molecular level, I characterized transcripts of established pluripotency markers by qRT-PCR in four independent clones for wild type and *Smad2/3*$^{-/-}$ ES cells under 2i+LIF conditions (see section 2.2 for validation of clones). As shown in Figure 9b, expression of the core pluripotency factors *Oct4*, *Sox2* and *Nanog* was unaffected by the loss of Smad2/3. Mouse ES cells grown in 2i+LIF are

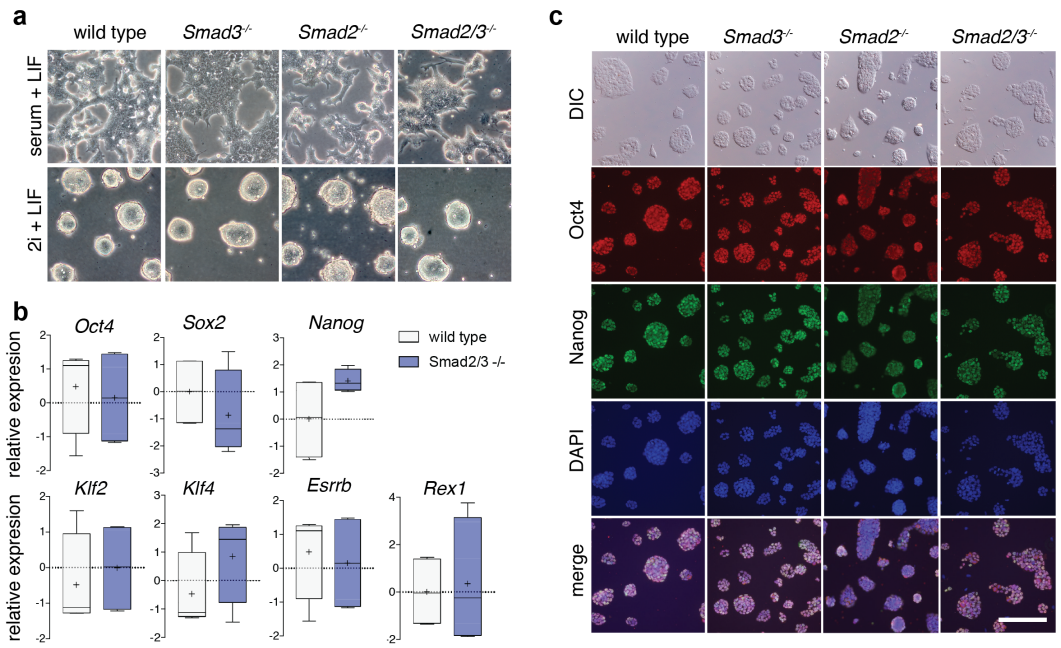


Figure 9 Loss of Smad2/3 signals does not affect ES cell morphology and the expression of pluripotency markers.

(**a**) Morphology of *Smad2/3*$^{-/-}$ embryonic stem cells grown under 2i+LIF and serum+LIF conditions. (**b**) qRT-PCR of core and naïve pluripotency markers of wild type and *Smad2/3*$^{-/-}$ ES cells grown in 2i + LIF. Box plots show median (line) and mean (+) and 25th to 75th percentile distribution of gene expression (normalized to *Hprt*) relative to averaged expression in wild type (fold change). Four biological replicates (cell lines) were averaged for each genotype. Whiskers represent the smallest and largest values. Each individual biological replicate was run in technical duplicate. Unpaired t-tests were used to assess the lack of statistical significance ($P<0.05$). (**c**) Immunofluorescence for Oct4 and Nanog in wild type, *Smad2*$^{-/-}$, *Smad3*$^{-/-}$ and *Smad2/3*$^{-/-}$ ES cells in 2i+LIF. Scale bar: 200 µm.

characterized by the expression of naïve markers of pluripotency including *Esrrb*, *Klf2*, *Klf4* and *Zfp42/Rex1*. These markers were also unaffected by the loss of Smad2/3. Oct4 and Nanog protein expression in cells grown in 2i+LIF and serum+LIF was indistinguishable between genotypes (Fig 9c and data not shown). In my qRT-PCR analysis I noticed a high variability in the expression levels of pluripotency marker genes in the four clones analysed irrespective of their genotype. I decided that it would be crucial to characterize multiple clones of each genotype in subsequent experiments to be confident about a biological effect rather than a mere effect of clonal variation. Pluripotent cells have the potential to differentiate into all three embryonic germ layers and primordial germ cells, but not extra-embryonic tissues (see chapter 1). I concluded that Smad2/3 signals are dispensable for ES cell viability and the expression of marker genes of pluripotency suggesting that the undifferentiated state is unaffected by the loss

of Smad2/3. Later in this chapter (see sections 2.5 and 2.6), I will address whether the potential to differentiate is affected upon loss of Smad2/3. First, however I wanted to test whether *Smad2/3* $^{-/-}$ ES cells maintain the ability to self renew and efficiently form pluripotent colonies when they are challenged to form colonies from single cells. I performed a colony-forming assay followed by assessment of colony number and size. As shown in Figure 10a and b, the ability to form colonies was unaffected upon loss of Smad2/3. The colony size at d5 was unaffected by the loss of Smad2/3 (Figure 10c and d).

Next, I performed alkaline phosphatase (AP) staining to assess undifferentiated pluripotent ES cells within these colonies (Pease et al. 1990). Loss of Smad2/3 had no effect on the formation of pluripotent, predominantly AP^{+} ES cell colonies (Figure 10e and f). When LIF was removed, the majority of ES cell colonies - irrespective of their genotype - changed from a pluripotent AP^{+} state to a flattened mixed or differentiated AP^{-} state. In agreement with a naïve homogenous state of pluripotency under 2i+LIF conditions, *Smad2/3*$^{-/-}$ colonies grown in 2i+LIF were homogenously AP^{+} and completely lost AP when 2i and LIF were withdrawn and cells cultured in pure neural differentiation medium (data not shown). These results suggested that loss of Smad2/3 in ES cells does not affect the ability to self-renew and form pluripotent colonies. Loss of AP and survival of *Smad2/3*$^{-/-}$ cells upon LIF withdrawal suggested that *Smad2/3*$^{-/-}$ cells possess the ability to differentiate.

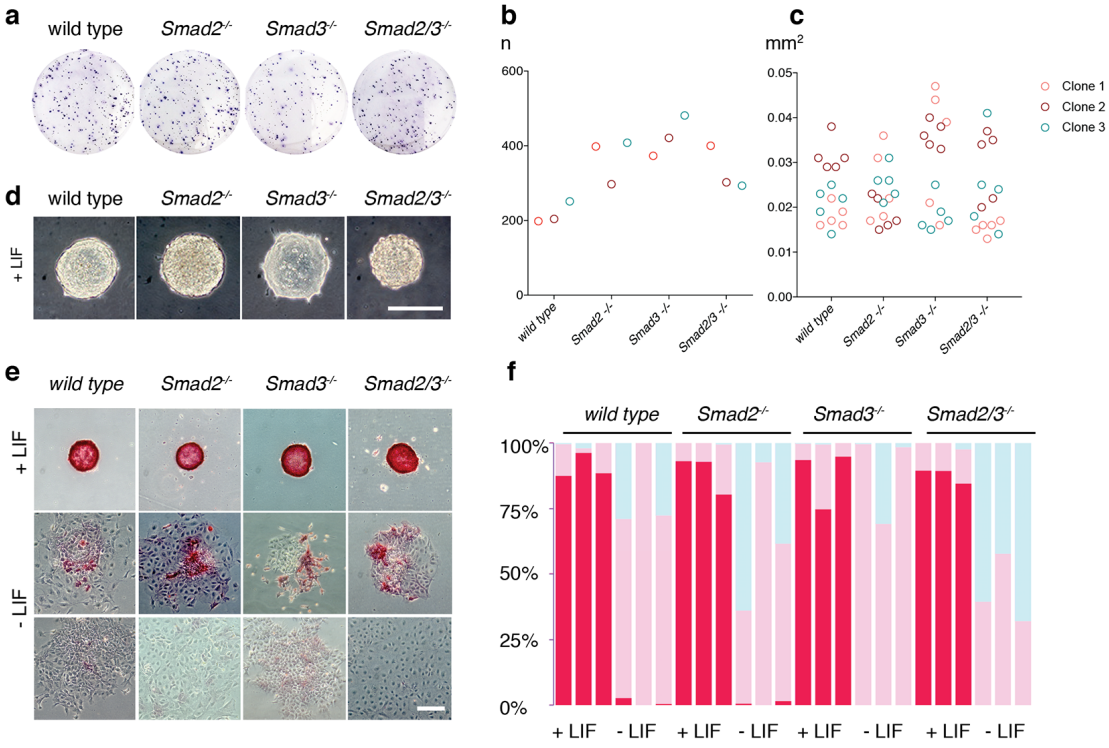


Figure 10 Smad2/3 expression is non-essential for self-renewal and the ability to form pluripotent ES cell colonies.

(**a**) Giemsa staining of wild type, *Smad2*$^{-/-}$, *Smad3*$^{-/-}$ and *Smad2/3*$^{-/-}$ embryonic stem cell colonies at d7. Colonies were obtained following seeding of 600 cells/plate in serum+LIF conditions. (**b**) Quantification of the averaged number of colonies (see a) for three clones of each genotype. (**c, d**) Close up of representative colonies five days after plating per genotype and assessment of colony surface area averaged for 15 colonies per genotype (five per clone) (**e**) Alkaline Phosphatase Staining of wild type, *Smad2*$^{-/-}$, *Smad3*$^{-/-}$ and *Smad2/3*$^{-/-}$ colonies at d5 after plating. Colonies were grown in the presence or absence of LIF from 600 cells in serum conditions. (**f**) Quantification of undifferentiated (red), mixed (pink) and differentiated (grey) colonies for three clones of each genotype. To calculate proportional values, the total number of colonies was set to 100%. Unpaired t-tests were used to assess lack of statistical significance in c and f ($p<0.05$). Scale bar: 200 µm.

2.4 Dose-dependent Smad2/3 signals are required for growth and differentiation in embryoid bodies and for the differentiation into definitive endoderm *in vitro*

To evaluate the extent to which *Smad2/3*$^{-/-}$ ES cells were able to differentiate and to assess how gradual loss of Smad2/3 signals would affect cell fate choice I exploited culture protocols that promote differentiation. Removal of feeder cells or LIF from ES cells grown in suspension triggers differentiation of ES cells to multicellular aggregates called embryoid bodies (EBs) (Martin 1981, Smith et al. 1988). To some extent, EBs

recapitulate cell fate specification in the post-implantation mouse embryo as EBs can form derivatives of the PrE and epiblast-derived germ layers (Doetschmann et al. 1985, Costello et al. 2011). Serum-derived cytokines in the culture medium bias EBs towards expression of mesodermal and endodermal cell fates making them suitable to mimic early differentiation events occurring in the primitive streak in developing mouse embryos (Wiles and Keller, 1991).

I therefore decided to differentiate wild type, *Smad2*$^{-/-}$, *Smad3*$^{-/-}$ and *Smad2/3*$^{-/-}$ ES cell lines into EBs by LIF removal (see chapter 5). To be able to compare EB growth and general morphology between the genotypes, I decided to form EBs in hanging drops by seeding 100 cells/microdrop. Analysis of EB morphology at d2, d3 and d4 of differentiation revealed that as for wild type ES cells *Smad3*$^{-/-}$ cells formed well-defined, round EBs that increased in size over the course of the four days of differentiation (Fig 11a). At d4 the first signs of cavitation (darker centre in (a)) could be detected in wild type and *Smad3*$^{-/-}$ EBs.

Smad2$^{-/-}$ ES cells initiated EB formation similar to wild type and *Smad3*$^{-/-}$ ES cells, but exhibited a more disorganized outer layer (representing PrE (Coucouvanis and Martin, 1999)) from d3 onwards and were significantly growth retarded at d4 (Fig 11a and c). D4 *Smad2*$^{-/-}$ EBs did not show any signs of cavitation (Fig 11a). This observed differentiation defect is in agreement with the described VE and definitive endoderm differentiation defect in mutant embryos and ES cells (Waldrip et al. 1998, Tremblay et al. 2000, Costello et al. 2011).

Similar to *Smad2/3*$^{-/-}$ embryos *in vivo* (Dunn et al. 2004), *Smad2/3*$^{-/-}$ ES cells showed the most severe phenotype. EB growth was compromised from d2 onwards, becoming more severe by d3, when *Smad2/3*$^{-/-}$ EBs started to lose their round shape. At d4, round morphology was completely lost and the outer EB layer was disorganized, a phenotype that was observed in four independent *Smad2/3*$^{-/-}$ cell lines derived from two parental *Smad2*$^{-/-}$ lines (Fig 11b). As for *Smad2*$^{-/-}$ EBs, I observed no sign of cavitation. Loss of

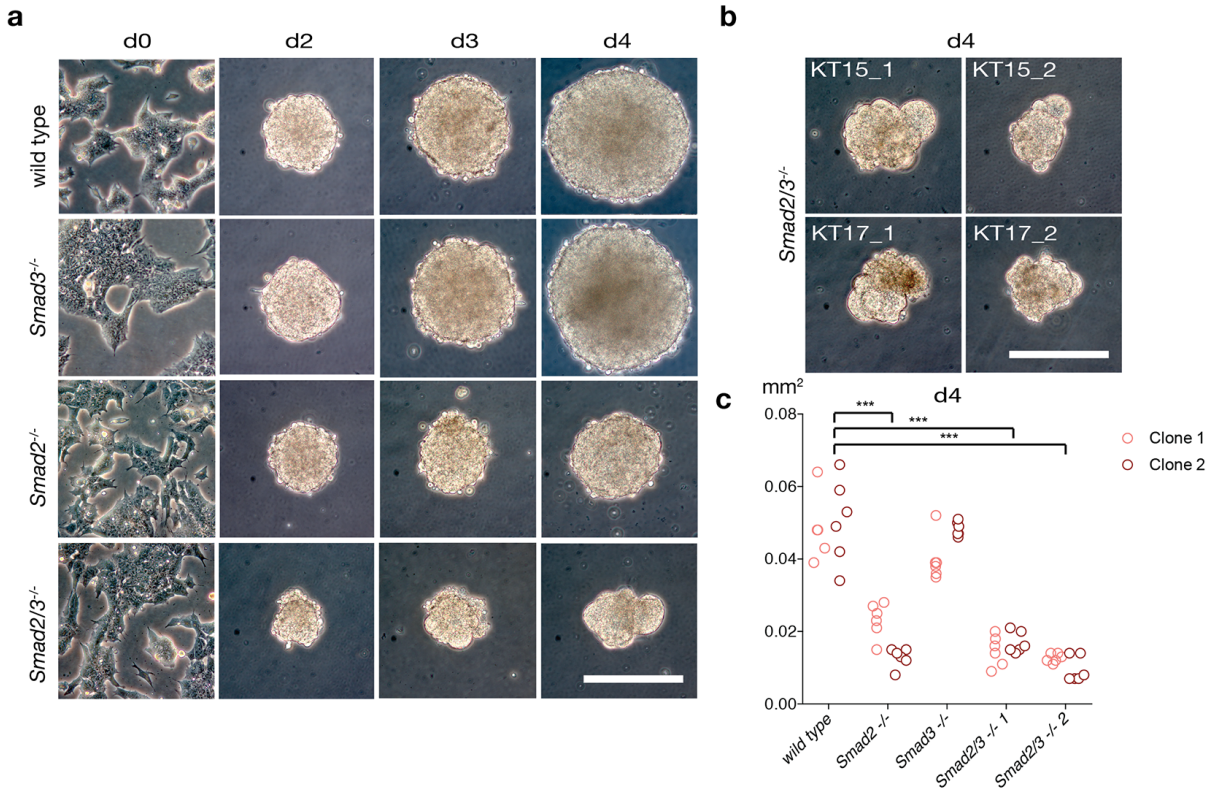


Figure 11 Loss of Smad2 and Smad2/3 affects embryoid body morphology.

(**a**) Morphology of undifferentiated ES cells and d2 and d3 embryoid bodies differentiated from 100 cells by removal of LIF. This phenotype was confirmed with one (wild type, *Smad3*$^{-/-}$, *Smad2*$^{-/-}$) or three (*Smad2/3*$^{-/-}$) additional clones per genotype. (**b**) Examples of d4 *Smad2/3*$^{-/-}$ EBs from four different clones (top and bottom row represent different parental *Smad2*$^{-/-}$ lines. (**c**) Morphometric measurements of the surface area of 12 d4 EBs (6 for two clones) per genotype (4 clones for Smad2/3). Unpaired t-tests were used to assess statistical significance (*P<0.05, **P<0.01, ***P<0.001). Scale bar: 200 µm.

Smad2/3 resulted in defects in EB proliferation and morphology consistent with a severe loss in the ability to initiate differentiation. To investigate differentiation into the three embryonic germ layers in mutant EBs, I isolated RNA and performed OneStep RT-PCR for key lineage markers. Wild type EBs expressed the primitive streak marker *Brachyury* (*T*) (Wilkinson et al. 1990), the endoderm marker *Foxa2* (Ang and Rossant 1994a), the primitive ectoderm marker *Fgf5* (Hébert et al. 1991) as well as *Cer1*, which marks the AVE and anterior primitive streak (Belo et al. 1997). *Smad3*$^{-/-}$ EBs were indistinguishable from wild type. As expected, *Smad2*$^{-/-}$ EBs failed to initiate endoderm and AVE marker expression (Costello et al. 2011). Similarly, *Smad2/3*$^{-/-}$ EBs failed to express these markers (Fig 12a). Notably, all EBs retained expression of the pluripotency marker *Oct4*. *Smad2*$^{-/-}$

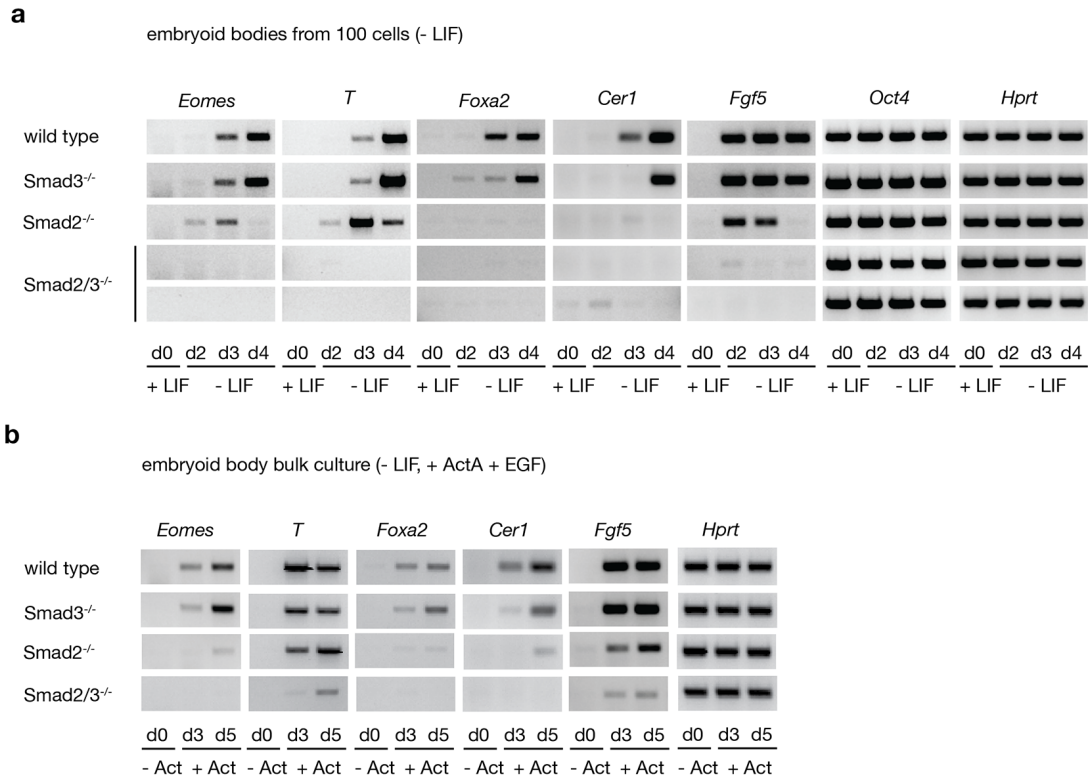


Figure 12 Loss of Smad2 and Smad2/3 affects marker gene expression of the primary germ layers during EB and definitive endoderm differentiation.

(**a**) OneStep RT-PCR analysis of marker genes of the primary germ layers and Hprt control on undifferentiated ES cells and EBs at d2, d3 and d4 of differentiation (see also main text). (**b**) OneStep RT-PCR analysis of marker genes of the primary germ layers on undifferentiated ES cells and *in vitro* differentiated endoderm at d3 and d5 after stimulation with Activin A and EGF (see also main text). Act: Activin A, LIF: leukemia inhibitory factor, EGF: epidermal growth factor, d: day

ES cells contribute to mesodermal lineages but lack the ability to form definitive endoderm *in vivo* and *in vitro* (Tremblay et al. 2000, Costello et al. 2011). To assess directed endoderm formation, I cultured *Smad2/3*$^{-/-}$ ES cells in the presence of exogenous Activin A and EGF (Costello et al. 2011, Morrison et al. 2008). OneStep RT-PCR marker analysis confirmed that, as for Smad2 loss of function mutants, *Smad2/3*$^{-/-}$ ES cells fail to form definitive endoderm. In contrast to observations made in d4 hanging drop EBs (Fig 12b), upon Activin A stimulation *Smad2/3*$^{-/-}$ cells weakly express *T* and *Fgf5* at d5 of differentiation (see chapter 4). Collectively, this analysis suggests that loss of Smad2/3 severely affects differentiation of the embryonic lineages.

2.5 *Smad2/3*$^{-/-}$ EBs lack mesoderm and endoderm marker gene expression and divert to an extra-embryonic-like profile

To learn more about these differentiation defects I collected mutant and wild type EBs at d2 and d3 of differentiation as well as undifferentiated ES cells and performed transcriptional profiling using the Illumina Mouse WG-6 v2 Expression BeadChip (see chapter 5). As controls, I included *Smad2*$^{-/-}$ and *Smad3*$^{-/-}$ ES cell and EB samples in my analysis. I profiled four clones per genotype at each time-point. The morphological phenotypes (Fig 13a and section 2.4), genotypes, as well as Smad2 and Smad3 protein expression, were confirmed for all these clones (Fig 8b and c in section 2.2).

Principal component analysis (PCA) on normalized data revealed clustering of most d0 samples, although the segregation was incomplete (Fig 13b). The majority of d2 and d3 samples clustered according to genotype with wild type and *Smad3*$^{-/-}$ samples as well as *Smad2*$^{-/-}$ and *Smad2/3*$^{-/-}$ clustering together. d2 samples lay closer together than d3 samples, suggesting progressing transcriptional divergence of mutants from wild type EBs.

We next identified statistically significant mis-regulated transcripts in wild type d3 EBs relative to undifferentiated cells ($p \leq 0.05$ and $\geq$ 2-fold changed). Among the top 20 up-regulated transcripts I identified key lineage markers expressed in early embryos (see Table 3 in Fig 13c). The early mesoderm markers *T* (Wilkinson et al. 1990), *Lhx1* (Barnes et al. 1994, Nowotschin et al. 2013), *Fgf8* (Crossley and Martin 1995), *Gsc* (Blum et al. 1992), *Mesp1* (Saga et al. 1999), *Mixl1* (Pearce and Evans 1999) and the primitive ectoderm marker *Fgf5* (Hébert et al. 1991) as well as the endothelial marker *Klhl6* (Kroll et al. 2005) were induced. The naïve pluripotency markers *Esrrb*, *Zfp42/Rex1* and *Fbxo15* normally expressed in the ICM *in vivo* and in undifferentiated ES cells (Martello et al. 2013, Guo et al. 2010, Rogers et al. 1991, Tokuzawa et al. 2003, Pelton et al. 2002) were among the strongest down-regulated transcripts.

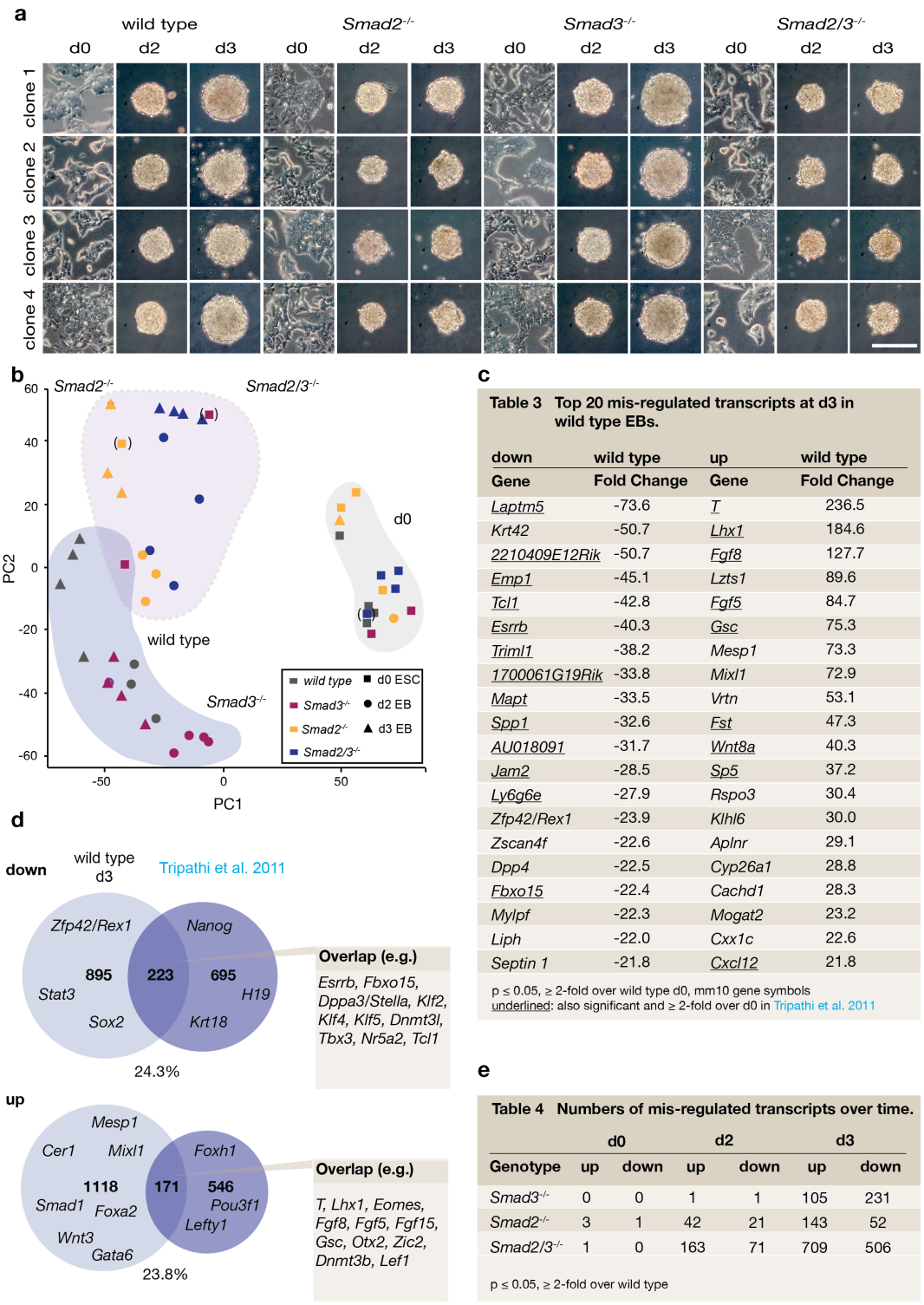


Table 3 Top 20 mis-regulated transcripts at d3 in wild type EBs.

down	wild type	up	wild type
Gene	Fold Change	Gene	Fold Change
Laptm5	-73.6	T	236.5
Krt42	-50.7	Lhx1	184.6
2210409E12Rik	-50.7	Fgf8	127.7
Emp1	-45.1	Lzts1	89.6
Tcl1	-42.8	Fgf5	84.7
Esrrb	-40.3	Gsc	75.3
Triml1	-38.2	Mesp1	73.3
1700061G19Rik	-33.8	Mixl1	72.9
Mapt	-33.5	Vrtn	53.1
Spp1	-32.6	Fst	47.3
AU018091	-31.7	Wnt8a	40.3
Jam2	-28.5	Sp5	37.2
Ly6g6e	-27.9	Rspo3	30.4
Zfp42/Rex1	-23.9	Klhl6	30.0
Zscan4f	-22.6	Aplnr	29.1
Dpp4	-22.5	Cyp26a1	28.8
Fbxo15	-22.4	Cachd1	28.3
Mylpf	-22.3	Mogat2	23.2
Liph	-22.0	Cxx1c	22.6
Septin 1	-21.8	Cxcl12	21.8

p ≤ 0.05, ≥ 2-fold over wild type d0, mm10 gene symbols
underlined: also significant and ≥ 2-fold over d0 in Tripathi et al. 2011

Table 4 Numbers of mis-regulated transcripts over time.

	d0		d2		d3	
Genotype	up	down	up	down	up	down
Smad3-/-	0	0	1	1	105	231
Smad2-/-	3	1	42	21	143	52
Smad2/3-/-	1	0	163	71	709	506

p ≤ 0.05, ≥ 2-fold over wild type

Figure 13 Transcriptional profiling of mutant and wild type EBs during differentiation: Sample clustering and validation of control differentiation.

(**a**) Bright field images of four independent clones of each genotype in undifferentiated ES cells and differentiated d2 and d3 EBs grown from 100 cells each. See also section 2.4 Fig 11a for comparison. Scale bar: 200 µm. (**b**) PCA analysis of all datasets obtained from transcriptional profiling of Smad2/3 EBs and ES cells. Outliers excluded in the further analysis are marked in brackets. (**c**) Table 3 with the top 20 significantly and > 2-fold up- and down-regulated transcripts in wild type d3 EBs. (**d**) Venn diagram of d3 wild type up- (top) and down- (bottom) regulated transcripts in comparison to wild type d3 EBs in Tripathi et al. 2011. (**e**) Table 4 with numbers of significantly and > 2-fold up- and down-regulated transcripts in comparison to wild type at each time-point (excluding outliers in (b)). ESC: ES cells, EB: embryoid body, d: day.

Overlaying my wild type d3 EB dataset with a published dataset reported for EBs generated via the hanging drop method (Tripathi et al. 2011) revealed considerable overlap, as approximately a quarter of my mis-regulated transcripts were also present in their dataset (Fig 13d). Among the 20 strongest regulated transcripts, the overlap comprised more than half of the regulated transcripts (Fig 13c and d). A full list of overlapping and exclusive significantly ($p \leq 0.05$ and $\geq$ 2-fold) regulated transcripts in my dataset and Tripathi et al. 2011 can be found in File S1 on the attached data disc.

Next, I analysed mutant samples in comparison to wild type at each time-point. The number of down- as well as up-regulated transcripts increased over time (Fig 13e). At d2, *Smad2*$^{-/-}$ and *Smad2/3*$^{-/-}$ EBs showed substantially increased numbers of mis-regulated transcripts. These differences were even more striking at d3. In agreement with their severe morphological phenotype (see section 2.4), *Smad2/3*$^{-/-}$ EBs had more mis-regulated transcripts than each of the single mutant EBs. *Smad2* mutant embryos are embryonically lethal, whereas *Smad3* mutants are viable and (consistent with this) *Smad2* but not *Smad3* mutant EBs show a phenotype (see section 2.4 and Waldrip et al. 1998, Tremblay et al. 2000, Datto et al. 1999). Thus, it was expected that *Smad3*$^{-/-}$ EBs were only affected at d3. The increased number of down-regulated transcripts in d3 *Smad3*$^{-/-}$ EBs in comparison to *Smad2*$^{-/-}$ EBs will be discussed in chapter 4.

Unbiased lists of significantly ($p \leq 0.05$) and $\geq$ 2-fold changed averaged transcript levels for all clones per genotype at each time-point can be found in File S2a on the attached data disc. File S2b contains a list of $\geq$ 2-fold changed transcripts without a significance restriction to assess fold-changes for those transcripts that varied too much among clones to achieve statistical significance. To assess individual clonal variation among the four clones profiled for each genotype, unbiased full lists of all probes assessed on the array with log2-fold changes for each individually assessed clone on heatmaps are also supplied (Files S3 and S4). These files allow unbiased assessment of relative expression changes. File S3 depicts fold changes of d0, d2 and d3 time-points of each genotype over the corresponding time-point in wild type controls and thus describes differences between mutant and wild type control samples during differentiation. File S4 depicts fold changes

of d0, d2 and d3 time-points over averaged d0 transcripts levels within each genotype and describes expression kinetics of mutant and wild type control samples during differentiation.

The absence of individual lineage marker transcripts in *Smad2/3*$^{-/-}$ EBs in the OneStep analysis (see section 2.4) prompted me to assess the expression of key lineage markers of the embryonic germ layers and extra-embryonic tissues of the early post-implantation embryo on a broader scale in mutant EBs in comparison to wild type controls. To gain mechanistic insight into Smad2/3-mediated transcriptional effects that can be related to the *Smad2/3*$^{-/-}$ phenotype *in vivo* (Dunn et al. 2004), I selected marker genes based on expression data in early post-implantation stage mouse embryos. Selected marker genes and their relative expression in comparision to wild type are shown in Fig 14.

Primitive Streak and Definitive Endoderm (PS, DE)

Strikingly, I observed down-regulation of all mesodermal and endodermal markers examined in d3 *Smad2/3*$^{-/-}$ EBs (Fig 14a, PS group). Down-regulated early mesoderm markers expressed in the primitive streak (PS) included *Wnt3a* (Liu et al. 1999) and the pan-mesodermal marker *Brachyury/T* (Wilkinson et al. 1990), expression of which depends on Wnt3a expression (Yamaguchi et al. 1999, Arnold et al. 2000), as well as the established Smad2/3 downstream effectors *Eomes* (Brennan et al. 2001) and its downstream effectors *Lhx1*, *Mesp1* and *Mixl1* (Nowotschin et al. 2013, Costello et al. 2011, Izumi et al. 2007). The PS marker *Fgf8* (Crossley and Martin, 1995), that is known to depend on Smad2 (Waldrip et al. 1998), was also down-regulated. In agreement with maintained expression or overexpression of selected mesodermal markers in *Smad2*$^{-/-}$ mutants (Waldrip et al. 1998), averaged mean expression levels of the seven PS markers shown in Figure 14a over time showed that Smad2 did not substantially contribute to the down-regulation of mesodermal markers, but rather resembled the average marker expression in wild type EBs (Fig 14b). When compared to wild type, the degree of mis-regulation was less pronounced than for *Smad2/3*$^{-/-}$ EBs and variable among the four

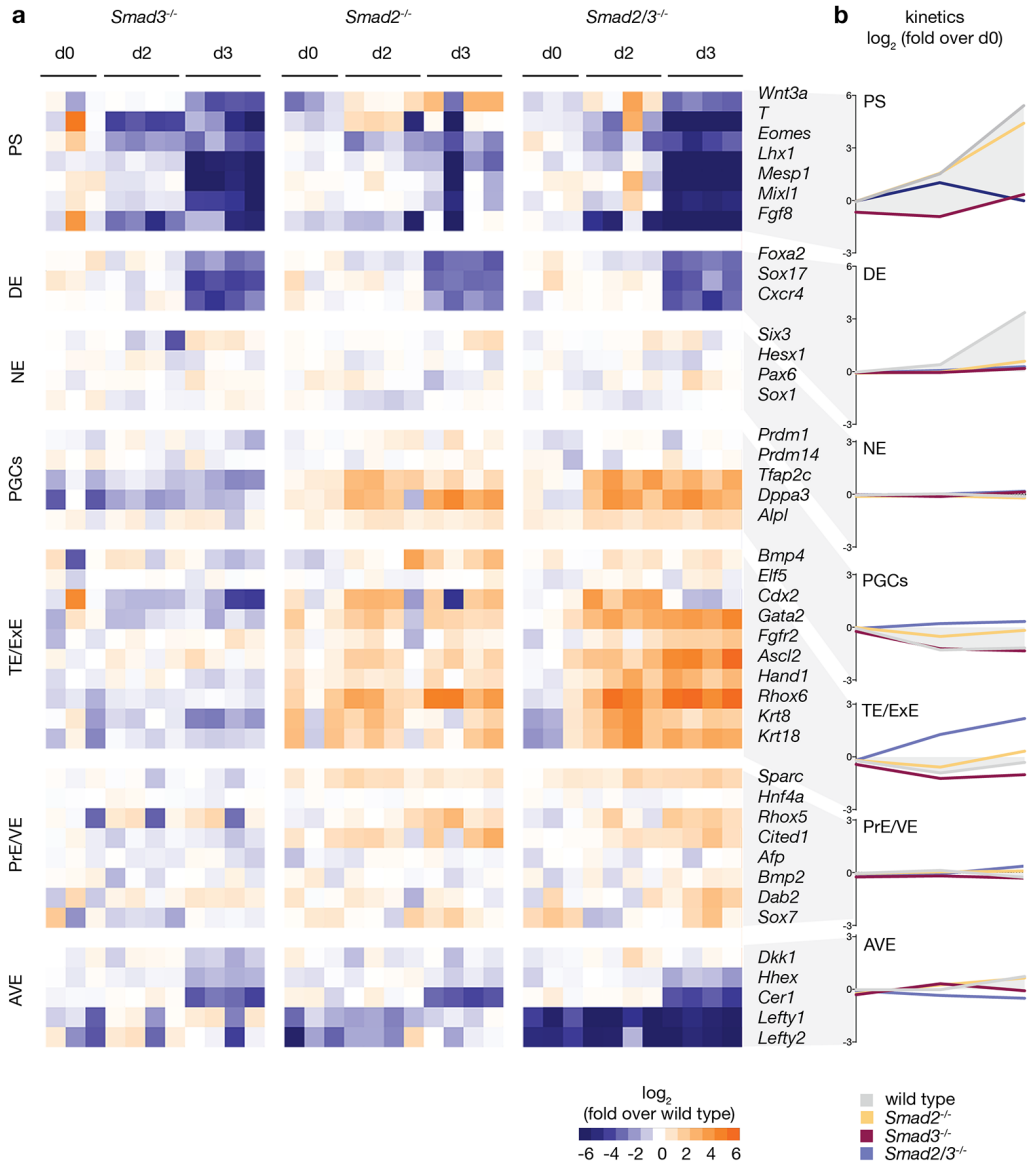


Figure 14 Expression changes of key lineage marker genes in *Smad3*$^{-/-}$, *Smad2*$^{-/-}$ and *Smad2/3*$^{-/-}$ EBs during differentiation.

(**a**) Heatmap displaying expression changes of selected key lineage marker transcripts of the embryonic and extra-embryonic lineages of the early post-implantation mouse embryo. Mutant undifferentiated ES cells (d0) and d2 and d3 EBs are compared to the average expression of wild type cells/EBs at the same time-point. Expression changes are displayed on a log2 scale. Marker gene names represent mm10 symbols. This heat map does not include information on the statistical significance of individual marker changes. (**b**) Averaged expression dynamics for the marker genes displayed in (a) for wild type and mutant samples over the three days of differentiation (assessed at d0, d2, d3). Differences of wild type expression levels to 0 are coloured in grey. Fold change was calculated in comparison to d0 samples within each genotype and is displayed on a log2 scale. See main text for details. PS: primitive streak, DE: definitive endoderm, NE: anterior markers of the neuroectoderm, PGCs: primordial germ cells, TE/ExE: trophectoderm/extra-embryonic ectoderm, PrE/VE: primitive endoderm/visceral endoderm, AVE: anterior VE.

clones and marker genes analysed (Fig 14a). In agreement with a primary requirement for Smad2 in the endodermal lineage (Tremblay et al. 2000), only *Eomes* and *Lhx1*, which are also involved in definitive endoderm specification (Costello et al. 2011, 2015), were significantly down-regulated at d3 (Fig 14a, DE group). I did, however, detect robust down-regulation of early mesodermal markers in *Smad3*$^{-/-}$ EBs (see chapter 4), although the degree of down-regulation was less pronounced than in *Smad2/3*$^{-/-}$ EBs and individual markers (e.g *T*) did not reach statistical significance due to clonal variation. The early definitive endoderm (DE) markers *Foxa2* and *Sox17* (Ang and Rossant 1994a, Kanai-Azuma et al. 2002, Blum et al. 1992) were down-regulated in all three mutants at d3 indicating an absolute requirement for combined Smad2 and Smad3 signalling in establishing the endoderm lineage (Dunn et al. 2004, 2005, Tremblay et al 2000). *Cxcr4*, which can be used as a surface marker to separate definitive from visceral endoderm *in vitro* (Yasunaga et al. 2005), was significantly down-regulated in *Smad2*$^{-/-}$ and *Smad2/3*$^{-/-}$ but not significant in *Smad3*$^{-/-}$ EBs.

Neuroectoderm and primordial germ cells (NE, PGC)

Early anterior/neuroectodermal (NE) markers such as *Six3* and *Hesx1* (Oliver et al. 1995, Thomas and Beddington 1996), *Pax6* and *Sox1* were unaffected (Fig 14a, NE group). Since the EB differentiation medium contains fetal bovine serum (see chapter 5), this differentiation protocol promotes mesodermal and endodermal cell fates (Wiles and Keller 1991). Selected neuroectodermal markers were not up-regulated during differentiation of wild type controls (Fig 14b, NE group). In agreement with an expanded cluster of Blimp1-expressing cells and multiple clusters of alkaline phosphatase^{+} cells in *Smad2* mutants (Ohinata et al. 2009, Tremblay et al. 2001), d3 *Smad2*$^{-/-}$ as well as d2 and d3 *Smad2/3*$^{-/-}$ EBs but not *Smad3*$^{-/-}$ EBs significantly up-regulated the PGC marker *Dppa3/Stella* (Sato et al. 2002) (Fig 14a, PGC group). Similarly, the PGC marker *Tfap2c/AP2γ* (Weber et al. 2010) was significantly up-regulated exclusively in d2 *Smad2*$^{-/-}$ and d2 and d3 *Smad2/3*$^{-/-}$ EBs, whereas *Alpl/Tnap* (encoding alkaline phosphatase), which is expressed in PGCs (Ginsburg et al. 1990), was only significantly up-regulated in d2 and d3 Smad2/3 EBs. *Tfap2c*, *Dpp3a* and *Alpl* are, however, also expressed in the early

TE, making a lineage distinction difficult (Winger et al. 2006, Latos et al. 2015, Sato et al. 2002, MacGregor et al. 1995). Early presumptive PGC (pPGC) markers *Prdm1* (encoding Blimp1) (Vincent et al. 2005, Ohinata et al. 2005) and *Prdm14* (Yamaji et al. 2008) were not significantly affected by loss of Smad2/3, but were also not induced in wild type EBs (Fig 14b, PGC group). At this point my analysis does thus not provide a definite answer as to whether Smad2/3 signals are required for PGC specification. Results above strongly suggest that Smad2/3 signals are crucially involved in mesoderm and endoderm differentiation with a bias of individual Smad2 and Smad3 involvement to the endodermal and mesodermal cell fate, respectively, whereas neural differentiation seemed unaffected in my experimental setup.

Trophectoderm and extra-embryonic ectoderm (TE, ExE)

I next examined a panel of established TE and early ExE markers (Fig 14a, TE/ExE group). TE and ExE cells in the mouse embryo are epithelial cells that express keratins (Ralston and Rossant 2008, Tamai et al. 2000, Marikawa and Alarcon 2012). Keratins such as *Krt8/18* were significantly up-regulated in *Smad2/3*$^{-/-}$ EBs. *Smad2*$^{-/-}$ EBs (but not *Smad3*$^{-/-}$ EBs) seemed to contribute to this effect, even though both *Krt8/18* were not significantly changed at d3 (likely due to clonal variation). The earliest known TE marker *Cdx2* (Nishioka et al. 2008) showed on average a 10-fold up-regulation in d2 of EB differentiation in *Smad2/3*$^{-/-}$ EBs but was not significant due to clonal variation. Other early extra-embryonic ectoderm markers such as *Bmp4* (Lawson et al. 1999) and *Elf5* (Latos et al. 2015) were not affected. Furthermore, *Gata2* (Ng et al. 1994), *Fgfr2* (Haffner-Krausz et al. 1999), *Ascl2* (Tanaka et al. 1999), *Hand1* (Cross et al. 1995) and *Rhox6* (also known as *Psx1*) (Chun *et al.* 1999) are all expressed in the extra-embryonic ectoderm and were significantly up-regulated in d3 *Smad2/3*$^{-/-}$ EBs.

Primitive endoderm, visceral endoderm and anterior visceral endoderm (PrE, VE, AVE)

Effects of Smad2/3 on the expression of markers of the extra-embryonic primitive and visceral endoderm (PrE/VE) lineages was milder (Fig 14a, PrE/VE group). *Smad2*$^{-/-}$ and

Smad2/3$^{-/-}$ EBs up-regulated *disabled-2* (*Dab2*), which is expressed in the PrE and VE (Morris et al. 2002, Yang et al. 2002) and acts downstream of *Gata6* (Morrisey et al. 2000). *Secreted Protein Acidic and Rich in Cysteine* (*Sparc*), which is expressed in the PrE (Holland et al. 1987) and *Cited1* (also known as *Msg1*), which is predominantly expressed in the extra-embryonic VE (Dunwoodie et al. 1998), were significantly up-regulated in d3 *Smad2/3*$^{-/-}$ EBs. Other PrE and VE markers such as *Rhox5* (also known as *Pem*, expressed in the extra-embryonic EPC, ExE and VE at E5.5 (Lin et al. 1994)), *Hepatic nuclear factor 4* (*Hnf4a*), which marks the PrE and VE (Duncan et al. 1994) and *α-fetoprotein* (*Afp*), which is expressed in the VE but not the PrE (Dziadek and Adamson 1978), were unaltered. *Sox7*, which is expressed in PrE in the blastocyst (Artus et al. 2011), was also unchanged. As for NE and PGC marker expression, up-regulation of PrE/VE markers in wild type EBs was not strong (Fig 14b, PrE/VE group). Anterior visceral endoderm (AVE) markers *Hhex*, *Cer1* and the Nodal antagonists *Lefty1* and *Lefty2,* which are crucial for restricting the site of primitive streak emergence in the mouse embryo and lost in *Smad2*$^{-/-}$ mutants (Waldrip et al. 1998) were down-regulated in d3 *Smad2/3*$^{-/-}$ EBs (Fig 14a AVE group). *Cer1* was down-regulated by d3 in both *Smad2*$^{-/-}$ and *Smad3*$^{-/-}$ EBs, whereas strong down-regulation of *Lefty1/2* was exclusive to *Smad2/3*$^{-/-}$ EBs.

Collectively, this marker gene analysis suggested that on a transcriptional level *Smad2/3*$^{-/-}$ EBs loose the ability to activate mesodermal and endodermal lineage markers and rather convert to an extra-embryonic-like state that is characterized by the up-regulation of mainly trophectodermal markers in addition to a subset of primitive and visceral endoderm-specific markers.

To investigate whether the lack or strong reduction of key lineage markers of mesoderm and endoderm lineages as well as the observed up-regulation of extra-embryonic TE/ExE markers reflected the most prominent changes upon loss of Smad2/3, I examined the top 20 mis-megulated transcripts (see Tables 5-8).

Top changes in undifferentiated ES cells (d0)

Statistically significant and ≥ 2-fold expression changes at d0 were minor. Down-regulated transcripts in *Smad2*$^{-/-}$ ES cells included ~3.8-fold down-regulation of *Bid3*, a gene involved in neuronal apoptosis (Coultas et al. 2007), a ~2.9-fold down regulation of the *Mannose receptor* (*Mrc1*), which is involved in modulating lutropin half-life upon implantation (Mi et al. 2002), and the ~2.7-fold down-regulation of the transcript encoding zinc finger protein Zfp493 with unknown function. The only significant and ≥ 2-fold up-regulated gene in *Smad2*$^{-/-}$ ES cells was *Kelch-like 15* (*Klhl15*) (2.1-fold up-regulated), which has been knoked-out *in vivo* but not yet characterized (Skarnes et al. 2011). *Smad2/3*$^{-/-}$ ES cells up-regulated the well-established Bmp signalling target *Inhibitor of differentiation 1* (*Idb1*) (also known as *Id1*) ~4.1-fold. *Idb1* has been shown to mediate Bmp signalling to prevent neural differentiation (Ying et al. 2003, Zhang et al. 2010, Malaguti et al. 2013). The lack of major significant expression changes in undifferentiated ES cells upon loss of Smad2/3 in my experimental setup will be discussed in chapter 4.

Top changes in day 2 and day 3 EBs (Tables 5-8)

On the next two pages I present the top 20 mis-regulated transcripts in the examined mutant EBs in comparison displayed as fold-change over wild type, followed by a limited description of selected targets.

Table 5 Top 20 down-regulated transcripts at d2.

Smad3$^{-/-}$		Smad2$^{-/-}$		Smad2/3$^{-/-}$	
Gene	**Fold Change**	**Gene**	**Fold Change**	**Gene**	**Fold Change**
Il18	-2.5	*Fgf5*	-12.7	*Lefty2*	-101.0
		Wt1	-5.5	*Lefty1*	-28.3
		Bcl11a	-4.6	*Fgf5*	-21.8
		Cbln4	-4.1	*Pitx2*	-17.6
		Mmp25	-3.9	*Fgf15*	-7.5
		Fam19a4	-3.8	*Nrcam*	-7.4
		Crct1	-3.7	*Slc27a2*	-6.4
		Mfap3l	-3.6	*Mmp25*	-6.3
		Slc27a2	-3.6	*Fam19a4*	-5.9
		Stk39	-3.6	*Utrn*	-5.6
		Fgf15	-3.3	*Cbln4*	-5.2
		Etv1	-3.0	*Grm6*	-5.0
		B130052F17Rik	-2.8	*Gsc*	-4.6
		Cyp2j13	-2.6	*Stk39*	-4.4
		Lin28b	-2.5	*Etv1*	-4.1
		Bcl11a	-2.5	*Ntrk2*	-4.1
		Pcdh17	-2.5	*Wt1*	-4.0
		B930076A02	-2.5	*Mfap4*	-4.0
		Amer1	-2.3	*Tmem63a*	-3.8
		Acsl4	-2.1	*Bcl11a*	-3.8

p ≤ 0.05, ≥ 2-fold over wild type at same time-point, *mm10* gene symbols

Table 6 Top 20 down-regulated transcripts at d3.

Smad3$^{-/-}$		*Smad2$^{-/-}$*		*Smad2/3$^{-/-}$*	
Gene	**Fold Change**	**Gene**	**Fold Change**	**Gene**	**Fold Change**
Lhx1	-53.2	*Fgf5*	-15.9	*Lhx1*	-219.9
Smad3	-37.9	*Gsc*	-10.0	*T*	-163.2
Mesp1	-37.5	*Lhx1*	-8.7	*Fgf8*	-137.7
Gata6	-26.1	*Cer1*	-8.5	*Fst*	-117.5
Agtrl1	-21.5	*Foxa2*	-7.9	*Mixl1*	-78.5
Klhl6	-19.3	*Adamts9*	-7.6	*Gsc*	-75.9
Mixl1	-19.0	*Sox17*	-5.2	*Fgf5*	-74.4
Sp5	-15.8	*Eomes*	-4.9	*Mesp1*	-48.9
Defcr-rs2	-15.4	*Bcl11a*	-4.9	*Lefty1*	-47.5
Defcr-rs7	-14.6	*1700007G11Rik*	-4.7	*Eomes*	-38.7
Cyp26a1	-14.3	*Chrd*	-4.4	*Sp5*	-36.9
Fgf10	-13.1	*Cbln1*	-3.8	*Lefty2*	-36.7
Pdgfra	-12.7	*Nrcam*	-3.8	*Agtrl1*	-30.2
C230098O21Rik	-12.3	*Otx2*	-3.7	*Klhl6*	-23.4
Gsc	-10.7	*Sema6d*	-3.6	*Cyp26a1*	-22.6
Foxq1	-10.5	*Cxcr4*	-3.5	*Rspo3*	-19.5
Adamts9	-10.0	*Tgfbr3*	-3.5	*Pitx2*	-19.1
Sox17	-9.8	*G2-pending*	-3.5	*Vrtn*	-18.3
Hs3st3b1	-9.8	*Prdm8*	-3.3	*Evx1*	-17.3
End2	-9.1	*Cxxc4*	-3.0	*Defcr-rs2*	-16.5

p ≤ 0.05, ≥ 2-fold over wild type at same time-point, *mm10* gene symbols

Table 7 Top 20 up-regulated transcripts at d2.

Smad3$^{-/-}$		*Smad2* $^{-/-}$		*Smad2/3*$^{-/-}$	
Gene	**Fold Change**	**Gene**	**Fold Change**	**Gene**	**Fold Change**
End2	4.7	*Tbx3*	9.3	*Cops8*	20.4
		6030495B01Rik	8.8	*Tcfap2a*	19.8
		Hs3st3b1	8.2	*H19*	17.6
		Wnt6	8.1	*Psx1*	16.2
		Tcfap2c	8.0	*Hs3st3b1*	15.5
		Ahnak	7.2	*Calcoco2*	15.1
		Gjb3	7.1	*Plac1*	14.8
		Anxa2	7.1	*Tbx3*	14.4
		Calcoco2	5.6	*6030495B01Rik*	13.8
		LOC380875	5.0	*Tcfap2c*	13.2
		4933402E13Rik	4.9	*Msx2*	12.8
		Mme	4.8	*Psx2*	12.6
		Elf3	4.6	*Sct*	11.8
		Stard8	4.1	*Gata3*	11.7
		Gadd45b	3.7	*Igf2*	11.4
		Cldn4	3.7	*Gjb3*	9.4
		Klf5	3.6	*Wnt6*	9.2
		Fabp3	3.5	*Gata2*	8.8
		Pdgfa	3.4	*LOC380875*	8.6
		Kirrel	3.4	*Dppa3*	8.6

p ≤ 0.05, ≥ 2-fold over wild type at same time-point, *mm10* gene symbols

Table 8 Top 20 up-regulated transcripts at d3.

Smad3$^{-/-}$		*Smad2*$^{-/-}$		*Smad2/3*$^{-/-}$	
Gene	**Fold Change**	**Gene**	**Fold Change**	**Gene**	**Fold Change**
Utf1	6.6	*Psx2*	21.7	*Plac1*	65.7
2610528J11Rik	4.8	*Psx1*	19.0	*Psx1*	56.6
LOC234741	4.8	*H19*	17.9	*Psx2*	47.8
Miat	4.7	*Dppa3*	14.3	*H19*	45.6
Pla2g10	4.0	*Krt1-14*	13.2	*Ascl2*	27.0
Gm691	3.9	*Lgals3*	12.9	*Pparg*	24.5
Pipox	3.9	*Calcoco2*	10.4	*Wnt7b*	23.1
Chrna1	3.8	*Esrrb*	9.6	*Nxf7*	21.3
Dtna	3.7	*Wnt7b*	9.4	*Cldn4*	20.0
Sox2	3.6	*Cldn4*	9.0	*Calcoco2*	20.0
Gdf3	3.6	*Cpsf4l*	8.8	*Pdgfb*	20.0
Uchl1	3.5	*Nr5a2*	7.6	*Vgll3*	18.6
Elavl3	3.5	*Sct*	7.2	*Gadd45g*	18.1
Syt4	3.4	*Klf2*	7.1	*Gata2*	16.9
1700019D03Rik	3.4	*Folr1*	7.1	*Wnt4*	16.6
Snca	3.4	*Edn1*	6.9	*Cops8*	16.2
Trim2	3.4	*Mylpf*	6.9	*Dlx3*	16.0
2900011O08Rik	3.3	*Cxcl16*	6.8	*Gjb3*	15.1
Stat4	3.3	*LOC245128*	6.7	*LOC385493*	14.8
Ntrk2	3.3	*2210409E12Rik*	6.7	*Pramef12*	14.4

p ≤ 0.05, ≥ 2-fold over wild type at same time-point, *mm10* gene symbols

a. Down-regulated transcripts (Tables 5 and 6)

Strikingly, early PS markers *Lhx1*, *T*, *Fgf8* and *Mixl1* were among the top five down-regulated transcript in d3 *Smad2/3*$^{-/-}$ EBs and changed more than 70-fold (Table 6). Interestingly, inhibitors of TGFβ signalling also belonged to the top affected transcripts. *Follistatin* (*Fst*), an inhibitor of both Bmp and Activin signalling that can directly bind Activin (Nakamura et al. 1990, Amthor et al. 2002, Fainsod et al. 1997) as well as the Nodal inhibitors *Lefty1* and *Lefty2* (Chen et al. 2004, formerly also known as *Ebaf* and *Leftb*, respectively) were all down-regulated >30-fold. The well-established Nodal downstream targets *Gsc*, *Eomes*, *Mesp1* and *Pitx2* (Brennan et al. 2001, Costello et al. 2011, Shiratori et al. 2001) also ranked high. In addition, early markers of differentiation including the primitive streak marker *Sp5* (Harrison et al. 2000, Treichel 2001), the primitive ectoderm marker *Fgf5* (Hébert et al. 1991) and *Cyp26a1,* which is expressed in the anterior headfold and required for patterning of the hindbrain, vertebrae and tailbud (Sakai et al. 2001), were down-regulated. The endothelial marker *Klhl6* (Kroll et al. 2005) as well as the Foxa2-dependent *Defa-rs2* transcript, that is expressed in the posterior epiblast and node (Tamplin et al. 2011), were also strongly down-regulated. I also saw a strong Smad/3-dependence of transcripts of the Apelin receptor *Agtrl1*/*Aplnr* normally expressed in the PS and involved in cardiac development *in vivo* and *in vitro* (Kang et al. 2013, D'Aniello et al. 2009, 2013). The zebrafish ortholog of the Apelin receptor has been shown to enhance Nodal signalling in cardiogenesis (Deshwar et al. 2016) and to be activated by the novel Nodal-dependent factor Toddler to mediate gastrulation movements (Pauli et al. 2014). The next top down-regulated transcript *Evx1* is expressed in the posterior streak from E6.5 onwards and was shown to promote expression of posterior transcripts related to cardiac differentiation (Dush and Martin 1992, Bell et al. 2016). Interestingly, *Evx1* expression in EBs is more strongly induced upon BMP4 or Wnt3a stimulation than with Activin A and its absence promoted expression of anterior markers such as *Cer1* and *Sox17* (Bell et al. 2016). Another connection of Smad2/3 signalling to the Wnt signalling pathway is seen by a ~20-fold down-regulation of *R-Spondin 3* (*Rspo3*, also known as *Thsd2*). *Rspo3* is expressed in the posterior streak and allantois and involved in vascular development in the embryo and placenta (Aoki et al. 2007, Kazanskaya et al. 2008). *Vtrn*, which was also among the top 20 down-regulated

transcripts, has not yet been characterized in the mouse embryo. At d2, top down-regulated transcripts already included *Lefty1* and *Lefty2, Fgf5, Fgf15* and *Pitx2*, *Gsc* and *Etv1* (among others).

Most prominent, down-regulated transcripts in *Smad2*$^{-/-}$ EBs included endodermal markers such as *Gsc*, *Lhx1, Foxa2, Sox17, Eomes* and *Cxcr4*. The primed pluripotency marker *Fgf5* was the top down-regulated target gene and *Otx2*, which is also expressed in the primed state, was also among the top 20 down-regulated transcripts at d3 (Buecker et al. 2014). Half of the top 20 down-regulated in *Smad2*$^{-/-}$ EBs (including, amongst others *Fgf5* and *Fgf15*) were also among the top 20 down-regulated transcripts in *Smad2/3*$^{-/-}$ EBs suggesting a strong contribution of Smad2 to Smad2/3 signalling. Top down-regulated transcripts in *Smad3*$^{-/-}$ EBs at d3 indicated that Smad3 contributes to mesoderm and endoderm specification. *Lhx1*, *Mesp1*, *Mixl1*, *Sp5* as well as *Gsc* and *Sox17* were among the top down regulated transcripts and all more than ~10-fold less induced than in wild type controls. Primed markers were not affected by the loss of *Smad3*.

b. Up-regulated transcripts (Tables 7 and 8)

Top up-regulated transcripts in d3 *Smad2/3*$^{-/-}$ EBs confirmed the diversion to an extra-embryonic-like fate that the marker analysis in Fig 14 had suggested (Table 8). The top hit *Placental specific protein 1* (*Plac1*) is a paternally imprinted X-linked gene expressed in the trophoblast lineage and loss of function leads to an expansion of the spongiotrophoblast layer resulting in placentomegaly (Jackman et al. 2012). *Ascl2* (also known as *Mash2*) was also up-regulated. *Ascl2* is also an imprinted gene expressed from the maternal allele in the ectoplacental cone (Guillemot et al. 1995, Tanaka et al. 1999) and required to establish the spongiotrophoblast layer of the placenta (Rossant et al. 1998, Tanaka et al. 1997). The next top up-regulated transcript *Peroxisome proliferator activated receptor gamma* (*Pparg*) is again required for spongiotrophoblast and labyrinth development (Barak et al. 1999, Parast et al. 2009). *Wnt7b* (> 20-fold increased) is also expressed in the chorion and null mutants show placental defects (Kemp et al. 2007, Parr et al. 2001). The *Nuclear RNA export factor 7* (*Nxf7*), a candidate TS cell marker (Kuales et al. 2015), is strongly up-

regulated in d3 *Smad2/3*$^{-/-}$ EBs. *Claudin 4* (*Cldn4*) is expressed in the extra-embryonic ectoderm and has been suggested to be required in tight junctions in TE cells during blastocyst expansion (Tamplin et al. 2008, Moriwaki et al. 2007). The *Calcium binding and coiled-coil domain 2* (*Calcoco 2*, also known as *Ndp52*) was also up-regulated. *Ndp52* was identified as an Oct4-related gene and shows enrichment in human *in vitro* differentiated trophoblast cells (Bortvin et al. 2003, Marchand et al. 2011). *Platelet derived growth factor B* (*Pdgfb*) regulates labyrinth layer development (Ohlsson et al. 1999) and is also up-regulated. *Vestigial like family member 3* (*Vgll3*) was reported to be up-regulated upon *Gata3* overexpression in a *Cdx2*-dependent fashion in TS cells (Ralston et al 2010). *Gata2* is expressed in TGCs (Ng et al. 1994), while *Wnt4* is expressed in the decidual stroma (Nelson et al. 2016). Loss of the *COP9 signalosome subunit 8* (*Cops8*) leads to early embryonic lethality and arrest during ICM outgrowth, but mutants have not been further characterized (Menon et al. 2007). Loss of *Distal-less homeobox 3* (*Dlx3*) leads to failure to specify the labyrinth layer of the placenta and is expressed in the chorion and EPC (Morasso et al. 1999). *Gap junction protein, beta 3* (*Gjb3,* also known as *Connexin 31*) is expressed in glycogen cells of the placenta and required for placenta development (Zheng-Fischhofer et al. 2007). Collectively, all top 20 up-regulated transcripts (except for those that have not been characterized in respect to early embryonic development) are expressed and have functions in trophoblast development, strongly suggesting that *Smad2/3*$^{-/-}$ d3 EBs divert to a trophoblast-like fate.

Overall changes in *Smad2*$^{-/-}$ EBs were less pronounced compared to *Smad2/3*$^{-/-}$ EBs, but a contribution of Smad2 to the diversion to the expression of extra-embryonic markers was observed as *Smad2*$^{-/-}$ EBs up-regulated TE markers including *Tcfap2c/AP2γ* and *Growth arrest and DNA-damage-inducible 45 beta* (*Gadd45b*), which is expressed in the chorion (Kaufmann et al. 2011) as well *Klf5*, which acts downstream of *Fgf4* and upstream of *Cdx2*, *Eomes* and *Krt8* in the TE (Lin et al. 2010) (Table 7). Top up-regulated transcripts in d2 *Smad2/3*$^{-/-}$ EBs included almost exclusively transcripts characteristic for the extra-embryonic trophectoderm. The closely related *Placenta-specific homeobox 1* and *2* genes (*Psx1* and *Psx2*, also known as *Rhox6* and *Rhox9*) were also strongly up-regulated. They are expressed in giant cells and the labyrinth layer of the developing placenta (Chun *et al.*

1999, Han et al. 2000, Kent et al. 2010). *Psx1*$^{-/-}$ mice are viable (Takasaki et al. 2001). *H19* was also upregulated. *H19* is an imprinted lincRNA gene expressed from the maternal allele in the pre-blastocyst stage during mouse development and in the TE (Doherty et al. 2000). *H19* can drive tropoblast lineage commitment in ES cells (Fujimori et al. 2013). *H19* is linked to the expression of the reciprocally imprinted *Insulin-like growth factor 2* (*Igf2*) transcript (Zemel et al. 1992). *Ifg2* is also ~7-fold up-regulated in d3 *Smad2/3*$^{-/-}$ EBs (see supplementary File S2a). *Smad2*$^{-/-}$ EBs furthermore exhibited strong up-regulation of the naïve pluripotency markers including *Tbx3* on d2 and *Dppa3*, *Esrrb*, *Nr5a2* and *Klf2* on d3 (Tables 6 and 8). By contrast, up-regulated transcripts in *Smad3*$^{-/-}$ d3 EBs were minor and did not indicate contribution to extra-embryonic transcript expression observed in *Smad2/3*$^{-/-}$ EBs (Table 8).

Taken together, analysis of the top 20 up- and down-regulated transcripts for each genotype suggested that mesoderm and endoderm marker transcription is severely compromised in *Smad2/3*$^{-/-}$ EBs, as marker transcripts of these lineages showed the most prominent changes upon loss of Smad2/3. Furthermore, the diversion to an extra-embryonic-like fate is the most prominent feature of *Smad2/3*$^{-/-}$ ES, as top up-regulated transcripts almost exclusively comprised trophectoderm-associated transcripts. Smad2 seems to primarily contribute to endodermal cell fate specification and could be involved in lineage priming as primed pluripotency markers were strongly down-regulated. Smad3, in contrast, does not strongly influence primed pluripotency or trophectodermal marker gene expression, but promotes mesodermal and endodermal cell fate, even though the observed effect upon loss of Smad3 were less dramatic than for combined loss of *Smad2/3*.

GO term analysis

GO term analysis of all significantly and ≥2 fold up- or down-regulated transcripts in all genotypes at d3 confirmed the suggested diversion of *Smad2/3*$^{-/-}$ EBs to an extra-embryonic-like fate. GO terms for d3 *Smad2/3*$^{-/-}$ up-regulated transcripts included 'placenta development', and 'epithelium formation' among others, whereas GO

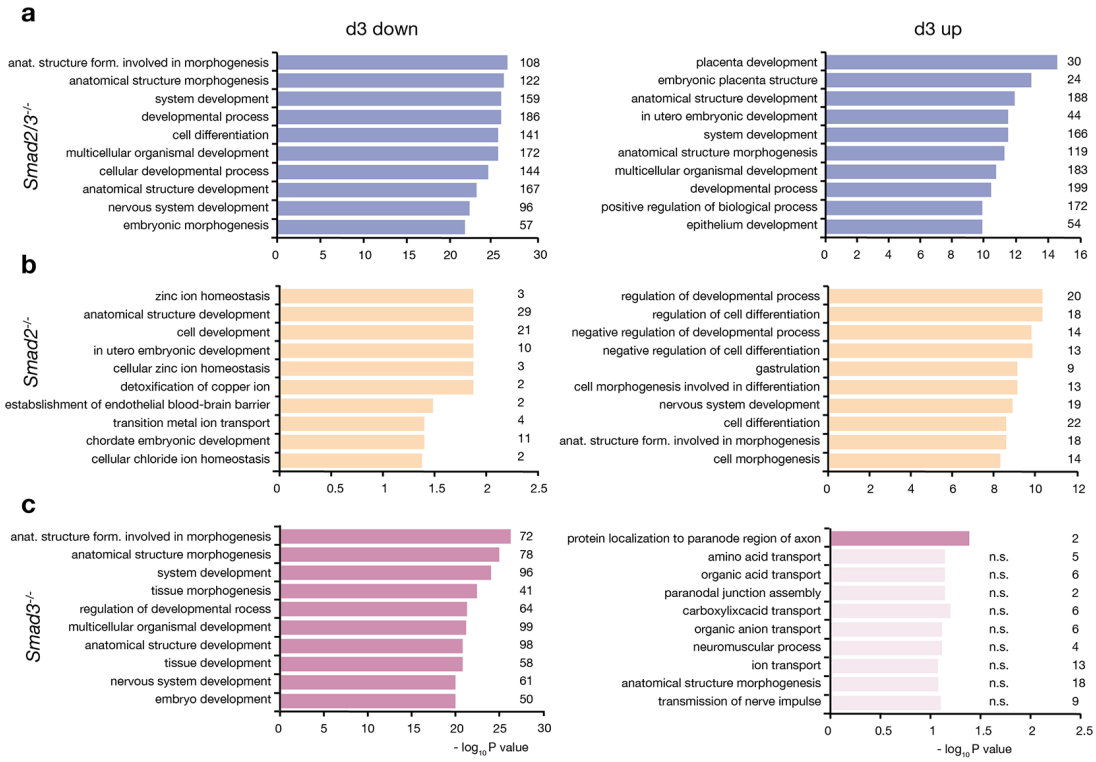


Figure 15 Biological function GO term analysis of d3 mis-regulated transcripts for *Smad2/3*$^{-/-}$, *Smad2*$^{-/-}$ and *Smad3*$^{-/-}$ EBs.

Gene ontology term analysis of deregulated transcripts in (**a**) *Smad2/3*$^{-/-}$, (**b**) *Smad2*$^{-/-}$ and (**c**) *Smad3*$^{-/-}$ d3 EBs ($p \leq 0.05$, $\leq \geq 2$-fold over wild type as mm10 gene symbols of probes) using (http://bioinfo.vanderbilt.edu/ webgestalt/). Numbers of transcripts in each category are indicated next to significance bars. Log10 scale of significance ($P<0.05$). n.s.: not significant.

terms for down-regulated transcripts included 'embryonic morphogenesis', 'cell differentiation' and 'developmental process' (Fig 15a). A full list of the genes categorized for each term can be found in File S5 on the attached data disc. *Smad2*$^{-/-}$ d3 EBs exhibited lesser significance for GO terms likely due to the smaller number of changed transcripts. GO terms for up-regulated transcripts did not include those directly associated with placenta development but showed enrichment for genes associated with 'cell differentiation', 'cell morphogenesis' and 'gastrulation' in agreement with the observed induction of exclusively posterior primitive streak derivatives in Smad2 mutant embryos (Fig 15b). GO terms resulting from analysis of down-regulated transcripts revealed only small numbers of genes and included 'cell development', 'anatomical structure development', 'in utero embryonic development' and 'chordate embryonic development', whereas the majority of other GO terms included only < 4 genes and were thus not considered as meaningful (Fig 15b).

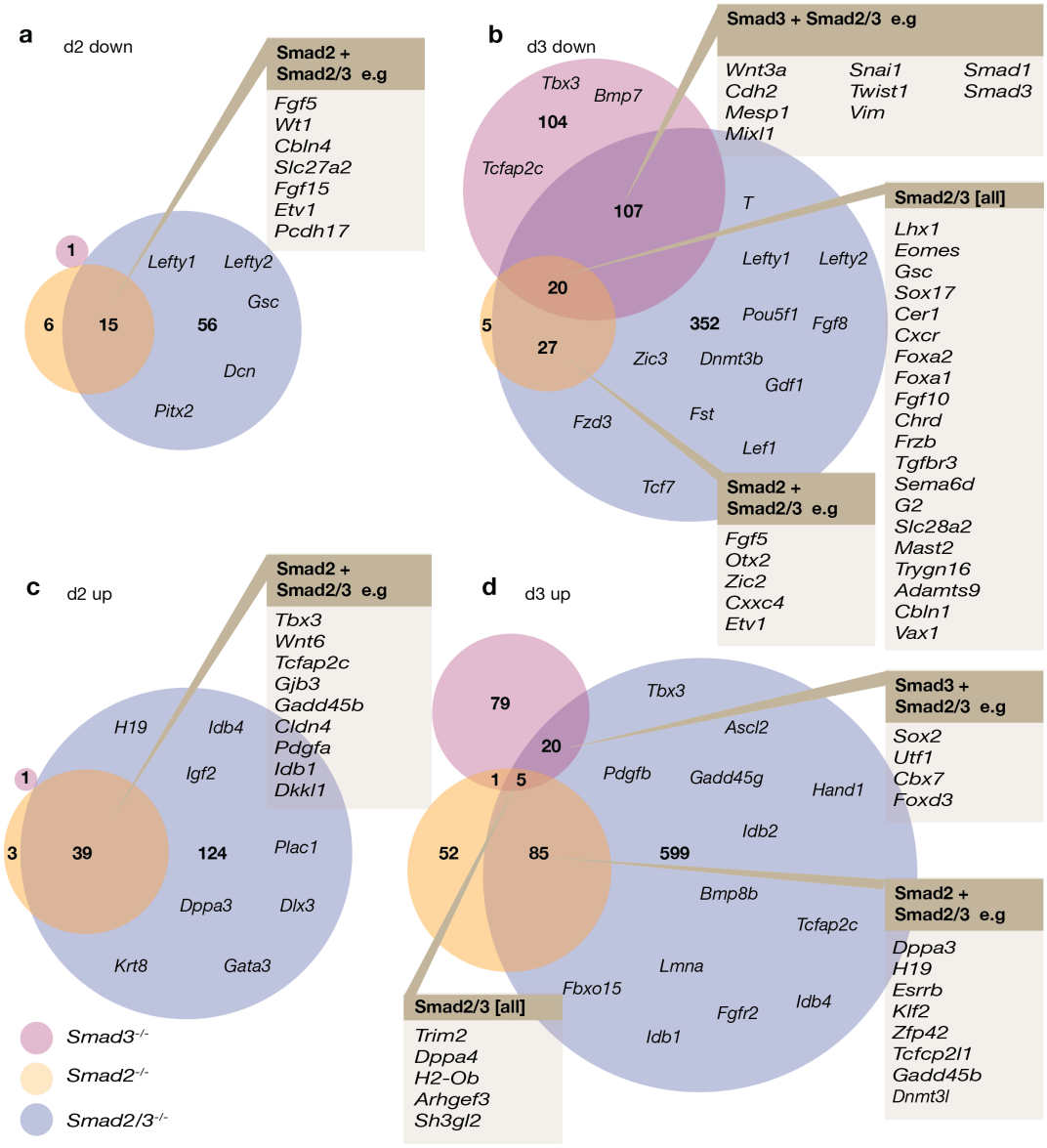


Figure 16 Venn diagrams of overlapping mis-regulated transcripts at d2 and d3 in *Smad2/3*$^{-/-}$, *Smad2*$^{-/-}$ *and Smad3*$^{-/-}$ EBs.

Venn diagrams of mis-regulated transcripts in *Smad2/3*$^{-/-}$, *Smad2*$^{-/-}$ *and Smad3*$^{-/-}$ d2 and d3 EBs ($P \leq 0.05$, $\leq \geq 2$-fold over wild type as mm10 gene symbols of probes). Example transcripts are shown. For a full list of overlapping transcripts see Table S6 on the attached data disc. Down-regulated transcripts at d2 and d3 are shown in (**a**) and (**b**), respectively, whereas up-regulated transcripts at d2 and d3 are shown in (**c**) and (**d**), respectively.

For *Smad3*$^{-/-}$ d3 EBs, no significant GO term with more than two genes was identified for up-regulated transcripts (Fig 15c). Down-regulated transcripts, however, were associated with top 10 biological GO terms related to embryonic development and included 'tissue morphogenesis' and 'embryo development' among others.

Comparison of Smad2, Smad3 and combined Smad2/3 target genes

A core set of 20 down-regulated transcripts was shared in *Smad2*$^{-/-}$, *Smad3*$^{-/-}$ and *Smad2/3*$^{-/-}$ d3 EBs (Fig 16). Core Smad2/3-dependent transcripts included endodermal markers including *Gsc*, *Sox17*, *Foxa2* as well as the established Nodal target genes *Eomes* and *Lhx1*. Commonly up-regulated transcripts included *Dppa4*, *Trim2* (*tripartite motif-containing 2*), *H2-Ob* (*histocompatibility 2, O region beta locus*), *Arhgef3* (*Rho guanine nucleotide exchange factor 3*) and *Sh3gl2* (*SH3-domain Grb2-like 2*). These genes have not been studied in early embryos. *Dppa4* is expressed in ES cells but not required for ES cell maintenance (Bortvin et al. 2003, Mandan et al. 2009). *Trim2* is expressed in the developing brain at E9.5, (Gray et al. 2004) but expression has not been examined in early development. Similar to *Smad2/3*$^{-/-}$ embryos *in vivo* which show a more dramatic phenotype than *Smad2*$^{-/-}$ and *Smad3*$^{-/-}$ embryos (Dunn et al. 2004), *Smad2/3*$^{-/-}$ d2 and d3 EBs exhibited a large number of exclusive mis-regulated transcripts. These included up-regulated extra-embryonic markers at d2 and d3 as well as selected naïve pluripotency markers. By contrast, exclusive down-regulated transcripts at d2 and d3 included the Nodal antagonists *Lefty1/2* as well as *Gdf1*, and the Wnt effectors *Lef1*, *Tcf7* and the Wnt target *T*. All but three up-regulated transcripts in *Smad2*$^{-/-}$ d2 EBs were also up-regulated in the *Smad2/3*$^{-/-}$ d2 EBs and the majority of down-regulated transcripts were also overlapping (Fig 16a and c). The majority of mis-regulated transcripts in *Smad2*$^{-/-}$ overlapped with mis-regulated transcripts in *Smad2/3*$^{-/-}$ EBs. These included a subset of up-regulated naïve pluripotency markers such as *Dppa3*, *Esrrb*, *Klf2*, *Zfp21/Rex1* and *Tcfcp2l1* as well as *Idb1*. Common down-regulated transcripts included primed pluripotency markers *Fgf5*, *Otx2* and *Zic2* as well as the endodermal marker *Cxxc4*. D3 *Smad3*$^{-/-}$ EBs only share 20 commonly up-regulated transcripts with d3 *Smad2/3*$^{-/-}$ EBs including the pluripotency marker *Sox2*. Common down-regulated transcripts at d3 for *Smad3*$^{-/-}$ and *Smad2/3*$^{-/-}$ EBs included markers that are normally expressed in mesodermal cells at gastrulation such as *Wnt3a*, *Smad1*, *Mesp1* and *Mixl1*. Commonly up-regulated markers also included EMT-associated transcripts *Snai1*, *Vim* and *Twist1* (Fig 16b, d). However, *Smad3*$^{-/-}$ and S*mad2*$^{-/-}$ exhibited several mutually exclusive differences at d3. For S*mad2*$^{-/-}$ these included *Fzd7*

(down) and *Klf5* (up). For S*mad3*$^{-/-}$ *Tcfap2c/AP2γ* (down) and *Gdf3* (up) are selectively changed.

I next wanted to analyse to what extent loss of Smad2/3 affects gene expression of the most up-regulated transcripts during EB differentiation. I therefore assessed expression dynamics of the top 20 up-regulated transcripts in d3 wild type EBs ('wild type differentiation genes', see also Table 3 in Fig 13c) and compared them to their expression in *Smad2/3*$^{-/-}$ ES cells, d2 and d3 EBs. This analysis demonstrated that 80% (16/20) of the top 20 wild type differentiation genes were significantly down-regulated in d3 *Smad2/3*$^{-/-}$ EBs (Fig 17a). Interestingly, several of these differentiation genes including *T*, *Fgf8*, *Fgf5*, *Mixl1*, *Fst*, *Wnt8a*, *Sp5* and *Rspo3* were weakly induced at d2 but even weaker or lost at d3. To extend this analysis, I overlapped all significantly up- and down-regulated transcripts in d3 wild types with significantly down-regulated transcripts in d3 *Smad2/3*$^{-/-}$ EBs. On a global scale about a quarter of both up-regulated (~27.2%) and down-regulated differentiation transcripts (~20.9%) were inversely regulated in d3 *Smad2/3*$^{-/-}$ EBs (Fig 17b). Smad2/3-independent gene expression changes included modest up- regulation of neural markers such as *Sox9* and *Nes* as well as down-regulation of *Bmp4*, *Fgf4* and *Klf4* transcripts.

2.6 *Smad2/3*$^{-/-}$ ES cells compromise the initiation of lineage priming in EpiLCs

ES cells grown in serum+LIF (core pluripotency) differ from ES cells grown in 2i+LIF (naïve pluripotency) as assessed by their transcriptional signature and tendency to differentiate (Marks et al. 2012, Kolodziejczyk et al. 2015). Naïve ES cells grown in 2i+LIF can be differentiated into a transient primed state of pluripotency in epiblast-like cells (EpiLCs) after culture in bFGF and Activin A-containing medium for two days (Hayashi et al. 2011). The inability of *Smad2/3*$^{-/-}$ EBs to initiate differentiation into embryonic lineages in my EB differentiation could potentially be caused by defects during

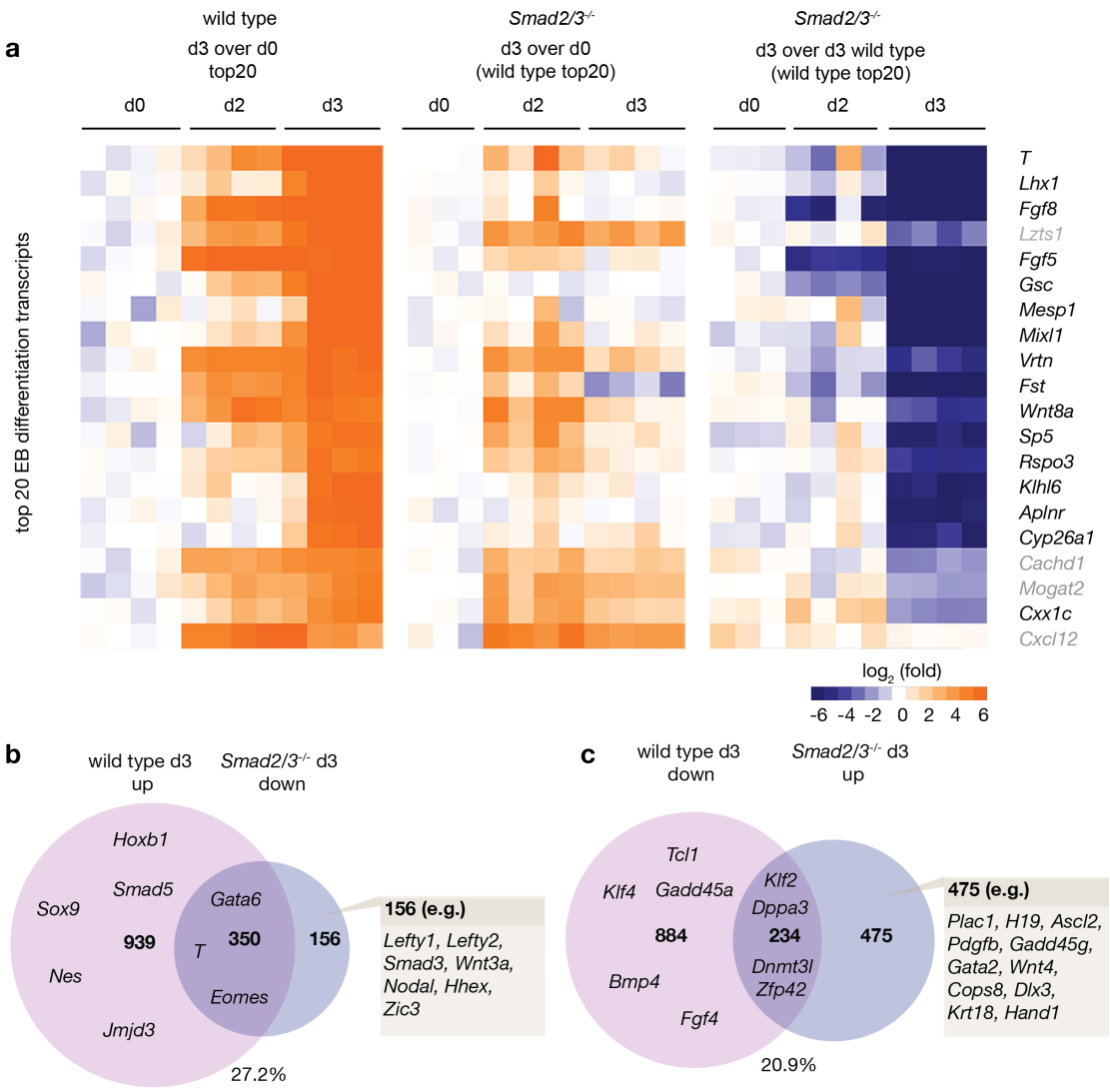


Figure 17 More than a fifth of all EB differentiation-associated transcripts regulated in wild type d3 EBs are antagonistically regulated in d3 Smad2/3$^{-/-}$ EBs.

(**a**) Top 20 differentiation genes in d3 wild type EBs and their expression dynamics in d3 *Smad2/3*$^{-/-}$ EBs compared to undifferentiated (middle panel) and d3 wild type EBs. All transcripts except those in grey were statistically significantly and >2 fold down-regulated in *Smad2/3*$^{-/-}$ EBs compared to wild type d3. (**b**) Venn diagrams of wild type d3 mis-regulated transcripts with inversely regulated transcripts in d3 *Smad2/3*$^{-/-}$EBs ($p \leq 0.05$, $\leq \geq 2$-fold over d0 and wild type, respectively, mm10 gene symbols of probes). For a full list of overlapping transcripts see File S7 on the attached data disc.

the transition from the undifferentiated state to lineage priming. I first assessed expression of pluripotency markers in my EB dataset. I distinguished between naïve, core and primed markers of pluripotency that I derived from published profiling studies of ESCs and EpiLC and their counterparts *in vivo* (i.e ICM cells and early post-implantation

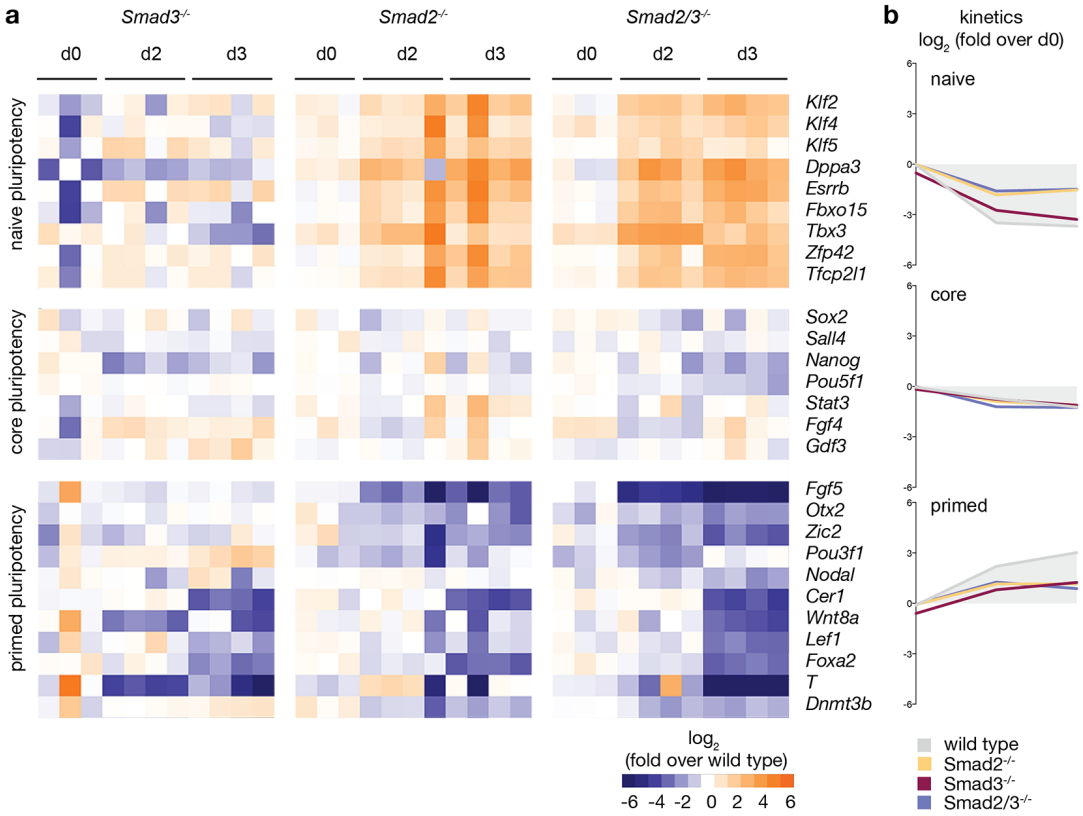


Figure 18 Expression changes of naïve, core and primed pluripotency marker transcripts in *Smad3*$^{-/-}$, *Smad2*$^{-/-}$ and *Smad2/3*$^{-/-}$ EBs during differentiation.

(**a**) Heatmap displaying expression changes of selected pluripotency marker transcripts of the naïve, core and primed pluripotency states in naïve and undifferentiated ES cells and EpiLCs *in vitro*. Mutant undifferentiated ES cells (d0) and d2 and d3 EBs are compared to the average expression of wild type cells/EBs at the same time-point. Expression changes are displayed on a log2 scale. Marker gene names represent mm10 symbols. This heat map does not include information on the statistical significance of individual marker changes. (**b**) Averaged expression dynamics for the marker genes displayed in (a) for wild type and mutant samples over the three days of differentiation (assessed at d0, d2, d3). Wild type expression levels are underlined in grey. Fold change was calculated in comparison to d0 samples within each genotype and is displayed on a log2 scale. See main text for details.

epiblasts) (Boroviak et al. 2014, 2015, Buecker et al. 2014, Kojima et al. 2014). In agreement with a lack of diversion to an extra-embryonic-like fate, *Smad3*$^{-/-}$ EBs did not significantly differ from wild type EBs in the down-regulation of naïve and core pluripotency markers (Fig 18). Up-regulation of primed markers was, to some extent, affected, albeit only markers that also mark early definitive endoderm (*Cer1*, *Foxa2*) were statistically significant in comparison to wild type. *Smad2*$^{-/-}$ and *Smad2/3*$^{-/-}$ EBs, in contrast, up- regulated naïve (but not core) pluripotency markers, whereas primed markers were down-regulated.

At d3, the majority of naïve markers (all but *Klf4* and *Klf5* for *Smad2/3*$^{-/-}$ EBs and all but *Klf4*, *Fbxo15* and *Tbx3* for *Smad2*$^{-/-}$ EBs) and primed markers (all for *Smad2/3*$^{-/-}$ EBs and *Fgf5*, *Otx2*, *Zic2*, *Cer1*, *Foxa2* for *Smad2*$^{-/-}$ EBs) reached statistical significance (see supplementary File S2 on the attached data disc). Kinetics of naïve marker expression revealed that *Smad2/3*$^{-/-}$ and *Smad2*$^{-/-}$ EBs down-regulated the majority of naïve markers during differentiation (except for *Dppa3* and *Tbx3* and, for *Smad2/3*$^{-/-}$ EBs, also *Klf2*), suggesting that the exit from the undifferentiated state does occur. Core pluripotency markers were similarly down-regulated or maintained as in wild type or *Smad3*$^{-/-}$ EBs. Primed markers (including *Fgf5*, *Wnt8a*, *T*, *Dnmt3b*) were induced in d2 *Smad2/3*$^{-/-}$ EBs, but dropped to levels similar to undifferentiated cells at d3. *Smad2*$^{-/-}$ EBs up-regulated primed markers similar to *Smad2/3*$^{-/-}$ EBs (albeit slightly stronger for *Fgf5*, *Wnt8a* and *T*) but these did not change further at d3.

Since d2 and d3 EBs represent mixed populations of differentiating rather than lineage primed cells, I next exploited a protocol that directs naïve ES cells (2i+LIF) to a transient primed EpiLC state by a 2-day induction via recombinant Activin A and bFGF which induces morphological and transcriptional changes of cells (Hayashi et al. 2011, Buecker et al. 2014) (Fig 19a). EpiLCs express a unique signature of primed markers including *Fgf5* and *Fgf15*, *Wnt3*, *Dnmt3b*, *Dnmt3l*, *Otx2*, while they down-regulate naïve pluripotency-associated markers including *Klf2*, *Klf4*, *Essrb*, *Zfp42/Rex1*, *Tbx3* (Hayashi et al. 2011, Buecker et al. 2014). While *Oct4* transcript levels remain unchanged in comparison to ES cells, *Sox2* and *Nanog* transcript and protein levels decrease upon EpiLC differentiation (Hayashi et al. 2011). Since primed markers were most affected in *Smad2/3*$^{-/-}$ EBs and I was particularly interested in the mechanism underlying the observed block in embryonic differentiation in these cells, I restricted this analysis to *Smad2/3*$^{-/-}$ and wild type control ES cells. *Smad2/3*$^{-/-}$ EpiLCs grown in 2i exhibited the characteristic flattening of cells that wild type cells undergo during EpiLC differentiation (Fig 19b).

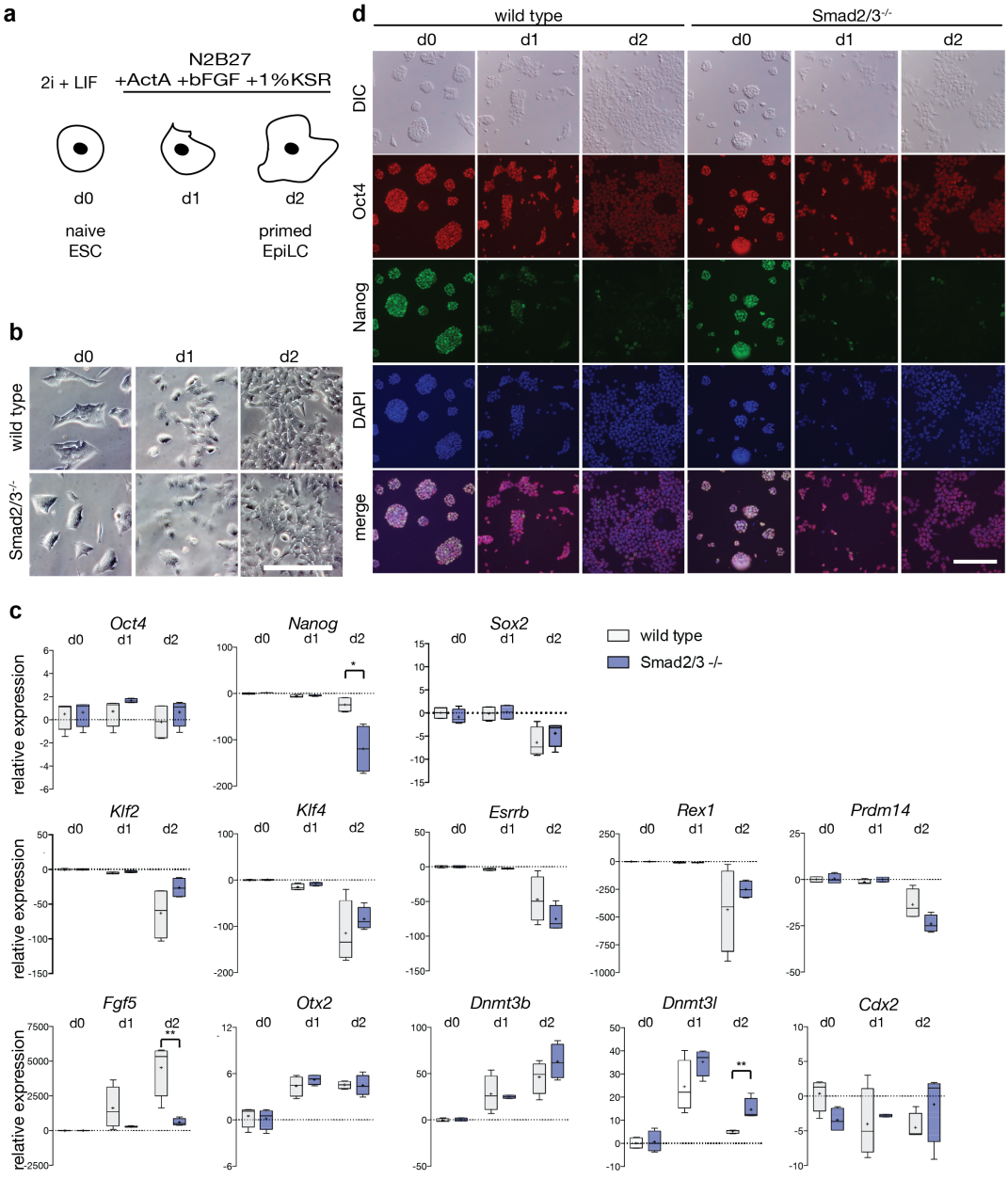


Figure 19 EpiLC differentiation of *Smad2/3*$^{-/-}$ ES cells.

(**a**) Schematic of EpiLC differentiation. (**b**) Morphology of *Smad2/3*$^{-/-}$ ES cells in 2i+LIF and cells grown in EpiLC medium for one and two days. (**c**) qRT-PCR marker gene analysis of d0 2i + LIF ES cells and d1 and d2 EpiLCs. Box plots show median (line) and mean (+) and 25th to 75th percentile distribution of gene expression (normalized to *Hprt*) relative to averaged expression in wild type ES cells (d0) (fold change). Four biological replicates (cell lines) were averaged for each genotype. Whiskers represent the smallest and largest values. Each individual biological replicate was run in technical duplicate. Unpaired t-tests were used to assess statistical significance (*P<0.05, **P<0.01, ***P<0.001). (**d**) Immunofluorescence staining of d2 *Smad2/3*$^{-/-}$ and wild type EpiLCs with antibodies specific to Oct4 and Nanog.

I confirmed this phenotype in four independent clones (data not shown). qRT-PCR for selected marker genes on four clones for *Smad2/3*$^{-/-}$ and wild type ES cells grown in

2i+LIF or in EpiLC differentiation medium for one and two days showed, however, significant changes in *Smad2/3*$^{-/-}$ EpiLCs compared to wild types (Fig 19c). The primed pluripotency marker *Fgf5* was significantly down-regulated compared to wild type controls, whereas the DNA methyltransferase *Dnmt3l* was up-regulated. Furthermore, *Smad2/3*$^{-/-}$ EpiLCs showed a more pronounced decrease in *Nanog* than in wild type control cells. *Otx2*, which plays important roles in EpiLC differentiation (Buecker et al. 2014), was, however, not significantly affected in *Smad2/3*$^{-/-}$ EpiLCs. Apart from *Nanog* down-regulation, core pluripotency markers did not significantly change (*Sox2*, *Oct4*). Naïve pluripotency markers (*Klf2, Klf4, Esrrb, Rex1, Prdm14*) were not significantly changed. The extra-embryonic marker *Cdx2* that was up-regulated in *Smad2/3*$^{-/-}$ EBs (see section 2.5) did not change significantly, suggesting that *Smad2/3*$^{-/-}$ EpiLCs do not undergo a diversion to an extra-embryonic-like fate. I failed to detect differences in Nanog proteins levels by immunofluorescence of *Smad2/3*$^{-/-}$ EpiLCs co-stained with Oct4 (Fig 19d). Future experiments will aim to extent the analysis of *Smad2/3*$^{-/-}$ EpiLCs to clarify the role of Smad2/3 in lineage priming.

2.7 Conclusion of project I

Taken together, the experiments presented here elucidate important aspects of cooperative Smad2/3-mediated TGFβ signalling during the transition of mouse embryonic stem cells from pluripotency to differentiation and contribute to answering the questions set out in the aims of the thesis.

1. Does combined loss of Smad2/3 function in ES cells have an impact on cell viability, self-renewal and pluripotency marker expression?

The generation of *Smad2/3*$^{-/-}$ ES cells and their initial characterization exclude an essential role for Smad2/3-mediated TGFβ signalling in ES cell viability, self-renewal and pluripotency marker expression in 2i+LIF and serum+LIF feeder-free culture and thereby refine our understanding of the role of TGFβ signalling in ES cells. Future

experiments will address whether Smad2/3-mediated signalling affects cell proliferation and levels of Nodal and Bmp signalling on the protein level. Furthermore, it will be interesting to assess whether *Smad2/3*$^{-/-}$ ES cells display the chromatin architecture typical for wild type ES cells (see below).

2. Can Smad2/3$^{-/-}$ *ES cells initiate cell fate specification during differentiation in embryoid bodies?*

I show here that *Smad2/3*$^{-/-}$ ES cells lack the ability to up-regulate selected markers of embryonic cell lineages during embryoid body differentiation and are unable to promote embryoid body growth and signalling to sustain further development. I show that loss of Smad2/3 does not lead to loss of *Oct4* expression within four days from the onset of differentiation.

3. How does loss of Smad2, Smad3 or the combined loss of Smad2/3 function affect gene expression profiles during differentiation?

Transcriptional profiling revealed that *Smad2/3*$^{-/-}$ EBs do not induce endodermal and mesodermal fates that are induced in wild type controls. Furthermore, combined loss of Smad2/3 leads to down-regulation of almost a quarter of all differentiation-associated transcripts in day 3 EBs and the concomitant expression of abundant extra-embryonic markers that are normally not induced. This suggests that *Smad2/3*$^{-/-}$ EBs have an early block in differentiation. Interestingly, loss of Smad2 and Smad3 alone only partially recapitulates these transcriptional changes. My analysis thereby refines the gene expression changes underlying the dose-dependent roles of Smad2/3 signalling *in vivo*. Clonal variation in my experiments necessitates further experiments to validate top targets of transcriptional profiling experiments by qPCR and on the protein level. Furthermore, it will be crucial to assess directed differentiation protocols into neural and germ cell fates and to validate differentiation potential in chimeras to clarify whether any embryonic cell fates can be correctly specified in the absence of Smad2/3.

4. Can *Smad2/3*$^{-/-}$ ES cells initiate lineage priming in EpiLCs?

Limited analysis of *Smad2/3*$^{-/-}$ EpiLCs suggests that lineage priming is affected upon loss of Smad2/3 as a subset of primed pluripotency markers is mis-regulated. Whereas *Fgf5* was substantially down-regulated in *Smad2/3*$^{-/-}$ EpiLCs compared to controls and *Nanog* levels seemed to decrease more drastically, expression of the methyltransferase *Dnmt3l* was up-regulated. As the primed state is characterized by re-arrangements of the chromatin landscape (Buecker et al. 2014, Factor et al. 2014), it will be interesting to assess in further experiments whether *Smad2/3*$^{-/-}$ ES cells can undergo chromatin changes accompanying the transition to a primed pluripotency state.

In conclusion, I have established an experimental system that allows the genetic dissection of roles of Smad2/3-mediated TGFβ signalling in ES-cell based *in vitro* models for differentiation and lineage priming. To date, my results have only provided a limited characterization of cooperative Smad2/3 functions. Much remains to be learned about their mechanistic roles *in vitro* and during development *in vivo* (see chapter 4).

3

The role of visceral endoderm- and epiblast-derived Smad signals in inducing the primordial germ cell marker Blimp1

3.1 Preface

In the mouse embryo, precursors of primordial germ cells (pPGCs) can first be identified by the expression of Blimp1 (encoded by the *Prdm1* gene) concomitant with the onset of gastrulation (Ohinata et al. 2005, Vincent et al. 2005). Blimp1 is, however, not required for initial pPGC formation and the direct upstream signal responsible for the inset of Blimp1 expression in pPGCs is unknown. The *Prdm1* locus contains a putative T-box regulated enhancer that has been shown to be bound by Brachyury (T) and Nanog in PGC like cells (PGCLCs) to reinforce but not initiate Blimp1 expression (Ohinata et al. 2005, Vincent et al. 2005, Aramaki et al. 2013, Murakami et al. 2016).

Blimp1$^+$ pPGCs form in response to Bmp4 signals from the extra-embryonic ectoderm and Wnt3A signals from the epiblast, both of which depend on Nodal signalling for their continuous expression (Lawson et al. 1999, Ohinata et al. 2009, Ben-Haim et al. 2006). Despite well-established roles of Nodal signalling in axis patterning and cell fate specification in the post-implantation embryo (reviewed in Robertson 2014), its role in germ cell specification is not understood. It is unknown whether downstream effectors such as the T-box factor Eomes (Brennan et al. 2001, Arnold et al. 2008) are required to induce Blimp1. Reduction or loss of PGCs upon loss of Bmp-dependent *Smad1*, *Smad5* and *Smad4* expression together with the expansion of the Blimp1$^+$ PGC cluster upon loss of Smad2 suggests antagonistic roles of Bmp and Nodal signalling in Blimp1 induction (Tremblay et al. 2001, Hayashi et al. 2002b, Chang et al. 1999, Chu et al. 2004, Waldrip et al. 1998, Ohinata et al. 2009). Tissue-specific roles of Bmp and Nodal-dependent Smads in the VE and epiblast have, however, not been genetically studied with respect to induction of Blimp1$^+$ pPGCs.

In this chapter, I set out to clarify the tissue-specific requirements of downstream TGFβ pathway components in defining the competence of epiblast cells for pPGC induction. This was accomplished by screening conditional mutant embryos lacking either *Eomes*, *Smad2*, *Smad4*, *Smad1* or *Prdm1* function in the VE or the epiblast. Null and conditional alleles for all genes except for *Smad1* were available at the start of these experiments. In section 3.2, I describe the preparations for my screen. I first derived animals carrying null

and conditional alleles for *Smad1* from an available targeted ES cell line. Subsequently, I bred mouse strains to conditionally ablate the candidate genes in the VE and epiblast using *Ttr.Cre* (Kwon and Hadjantonakis 2009) and *Sox2.Cre* (Hayashi et al. 2002a) deleter transgenes. I then validated a protocol for immunohistochemical staining for Blimp1 in PGCs at E7.5.

Using these mouse lines in combination with Blimp1 immunohistochemistry, I show in section 3.3 that Eomes in the epiblast is dispensable for initial Blimp1 induction in the epiblast but is required to restrict the number of Blimp1$^+$ cells. *Eomes* expression from the VE is also non-essential for induction of Blimp1$^+$ cells. In section 3.4 I demonstrate that VE-specific ablation of Smad2 phenocopies the expansion of Blimp1$^+$ cells in global Smad2 mutants. Sections 3.5 and 3.6 show that in contrast to Smad2-dependent Nodal signalling, Bmp signalling via Smad1 and Smad4 in the VE seems not to affect induction of Blimp1$^+$ epiblast cells. However, both effectors are required in the epiblast to faithfully induce Blimp1 in the posterior epiblast. Finally, I show that Blimp1 expression in the VE is dispensable for PGC formation and embryonic development (section 3.7). My analysis also suggests that expression of Blimp1 in the VE – in contrast to its expression in the epiblast – is not regulated by TGFβ signalling.

Collectively, my results exclude Eomes as an essential transcription factor required for Blimp1 induction in pPGCs. They thereby strengthen the VE-specific requirement of Smad2 and Eomes-mediated Nodal signalling in the VE to restrict Blimp1 expression to the posterior epiblast. By contrast, VE-derived Smad4 and Smad1 signals are dispensable for Blimp1 induction in the epiblast. Finally, I established a resource of mouse strains, mutant Blimp1 reporter ES cell lines and methods (section 3.8) that allow the continuation of this project to characterize further the role of TGFβ signals in establishing competence to form pPGCs, discussed in chapter 4.

3.2. Preparation for the screen

3.2.1 Derivation of Smad1$^{+/-}$ and Smad1$^{CA/CA}$ mouse strains from the Smad1^{RobPC} allele

Our lab had previously established a modified *Smad1* allele (*Smad1*^{RobPC}) from which a conditional (*Smad1*^{RobCA}, here referred to as *Smad1*^{CA}) and a null allele (*Smad1*^{RobCN}, here referred to as *Smad1*$^{-}$) can be generated (Tremblay et al. 2001). In the *Smad1*^{RobPC} allele, the first coding exon of *Smad1* encoding most of the MH1 domain required for DNA binding is flanked by lox P sites (Fig 20a). ES cells harbouring the *Smad1*^{RobPC} allele in the heterozygous state were available from the Robertson lab frozen archive.

I derived heterozygous ES cells harbouring one *Smad1*^{CA} or *Smad1*$^{-}$ allele from the *Smad1*^{RobPC} allele using Cre-mediated recombination (see Fig 20a). Screening by Southern blotting and PCR identified both alleles (see Fig 20b-d). I confirmed the respective alleles by sequencing (data not shown). We injected excised clones into blastocysts to produce chimeras. Germ line chimeric mice were bred to generate mice harbouring the *Smad1*^{CA} or *Smad1*$^{-}$ allele. I confirmed mutant alleles by PCR genotyping of ear notches (data not shown). Heterozygous *Smad1*$^{CA/+}$ mice were intercrossed to obtain a homozygous *Smad1*$^{CA/CA}$ stock, whereas *Smad1*$^{-/+}$ mice were maintained as heterozygous stock due to embryonic lethality of homozygotes (Tremblay et al. 2001). For strain maintenance, I genotyped litters by PCR and maintained heterozygotes (see chapter 5). Both strains were expanded to obtain pools of female *Smad1*$^{CA/CA}$ mice and heterozygous male studs harbouring the *Smad1*$^{-}$ allele.

3.2.2 Breeding of mouse lines to allow the conditional ablation of Eomes, Smad2, Smad1, Smad4 and Prdm1 in the visceral endoderm and epiblast

I first obtained double-heterozygous male mice by breeding heterozygous mice harbouring null alleles of *Smad1* (Tremblay et al 2001, see section 3.2.1), *Smad2* (Waldrip et al. 1998), *Smad4* (Chu et al. 2004), *Eomes* (Arnold et al 2008) and *Prdm1* (Vincent et al.

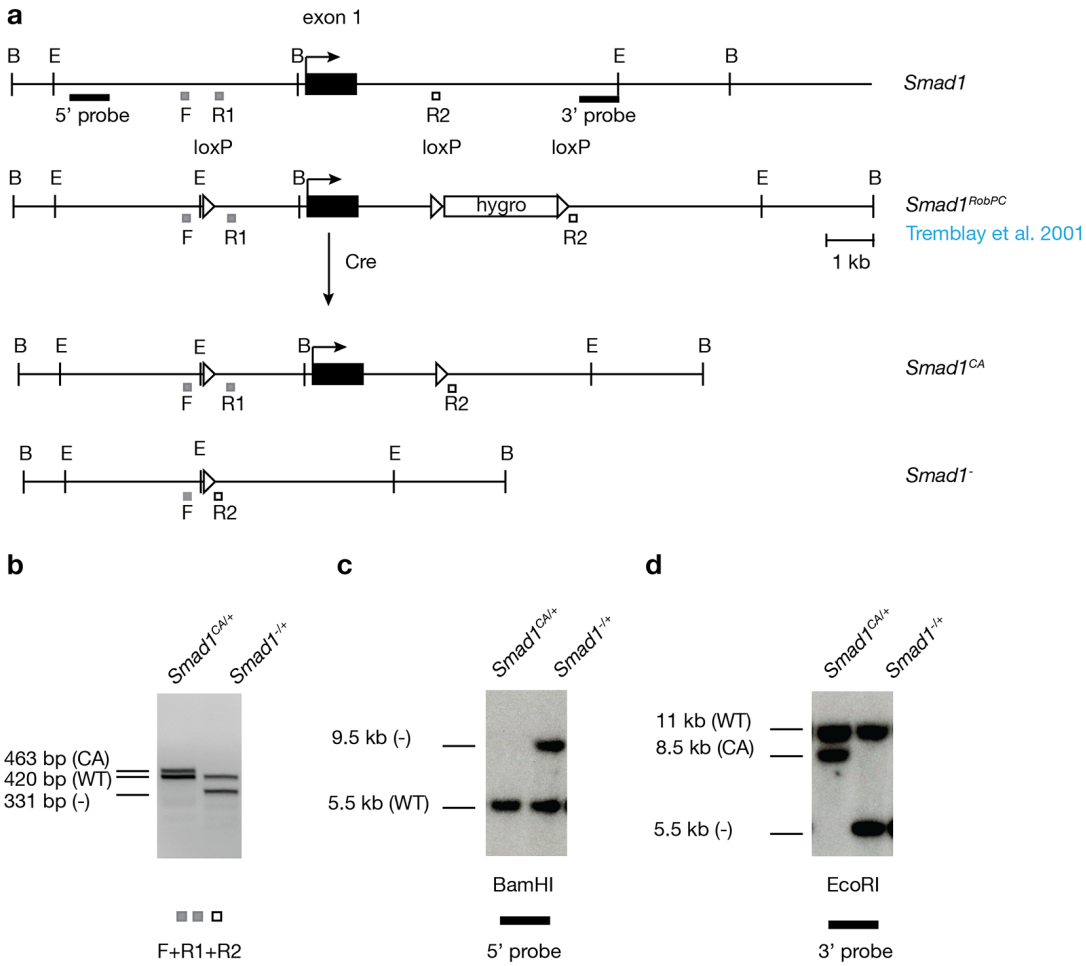


Figure 20 Generation of the null *Smad1*$^{-}$ and conditional *Smad1*^{CA} allele from the modified *Smad1*^{RobPC} allele.

(**a**) Cre-mediated excision of the *Smad1*^{RobPC} allele (Tremblay et al. 2001) in ES cells leads to loss of the lox P-flanked first coding exon, thereby generating the *Smad1*$^{-}$ null allele or excision of the hygromycin (hygro) selection cassette generating the *Smad1*^{CA} conditional allele. A third recombination outcome generates the null allele with the hygromycin cassette (not used in this study, therefore not shown). (**b-d**) PCR and Southern blot of heterozygous ES cell subclones harbouring the *Smad1*$^{-}$ or *Smad1*^{CA} allele. Primers F, R1 and R2 were used for PCRs in (b). 5' and 3' probes indicated in (a) were used on BamHI (B) or EcoRI (E)-digested genomic DNA for Southern blotting in (c and d). Identical PCR genotyping primers as in (b) were used to confirm and maintain mouse strains derived from these alleles (see chapter 5). CA: *Smad1*^{CA} allele, WT: wild type allele, -: *Smad1*$^{-}$ allele derived from the modified *Smad1*^{RobPC} allele.

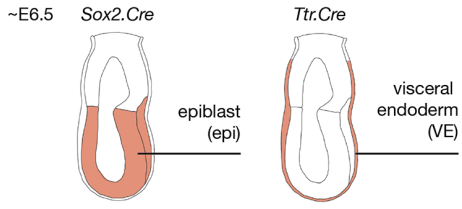
2005) with mice harbouring the VE-specific *Ttr.Cre* (Kwon and Hadjantonakis 2009) or epiblast-specific *Sox2.Cre* (Hayashi et al. 2002a) transgenes. Both Cre transgenes are expressed prior to the onset of Blimp1 induction at ~E6.25. *Sox2.Cre* is activated at the

blastocyst stage and exclusively expressed in the epiblast derivatives[1], whereas *Ttr.Cre* mediates complete deletion throughout the VE by E5.5 (Hayashi et al. 2002a, Kwon and Hadjantonakis 2009). Table 9 summarizes the male deleter studs and conditional female mice that were used for experiments. Subsets of studs were bred to mice harbouring the fluorescent Blimp1 reporter transgene *Prdm1.Venus* that expresses membrane-targeted Venus, a brighter variant of yellow fluorescent protein, under the control of *Prdm1* (encoding Blimp1) regulatory elements (Ohinata et al. 2008). This allowed obtaining triple heterozygous strains to facilitate whole-mount Blimp1 expression analysis (see chapter 4). I also collected double-heterozygous male studs harbouring just the null allele and the *Prdm1.Venus* transgene to derive Blimp1 reporter ES cell lines on a variety of mutant backgrounds. For this purpose, I also included the *Smad5* (Chang et al. 1999) and *Wnt3* (Liu et al. 1999) null alleles (see section 3.8.2).

To obtain embryos conditionally lacking individual factors in the VE or the epiblast, I set up timed matings of double heterozygous male studs with homozygous females harbouring conditional alleles for *Eomes* (Arnold et al. 2008), *Smad2* (Vincent et al. 2003a), *Smad1* (Tremblay et al 2000), *Smad4* (Chu et al. 2004) and *Prdm1* (Shapiro-Shelef et al. 2003). Mendelian inheritance predicts that 25% of embryos will harbour the null allele and the respective Cre deleter transgene, thereby producing a null from the maternally inherited conditional allele (see Table 9). I refer to this genetic configuration as either VE or epiblast-specific mutants throughout this thesis, abbreviated as *ΔVE* and *Δepi,* respectively. For obtaining VE or epiblast-specific mutant embryos that also harbour the *Prdm1.Venus* reporter, the predicted percentage of mutants drops to 12.5%.

[1] Since *Sox2* is also expressed in oocytes in females (Vincent et al. 2003b, Pan and Schultz 2011)I transmitted the transgene from the paternal side to obtain the desired conditional deletion instead of a complete deletion.

Table 9 Mouse lines used for conditional deletions.



Hayashi et al. 2002a ♂1	Kwon and Hadjantonakis 2009 ♂2	♀	desired embryo from cross ♂1 x ♀ or ♂2 x ♀ [25% off offspring]	References
Double-heterozygotes*	**Double-heterozygotes***	**Conditional allele**		
Eomes$^{+/-}$*; Sox2.Cre*$^{+/-}$	*Eomes*$^{+/-}$*; Ttr.Cre*$^{+/-}$	*Eomes*$^{CA/CA}$	*EomesΔepi (1)* *EomesΔVE (2)*	Arnold et al. 2008
Smad2$^{+/-}$*; Sox2.Cre*$^{+/-}$	*Smad2*$^{+/-}$*; Ttr.Cre*$^{+/-}$	*Smad2*$^{CA/CA}$	*Smad2Δepi (1)* *Smad2ΔVE (2)*	Waldrip et al. 1998 Vincent et al. 2003a
Smad1$^{+/-}$*; Sox2.Cre*$^{+/-}$	*Smad1*$^{+/-}$*; Ttr.Cre*$^{+/-}$	*Smad1*$^{CA/CA}$	*Smad1Δepi (1)* *Smad1ΔVE (2)*	Tremblay et al. 2001
Smad4$^{+/-}$*; Sox2.Cre*$^{+/-}$	*Smad4*$^{+/-}$*; Ttr.Cre*$^{+/-}$	*Smad4*$^{CA/CA}$	*Smad4Δepi (1)* *Smad4ΔVE (2)*	Chu et al. 2004
Prdm1$^{+/-}$*; Sox2.Cre*$^{+/-}$	*Prdm1*$^{+/-}$*; Ttr.Cre*$^{+/-}$	*Prdm1*$^{CA/CA}$	*Prdm1Δepi (1)* *Prdm1ΔVE (2)*	Vincent et al 2005 Shapiro-Shelef et al. 2003

* Subsets of each class of males were further bred to produce triple-heterozygotes harbouring the *Prdm1.Venus* reporter transgene (Ohinata et al. 2008), Abbreviations (*EomesΔepi*) refer to offspring with the genetic conformation *Eomes*$^{CA/-}$*; Sox2.Cre*$^{+/-}$.

3.2.3 Blimp1 immunohistochemistry validates Blimp1 expression in primordial germ cells of wild type mouse embryos at E7.5

To assess induction of the earliest known pPGC marker Blimp1 in post-implantation mouse embryos, I decided to perform immunohistochemical staining with a Blimp1-specfic antibody. Blimp1^{+} pPGCs first arise at ~E6.25 (Ohinata et al 2005). By E7.25-E7.5, a cluster of ~40 PGCs is evident at the base of the developing allantois (Ginsburg et al. 1990) and thus would allow faithful assessment of whether Blimp1 induction had occurred in the different mutant contexts (see section 3.2.2). I therefore focussed the staining on the E7.5 developmental stage. First, it was necessary to validate expression of Blimp1 in PGCs of wild type embryos. Previous work in our lab had established protocols for Blimp1 nuclear staining by immunohistochemistry on paraffin sections in multiple cell types and tissues. These include diploid trophoblast and trophoblast giant cells of the ectoplacental cone at E7.5. They will form the spongiotrophoblast layer of the placenta, as well as a subset of maternal decidual stroma cells, and enterocytes of the developing villus epithelium of the E16.5 intestine (Mould et al. 2012, 2015). To take advantage of Blimp1 expression in the maternal decidual tissue as a positive control and

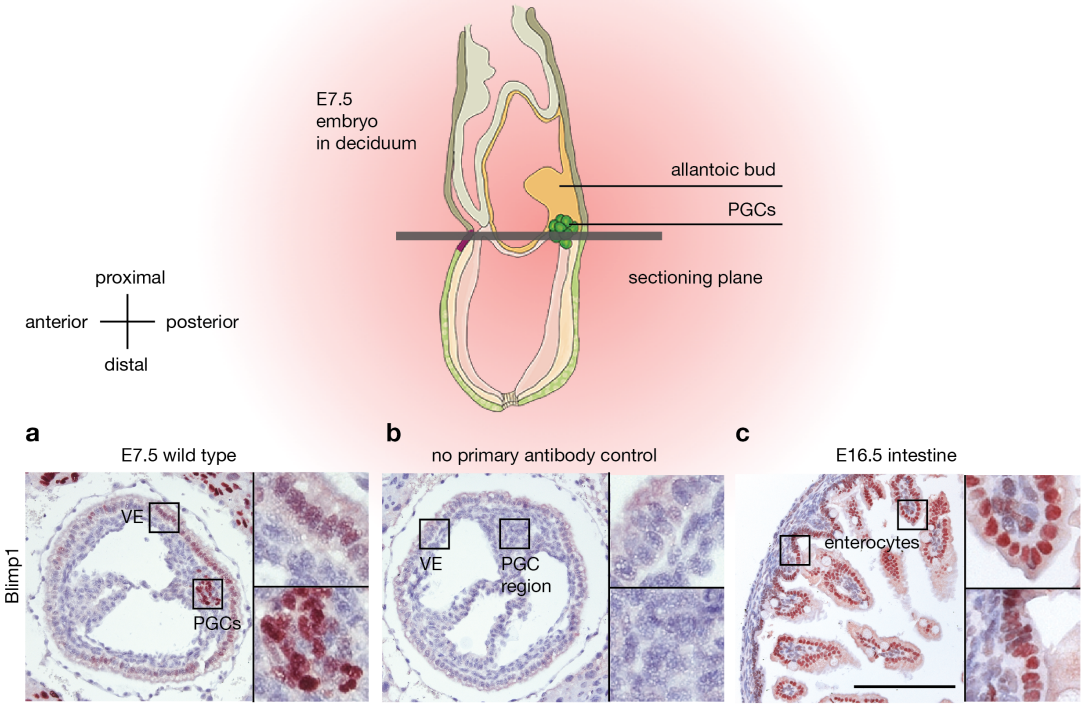


Figure 21 Blimp1 immunohistochemistry on sections of E7.5 mouse embryos validates expression in primordial germ cells and the visceral endoderm.

(**a**) Blimp1 immunohistochemistry on transverse sections through paraffin-embedded E7.5 mouse embryos within the maternal deciduum. Red staining marks primordial germ cells at the base of the allantoic bud. Blimp1 is also expressed in the visceral endoderm surrounding the epiblast. Strong expression of Blimp1 in cells within the maternal deciduum serves as a positive control. (**b**) Section processed as in (a) without the primary antibody (negative control). (**c**) Blimp1 immunohistochemistry on E16.5 intestinal epithelium (positive control, Mould et al. 2015). Scale bar: 200 µm, boxed areas are shown magnified to the right. E: embryonic day, VE: visceral endoderm, PGCs: primordial germ cells. For a comprehensive estimation of sectioning planes through embryos at ~E7.5, see Pereira et al. 2011.

to avoid damage of embryos, I embedded E7.5 embryos within the deciduum and sectioned embryos transversely through the developing allantoic bud (Fig 21). Blimp1 immunohistochemistry validated nuclear staining in PGCs of E7.5 embryos (Fig 21a, Vincent et al. 2005; Ohinata et al. 2005). Blimp1 expression in VE cells as well as strong expression in a subset of decidual cells was also observed. A control with no primary antibody proved specificity of the staining for Blimp1 (Fig 21b). Parallel staining of transverse sections through E16.5 intestine specifically stained Blimp1$^+$ enterocytes in the villus epithelium (Fig 21c, Mould et al. 2015).

3.3 Eomes signals in the epiblast and the VE are dispensable for Blimp1 induction but required to restrict Blimp expression to the posterior epiblast

A recent report (Aramaki et al. 2013) showed binding of the mesodermal T-Box factor *Brachyury/T* to a T-box site 10 kb upstream of the *Prdm1* transcriptional start site. *Brachyury/T* is not essential for initial Blimp1 induction but is required for strong up-regulation of Blimp1 in PGCs at later stages. The authors speculated about possible involvement of Eomes binding to this T-box site for initial pPGCs induction (or alternative T-box factors expressed at E6.0-E6.25) (Aramaki et al. 2013). Intriguingly, overexpression of Eomes in BMP4-treated *Wnt3*$^{-/-}$ PGCLCs (which are devoid of *Prdm1* expression) induced *Prdm1.Venus* (Aramaki et al. 2013).

Previous studies showed that the epiblast expresses *Eomes* prior to and independently of *Brachyury/T* many hours before the onset of overt PS formation (Arnold et al. 2008, and Simon et al. 2017). Furthermore, Eomes epiblast-mutants accumulate epiblast cells in the developing streak that fail to undergo EMT, but continue to express T (Arnold et al. 2008). Single-cell transcriptional profiling suggested that PGCs do not undergo EMT, as EMT-associated transcripts were down-regulated when compared to somatic cells (Kurimoto et al. 2008). *Eomes* expression in the VE is required for AVE specification (Nowotschin et al. 2013). The AVE has been implicated in restricting the pPGC fate, as AVE expansion (e.g. in *Bmp8b* mutants) reduces Blimp1 induction, whereas failure to specify the AVE (e.g. in *Smad2* mutants) expands the cluster of Blimp1^{+} cells (Ohinata et al. 2009). These combined data prompted me to assess the role of Eomes in the induction of Blimp1.

Since *Eomes*$^{-/-}$ mutant embryos arrest at implantation prior to pPGC induction (Russ et al. 2000), I investigated Blimp1 induction in *EomesΔVE* and *EomesΔepi* mutant embryos (Arnold et al. 2008, Nowotschin et al. 2013) using the breeding strategy outlined in section 3.2.2. I performed immunohistochemical staining (section 3.2.3) to assess whether Blimp1 induction had occurred in E7.5 mutant embryos.

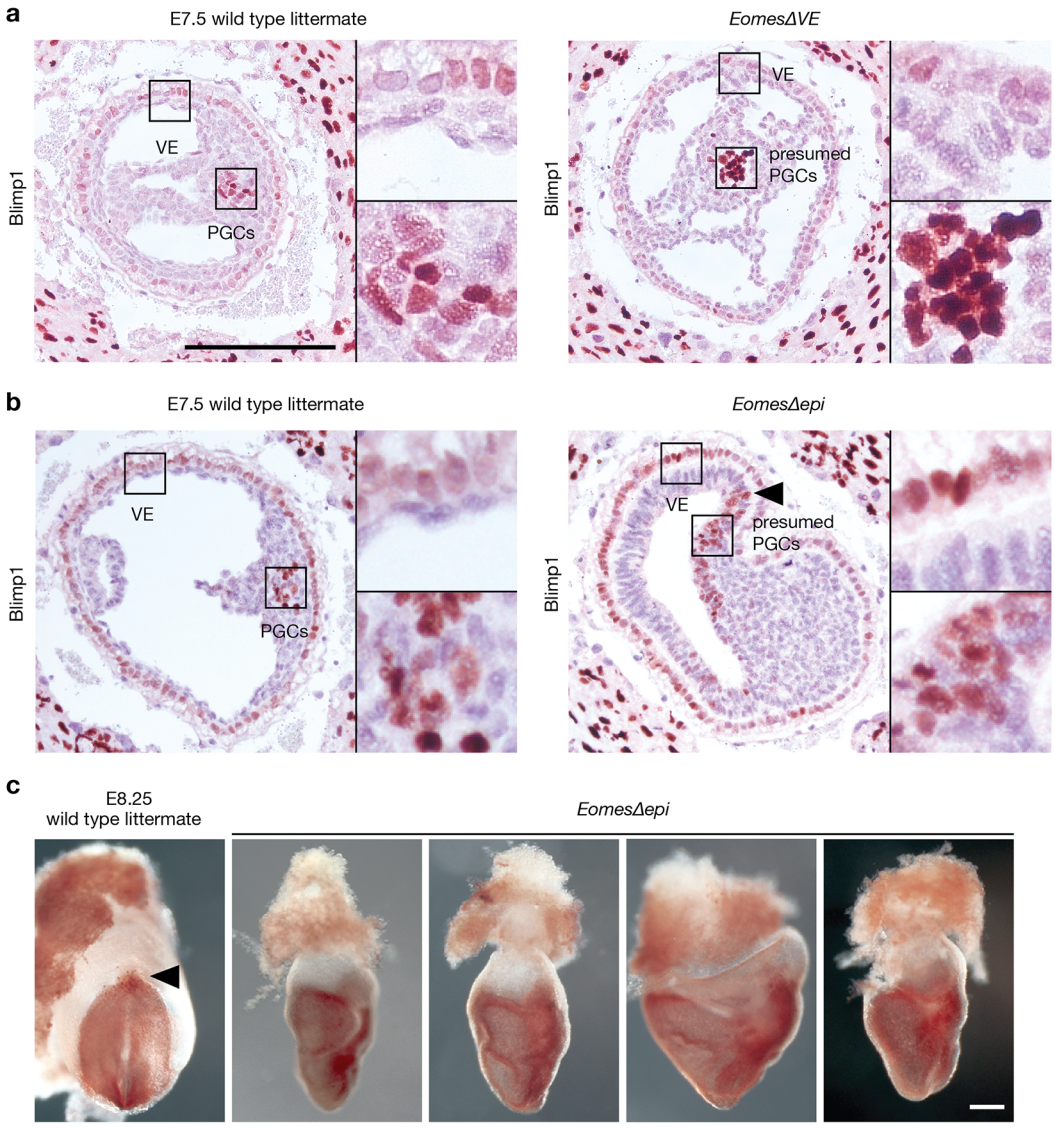


Figure 22 Epiblast and visceral endoderm-derived Eomes expression is dispensable for emergence of Blimp1⁺ cells in the epiblast.

(**a-b**) Representative images of Blimp1 immunohistochemistry on histological sections of E7.5 *EomesΔVE* (a) or *EomesΔepi* mutant embryos (b) in comparison to wild type littermates. The arrowhead in (b) indicates expansion of the Blimp1⁺ cluster into the ectodermal layer of the embryo. High magnification images of the boxed areas are shown to the right. (**c**) Alkaline phosphatase staining of whole-mount E8.25 *EomesΔepi* mutants in comparison to a wild type littermate. The arrowhead in (c) indicates PGCs in the wild type. VE: visceral endoderm; epi: epiblast; PGCs: primordial germ cells. Scale bars: 200 μm.

PCR genotyping on sectioned material was used to identify *Ttr.Cre* or *Sox2.Cre* –positive embryos (13/28 for *EomesΔVE* and 6/11 for *EomesΔepi* crosses, data not shown, see chapter 5). These were subsequently scored histologically for the respective mutant phenotypes (Arnold et al. 2008, Nowotschin et al. 2013). For *EomesΔVE* crosses, I identified five obvious mutants and two very small concepti that could not be identified

as mutant or wild type, i.e. 5 or 7/13. Four of these were screened by Blimp1 immunohistochemistry. For *EomesΔepi* crosses, I identified two obvious mutants and one very small embryo that could not be identified as mutant or wild type. Embryos from two additional litters were sectioned and allowed identification of two obvious mutants. A total of four *EomesΔepi* mutants for subsequently stained by Blimp1 immunohistochemistry.

Representative mutants shown in Fig 22a-b show that Blimp1 is expressed in the epiblast cells of both *EomesΔVE* and *EomesΔepi* mutant embryos at E7.5, thus excluding an essential role of epiblast or VE-derived Eomes in initial Blimp1 induction. In comparison to wild types, I observed a single, more compact strongly Blimp1$^+$ cell cluster in the mesoderm of all four stained *EomesΔVE* mutants.

In all four *EomesΔepi* mutants screened, I also detected one continuous area of Blimp1$^+$ cells in mutant embryos. Here, however, the cluster extended along the proximal-distal axis of the epiblast and comprised substantially more Blimp1$^+$ cells than in wild type littermates. Strikingly, I observed mis-localisation of Blimp1$^+$ cells out of the accumulating posterior cells (which fail to undergo EMT, Arnold et al. 2008) into the adjacent, more anterior ectodermal layer of the embryo (arrowhead in Fig 22b). Interestingly, Blimp$^+$ cells in the VE were not affected by loss of *Eomes* in the VE or in the epiblast, suggesting that Eomes is also non-essential for Blimp1 induction in the VE.

Staining of four whole-mount E8.25 mutant embryos (identified from 13 embryos) with alkaline phosphatase (AP), which marks PGCs (Ginsburg et al., 1990) suggested an expanded AP$^+$ cluster, whereas a wild type embryo showed single AP$^+$ PGCs (Fig 22c) and indicated that Blimp1$^+$ cells progress to AP$^+$ PGCs. The genotype of the four stained mutants was confirmed by PCR of ectoplacental cones from individual embryos (data not shown). This experiment could be enhanced in future by sectioning of stained embryos to define whether AP$^+$ cells are located within epithelial ectodermal cells or in the bulk mesoderm population.

Taken together, I show that Eomes signals in the VE and epiblast are individually dispensable for the induction of Blimp1$^+$ and AP$^+$ cells from the epiblast but are individually required to confine the location and size of the Blimp1$^+$/AP$^+$ cell cluster. The formation of abundant Blimp1$^+$ cells in *EomesΔVE* mutants lacking the AVE (Nowotschin et al. 2013) further strengthens the role of VE-derived signals in restricting the site and domain of Blimp1 expression. I noticed an expanded cluster of Blimp1$^+$ or AP$^+$ cells within the expanded posterior region in EomesΔepi mutants. This confirms that pPGCs do not undergo EMT as has been proposed previously (Kurimoto et al. 2008).

3.4 Deletion of *Smad2* from the VE leads to an expanded Blimp1$^+$ cell cluster thereby phenocopying *Smad2*$^{-/-}$ mutants

In contrast to *EomesΔepi* mutant embryos that fail to undergo EMT, *Smad2* mutants expand the region of Eomes$^+$ and T$^+$ epiblast cells and undergo EMT (Arnold et al. 2008, Waldrip et al. 1998, Brennan et al. 2001). This is due to the failure to establish the AVE (and earlier the DVE) (Waldrip et al. 1998, Yamamoto et al. 2009). Delaminating epiblast cells form a loose mesenchymal population that express extra-embryonic mesoderm markers as well as Blimp1 and alkaline phosphatase at the expense of anterior or distal streak derivatives (Waldrip et al. 1998, Tremblay et al. 2001, Ohinata et al. 2009).

With respect to PGC formation, *EomesΔVE* mutants are reminiscent of early *Smad2* mutants (Tremblay et al. 2001, Ohinata et al. 2009). *Eomes* expression in the VE is lost in *Smad2* mutants (Nowotschin et al. 2013). This indicates that the observed expansion of Blimp1$^+$ cells in *Smad2* mutants could be mediated by *Eomes* expression in the VE. Chimera experiments demonstrated that the *Smad2*$^{-/-}$ phenotype cannot by rescued by Smad2 activities in the epiblast, suggesting the abundant formation of Blimp1$^+$ cells is likely due to loss of *Smad2* signalling in the VE (Waldrip et al. 1998, Ohinata et al. 2009). To establish this point unequivocally, I next genetically inactivated Smad2 signals in the VE. I screened for mutant embryos by *Tr.Cre*-specific PCR (see chapter 5), which

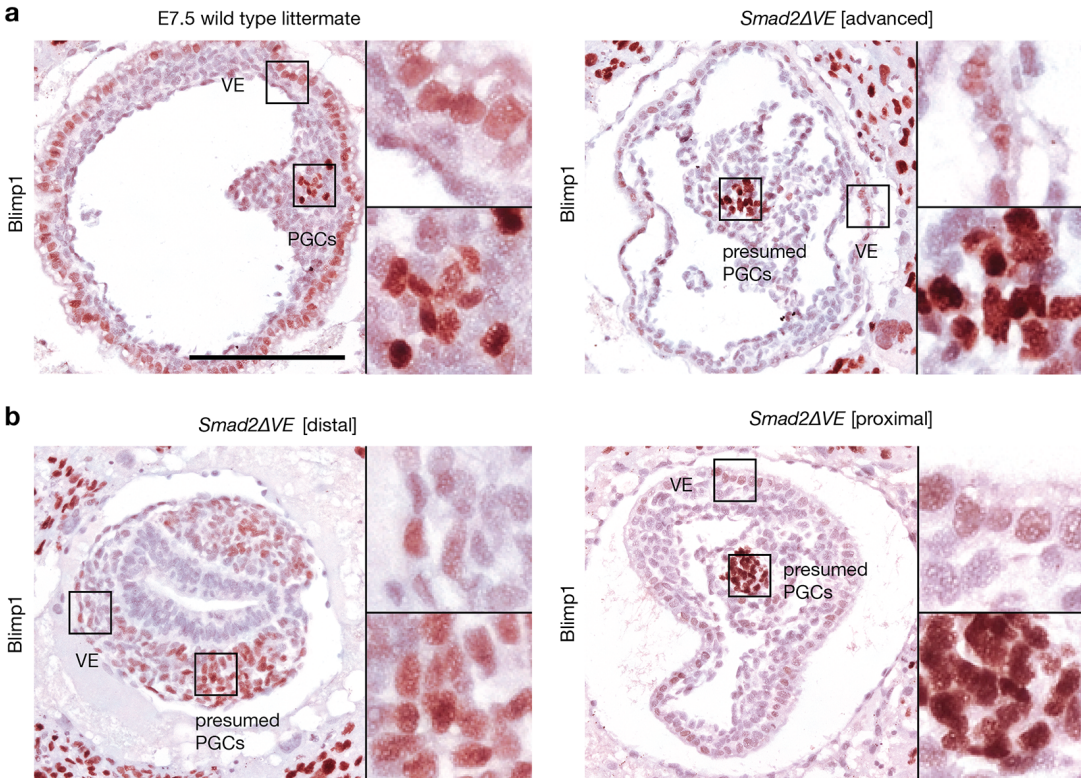


Figure 23 Visceral endoderm-specific ablation of *Smad2* leads to an expansion of Blimp1⁺ cells in the epiblast.

(**a-b**) Representative images of Blimp1 immunohistochemistry on histological sections of E7.5 conditional mutants that specifically lack Smad2 function in the VE in comparison to a wild type littermate. Two representative mutants are shown: (a) wild type control and mutant showing loose mesenchymal cells that contain a cluster of Blimp1⁺ cells. (b) distal and proximal section through a second mutant showing abundant Blimp+ cells in the distal region (left) and a cluster of Blimp1⁺ cells in a more proximal region (right). High magnification images of the boxed areas are shown to the right. VE: visceral endoderm; epi: epiblast; PGCs: primordial germ cells. Scale bar: 200 μm.

identified 7/20 embryos. Four of the seven *Ttr.Cre*⁺ embryos displayed a morphology that resembled *Smad2* mutants (Waldrip et al. 1998) and were selected for Blimp1 immunohistochemistry. Overall morphology of the sectioned mutant embryos was indistinguishable from the published Smad2 phenotype (Waldrip et al. 1998, Ohinata et al. 2009) suggesting that *Smad2ΔVE* mutants phenocopy *Smad2* mutants at E7.5. As shown in Fig 23, loss of Smad2 from the VE leads to abundant formation of Blimp1⁺ cells at the onset of gastrulation, that resolved into clumps of Blimp1⁺ cells. I verified this observation in two additional *Smad2ΔVE* mutant embryos (data not shown). Strikingly, Blimp1 expression in the VE was unaffected in *Smad2ΔVE* mutant embryos which

suggests that Smad2 expression in the VE is not essential for Blimp1 induction in the VE.

Previous experiments showed that removal of Smad2 from the epiblast blocks induction of the definitive endoderm lineage, whereas mesodermal specification is unaffected (Vincent et al. 2003a, Tremblay et al. 2000). Even though Blimp1 transcripts in *Smad2Δepi* mutants were assessed, analysis focussed on its expression in the endoderm and was inconclusive in respect to expression in PGCs (Vincent et al. 2003a) (see chapter 4). Collectively, my data analysing conditional Eomes and Smad2 mutants suggest that Nodal signalling is crucial for restricting epiblast cells from adopting a pPGC fate. In light of the essential role of Bmp signalling in inducing pPGCs and Blimp1 (Ohinata et al. 2009) and the suggestion that antagonistic interactions between Smad2 and Smad1 signaling pathways pattern the VE (Yamamoto et al. 2009), we wanted to evaluate a possible interplay of Nodal and Bmp signalling that influences acquisition of pPGC competence. To test this, I next investigated the tissue-specific roles of Smad4, which acts downstream of both Nodal and Bmp signalling, and the Bmp-effector Smad1.

3.5 Smad4 signals in the visceral endoderm are dispensable for Blimp1 induction in the E7.5 epiblast whereas epiblast-derived Smad4 is required to faithfully induce Blimp1

Previous work established that mutant embryos lacking Smad4 in the epiblast lack PGCs as assessed by alkaline phosphatase staining (Chu et al. 2004). Blimp1 induction (and thus the emergence of pPGCs) has, however, not been assessed. VE-derived Smad4 contributes essential cues for early embryonic patterning and development, as Smad4 null mutants display an earlier embryonic lethal phenotype than Smad4Δepi mutants (Sirard et al. 1998, Yang et al. 1998, Chu et al. 2004, Costello et al. 2009, Li et al. 2010). Due to a potential involvement of ALK2 receptor-mediated Bmp signaling in the VE (de Sousa Lopes et al. 2004, 2007), I hypothesized that Smad4 activities are possibly also required in the VE for the emergence of Blimp1$^+$ pPGCs. Presumptive mutants were selected by PCR genotyping for *Ttr.Cre* or *Sox2.Cre,* respectively, and morphological criteria (Chu et

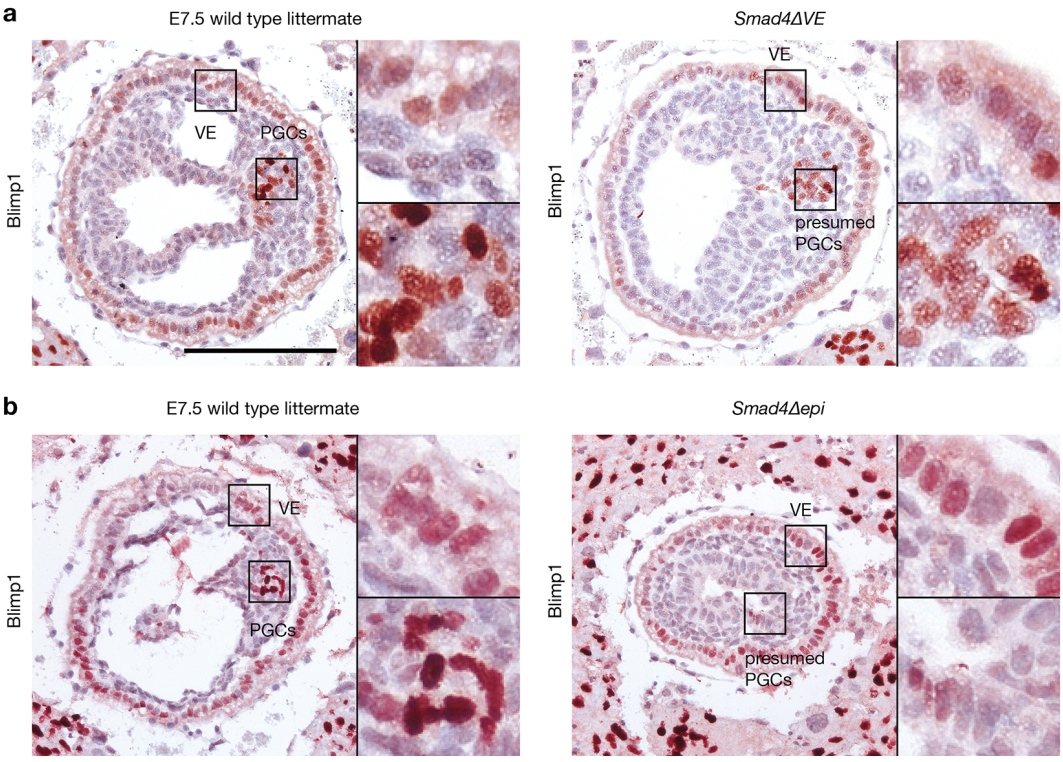


Figure 24 Visceral endoderm-derived Smad4 is dispensable for emergence of Blimp1⁺ cells in the epiblast, whereas epiblast-derived Smad4 is essential for robust Blimp1 induction in the posterior epiblast.

(**a-b**) Representative images of Blimp1 immunohistochemistry on histological sections of E7.5 conditional mutants that specifically lack Smad4 function in the visceral endoderm (a) or the epiblast (b) in comparison to wild type littermates. High magnification images of the boxed areas are shown on the right. VE: visceral endoderm; epi: epiblast; PGCs: primordial germ cells. Scale bar: 200 μm.

al. 2004, Li et al. 2010). VE-specific mutants can be easily identified by their disturbed mesoderm formation (Li et al. 2010).

From a screen of 24 embryos I identified ten that harboured *Ttr.Cre*, of which four also carried the *Smad4* mutant allele. Unfortunately, this PCR does not distinguish between the conditional deleted and null allele and thus cannot be used to identify conditionally deleted mutants (Chu et al. 2004). During sectioning, I inadvertently lost relevant sections for one of the four embryos. Two embryos with abnormal morphology (prospective mutants) showed a cluster of Blimp1⁺ cells (Fig 24) suggesting that Smad4 signalling in the VE is dispensable for Blimp1 induction. The remaining third embryo looked morphologically normal and possessed a defined cluster of Blimp⁺ cells (data not shown).

Smad4Δepi mutant embryos display a less severe phenotype at gastrulation stages but exhibit a thickened primitive streak and lack the definitive endoderm (Chu et al. 2004). Migrating mesoderm in *Smad4Δepi* mutant embryos traverses the ventral midline without interruption, resulting in the formation of fused somites (Chu et al. 2004). As I was unable to unambiguously identify mutants from strips of un-mounted paraffin sections, I re-sorted to screening all *Sox2.Cre*$^+$ embryos by Blimp1 immunohistochemistry on serial sections. Strikingly, I failed to detect robust Blimp1 expression in the entire proximal-distal epiblast of four out of eight *Sox2.Cre*$^+$ embryos suggesting that these represent *Smad4Δepi* embryos (Fig 24b). These embryos were also smaller than their Cre$^-$ littermates and displayed abnormal primitive streak morphology (Fig 24b). I did, however, detect rare single Blimp1$^+$ cells in prospective Smad4 mutant epiblasts in single sections that did not expand into a Blimp1$^+$ cluster in immediately adjacent sections (Fig 24b and data not shown).

Overall, these results suggest that VE-derived Smad4 signals are dispensable for Blimp1 induction in presumed PGCs and the VE, whereas Smad4 in the epiblast is required to efficiently induce Blimp1$^+$ pPGCs.

3.6 Smad1 in the epiblast, but not the visceral endoderm, is required for the induction of Blimp1$^+$ epiblast cells at E7.5

Previous work has established that mutant embryos lacking *Smad1* have drastically reduced numbers of AP$^+$ PGCs or Blimp1$^+$ pPGCs (Tremblay et al. 2001, Hayashi et al. 2002b, Ohinata et al. 2009). However, VE- versus epiblast-specific roles for *Smad1* have not been studied genetically. Blimp1 induction (and the emergence of pPGCs) has not been shown to result unambiguously from Smad1 signalling in the epiblast alone. This scenario had been suggested by chimera experiments and by exposure of *ex vivo* cultures of isolated epiblast tissue to recombinant Bmp4 (Ohinata et al. 2009). Furthermore, VE-derived Bmp signalling by Bmp2 (Hoodless et al. 1996) via Alk2 has also been implicated in PGC specification (Ying and Zhao, 2001, de Sousa Lopes et al. 2004).

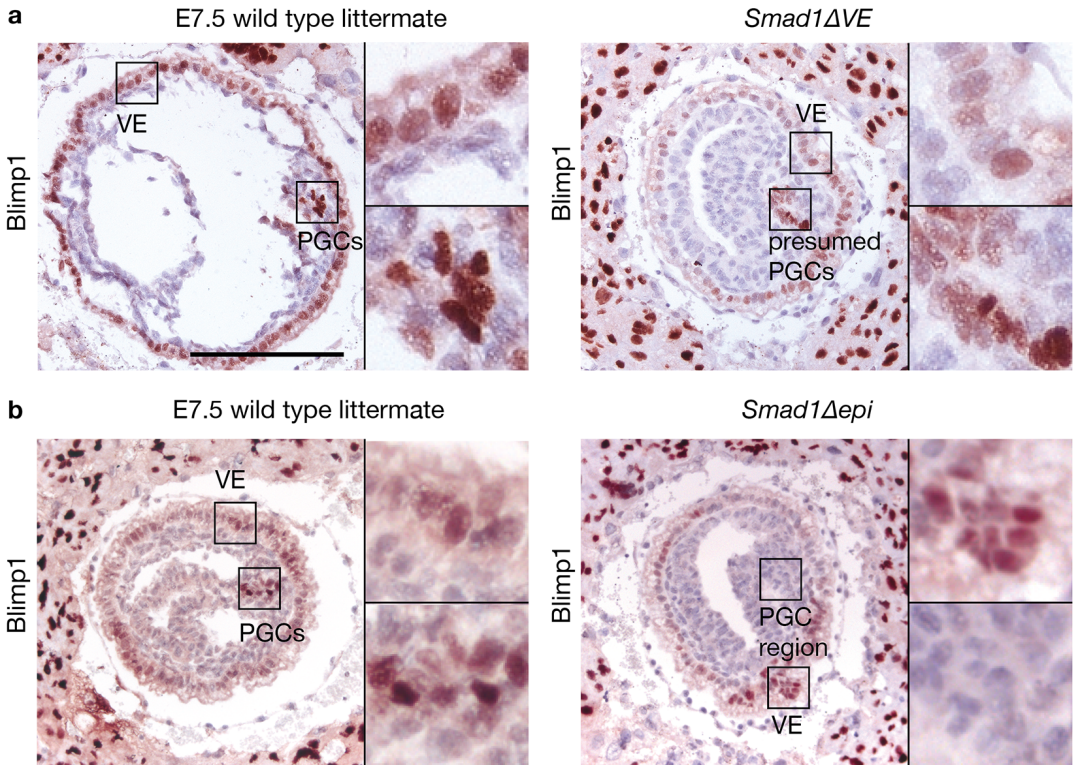


Figure 25 Visceral endoderm-derived Smad1 is dispensable for emergence of Blimp1⁺ cells in the epiblast, whereas epiblast-derived Smad1 is essential for Blimp1 induction in the posterior epiblast.

(**a-b**) Representative images of Blimp1 immunohistochemistry on histological sections of E7.5 conditional mutants that specifically lack Smad4 function in the visceral endoderm (a) or the epiblast (b) in comparison to wild type littermates. High magnification images of the boxed areas are shown to the right. VE: visceral endoderm; epi: epiblast; PGCs: primordial germ cells. Scale bar: 200 μm.

I used *Smad1* conditional and null alleles to delete *Smad1* either from the VE or epiblast. Potential mutant embryos were identified by Cre PCR performed on sections of E7.5 embryos within the deciduum (see section 3.2.1, 3.2.2 and data not shown). Screening 15 embryos derived from *Smad1ΔVE* crosses identified four *Ttr.Cre*⁺ embryos. Three of these exhibited thickening and/or ruffling of the VE or had an abnormally distorted epiblast similar to that described for *Smad1* mutant embryos (Tremblay et al. 2001). One embryo was morphologically normal and therefore not classified as a *Smad1ΔVE* mutant. Of the three likely *Smad1ΔVE* mutants two contained a cluster of Blimp1⁺ cells (Fig 25a), whereas a third embryo (that showed a profoundly distorted shape) exhibited fewer

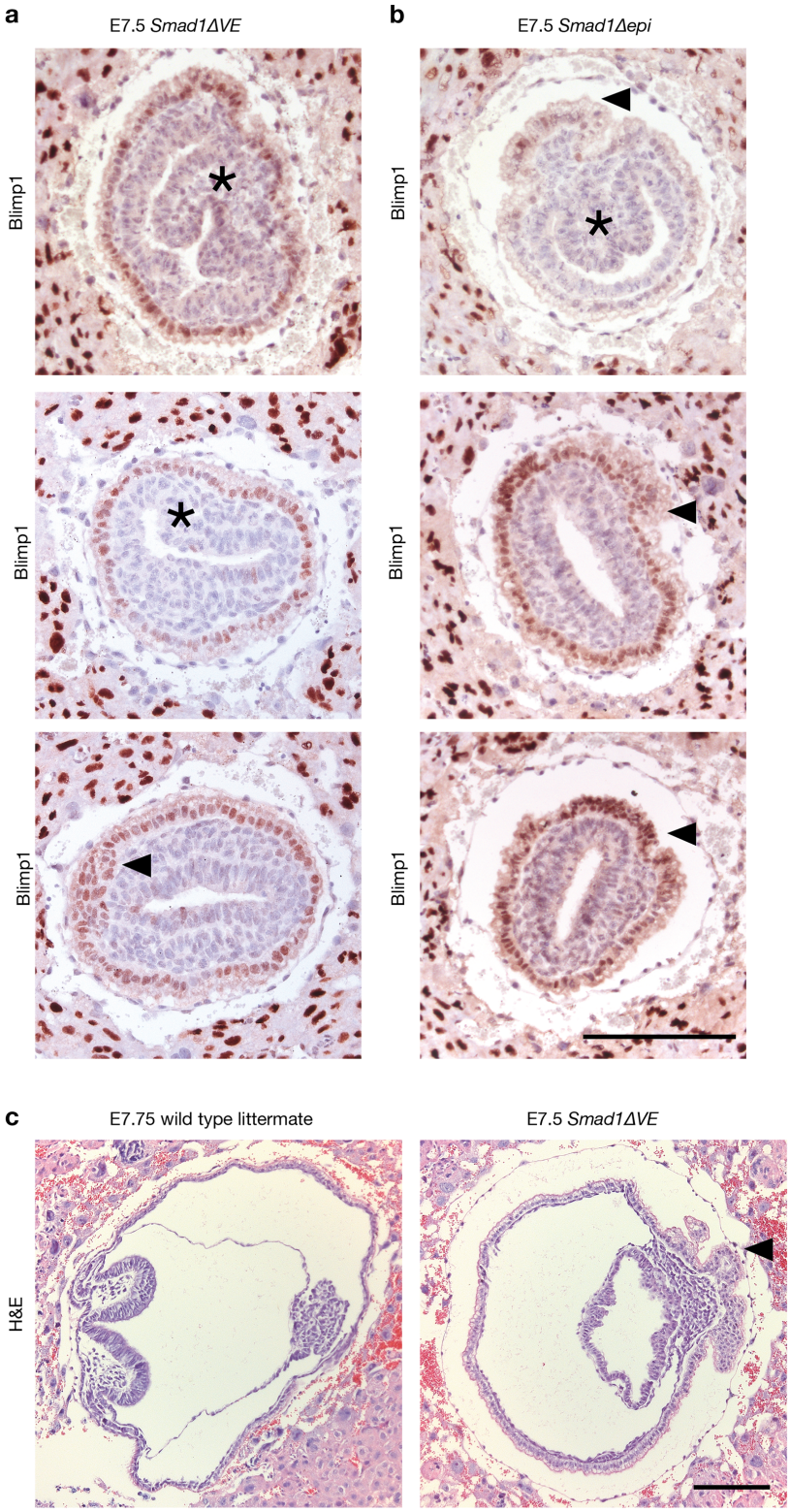


Figure 26 Examples of the observed thickening and ruffling of visceral endoderm in VE- and epiblast-specific Smad1 mutants at E7.5.

(**a-b**) Representative images of Blimp1 immunohistochemistry on histological sections of three individual E7.5 conditional mutants that specifically lack Smad1 function in the visceral endoderm (a) or the epiblast (b). Arrowheads indicate ruffled VE and stars indicate disturbed epiblast morphology. (**c**) Ruffling of the VE in VE-specific Smad1 mutants at E7.75. VE: visceral endoderm; epi: epiblast; pPGCs: precursors of primordial germ cells. Scale bars: 200 μm.

Blimp1$^+$ cells suggesting variability in the level of Blimp1 induction. Due to the small number of prospective mutants screened and the necessity to evaluate sectioned material, the extent of variation in Blimp1 induction remained unclear (see chapter 4). The VE ruffling and distorted morphology of mutants are illustrated in Fig 26a. For *Smad1Δepi* crosses, a screen of four embryos identified three *Sox2.Cre*$^+$ which were used for Blimp1 immunohistochemistry at E7.5. In addition, a litter of seven embryos (not genotyped) was also stained. I failed to detect Blimp1$^+$ clusters in 1/3 and 2/7 embryos screened, respectively (Fig 25b). These embryos also showed thickening and ruffling of the Blimp1$^+$ VE and varying degrees of disorganisation of the epiblast reminiscent of the Smad1 phenotype (Tremblay et al. 2001). It is thus likely that these embryos represent prospective *Smad1Δepi* mutants. This analysis suggests that Smad1 in the epiblast is required to robustly induce Blimp1 in epiblast cells. Occasional, single AP$^+$ cells have been detected in *Smad1*$^{-/-}$ embryos (Tremblay et al. 2001, Hayashi et al. 2002b). In *Smad1Δepi* mutants, I also found very few, single Blimp1$^+$ epiblast cells (data not shown). The thickening and ruffling of the VE in prospective VE-specific mutants is further illustrated in Fig 26c.

At this point, I am unable to attribute the thickening and ruffling of the VE and distortion of the epiblast to loss of Smad1 from the epiblast- or VE, since the small number of embryos screened showed a varying degree of similar abnormalities irrespective of which tissue Smad1 was deleted from (see Fig 26). Strikingly, Blimp1 expression in the VE was unaffected by the loss of Smad1 in the epiblast or VE.

3.7 *Prdm1*/Blimp1 in the visceral endoderm is dispensable for germ cell specification and embryonic development

Expression of Blimp1 in the VE precedes expression in pPGCs (Vincent et al. 2005, Ohinata et al. 2005). *Prdm1*$^{-/-}$ embryos lack any obvious defects at early post-implantation stages suggesting that its expression in the VE is dispensable for early axis patterning (Vincent et al. 2005). Initial characterization of Blimp1 mutants included experiments that showed that the lack of AP$^+$ PGCs in Blimp1 mutants could not be rescued by wild type

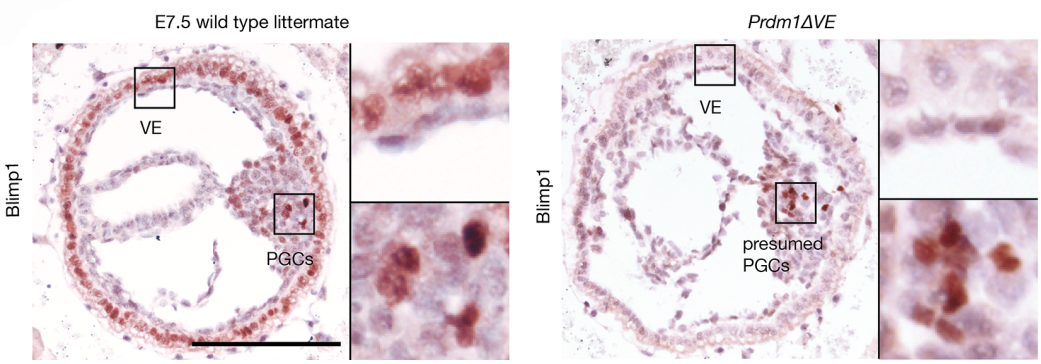


Figure 27 Visceral endoderm-derived *Prdm1* is dispensable for the emergence of Blimp1⁺ cells in the epiblast.

Representative images of Blimp1 immunohistochemistry on histological sections of a E7.5 conditional mutant that specifically lacks *Prdm1* in the visceral endoderm in comparison to a wild type littermate. High magnification images of the boxed areas are shown to the right. VE: visceral endoderm; PGCs: primordial germ cells. Scale bar: 200 µm.

extra-embryonic tissues in chimeras (Ohinata et al. 2005). Together with the failure of *Prdm1*$^{-/-}$ PGCLCs (derived from mutant ES cells) to activate PGC marker transcripts (Murakami et al. 2016), this suggests that Blimp1 acts directly in the epiblast. However, a role for Blimp1 signals from the VE for germ cell maintenance or embryonic development cannot be ruled out. In order to unambiguously assign a role for Blimp1 expression in the VE, I deleted *Prdm1* from the VE using the alleles and strategy described in section 3.2.1 and 3.2.2. Blimp1 immunohistochemistry of E7.5 sectioned embryos revealed complete absence of Blimp1 expression in the VE (Fig 27), thereby validating the conditional deletion. Since the *Prdm1* null allele (Vincent et al. 2005) deletes an upstream exon, while the *Prdm1* conditional allele deletes a downstream region from the *Prdm1* locus (Shapiro-Shelef et al. 2003), I could unambiguously identify mutant embryos by PCR genotyping for the null allele and *Ttr.Cre*-expression.

I identified seven of 18 embryos as *Prdm1ΔVE* mutants of which three were stained for Blimp1. I detected Blimp1⁺ epiblast cells in all three embryos confirming that Blimp1 in the VE is indeed dispensable for Blimp1 expression in the posterior epiblast. To evaluate possible later contributions by VE-specific Blimp1 expression in development, I genotyped the offspring of *Prdm1*$^{-/+}$;*Ttr.Cre*$^{+/-}$ x *Prdm1*$^{CA/CA}$ crosses at weaning (see chapter 5). From eleven offspring, I obtained three that were positive for *Ttr.Cre* transgene and the *Prdm1*$^{-}$ allele (data not shown). Furthermore, an intercross of two

Prdm1ΔVE mutants produced a litter of nine pups establishing the fertility of *Prdm1ΔVE* mutants (data not shown).

The *Ttr.Cre* transgene mediates deletion in both the VE derivatives as well as a subset of the intestinal epithelium at E12.5, E14.5 and E16.5 (Kwon and Hadjantonakis 2009). It is not clear whether *Ttr* activity at these later stages is due to *de novo* activation of *Ttr.Cre* or expansion of cells that had undergone earlier activation of *Ttr.Cre* (Kwon and Hadjantonakis 2009). Blimp1 is strongly expressed throughout the embryonic gut endoderm and continues to be expressed in the immature enterocytes of the intestinal epithelium up to birth (Robertson et al. 2007, Ohinata et al. 2008, Harper et al. 2011). Loss of Blimp1 in intestinal epithelium by *Villin.Cre*-mediated deletion (which is activated in enterocytes from E12.5 onwards, el Marjou et al. 2004) leads to early postnatal death due to a failure in intestinal epithelium maturation (Harper et al. 2011).

Collectively, these experiments suggest that Blimp1 has no role in either primordial germ specification or embryonic development and adult fertility. Furthermore, complete loss of Blimp1 in the VE validates the *Ttr.Cre* delete strains used for these experiments.

3.8 Protocols and reagents established for future experiments

3.8.1 Validation of a published PGC-LC differentiation protocol

A differentiation protocol has been established to generate primordial germ cell-like cells (PGCLCs) from naïve ES cells via differentiation into transient epiblast-like cells (EpiLCs) (Hayashi et al. 2011, see Fig 28d). I aimed to validate this protocol for use in future experiments (see chapter 4).

To assess induction of the pPGC marker Blimp1 in PGCLCs, I made use of a wild type ES cell line generated from the *Blimp1.Venus* reporter strain (Ohinata et al. 2008). An ES cell line lacking the Blimp1 reporter was included as a control. Induction of ES cell lines into EpiLCs for two days followed the dynamics described in Hayashi et al. 2011. ES

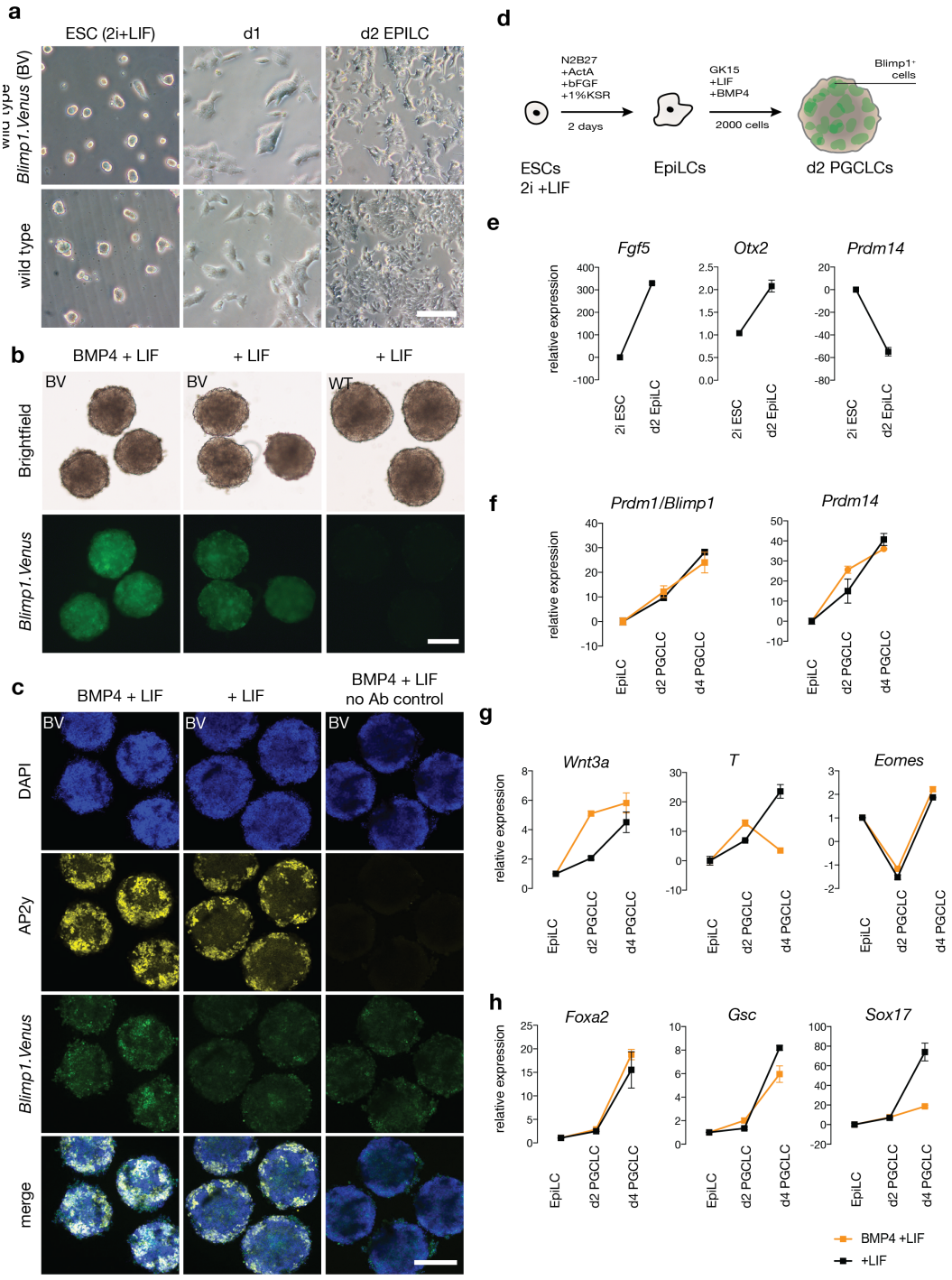


Figure 28 Validation of Blimp1 expression in a published PGCLC differentiation protocol.

(**a**) Cell morphology during EpiLC differentiation from wild type ES cells with or without the *Prdm1.Venus* reporter (Ohinata et al. 2008, abbreviated as BV). (**b**) Brightfield and epifluorescence images of d2 PGCLCs. A wild type line was included to assess variability in the morphology of PGCLCs in different cell lines. (**c**) Immunofluorescence staining on d2 PGCLCs with an antibody specific to the PGC marker Tcap2c/Ap2γ. (d) Schematic representation of the PGCLC differentiation protocol described in Hayashi et al. 2011. (**e-h**) qRT-PCR on EpiLCs and d2 and d4 PGCLCs with primers specific for primed and naïve pluripotency markers (e), PGC markers (f), early primitive streak markers (g) and early endodermal/visceral endodermal markers (h). qRT-PCR plots represent average fold changes over *Hprt* expression with standard (*continued on next page*)

cells gradually adopted a flattened morphology (Fig 28a). qRT-PCR analysis on wild type EpiLCs confirmed the induction of the primed pluripotency markers *Fgf5* and *Otx2* (Buecker et al. 2014), while the naïve pluripotency marker *Prdm14* was down-regulated in EpiLC compared to ES cells (Fig 28e).

Induction of EpiLCs for two days with recombinant BMP4 and LIF induced *Blimp1.Venus* (BV) expression (Fig 28b). BV+ areas in cell aggregates co-expressed the PGC marker *Tcap2c/Ap2γ* (Fig 28c). qRT-PCR on wild type PGCLCs confirmed induction of *Prdm1/Blimp1* and *Prdm14* at d2 and d4 (Fig 28f). Early primitive streak markers *Wnt3* and *T* were also increased in PGCLCs, whereas *Eomes* expression dropped at d2 and increased at d4 (Fig 28g). Embryonic and extra-embryonic endodermal markers *Foxa2*, *Gsc* and *Sox17* were also induced in PGCLCs (Fig 28h). PGCLCs induced by BMP4 and LIF resembled EpiLCs treated with LIF alone in activation of BV expression and marker transcript expression.

3.8.2 Establishing a resource of mutant and reporter ES cell lines for PGCLC differentiation experiments

Transgenic ES cell lines have been successfully differentiated into PGCLCs *in vitro* to explore the genetic requirement for PGC specification and development (Hayashi et al. 2011, Aramaki et al. 2013, Kurimoto et al. 2015, Murakami et al. 2016). To characterize the roles of Eomes, Smad2/3, Smad4 and Smad1/5 in establishment of the pPGC fate further, I sought to derive 2i-adapted homozygous mutant ES cells lines from mouse lines available in the lab. To facilitate assessment of PGCLC induction, I also exploited the *Prdm1.Venus* reporter (Ohinata et al. 2008), which I introduced into respective mutant backgrounds (see section 3.2.2). I also decided to derive *Wnt3* mutant lines harbouring *Prdm1.Venus* which have previously been shown to fail to induce Blimp1 in PGCLCs (Aramaki et al. 2013). *Wnt3*$^{-/-}$ PGCLCs can be forced to express Blimp1 by

---

(*continued from last page*) deviation from two technical duplicates for EpiLCs stimulated with LIF with (yellow) or without recombinant BMP4 (black). BV: *Prdm1.Venus* transgene, WT: wild type, ESC: embryonic stem cells, EpiLC: epiblast-like cells, PGCLCs: primordial germ cell-like cells. Scale bars: 200 μm.

Table 10 ES cell lines established to date.

Allele	genetic conformation	*Reporter*	n (clones)	Adopted to
Smad1^{-}	- / -		6	2i + LIF
	- / -		4	serum + LIF
	- / -	*Prdm1.Venus*	7	2i + LIF
	+ / -		1	2i + LIF
	+ / -	*Prdm1.Venus*	1	2i + LIF
Smad5^{-}	- / -		1	2i + LIF
	+ / -	*Prdm1.Venus*	2	2i + LIF
Smad2^{-}	- / -		4	serum + LIF
	- / -		4	2i + LIF
Smad3^{CRISPR}	- / -		4	serum + LIF
	- / -		4	2i + LIF
Smad2/3^{CRISPR}	- / -		4	serum + LIF
	- / -		4	2i + LIF
Eomes^{-}	- / -		2	2i + LIF
	- / -	*Prdm1.Venus*	4	2i + LIF
	+ / -	*Prdm1.Venus*	1	2i + LIF
Wnt3^{-}	- / -		4	2i + LIF
	- / -	*Prdm1.Venus*	9	2i + LIF
	- / -	*Eomes.GFP*	3	2i + LIF
	+ / -	*Eomes.GFP*	1	2i + LIF
wild type	+ / +		4	serum + LIF
	+ / +		4	2i + LIF
	+ / +	*Prdm1.Venus*	1 (+1)	2i + LIF

Cell lines indicated in grey were not derived or generated by me, but by previous work in the lab (Tremblay et al. 2001 and Elizabeth Robertson, unpublished). For refrences for the alleles used see Table 11 in the chapter 5.

overexpression of Eomes (Aramaki et al. 2013). Eomes is absent in epiblasts of epiblast-specific Wnt3 mutants (Barrow et al. 2007) suggesting that Eomes is not normally expressed in *Wnt3*$^{-/-}$ PGCLCs. We hypothesized that assessment of Eomes expression changes in Wnt3 mutant lines could thus be used as a readout for rescue screens. I therefore also aimed to derive *Wnt3*$^{-/-}$ lines harbouring the *Eomes.GFP* reporter (Arnold et al. 2009). Table 10 summarizes the mutant and transgenic ES cell lines generated to date including the Smad2/3 and Smad3 mutant ES cell lines described in chapter 2. The list also includes established wild type and Smad2 mutant lines (Tremblay et al. 2001) that I adapted to 2i conditions. I am currently working on deriving Smad2, Smad4 and Smad5 mutant ES cell lines harbouring the *Prdm1.Venus* reporter.

3.8.3 Validation of Stella, p-Smad1/5/8 and Blimp1 antibodies for future experiments

To validate the identity of Blimp1^{+} pPGCs/PGCs in the epiblast of conditional mutants, I wanted to stain whole-mount embryos with the PGC marker Stella, which is co-

expressed in nuclei of PGCs from E7.25 onwards (Sato et al. 2002, Ancelin et al. 2006). Stella expression is retained in developing germ cells in the genital ridges (Ohinata et al. 2008). I searched for published validated Stella antibodies and identified a polyclonal antibody raised against full-length mouse Stella protein used to detect germ cells in genital ridges (Chen et al. 2013). Sections of both male and female E12.5 genital ridges from wild type embryos showed strong Stella staining in developing germ cells (Fig 29a and data not shown) which was not observed in controls with no primary antibody. However, the staining showed unspecific background. Since this background was also detected in the red fluorescence channel I attributed this to auto-fluorescence from erythroid cells as has been reported by others (Hu et al. 2015). Future experiments will assess the utility of the Stella antibody for staining whole-mount and sectioned E7.5 embryos.

To assess a possible antagonism of Smad1 and Smad2 signalling in pPGC specification, I aimed to establish an antibody staining protocol for pSmad1/5/8 and pSmad2/3. To date, I have failed to establish suitable staining conditions for pSmad2/3 on E7.5 paraffin sections (data not shown). However, I can detect strong pSmad1/5/8 staining in cells exiting the primitive streak and in the visceral endoderm overlying the embryonic-extra-embryonic interface as well as in the allantois and mesoderm of the amnion. The staining is specific as the control with no primary antibody shows no background (Fig 29b). To assess Blimp1 expression in cells or embryos not bearing the *Prdm1.Venus* reporter (such as *Smad2/3*$^{-/-}$ cells), I aimed to establish immunofluorescence staining protocols for Blimp1. I tested the Blimp1 antibody used in immunohistochemical experiments (see previous sections), by standard and triple amplification staining (i.e with an intermediate secondary IgG antibody that is subsequently detected by a third antibody). Only triple amplification showed specific staining in the PGCs (arrowhead in Fig 29c) and VE (specifically in the AVE). However, there is unspecific background staining in the control with no primary antibody.

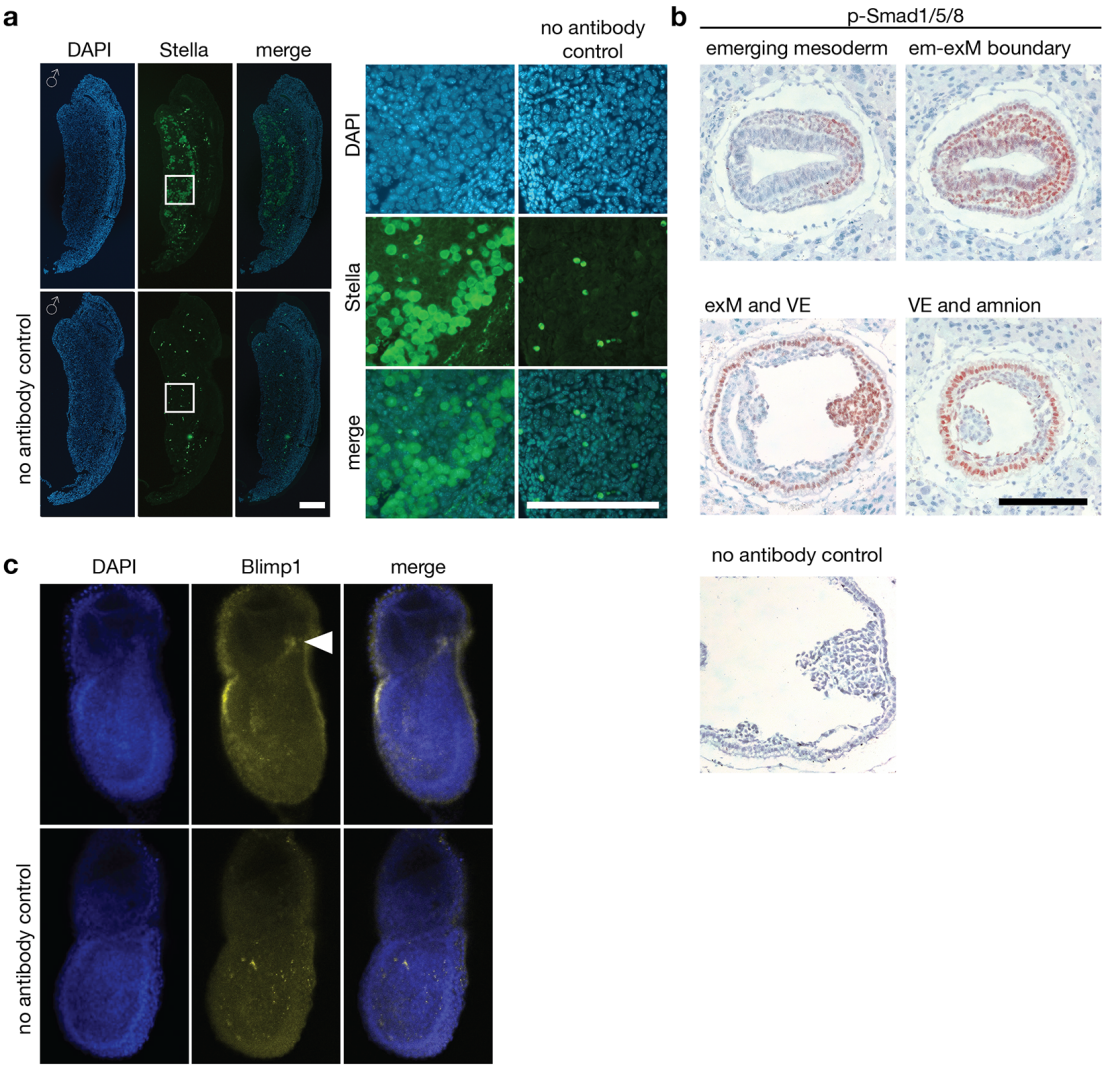


Figure 29 Testing of antibody stainings for Stella, pSmad1/5/8 and Blimp1 in mouse embryos.

(**a**) Immunofluorescence staining of paraffin sections of E12.5 male genital ridges with a Stella-specific antibody, co-stained with DAPI. Boxed areas are shown on the right showing developing germ cells. Small fluorescent cells present in the control with no antibody represent auto-fluorescent erythroid cells. (**b**) Immunofluorescence staining of paraffin sections of E7.5 wild type embryos in the deciduum with an antibody specific to phosphorylated forms of Smad1/5/8. All sections but section "exM and VE" and the control with no antibody are from the same sectioned embryo. (**c**) Immunofluorescence staining on whole-mount E7.5 embryos with an antibody specific to Blimp1. em: embryonic, exM: extra-embryonic mesoderm, VE: visceral endoderm. Scale bars: 200 μm.

3.8.4 Optimization of flow cytometric analysis of Eomes.GFP reporter cells in gastrulating embryos

To enable the characterisation of Eomes roles in the primitive streak and other sites in the embryo e.g. by analysing transcriptional profiles of Eomes^{+} cells, I established a protocol to recover *Eomes.GFP*$^{+}$ cells via fluorescent activated cell sorting (FACS)

(Arnold et al. 2009). *Eomes.GFP* is a knock-in allele and homozygotes phenocopy the null allele, but heterozygotes develop normally (Arnold et al. 2009, see Fig 30a). *Eomes.GFP* reporter expression in E7.5 heterozygous embryos recapitulated Eomes transcript expression in the primitive streak, nascent definitive endoderm and chorion (Fig 30b). I dissociated pooled embryos into a single cell suspension (Fig 30c, see chapter 5). Subsequent flow cytometric analysis of E7.5 embryo suspensions showed that $Eomes^{GFP}$ is expressed in ~75% of dissociated cells (Fig 30c). The high proportion of $Eomes^{+}$ cells (compared to the proportion of Eomes expression in embryos, see Fig. 30a) likely results from the preferential dissociation of loose mesenchymal cells of the streak, while anterior epiblast and extra-embryonic tissues are more adherent and resistant to dissociation. I also dissociated E6.5 embryos with similar results (data not shown).

To allow sorting and transcriptional profiling of (presumptive) $Eomes^{+}$ cells from wildtype and epiblast-specific Eomes mutants, I introduced the *Eomes.GFP* allele into conditional *Eomes* null background. $Eomes.GFP^{-/+}$; $Sox2.Cre^{/+}$ males (Arnold et al. 2008, Hayashi et al. 2002a) can be mated to $Eomes^{CA/CA}$ females (Arnold et al. 2008) to produce epiblast-specific ablation of Eomes. Preliminary analysis showed activation of *Eomes.GFP* in E7.5 *EomesΔepi* mutants (data not shown). Future experiments aim to use the established dissociation and flow cytometry protocol.

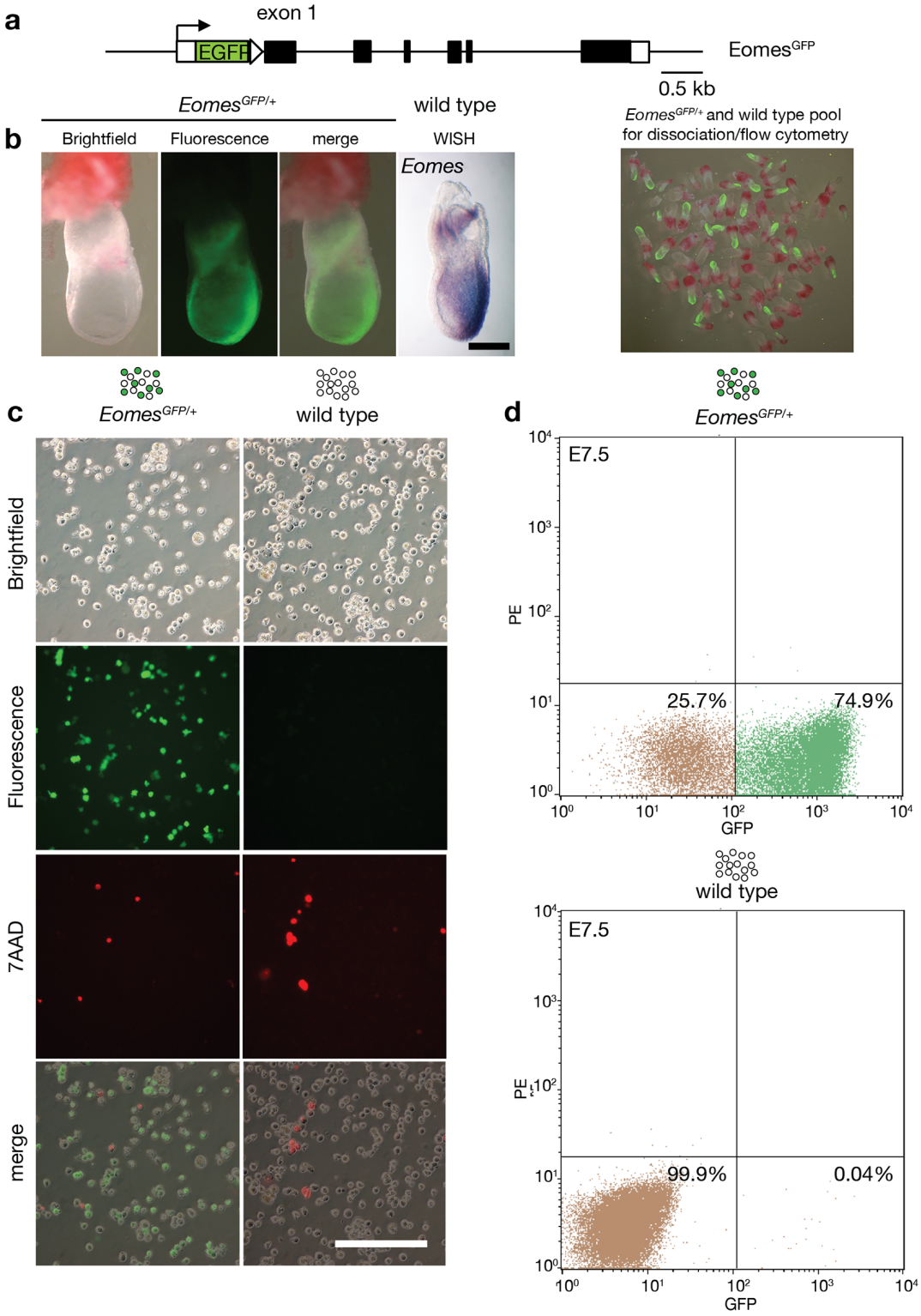


Figure 30 Flow cytometric analysis of *Eomes.GFP*⁺ cells from E7.5 embryos.

(**a**) The Eomes^{GFP} knock-in reporter allele (Arnold et al. 2009). (**b**). Brightfield and epifluorescence images of E7.5 *Eomes*$^{GFP/+}$ embryos in comparison to *Eomes* WISH on wild types. Pools of embryos used for dissociation and FACS are shown on the right. (**c**) Immunofluorescence images of dissociated cells of E7.5 *Eomes*$^{GFP/+}$ embryos and wild type littermates costained with 7AAD. (**d**) Flow cytometry of dissociated cells of of E7.5 *Eomes*$^{GFP/+}$ embryos and wild type littermates. Scale bars: 200 µm.

3.9 Conclusion of project II

Taken together, the presented experiments refine our understanding of the role of T-box factors in the initiation of Blimp1 expression in pPGCs and further characterize the role of the visceral endoderm in the initiation of Blimp1 expression in pPGCs. My experiments contribute to answering the questions set out in the aims of the thesis.

1. Is Eomes expression in the VE or in the epiblast required to induce Blimp1⁺ pPGCs?

The data presented exclude an essential role of the T-box factor Eomes either in the visceral endoderm or the epiblast to initiate expression of Blimp1 in pPGCs. Instead, Eomes signalling in the visceral endoderm and epiblast is crucial for restricting the induction of Blimp1⁺ cells to the posterior epiblast by enabling AVE development and EMT, respectively. Further experiments aim to address whether the EMT phenotype of *EomesΔepi* mutant embryos contributes to enhanced Bmp signalling, thereby leading to enhanced formation of Blimp1⁺ cells.

2. Does specific ablation of Smad2 expression in the VE phenocopy the expansion of Blimp1⁺ pPGCs observed in global Smad2 loss of function mutants?

My experiments to date suggest that *Smad2ΔVE* mutant embryos morphologically phenocopy the *Smad2* mutant phenotype at E7.5 and also lead to the expansion of Blimp1⁺ cell clusters in the epiblast at the onset of gastrulation. Further experiments aim to validate Blimp1⁺ cells as pPGCs and to characterize further the mechanism of how the AVE phenotypes of *Smad2ΔVE* and *EomesΔVE* mutant embryos lead to the mis-localization and expansion of the cluster of Blimp1⁺ cells.

3. Does ablation of Smad4 expression in the VE affect the induction of Blimp1⁺ pPGCs?
4. Is Smad1 expression in the VE required to induce Blimp1⁺ pPGCs?

My experiments strengthen a model in which Bmp-dependent signalling via Smad signals in the visceral endoderm is dispensable for the induction of Blimp1 in pPGCs. The small number of mutant embryos examined and the limitations of my analysis using histological

sections necessitates further experiments to validate findings in additional mutants and furtherrmore via whole-mount assessment of Blimp1 expression. The latter experiments will also allow me to draw conclusions about subtle effects on the epiblast population that is induced to become Blimp1$^+$ in *Smad4ΔVE* and *Smad1ΔVE* mutant embryos. Furthermore, it will be important to validate the dramatic reduction in Blimp1$^+$ cells in *Smad4Δepi* and *Smad1Δepi* mutant embryos using whole-mount Blimp1 assessment.

5. Does Prdm1 expression in the VE have a role in the induction of Blimp1$^+$ pPGCs and/or in later development?

My experiments to date exclude a role of Blimp1 expression in the visceral endoderm for the induction of Blimp1 in pPGCs. Furthermore, VE-derived Blimp1 signals seem to be dispensable for embryonic development and adult fertility.

In conclusion, the experiments presented suggest a dispensable role of the T-box factor Eomes in the induction of the primordial germ cell fate. They expand our understanding of the role of Nodal signalling and VE-derived Bmp signalling in establishing the competence to induce Blimp1$^+$ cells in the posterior epiblast. Reagents and tools established in this chapter will enable the validation and further characterization of these initial findings (see chapter 4).

4

Discussion

4.1 Summary of findings

Project I

Here I describe an experimental system that allows the dissection of transcriptional changes underlying graded Smad2/3 activities guiding the differentiation of mouse embryonic stem cells. I have shown that combined deletion of Smad2 and Smad3 in ES cells leads to the acquisition of a unique expression profile during differentiation, characterized by impaired induction of embryonic lineage specific genes and acquisition of a more extra-embryonic-like state. Parallel profiling of individual Smad2 or Smad3 mutant ES cells shows that loss of either transcription factor only partially recapitulates the defects apparent in the compound mutant ES cells. This emphasizes individual contributions of Smad2 and Smad3 and dose-dependency of Nodal signals. Preliminary data suggest that the underlying mechanism of the differentiation defect does not lie in a compromised undifferentiated state. Rather *Smad2/3*$^{-/-}$ cells seem unable to adopt an epiblast-like state that is competent to initiate lineage priming. Collectively, my results have identified novel downstream targets of Smad2/3 signals and suggest an absolute requirement for Smad2/3 during embryonic differentiation.

Project II

Here I present a genetic study that analyses induction of Blimp1 protein expression, which marks precursors of primordial germ cells, in VE- or epiblast-specific *Eomes*, *Smad2*, *Smad4*, *Smad1* and *Prdm1* mutants to define their tissue-specific contribution to the establishment of the germ cell fate. I have shown that Eomes functions in the epiblast and visceral endoderm are dispensable for Blimp1 induction in PGCs. Instead, lack of the AVE in VE-specific Eomes and Smad2 mutants leads to a failure to restrict Blimp1 induction to posterior epiblast cells. Establishment of an AVE, but failure to undergo EMT at gastrulation in epiblast-specific Eomes mutants similarly leads to a mis-localization and expansion of the region of Blimp1 induction. In contrast to Nodal signalling, lack of Bmp signalling via *Smad4* and *Smad1* in the epiblast leads to a failure to robustly induce Blimp1, whereas lack of either gene in the VE does not overtly affect Blimp1 induction. Finally, I clarify that *Prdm1* expression (encoding Blimp1) in the VE is

dispensable for Blimp1 induction in PGCs and for embryonic development and is induced independently of *Smad1/Smad4/Smad2/Eomes*. Collectively, my results have identified antagonistic roles of tissue-specific Nodal signalling and Bmp signalling in Blimp1 induction. They suggest that competence to induce the primordial germ cell fate is dependent on the interplay of Nodal and Bmp-dependent Smad signals.

4.2 Discussion of project I

Previous genetic analyses of cooperative Smad2/3 functions have focused on early mouse embryos. They showed that loss of Smad2/3 leads to a block in embryonic development prior to cavitation and gastrulation (Dunn et al. 2004). Here, I refine the underlying cause of this differentiation block *in vitro* using combined genetic ablation of Smad2/3 in ES cells.

4.2.1 Are Smad2/3 functions dispensable in undifferentiated ES cells?

Nodal$^{-/-}$ ES cells can be maintained and are pluripotent, as they can differentiate into tissues of the three germ layers and germ cells (Conlon et al. 1991). TGFβ signalling is mediated by multiple and redundant ligands and ablation of individual ligands thus does not unambiguously prevent signalling. Furthermore, the intracellular Smad2/3 signalling machinery in *Nodal*$^{-/-}$ ES cells is intact and in chimeras *Nodal*$^{-/-}$ cells can respond to Nodal signals from wild type ES cells. Furthermore, the original characterization of *Nodal*$^{-/-}$ ES cells was done on cells cultured exclusively on feeders in fetal calf serum-containing medium, thus exposing cells to a variety of cytokines. Here, I refined the role of Nodal signalling in ES cells by demonstrating that the intracellular effectors of Nodal/TGFβ/Activin signalling, Smad2/3, are not functionally implicated in self-renewal or pluripotency marker expression both in serum-free and serum-dependent culture without feeders. Other studies that have assessed the role of Nodal and Bmp signalling in undifferentiated ES cells came to similar conclusions about the dispensable role of TGFβ signalling in undifferentiated ES cells (James et al. 2005, Gomes Fernandes et al. 2016).

Intriguingly, two other studies assessing Smad2/3 and Smad4 signalling in ES cells reported interdependence of Nodal and Bmp signalling in undifferentiated ES cells (Galvin et al. 2010, Costello et al. 2009). Galvin et al. showed that treatment of ES cells with 5 μM SB431542 (which blocks Alk4/5/7 receptors upstream of Smad2/3) reduced p-Smad2 levels, but elevated levels of p-Smad1/5 and transcript levels of the Bmp downstream targets *Idb1/2/3* as well as the TE markers *Ascl2* (*Mash2*) and *Gata2*, whereas Activin A treatment had the opposite effect (Galvin et al. 2010). Costello et al. similarly showed genetically that *Smad4*$^{-/-}$ ES cells down-regulated *Idb1/2/3* transcripts as well as *Gdf1*, *Tgfb2* ligand and the Nodal antagonist *Lefty2*. Intriguingly, gastrulation markers including *T*, *Fgf8*, *Sp5* and modulators of the extra-cellular matrix were also down-regulated in the undifferentiated state, whereas early ICM markers *Zscan4* and *Tbx3* and VE marker transcripts *Dpp4, H19* and *Gata6* were up-regulated (Costello et al. 2009).

Both these studies used fewer biological replicates and less stringent criteria in their profiling experiments than in the current study. The strength and weakness of my experimental setup with four biological clones for each genotype is clonal variation. When I assessed averaged transcript changes that were greater than two fold but not statistically significant due to clonal variation, undifferentiated *Smad2/3*$^{-/-}$ ES cells also up-regulated *Idb1/2/3* as well as *Plac1* and *Cops8,* the latter of which were among the top 20 up regulated transcripts at later time-point of my analysis (see Tables 7 and 8 and File S2a and S2b). Among these, only *Idb1* was statistically significant. Similarly, the Nodal antagonists *Lefty1/2* and the Nodal target *Pitx2* were down regulated and later among the top 20 down-regulated transcripts, but not significantly altered in undifferentiated *Smad2/3*$^{-/-}$ cells (see Files S2a and S2b). *Smad2*$^{-/-}$ and *Smad3*$^{-/-}$ undifferentiated ES cells showed a similar trend in mis-regulation of transcripts which became statistically significant at later time-points. This interpretation was further supported by the assessment of relative expression levels and expression level changes in individual clones (see Files S3 and S4). As statistically significant changed transcript levels in undifferentiated ES cells did not suggest a changed state, future experiments will assess a possible interdependence of Nodal and Bmp signalling on a protein level by probing

undifferentiated *Smad2/3*$^{-/-}$ ES cell clones by Western blotting using the p-Smad1/5/8 antibody validated in section 3.8.3.

Clonal variation was not restricted to my transcriptional analysis, as my colony formation assay also showed considerable variance between individual clones as well as between wild type, *Smad3*$^{-/-}$, *Smad2*$^{-/-}$ and *Smad2/3*$^{-/-}$ ES cells (see Fig 11b). As Nodal and Bmp signalling have been implicated in the modulation of cell proliferation and self-renewal (Ying et al. 2003, Mishina et al., 2002, James et al. 2005, Li et al. 2013, Zhu et al. 1998), future experiments aim to extend my analysis by performing a commercial cell proliferation assay. It will further be interesting to see whether chromatin architecture in undifferentiated ES cells is altered upon loss of Smad2/3 (see below).

4.2.2 To what extent do cooperative Smad2/3 signals drive embryonic differentiation?

Loss of *Smad2/3* (and to a lesser extent also of *Smad2*) in ES cells affects embryoid body formation. Even though *Smad3*$^{-/-}$ ES cells aggregated to form EBs, *Smad2/3*$^{-/-}$ EBs quickly became growth retarded, showed a disorganized outer extra-embryonic endoderm layer and failed to cavitate (Figure 12). This phenotype was also seen for *Smad2*$^{-/-}$ EBs. This requirement of Smad2/3 for EB formation could be conserved in human, as EBs formed from hESCs treated with the Alk4/5/7 inhibitor SB431542 were also described as abnormal (James et al. 2005). Signalling between the outer and inner EB layers have been shown to be required for cavitation (Coucouvanis and Martin 1995). It is thus likely that this phenotype arises from a failure of signalling between the two layers, especially since Smad2 has essential roles in the extra-embryonic visceral endoderm tissue (Waldrip et al. 1998). We employed transcriptional profiling to investigate the cause for this morphological defect.

4.2.2.1 Cooperative Smad2/3 signals drive mesoderm and endodermal cell fate specification

Transcriptional profiling of *Smad2/3*$^{-/-}$ EBs showed a severe block in endoderm and mesoderm differentiation. In agreement with the published *Smad2* mutant phenotypes

(Waldrip et al. 1998, Tremblay et al. 2000, Vincent et al. 2003a, Costello et al 2011), *Smad2*$^{-/-}$ EBs also blocked endoderm specification but did not affect mesoderm differentiation. Smad2/3-regulated transcripts represent a useful resource for further studies, as genetic ablation in my experiment - in contrast to use of Alk4/5/7 inhibitors - allows specific assessment of Smad2/3-regulated genes. My preliminary analysis of the observed gene expression changes indicates that Smad2 contributes to the activation of primed pluripotency marker expression and endodermal transcripts, while it represses naïve pluripotency markers and prevents expression of extra-embryonic trophectodermal markers. Surprisingly, I detected a strong contribution of *Smad3* to mesoderm and a subset of endoderm differentiation.

4.2.2.2 The contradictory role of Smad3 in the mouse embryo and in differentiating ES cells

Viability of *Smad3* null mice (Datto et al. 1999, Yang et al. 1999, Zhu et al. 1998) contradicts the observed effects upon loss of *Smad3* in EB differentiation and suggest that this finding does not translate into a requirement of *Smad3* for early differentiation in the embryo *in vivo*. In agreement with this scenario, EB growth and morphology were unaffected by *Smad3* ablation. Furthermore, OneStep analysis indicated comparable induction of marker transcripts in wild type and *Smad3*$^{-/-}$ EBs. Also, expression changes detected in *Smad3*$^{-/-}$ EBs via transcriptional profiling were less pronounced than in *Smad2/3*$^{-/-}$ EBs. Possible scenarios that could explain this discrepancy include altered differentiation dynamics due to cooperative functions of Smad3 with Smad2 in the early embryo (Dunn et al. 2004) that are resolved during subsequent development. As Smad3 null mice are viable, early developmental stages of mutants have not been assessed (Datto et al. 1999, Yang et al. 1999, Zhu et al.1998). In addition, the use of Activin A used in *in vitro* experiments might not recapitulate the complex actions of multiple ligands (including Nodal, Gdfs and Activins) in the early embryo *in vivo*. Thus, *in vitro* differentiation is an imprecise model for assessing gene function *in vivo*. For example, Bogani et al. showed that loss of *Prdm4* affects pluripotency marker gene expression in ES cells but does not perturb embryonic development (Bogani et al. 2013).

Clonal variation among individual *Smad3*$^{-/-}$ clones did not allow identification of substantial significant changes in the *Smad3*$^{-/-}$ undifferentiated state. Averaged clones showed ≥ 2 fold but non-significant up-regulation of differentiation markers including *Wnt8a*, *T* and *Fst*, whereas naïve pluripotency markers *Dppa3/Stella*, *Fbxo15* and *Tcl1* were down-regulated (see File S2b). These expression changes could bias *Smad3*$^{-/-}$ ES cells to a differentiation-prone state. Furthermore, the degree of clonal variation in *Smad3*$^{-/-}$ ES cell lines could differ from *Smad2*$^{-/-}$ ES cell lines, as CRISPR-Cas9-modified and conventionally generated null cell lines were compared (see chapter 5).

4.2.2.3 Are *Smad2/3*$^{-/-}$ cells capable of inducing neural or germ cell fates?

EB differentiation in serum-containing medium favours mesodermal and endodermal differentiation, while populations of neural or germ cell fates are not specifically enriched (Wiles and Keller, 1991, Ying et al. 2003, West et al. 2006). Future experiments will therefore exploit directed differentiation protocols towards serum-free neural (Ying et al. 2003, Abranches et al. 2009, Tesar et al. 2007, Iwafuchi-Doi et al. 2012) and germ cell fates (Hayashi et al. 2011, see section 3.8.1) followed by qRT-PCR analysis to assess the extent to which loss of Smad2/3 signalling affects induction of these fates. *Smad2/3*$^{-/-}$ PGCLCs will also be screened for the induction of protein levels of the germ cell markers Blimp1, Stella or AP2γ staining (see section 3.8.1 and 3.8.3).

a. Neural fate

Inhibition of Smad2/3 signaling with the ALK4/5/7 inhibitor SB431542 in EpiSCs (Inman et al. 2002) leads to acquisition of neural identity and *Nodal*$^{/-}$ embryos (that exhibit reduced Bmp signaling, Mesnard et al. 2006) convert to a neural fate (Camus et al. 2006, Vallier et al. 2009). *Smad2/3*$^{-/-}$ EBs exhibit enhanced expression of Bmp-dependent *Idb1/3/4* transcripts suggesting that Bmp signalling is enhanced upon loss of Smad2/3. As Bmp signalling blocks neural differentiation (Ying et al. 2003), it therefore seems unlikely that Smad2/3 mutants adopt a neural fate. At the present time, I cannot, however, exclude that *Smad2/3*$^{-/-}$ ES cells adopt a neural fate upon differentiation, as the respective experiment has not been done. Genetic ablation of Smad2/3 does, however,

represent a better system to assess specific Smad2/3 functions in cell fate specification than pharmacological inhibition of Alk4/5/7 (Vallier et al. 2009), thereby allowing a definitive answer to this question.

b. Germ cell fate

Single cell transcriptional profiling of ~E6.75 Blimp1^{+} pPGCs identified transcripts enriched and repressed in PGCs and their somatic neighbours. It also included the down regulation of EMT-associated transcripts *Snai1*, *Fgfr1*, *Cdh2* and *Vim* in pPGCs (Kurimoto et al. 2008). *Eomes* in the epiblast is required for EMT and acts downstream of *Nodal* (Brennan et al. 2001). Smad2/3 binds to the *Eomes* locus during human endoderm differentiation (Teo et al. 2011). Smad2 mutants expand *Eomes* expression in the epiblast (Brennan et al. 2001). *Smad2/3*$^{-/-}$ EBs display completely abolished *Eomes* expression suggesting that EMT is blocked upon loss of *Smad2/3*. Furthermore, enhanced Bmp signalling upon loss of *Smad2/3* could block EMT, as *Idb1* has been implicated in *Cdh1* (*E-Cadherin*) maintenance in the epiblast prior to gastrulation (Malaguti et al. 2013). In agreement with this hypothesis, *Smad2/3*$^{-/-}$ EBs have a lower expression level of *Snai1*, *Cdh2* and *Vim* than wild type controls (File S2). Whether this allows *Smad2/3*$^{-/-}$ EBs to enter the germ cell fate remains an open question. As *Nanog* has been implicated in germ cell specification (Murakami et al. 2016), it would be interesting to investigate whether lowered Nanog levels in *Smad2/3*$^{-/-}$ EpiLCs translate into an inability to re-activate *Nanog* in PGCLCs (see also below).

4.2.3 Does the extra-embryonic fate represent the default state if embryonic cell fate is blocked?

The Smad2/3 double mutant phenotype *in vivo* suggested a model in which proper maintenance of the early post-implantation epiblast requires Smad2/3 signals, as the epiblast marker transcript *Oct4* was lost while trophectoderm was able to form (Dunn et al. 2004). Analysis of *Smad2/3*$^{-/-}$ ES cells and EBs refines this model by showing that *Smad2/3*$^{-/-}$ ES cells are viable and have limited differentiation potential upon LIF withdrawal. D3 *Smad2/3*$^{-/-}$ EBs showed statistically significant ~2-fold down-regulation

of *Oct4*. Similarly, treatment with 10 µM of the Alk4/5/7 inhibitor SB431542 did not down regulate Oct4 protein levels in ES cells in serum+LIF. However, Oct4 levels in the ICM upon blastocyst outgrowth for four days was reduced but not completely abolished (James et al. 2005). This suggests that Oct4 is initially induced in Smad2/3 mutants but lost by E7.5 (Dunn et al. 2004). In agreement with this interpretation, *Smad4*$^{-/-}$ EBs and *Smad4* mutants (Costello et al. 2009) as well as Nodal mutants induce *Oct4*, but in the case of *Nodal* mutants expression is not maintained (Brennan et al. 2001).

Oct4 protein levels are maintained during EB differentiation but display dynamic heterogeneity in subpopulations of cells (Sajini et al. 2012). In the mouse embryo, *Oct4* is expressed in the pre-implantation embryo but progressively declines in the TE during expansion of the blastocyst (Schöler et al. 1990). *Oct4* remains expressed in the early PrE, but declines upon differentiation into VE and PE (Palmieri et al. 1994). While the egg cylinder expresses *Oct4*, *Oct4* is maintained in the posterior epiblast (including the PGCs), but down-regulated in anterior parts of the embryo (Yeom et al. 1996, Kehler et al. 2004). From E8.5 onwards, *Oct4* becomes restricted to PGCs (Schöler et al. 1990). Thus, ablation of *Pou5f1* (encoding Oct4) leads to the formation of an inner cell mass that fails to acquire ICM characteristics and eventually diverts to a TE-like fate, that is unable to proliferate due to a lack of *Fgf4* (Nichols et al. 1998). Similarly, lowering Oct4 levels in ES cells leads to differentiation into TE, whereas a less than 2-fold increase is sufficient to drive PrE and mesoderm differentiation (Hay et al. 2004, Niwa et al. 1998, 2000). Thus, even slight changes in the expression of critical factors such as *Oct4* can promote loss of a particular cell fate.

Epiblast cells in the embryo and ES cells do not normally contribute to the TE lineage (Beddington and Robertson 1989). However, once LIF is removed from *Smad2/3*$^{-/-}$ ES cells and EB formation is initiated, cells start to up-regulate both trophectodermal and extra-embryonic endoderm markers. It remains unclear whether undifferentiated *Smad2/3*$^{-/-}$ ES cells are already predisposed for this lineage diversion, as clonal variation obscures the analysis (see 4.2.2). Galvin et al. also showed up-regulation of trophectodermal markers *Ascl2/Mash2* and *Gata2* upon SB431542 treatment of ES cells

(Galvin et al. 2010). Similarly, another study used the same inhibitor or recombinant Lefty2 to induce trophectodermal markers in ES cells (Lee et al. 2011). Does the TE fate therefore represent the default state? Attempts by Davor Solter's lab showed that repeatedly mechanically separated blastomeres from the 2-cell stage through to the 32-cell stage exhibited transcriptional profiles with selective loss of some but not all ICM characteristics, while selective TE markers became expressed (Lorthongpanich et al. 2012). This suggested that individual blastomeres are biased towards the TE fate if cell-cell interactions are reduced. This is in agreement with recent experiments attributing TE-ICM segregation with cell-cell interactions (Maître et al. 2016). *Smad2/3*$^{-/-}$ EBs do not show up-regulation of crucial TE markers such as *Eomes* and *Elf5* (Russ et al. 2000, Strumpf et al. 2005, Latos et al. 2015), while core pluripotency genes are only partially affected. I therefore prefer a model in which the lack of Smad2/3 signalling does not lead to a complete fate diversion, but to the acquisition of an extra-embryonic-like state. Beyond the scope of this thesis, it would be interesting to test the cell fate diversion of *Smad2/3*$^{-/-}$ ES cells during differentiation *in vivo*. To this end, contribution to the extra-embryonic lineages could be assessed in Smad2/3<>wild type chimeric embryos.

4.2.4 Could Smad2/3 signalling mediate enhancer switching during the acquisition of primed pluripotency?

It remains unclear whether the ability of *Smad2/3*$^{-/-}$ ES cells to differentiate is blocked at its earliest stages. Analysis of transcriptional changes in *Smad2/3*$^{-/-}$ EBs by OneStep indicated a block in inducing markers of embryonic differentiation, whereas selected differentiation markers (*T* and *Fgf5*) were barely induced in Activin A-treated *Smad2/3*$^{-/-}$ EBs. Similarly, expression dynamics of the top 20 differentiation genes indicated that a subset of differentiation-associated transcripts are weakly induced at d2 but reduced or lost by d3. This suggests that expression of marker transcript of primed and differentiated states can be initiated at least to some extent. My preliminary analysis of *Smad2/3*$^{-/-}$ EpiLCs suggested that the underlying differentiation defect of *Smad2/3*$^{-/-}$ EBs could originate from incomplete lineage priming. Smad2/3 and Smad4 are required for EpiSC maintenance. ES-specific (but not EpiSC-specific) enhancers exhibit Smad2/3 and Smad4 binding motifs suggesting a potential involvement of Smad2/3 in the repression

of naïve pluripotency genes (Tesar et al. 2007, Brons et al. 2007, Factor et al. 2014). During the transition from naïve to primed pluripotency in EpiLCs enhancer chromatin landscapes change concomitant with a re-localization of Oct4, p300 and H3K27ac from naïve to EpiLC enhancers (hereafter referred to as 'ES' and 'primed' enhancers, Buecker et al 2014). Overexpression of the transcription factor Otx2, which interacts with Oct4 in EpiLCs, can partially recapitulate this enhancer switch, but does not lead to Otx2 binding to 'ES' enhancers suggesting a secondary role of Otx2 in the acquisition of lineage priming (Buecker et al 2014). Consequently, *Otx2*$^{-/-}$ ES cells initiate lineage priming but lack a subset of EpiLC induced transcripts including *Fgf5* and *Oct6* and are unable to maintain the EpiSC state due to premature neural progenitor differentiation (Buecker et al 2014, Acampora et al. 2013). Thus, Otx2 requires cooperative functions of other factors to mediate the transition from the naïve to a primed state of pluripotency both in the embryo and *in vitro*. In support of this hypothesis, *Otx2*$^{-/-}$ embryos initiate gastrulation, but fail to induce and specify prechordal mesoderm and anterior neural tissues due to requirements of independently regulated Otx2 isoforms in the VE and anterior epiblast (Acampora et al. 1995 and 2009, Matsuo et al. 1995, Ang et al. 1994b, 1996, Rhinn et al. 1998). Due to this role of Otx2 *in vivo*, ES cells or embryo-derived *Otx2*$^{-/-}$ EpiSCs failed to differentiate further along the neural fate despite the induction of neural progenitors (Acampora et al. 2013). Interestingly, loss of *Otx2 in vivo* does not lead to premature neural induction and it has been argued that EpiSCs lack exposure to Bmp signals present in the embryo that normally prevent neural differentiation (Acampora et al. 2013).

Smad2/3 mutants arrest earlier than Otx2 mutants (Dunn et al. 2004, Ang et al. 1996). I show here that *Smad2/3*$^{-/-}$ ES cells lack the ability to induce robustly marker transcripts of embryonic lineages during differentiation *in vitro* and to down-regulate a subset of primed pluripotency markers. I therefore hypothesize that Smad2/3 could mediate enhancer switches during the acquisition of primed pluripotency. In order to test this hypothesis, chromatin accessibility in *Smad2/3*$^{-/-}$ EpiLCs could be assessed by ATAC-seq and compared to wild type controls. Ideally, transcriptional profiles would be assessed in parallel to compare architectural change with differential gene expression.

At present, my preliminary analysis shows that d3 *Smad2/3*$^{-/-}$ EBs significantly down-regulated *Otx2* (4-fold) and *Oct4* (2-fold), whereas *Otx2* and *Oct4* transcripts in *Smad2/3*$^{-/-}$ EpiLCs remained unchanged. It is not clear whether repressed *Otx2* reflects *Otx2* expressed in the neuroectoderm or early epiblast/VE. It will be interesting to investigate whether loss of Smad2/3 affects Otx2-dependent aspects of lineage priming. First, I will assess protein level of Oct6 and Otx2 (Buecker et al. 2014). To confirm that *Smad2/3*$^{-/-}$ EpiLCs do not recapitulate the diversion to an extra-embryonic-like fate that I observed in *Smad2/3*$^{-/-}$ EBs, I will also assess protein levels of the trophectodermal marker Cdx2 (Beck et al. 1995).

Preliminary comparison of deregulated transcripts in d3 *Smad2/3*$^{-/-}$ EBs and *Otx2*$^{-/-}$ EpiLCs revealed common down-regulation of *Fgf5*, whereas *Klf2* was commonly up regulated (Buecker et al. 2014). No major other overlap is evident (data not shown). Genomic loci encoding top affected transcripts in my *Smad2/3*$^{-/-}$ EB and EpiLC differentiation screen (including *Fgf5*, *Nanog* and *Klf2*) show proximal Smad2/3 binding at 'ES' and 'primed' enhancers (as defined by DNaseI hypersensitive sites and binding of Otx2 and Oct4, Buecker et al. 2014) in ES cells and differentiated definitive endoderm, respectively (Yoon et al. 2015, Mullen et al. 2011). It will be interesting to investigate whether differential Smad2/3 binding is functionally involved in enhancer switches during the acquisition of lineage priming. Interestingly, comparison with Smad1 ChIP-seq data in mouse ES cells revealed that Smad1 co-occupies the 'ES' enhancer of the *Nanog* locus together with Oct4 and Smad2/3 (Chen et al. 2008). It is tempting to speculate that Smad2/3 and Smad1 could be involved in the antagonistic regulation of target genes in the undifferentiated and primed state. In support of this hypothesis, loss of *Smad1/5* elevated DNA methylation levels in undifferentiated, naïve ES cells and increased the propensity of ES cells to differentiate. This implicates Smad1/5 signalling as a negative regulator of lineage priming (Gomes Fernandes et al. 2016).

As DNA methylation changes have been implicated in different pluripotency states *in vitro* and *in vivo* (Habibi et al. 2013, Hackett et al. 2013, Smallwood et al. 2014, Smith et al. 2012), it is interesting to speculate whether Smad2/3 antagonistically influences DNA

methylation during the acquisition of the primed state. I have not assessed DNA methylation changes, but d3 *Smad2/3*$^{-/-}$ EBs down-regulated *Dnmt3b* (a de novo DNA methyltransferase, Okano et al. 1999) by ~2.7-fold, whereas *Dnmt3l* was ~4-fold up-regulated. ~4-fold elevated *Dnmt3l* transcripts levels were also observed in d3 *Smad2*$^{-/-}$ EBs further strengthening the involvement of Smad2 in a possible lineage priming defect. Moreover, *Dnmt3l* is significantly up-regulated compared to controls in *Smad2/3*$^{-/-}$ EpiLCs. Dnmt3l lacks DNA methyl transferase activity and is thought to establish maternal imprints as embryos from female *Dnmt3l*$^{-/-}$ mice die at mid-gestation due to placental defects (Bourc'his et al. 2001, Hata et al. 2002, Arima et al. 2006). The trophectodermal lineage is hypo-methylated and loss of the DNA methyl transferase Dnmt1 leads to trophectodermal marker expression (Ng et al. 2008, reviewed in Hemberger et al. 2009). As *Smad2/3*$^{-/-}$ EBs up-regulate trophectodermal markers it is thus difficult to attribute expression changes of transcripts for DNA methyltransferase to lineage priming.

4.2.5 Could Smad2/3 and Smad1 signalling antagonistically regulate Nanog expression during the transition from pluripotency to differentiation?

EpiLC differentiation leads to a decrease in *Nanog* transcript and protein expression (Hayashi et al. 2011). In my experiments, Nanog protein levels decreased during EpiLC differentiation in wild type and *Smad2/3*$^{-/-}$ alike, whereas *Nanog* transcript was significantly reduced in *Smad2/3*$^{-/-}$ EpiLCs compared to wild type controls. In the mouse embryo, *Nanog* is expressed from compaction onwards (Chambers et al. 2003, Dietrich and Hiiragi, 2007). It subsequently becomes restricted to the ICM and nascent epiblast, but is down-regulated following implantation (Chambers et al. 2003). Nanog is reactivated specifically in the posterior epiblast in the post-implantation embryo and is lost as cells delaminate to move through the primitive streak (Hart et al. 2004, Osorno et al. 2012, Sun et al. 2014, Hoffman et al. 2013). Expression is completely lost at the onset of somitogenesis and persists only in primordial germ cells (Chambers et al. 2003, Yamaguchi et al. 2005). Loss of *Nanog* leads to degeneration of the ICM and failure to form an epiblast (Mitsui et al. 2003, Silva et al. 2009). Intriguingly, Bmp and Nodal signalling have been reported to maintain heterogeneous Nanog expression in ES cells (Galvin-Burgess et al. 2013). Similar to *Nanog* reactivation in the posterior epiblast and

PGCs, *in vitro* differentiation into PGCLCs leads to reacquisition of *Nanog* expression at the transcriptional level via assessment of a *Nanog* reporter transgene (Hayashi et al. 2011, Murakami et al. 2016). Induction of *Nanog* has, however, only been documented in iPS cell-derived PGCLCs (Hayashi et al. 2011). As I plan to assess the induction of the germ cell fate in *Smad2/3*$^{-/-}$ PGCLCs and also *Smad1*$^{-/-}$ ES cell lines (see above) *Nanog* reactivation in these lines could be assessed in parallel. If wild type PGCLCs fail to induce Nanog expression, differentiation of ES cells into EpiSCs could provide an alternative system to assess effects on Nanog expression as these cells express Nanog protein (Hayashi et al. 2011, Guo et al. 2009).

In conclusion, my experiments show that Smad2/3 signals are dispensable for viability and self-renewal in ES cells, but are required for Smad2/3-mediated TGFβ signalling at the onset of embryonic differentiation. I demonstrate that Smad2/3 signals sustain embryoid body growth and that cooperative Smad2 and Smad3 functions are required for mesodermal and endodermal cell fate specification. In the absence of Smad2/3 signals, differentiating ES cells divert to an extra-embryonic-like state. Preliminary analysis of *Smad2/3*$^{-/-}$ EpiLCs indicates that Smad2/3 might be required for lineage priming prior to differentiation as critical markers of the primed state including *Fgf5* were down-regulated. Ongoing and future studies will be required to provide mechanistic insights into how Smad2/3 binding regulates this critical event in lineage priming in EpiLCs and in the early mouse embryo.

4.3 Discussion of project II

4.3.1 T-box transcription factors in the induction of Blimp1 in primordial germ cell specification

A recent report suggested that T-box factors could mediate initial induction of *Prdm1* expression (encoding Blimp1) in pPGCs, as the *Prdm1* locus contains a putative T-box-regulated enhancer. This enhancer is bound by the T-box factor Brachyury/T during PGC specification to reinforce Blimp1 expression (Aramaki et al. 2013). T-box transcription factors are defined by their T-box DNA recognition domain (Herrmann et al. 1990, Kispert and Herrmann 1993, Kispert et al. 1995, reviewed in Papaioannou 2014). At ~E5.5 - E6.25, when cells of the posterior epiblast acquire competence to induce Blimp1$^+$ pPGCs, only four of the 17 known T-box factors in mice are expressed. These are *Eomes*, *T*, *Tbx3* and the *MAX associated protein (Mga)* (Papaioannou 2014). As *Eomes* is expressed prior to *T* in the posterior epiblast (Simon et al. 2017), I sought to investigate its involvement in activation of Blimp1 in pPGCs. Contrary to previous speculation (Aramaki et al. 2013), I demonstrate here that the T-box factor Eomes in the epiblast and visceral endoderm is dispensable for initial Blimp1 expression.

Preliminary data from my colleague Dr Ita Costello show that Tbx3 protein is excluded from pPGCs at E6.5. *Tbx3*, which was shown to be expressed later in established late-streak stage PGCs (Kurimoto et al. 2008), probably does not bind to the T-box site at the *Prdm1* locus at this early time-point. Unique among the T-box factors, *Mga* contains a basic helix-loop-helix (bHLH) domain (Hurlin et al. 1999). *Mga* is expressed in the E5.5 - E6.5 epiblast, but its role in the early post-implantation embryo is as yet undefined. Homozygous mutant embryos arrest at peri-implantation stages and *Mga*$^{-/-}$ ES cells cannot be maintained (Washkowitz et al. 2015). *Mga*$^{-/-}$ blastocysts also failed to maintain Nanog$^+$ cells (a marker of the pluripotent inner cell mass) during diapause (Washkowitz et al. 2015). Thus, the present data do not support involvement of T-box factors in initial Blimp1 induction. Investigation of *Mga* awaits further study. Interestingly, *Mga* was identified as a repressor of germ cell-related gene expression in a RNAi screen in ES cells that assessed *Vasa* reporter gene expression (Maeda et al. 2013). However, in mice *Vasa* is not expressed in early PGCs (Fujiwara et al. 1994). It would be interesting to assess *Mga* expression e.g. by WISH in *Smad1Δepi* and *Smad2ΔVE* mutant embryos in which

Blimp1 expression is either drastically reduced or expanded to see whether *Mga* expression is altered in either context.

4.3.2 What is the role of Nodal signalling in primordial germ cell specification?

In this thesis I show that *EomesΔepi* mutants accumulate abundant Blimp^{+} cells in epithelial cells within the posterior epiblast. Epiblast cells in *EomesΔepi* mutants fail to undergo EMT and down-regulate E-Cadherin (Arnold et al. 2008). E-Cadherin function has been implicated in establishment of the germ cell fate (Okamura et al. 2003). Interestingly, not all accumulating posterior epiblast cells in *EomesΔepi* mutants become Blimp1^{+} cells suggesting that the escape from EMT at gastrulation and the continued expression of E-Cadherin is not the instructive signal for the pPGC fate (Kurimoto et al. 2008). Interestingly, Bmp signalling via *Idb1* inhibits E-Cadherin expression, blocks EMT and inhibits neural differentiation, but PGC formation was not assessed (Malaguti et al. 2013). *EomesΔepi* mutants expand *Bmp4* expression from the ExE into the posterior epiblast (Arnold et al. 2008). Eomes acts downstream of Nodal and Smad2/3 signals in both the epiblast and VE (Brennan et al. 2001, Nowotschin et al. 2013 and present data in chapter 2). *Smad2* mutants express abundant *Eomes* in the epiblast (Brennan et al. 2001), and *Bmp4* expression is also expanded into the epiblast. D2 *Smad2*$^{-/-}$ EBs also up regulate *Idb1* suggesting that the up-regulation of Bmp signalling is ultimately Smad2-dependent (Waldrip et al. 1998 and the present data). *Smad2/3*$^{-/-}$ EBs also enhance Bmp signalling via *Idb1* (and *Idb2/3* and *Idb2/4*, respectively). Furthermore, antagonistic Smad1 and Smad2 functions in DVE specification have been described (Yamamoto et al. 2009). It is tempting to speculate that compromising Nodal signalling via Smad2 and Eomes in the VE enhances Bmp signalling.

In agreement with this, *Smad2ΔVE* mutants phenocopy *Smad2* mutants. Both show enhanced expression of Blimp1 within the epiblast, which defaults entirely to posterior extra-emvbryonic mesodermal streak fates in response to the lack of an AVE (Waldrip et al. 1998). In *EomesΔVE* mutants induction of the primitive streak occurs radially throughout the proximal epiblast due to an AVE migration defect. As a result Blimp1^{+}

cells mis-localize. At present, my analysis of *EomesΔVE* mutants by sectioning and immunohistochemistry alone has not allowed me to draw conclusions about the 3D distribution of possibly enhanced numbers of Blimp1$^+$ cells. To extend this analysis, I am currently collaborating with Dr Ita Costello to assess whole-mount Blimp1 induction in the conditional mutant embryos described in this chapter. I have established triple-mutant male mice harbouring mutant alleles, conditional deleter transgenes and the *Prdm1.Venus* transgenic reporter (Ohinata et al. 2008, see section 3.2.2) in combination with homozygous female conditional strains. To complete the analysis of Smad2 and Eomes-dependent tissue-specific Nodal signalling in Blimp1 induction, we will assess Blimp1$^+$ cells using *Prdm1.Venus* fluorescence and confocal imaging.

Co-staining with an antibody specific for the PGC marker Stella (Sato et al. 2002, see section 3.8.3) will allow me to assess whether Blimp1$^+$ cells are also Stella$^+$ and thus indicate whether specification of the PGC fate has occurred. This analysis will enable me to draw conclusions about the expansion of the Blimp1$^+$ cluster formed in *Smad2ΔVE* and *EomesΔepi* and confirm the almost complete lack of Blimp1$^+$ cells in *Smad4Δepi* and *Smad1Δepi* mutants. Furthermore, Blimp1$^+$ cells in *Smad4ΔVE* and *Smad1ΔVE* mutants can be verified as PGCs to clarify that VE-derived Smad1 and Smad4 signals are dispensable for PGC specification.

To further test the hypothesis of antagonistic Nodal and Bmp signalling, future experiments will assess p-Smad1/5/8 activation with a specific antibody in whole-mount *Smad2ΔVE*, *EomesΔepi* and *EomesΔVE* (and potentially also *Smad2Δepi*) mutants. If resolution on a single-cell level will be required to draw conclusions, I will apply p-Smad1/5/8 staining on sections as established in section 3.8.3.

If p-Smad1/5/8 staining shows an expansion of Bmp signalling, it will be interesting to assess expression of VE-expressed Bmp ligands such as Bmp2 and Bmp target genes in the epiblast (such as Idb proteins, Malaguti et al. 2013) as well as Gdf1 or Gdf3. Gdf1 and Gdf3 have also been reported to act as Bmp inhibitors. They are expressed at gastrulation stages and could mechanistically link both pathways (Levine et al. 2006, 2009,

Fuerer et al. 2014, Andersson et al. 2006). Furthermore, it would be interesting to assess antagonistic roles of Smad2 and Smad1 signalling on the expression of Nanog and Sox2. The latter have been implicated in promoting or inhibiting the germ cell fate, respectively. Furthermore, it has been suggested that Nanog and Sox2 are influenced by Bmp and Nodal-dependent signalling in other systems (Murakami et al. 2016, Hayashi et al. 2011, Kurimoto et al. 2008).

If this analysis points to a possible mechanism, I plan to use established mutant ES cell lines harbouring the *Prdm1.Venus* reporter as well as *Smad2* and *Smad4* lines currently being generated (see section 3.8.2) and apply the PGCLC differentiation protocol validated in section 3.8.1 and/or XENLC differentiation to further characterize antagonistic actions. At this point, the focus is likely going to lie on antagonistic effects of Smad2 and Eomes in comparison to Smad1 and Smad4 on germ cell marker and possible antagonists induction. It would also be possible to sort Blimp1.Venus^{+} cells from mutant PGCLCs (using a protocol modified form the established protocol in section 3.8.4) to compare different mutant to wild type via transcriptional profiling.

To assess transcriptional signatures of ectopically formed presumptive PGCs in *EomesΔepi* mutants or *Smad2ΔVE* mutants, Blimp1.Venus^{+} positive cells from mutant embryos also harbouring the *Prdm1.Venus* transgene (see 3.8.4) could also be subjected to FACS or manually be picked for single-cell RNA profiling.

At this point, enhancers of *Prdm1* locus are ill-defined. A central focus of my experiments has been to explore the hypothesis put forward by Aramaki et al. that PGC fate is mediated via T-box proteins (Aramaki et al. 2013). My experiments suggest this is not the case, as I have shown genetically that Eomes is dispensable both in the VE and epiblast for activation of Blimp1 transcription in pPGCs. Formal proof of this will require deletion of the putative T-box enhancer to test the effect on Blimp1 expression. Future studies using conventional transgenic approaches will be required to identify enhancer regions critical for Blimp1 activation in pPGCs.

5

Methods

5.1 Mice and embryos

5.1.1 Mouse strains and alleles

Table 11 Mouse strains and alleles.

Mouse strain symbol in this thesis	MGI allele name	Reference
Smad1^{RobPC}	*Smad1*^{RobPC}	Tremblay et al. 2001
Smad2^{-}	*Smad2*^{Robm1}	Waldrip et al. 1998
Smad2^{CA}	*Smad2*^{RobCA}	Vincent et al. 2003a
Smad3^{tm1Xfw}	*Smad3*^{tm1Xfw}	Datto et al. 1999
Smad4^{-}	*Smad4*^{RobN}	Chu et al. 2004
Smad4^{CA}	*Smad4*^{RobCA}	Chu et al. 2004
Smad5^{-}	*Smad5*^{m1}	Chang et al. 1999
Eomes^{-}	*Eomes*^{N}	Arnold 2008
Eomes^{CA}	*Eomes*^{CA}	Arnold 2008
Eomes.GFP	*Eomes*^{GFP}	Arnold et al. 2009
Prdm1^{-}	*Prdm1*^{BEH}	Vincent et al. 2005
Prdm1^{CA}	*Prdm1*^{flox}	Shapiro-Shelef et al. 2003
Prdm1.Venus	*Prdm1*^{Venus*}	Ohinata et al. 2008
Wnt3^{-}	*Wnt3*^{tm1Brd}	Liu et al. 1999
Sox2.Cre or *(Δepi)*	*Sox2*^{Cre*}	Hayashi et al. 2002b
Ttr.Cre or *(ΔVE)*	*Ttr*^{Cre*}	Kwon and Hadjantonakis 2009
R26R	*Gt(ROSA)26Sor*^{tm1Sor}	Soriano 1999

transgenes and gene traps indicated as * and Gt, respectively, allele names were deduced from the MGI database (http://www.informatics.jax.org) or the listed reference. Null and conditional alleles in this thesis are predominantly abbreviated, e.g. *Smad1*^{Robm1} and *Smad1*^{RobCA} as *Smad1*$^{-}$ and *Smad1*^{CA}, respectively. Null alleles derived from Cre-excised conditional alleles are, in this case, abbreviated as *Smad1*^{CAN}. In several cases throughout this thesis, Cre-excised conditional alleles are identical to null alleles. Strains used in this thesis were maintained on a *C57BL/6* genetic background.

5.1.2 Animal breeding and timed matings

To obtain double heterozygous conditional deleter males (studs), heterozygous or homozygous *Sox2.Cre* and *Ttr.Cre* males were bred with heterozygous *Smad1*$^{-}$, *Smad2*$^{-}$, *Smad4*$^{-}$, *Smad5*$^{-}$, *Eomes*$^{-}$ or *Prdm1*$^{-}$ females. To introduce the *Prdm1.Venus* reporter transgene in these lines, double-heterozygous studs were bred with homozygous *Prdm1.Venus* females to obtain triple-heterozygous studs. Studs were mated to females carrying homozygous conditional alleles of the corresponding genotype to obtain a conditionally deleted allele in combination with a second null allele (here referred to as *Δepi* or *ΔVE*, respectively). As an example, a *Smad2*$^{-/+}$; *Ttr.Cre*$^{-/+}$ stud was mated to a *Smad2*$^{CA/CA}$ female to obtain 25% of embryos that are *Smad2*$^{-/CAN}$, *Ttr.Cre*$^{-/+}$. To obtain null embryos with or without the

Prdm1.Venus reporter transgene, heterozygous or double-heterozygous studs and females were generated. For timed matings, a vaginal plug in the morning was set as E0.5 and pregnant females were sacrificed at the desired developmental stage by a rising concentration of CO_2 followed by cervical dislocation. For large-scale experiments (e.g. flow cytometry), timed matings were set up with oestro-selected females (see Manipulating the mouse embryo 4th ed. p.103f). *Smad3*$^{tm1Xfw/tm1Xfw}$ animal tissue was obtained from viable homozygous offspring of *Smad3*$^{tm1Xfw/+}$ intercrosses.

5.1.3 Genotyping Primers

Table 12 Primer sequences used for genotyping.

Mouse Strain/allele	Primer sequences (5'->3')	Genotyping reference
Smad1^{CA}	F: CTCGTGACTTAAATGCTGCAC R: ATTATGTGGCTCCCCTCCCT Annealing temperature: 60°C. Products: WT 171BP, CA 221bp	*
Smad1^{-}	F: TCCTCATCAGAAAAGAACCCTAAGG R: TGGAGATAAATGTGCGATTCCG Annealing temperature: 57°C. Products: N 324bp	*
Smad2^{-}	F1: TGGCCTTAGAAAAGTTAATTGCCC R1: TATTGCTGAAGAGCTTGGCG R2: GCAAACCACAGCACACAACA Annealing temperature: 60°C . Products: WT 204bp, N 303bp	*
Smad2^{CA}	F: TTTCAAAACTATATTTGCCCAAG R: GCTTAAAAGTCACTACTCAAG Annealing temperature: 55°C. Products: WT 650bp, CA 700bp, N 200bp	Vincent et al. 2003a
Smad3^{tm1Xfw}	F1: CTCCAGAGTTAAAAGCGAAGTTCG R1: AAAATGCTGCACGGAAGCCAGGTC neo: ATTTGTCACGTCCTGCACGACG Annealing temperature: 60°C. Products: WT 489bp, N 347bp	Robertson lab manual
Smad4^{-} *Smad4*^{CA}	F1: CTTTTATTTTCAGATTCAGGGGTTC F2: AAAATGGGAAAACCAACGAG R: TACAAGTGCTATGTCTTCAGCG Annealing temperature: 52°C . Products: WT 625bp, CA 675bp, N 512bp	Chu et al. 2004
Smad5^{-}	F: GAGACTAGTGAGACGTGCTACTTCC R: TCTGGCCTCTTAATCCTGGACTTTC Annealing temperature: 60°C. Products: WT 700bp, N 520bp	Chang et al. 1999

(continued from last page)

Eomes^{N} *Eomes*^{CA}	F: CCTTACTTCCTAAGGCACACCTGTAGC R1: AGCTCAAACCGACTTCTTTCTGCTC R2: AATATGTCCTCAGGGAGATGATGACT Annealing temperature: 59°C. Products: WT 313bp, CA 356bp, N 435bp	Arnold et al. 2008
Eomes.GFP	F: AAGGAAAGGGGCACCTACAATC R1: AGCACTCTCCAGCGAGTAGAAGTG R2: CAGATGAACTTCAGGGTCAGCTTG Annealing temperature: 59°C. Products: WT 302bp, GFP 373bp	Arnold et al. 2009
Prdm1^{-}	F: TTGGTAAAGAAGTCTGCGGC R: ATTATACGAAGTTATGGATCATC Annealing temperature: 57°C. Products: N 188bp	Robertson lab manual
Prdm1.Venus	F: ACTCATCTCAGAAGAGGATCTG R: CACAGTCGAGGCTGATCTCG Annealing temperature: 55°C. Products: Venus ~200bp	Ohinata et al. 2008
Wnt3^{-}	F: GAAGACGCAATGGCATTTCTC R1: GACTTCCTCAAGGACAAGTACG R2: CCAACTTGTTCAAATTATTACCAGTG Annealing temperature: 61°C. Products: WT 309bp, N 300bp	Liu et al. 1999
Sox2.Cre	F: GCATAACCAGTGAAAGAGCATTGCTG R: GGACATGTTCAGGGATCGCCAGGCG Annealing temperature: 55°C. Products: Sox2.Cre 280bp	Robertson lab manual
Ttr.Cre	F: TCTTGCGAACCTCATCACTCG R: TTCTCTTGTCTCCTCTGTGCCCAG Annealing temperature: 55°C. Products: Ttr.Cre 187bp	Primers obtained from Ita Costello
R26R	F: TTACCAGGCCGAAGCAGCGTTGTTG R: GCGGCAGTAAGGCGGTCGGGATAGT Annealing temperature: 59°C. Products: LacZ 300bp	Robertson lab manual
Ube1x or *Ube1y1*	F: TGGATGGTGTGGCCAATG R: CACCTGCACGTTGCCCTT Annealing temperature: 57°C. Products: X-linked 253bp, Y-linked 335bp	Warr et al. 2009
3' SB probe Smad3	F: CAGGCGATGGTTCTGTCCTT R: GCCAGGGCAGGATTCAAGAT Annealing temperature: 65°C. Product: 564bp	*

*indicates that primer sequences were designed and optimized by myself.

 indicated usage of an alternative PCR mix, see PCR methods section.

See section 5.2.4 for lysis protocol. WT: wild type, CA: conditional, CAN: conditional null allele, N: null allele.

5.1.4 Isolation of blastocysts

E3.5 embryos were flushed out of uterine horns of timed mated females with FF ES medium using a syringe and needle (see Manipulating the Mouse Embryo 4th ed. p.146ff). Blastocysts were collected in a 3 cm dish and subsequently transferred to a drop of FF ES medium under mineral oil (see 5.4.1 for derivation of ES cell lines).

5.1.5 Isolation of early post-implantation stage embryos

E6.0-E8.5 embryos were dissected out of deciduae of timed mated females in PBS(-Mg_2Cl_2) supplemented with 1% FCS. Reichert's membrane was removed with needles (see Manipulating the mouse embryo 4th ed. p.159-166). For Blimp1 immunohistochemistry, whole deciduae were dissected out of uterine horns following removal of the outer muscular layer.

5.1.6 Isolating of genital ridges from E12.5 embryos

Female and male genital ridges of E12.5 embryos were dissected in PBS /1% FCS as described in Manipulating the mouse embryo 4th ed. p.175. Tail tips of embryos were used for confirmatory genotyping of the sex and lysed in 100ul ear lysis buffer (see below). Individual genital ridges were fixed in 4% PFA/PBS(-Mg_2Cl_2) at 4°C overnight and paraffin embedded (see below).

5.2 Molecular Biology

5.2.1 CRISPR/Cas9n

Two sets of four sgRNA to induce double-nicks 5' and 3' of exon 1 of murine *Smad3* were designed using the Zhang lab CRISPR design tool (http://crispr.mit.edu) taking care to avoid T-rich 3' ends and to keep offsets between nickase-sgRNAs < 10 bp. The PAM sequence was removed and *BbsI* sites engineered at the ends. Annealing standard desalted oligos, cloning into pX461 (Addgene®, Cas9n with GFP, see http://www.addgene.org/48140/, also Ran et al. 2013) using the *BbsI* site (FastDigest, Fermentas®) and transfection into Stbl3 cells (Invitrogen®) were performed in collabo-

ration with Dr Andy Basset. Dr Basset supplied me with sequence-verified mini preps of pairs of generated plasmids that had been positively screened by High Resolution Melt Analysis in N2A cells for inducing a cut. MaxiPreps of sgRNA plasmids with highest efficiencies (see Table 13) were performed and non-linearized plasmid DNA in elution buffer EB (Qiagen®) used for transfection into ES cells (see section 5.4.3).

Four independent clones of each established null ES cell line were used in subsequent experiments. These refer - in case of wild type and *Smad2*$^{-/-}$ - to individual ES cell lines derived from different blastocysts. In case of *Smad2/3* $^{-/-}$ and *Smad3*$^{-/-}$ lines, four independent clones represent individual CRISPR/Cas9n-modified deletion alleles that are all derived from a single *Smad2*$^{-/-}$ or wild type ES cell line. Hence the latter clones represent descendants from one single blastocyst. This discrepancy is inherent to the usage of established conventionally targeted or established wild type ES cell lines as controls for the *Smad3* CRISPR/Cas9n targeting.

Table 13 sgRNA primer sequences and CRISPR plasmid genotyping primer.

Location	**Primer sequences (5'->3')** (incl. *BbsI* overhang, target site in green)	**Application**	**Internal reference name**
Smad3 5' nick 1	F: CACCGCCCACGTGGGCCACCGGGTAGGG R: AAACTACCCGGTGGCCCACGTGGGC	sgRNA oligo	*Bassett C81 plasmid*
Smad3 5' nick 2	F: CACCGCGCTGGCGGCGCTGGGCGGGG R: AAACCGCCCAGCGCCGCCAAGCGC	sgRNA oligo	*Bassett C82B plasmid*
Smad3 3' nick 1	F: CACCGTGTCCCGCCCCACTCGAAGCGG R: AAACCCGCTTCGAGTGGGGCGGGACAC	sgRNA oligo	*Bassett C85 plasmid*
Smad3 3' nick 2	F: CACCGTCAGTACATTCTGTCAGATCTGG F: AAACCCAGATCTGACAGAATGTACTGAC	sgRNA oligo	*Bassett C86 plasmid*
CRISPR U6	F: GACTATCATATGCTTACCGT	Sequencing	*Synthesised by GATC*

5.2.2 RNA and DNA isolation

RNA was isolated using Qiashredder homogeniser (79654; Qiagen), RNeasy micro (74004; Qiagen, for EBs, EpiLCs and PGCLCs) or mini kits (74104; Qiagen, for ES cells) and RNase-Free DNase Set (79254; Qiagen) according to the manufacturer's protocol. 350 µl (micro kit)/600 µl (mini kit) RLT buffer containing 1% ME were used for

lysis. Elution was in 14 µl (micro kit)/30ul (mini kit) RNase-free water. Samples were stored at - 80°C. For DNA isolation from cells, confluent 6 cm dishes were lysed in 500 µl of Southern blot DNA lysis buffer supplemented with 1 mg/ml Proteinase K in 1.5 ml microcentrifuge tubes at 55°C overnight. Subsequently, DNA was extracted by phenol:chloroform and isopropanol precipitation and dissolved in elution buffer (Qiagen® EB buffer) to a final concentration of 1 µg/µl. Samples. Plasmid DNA was isolated using HiSpeed Plasmid Maxi kit (12663; Qiagen), Qiaprep Spin Miniprep kit (27104; Qiagen) or High Pure PCR Product Purification kit (11732668001; Roche) and diluted in supplied EB buffer or H_2O. DNA samples were stored at 4°C for DNA intended for Southern blotting or - 20°C for plasmid or other DNA samples.

For PCR genotyping of mice, ear notches from weaned mice were taken and lysed in 100µl crude lysis buffer with 0.5 mg/ml Proteinase K and incubated at 55°C overnight. Proteinase K was inactivated the next day by incubation at 95°C for 10 minutes. For genotyping embryos, EPC (E6.5 to E7.5) or yolk sac (E8.0 - 9.5) was removed and lysed as for ear notches but in reduced volume (20 µl). Genotyping from individual sections of E7.5 deciduae was performed the same way in further reduced volume (10 µl). Crude DNA samples were kept at 4°C.

For Southern blotting in 96 well format, DNA isolation was performed as described (see Manipulating the mouse embryo 4th ed. p.569f). Briefly, 50 µl of Southern Blot DNA lysis buffer was added per well and incubated at 60°C in a humid chamber overnight. The next day, DNA was precipitated by the addition of 100 µl ice-cold 75 mM NaCl in 98.5% ethanol per well for 30 minutes at room temperature. DNA was washed three times with 70% ethanol and dried overnight. DNA was either digested immediately for Southern blot analysis, or stored at -20°C until required.

5.2.3 Transcriptional Profiling

RNA was isolated from pools of ~1250 EBs for wild type/*Smad3*$^{-/-}$ at d2, d3 and ~2500 and ~5000 EBs for *Smad2*$^{-/-}$ and *Smad2/3*$^{-/-}$ at d2 and d3, respectively as well as from undifferentiated ES cells harvested from a confluent 6 cm dish (after the EB set-up).
1500 ng per sample were used for cRNA generation and transcriptional profiling performed by the Wellcome Trust Centre for Molecular Genetics, Oxford. Biotinylated cRNA was hybridized to Illumina Mouse WG-6 mouse v2 Expression BeadChips. Samples were randomly loaded onto the six array positions within each BeadArray. BeadStation data were extracted using the Gene Expression Analysis Module V1.6.0 of GenomeStudio V2009.2 (Illumina) and imported into an Illumina pre-processing package (http://arrayanalysis.org) for background correction, quantile normalisation, PCA and hierarchical clustering. Clustering analysis identified three outlier samples in undifferentiated ES cells that were excluded from subsequent analysis (indicated in brackets in Fig 13b). To not compromise clone numbers and thus biological significance of the experiment, we decided not to exclude more than one sample at d0 per genotype and not to omit any samples from later time-points. Differential probe expression was determined using a Statistical analysis module (http://arrayanalysis.org) with Benjamini-Hochberg (FDR) corrected p-values. mm10 symbols of probes with significantly different expression (adjusted P values of ≤ 0.05 and ≥ 2 fold change) compared to the averaged wild type signal at the same time-point were analysed using GO term analysis (Webgestalt, http://www.webgestalt.org/) and Venn diagram overlaps (http://www.cmbi.ru.nl/cdd/biovenn/). For wild type EB validation and expression kinetics within different genotypes, d3 datasets were compared to the average d0 dataset within each genotype to identify up and down regulated probes.

5.2.4 PCR

Standard desalted oligonucleotides for PCR reactions were obtained from Life Technologies® and reconstituted in H_2O at 100 µM. 0.5-1 µl of 10 µM dilutions were used in PCR reactions of 15 µl in ReddyMix PCR Mastermix (AB-0575; Thermo Scientific). If required, 1 µl of Mg_2Cl_2 (stock: 25 mM) was added. 0.2 - 1 µl crude DNA lysate from ear

notches or embryonic tissue, or 100 ng of phenol:chloroform purified cell DNA was used as a template. PCRs were performed on a T100 Thermal Cycler (Biorad) and cycling conditions were optimised for each primer pair. Genotyping primers used for mice, embryos and blastocyst-derived ES cell lines are listed in Table 12 in section 5.1.3. For problematic primer sets (indicated by * in Table 12), REDExtract-N-Amp™ PCR ReadyMix™ (4775; Sigma®) was used in a 10 µl reaction. PCR reactions were run out on 2% agarose/1xTAE gels supplemented with EtBr (~100 ng/300ml). A 1 kb Plus DNA Ladder (Invitrogen®) was loaded to assess product sizes. Gels were electrophoresed for 30 - 50 minutes at 140-190 volts depending on gel and tank size and then visualised and photographed using a Gel Doc system (BioRad).

5.2.5 Quantitiative qRT-PCR and OneStep

Oligonucleotides were obtained and diluted as for standard PCR (see section 5.2.4). 1 µg RNA was reverse transcribed to cDNA using Superscript III First Strand Synthesis System (18080-051; Life Technologies) and diluted to a final volume of 160 µl in H_2O. Quantitative RT-PCR was carried out on 2 µl (~100 ng input RNA converted to cDNA) in triplicates using SYBR-green kit (204143; Qiagen) with 1ul of each primer in a total volume of 15 µl on a Rotagene cycler (Qiagen). Two of three replicates were selected for analysis. Relative gene expression was normalized to *Hprt* expression and calculated as $2^{-\Delta\Delta Ct}$. OneStep analysis was performed using the Qiagen OneStep RT-PCR kit (210210; Qiagen) following the manufacturers protocols. 50 ng total RNA was used in each reaction and samples were run on 2 % agarose /1x TAE gels as described in section 5.2.4. The annealing temperature for the qPCR primers used in this study was 55 °C, if not indicated otherwise. For primer sequences used see Table 14.

Table 14 qPCR primer sequences.

Transcript	Primer sequences (5'->3')	Internal reference name	Reference (if applicable)
Nanog	F: CTTTCACCTATTAAGGTGCTTGC R: TGGCATCGGTTCATCATGGTAC Product: 112bp	*ADS_151* *ADS_152*	Hayashi et al. 2011

(continued from last page)

Oct4	F: AGCCGACAACAATGAGAACC R: TGATTGGCGATGTGAGTGAT Product: 168bp	*Oct4ex3_F* *Oct4ex4_R*	Primers obtained from Ita Costello
Sox2	F: CATGAGAGCAAGTACTGGCAAG R: CCAACGATATCAACCTGCATGG Product: 127bp	*ADS_159* *ADS_160*	Hayashi et al. 2011
Klf2	F: CAGTAAACTCAAAGGCATTTCTCAC R: CTGTGGCAGGTTCCAC-GCGCGGGGC Product: 267bp	*Klf2_F* *Klf2_R*	Ema et al. 2008
Klf4	F: AGAACAGCCACCCACACTTG R: AGTGCCTGGTCAGTTCATCG Product: 166bp	*Klf4_F* *Klf4_R*	Primers obtained from Ita Costello
Dnmt3b	F: GACGTCGAGCATCATCTTCA R: AACTGATGGGGTACTGACGC Product: 103bp	*Dnmt3b_F1* *Dnmt3b_R1*	Primers obtained from Ita Costello
Dnmt3l	F: TTCATGGACAATCTGCTGCT R: TGACTTGGGCTTGCAGATAC Product: 199bp	*Dnmt3l_F1* *Dnmt3l_R1*	Costello et al. 2009
Otx2	F: GCTATGCTGGCTCAACTTCC R: TTGAAGCTCCATATCCCTGG Product: 177bp	*ADS_153* *ADS_154*	Primers obtained from Ita Costello
Fgf5	F: TTGCGACCCAGGAGCTTAAT R: CTACGCCTCTTTATTGCAGC Product: 209bp	*Fgf5_F1* *Fgf5_R1*	Karwacki-Neisius et al. 2013
Hprt (OneStep)	F: GCTGGTGAAAAGGACCTCT R: CACAGGACTAGAACACCTGC Product: 249bp	*ADS_194* *ADS_195*	Elias et al. 2015
Eomes (OneStep)	F: TGTTTTCGTGGAAGTGGTTCTG-GC R: AGGTCTGAGTCTTGGAAGGTT-CATTC Product: 323bp	*Eomes_103* *Eomes_104*	Costello et al. 2011
T (OneStep)	F: AACTTTCCTCCATGTGCTGAGAC R: TGACTTCCCAACACAAAAAGCT Product: 533bp	*Brachyury_183* *Brachyury_184*	Costello et al. 2011
Foxa2 (OneStep)	F: TGGCTGCAGACACTTCCTACT R: CAACATCAGTACAACCCTCTGGT Product: 487bp	*Foxa2_193* *Foxa2_194*	Costello et al. 2011
Cer1 (OneStep)	F: GGAGGAAGCCAAGAGGTTCT R: GTCTTCATGGGCAATGGTCT Product: 145bp	*Cer1_F1* *Cer1_R1*	Primers obtained from Ita Costello
Oct4 (OneStep)	F: CGTTCTCTTTGGAAAGGTGTTC R: GAACCATACTCGAACCACATCC Product: 319bp	*Oct4_274* *Oct4_275*	Tesar et al. 2007

	(continued from last page)		
Esrrb	F: TGTGGAGAGATTGCTTTATTTTCTG R: GGACTGGATGGGAGATAATCC Product: 171bp	*Esrrb_F* *Esrrb_R*	Bogani et al. 2013
Cdx2	F: AGGCTGAGCCATGAGGAGTA R: TGAGGTCCATAATTCCACTCA Product: 124bp	*Cdx2_F1* *Cdx2_R1*	Ishiuchi et al. 2015
Prdm14	F: ACAGCCAAGCAATTTGCACTAC R: TTACCTGGCATTTTCATTGCTC Product: 126bp	*ADS_155* *ADS_156*	Aramaki et al. 2013
Rex1	F: GCAAAGA-CAAGTGGCCAGAAAGGGC R: CCTCGTATGATGCACTCTAGGTATC Product: 200bp	*Rex1_F1* *Rex1_R1*	Ema et al. 2008
Wnt3	F: CAAGCACAACAATGAAGCAGGC R: TCGGGACTCACGGTGTTTCTC Product: 199bp	*ADS_165* *ADS_166*	Aramaki et al. 2013
T	F: ATCAGAGTCCTTTGCTAGGTAG R: GTTACAATCTTCTGGCTATGC Product: 194bp	*ADS_163* *ADS_164*	Aramaki et al. 2013
Foxa2	F: CCCTGCTAGCTCTGGTCACT R: AGGTGAGACTGCTCCCTTGA Product: 116bp	*ADS_147* *ADS_148*	Aramaki et al. 2013
Gsc	F: GCACCATCTTCACCGATGAG R: CGGCGGTTCTTAAACCAGAC Product: 145bp	*Gsc_F* *Gsc_R2*	Primers obtained from Ita Costello
Sox17	F: TTCTGTACAC-TTTAATGAGGCTGTTC R: TTGTGGGAAGTGGGATCAAG Product: 134bp	*ADS_157* *ADS_158*	Aramaki et al. 2013
Eomes	F: CCTGGTGGTGTTTTGTTGTG R: TTTAATAGCACCGGGCACTC Product: 292bp	*ADS_143* *ADS_144*	Niwa et al. 2005

5.2.6 Southern Blotting

Southern blotting to screen for the CRISPR/Cas9n-mediated deletion of *Smad3* and for Cre-excision of the *Smad1*^{RobPC} allele was essentially performed as described in Manipulating the mouse embryo 4th ed. p.556f. Endonuclease digestion of DNA was carried out by adding 50 µl restriction enzyme mix (1x recommended NEB Buffer(NEB), 1xBSA (NEB), 100 µg/ml RNaseA (Qiagen®), 1 mM spermidine and 100 units of enzyme (NEB), per well and incubating overnight at 37°C in a humid chamber, with shaking. The next day, samples were run on a 0.8 % agarose gel to separate DNA fragments. Following

electrophoresis, the gel was incubated in depurination solution for 10 minutes, and then denaturation solution for 30 minutes.

The DNA was transferred onto Hybond XL membrane (RPN303S; GE Healthcare) overnight by capillary action. The following day, DNA was UV cross-linked using Stratagene UV-crosslinker. Before hybridisation, membranes were incubated with modified Church and Gilbert buffer for 2 hours at 65°C. Probes were radioactively labelled using a Random Primers DNA Labelling System (18187013; Invitrogen). 50 ng of probe DNA was dissolved in H_2O to a final volume of 23 µl, heated to 95°C for 5 minutes and immediately cooled on ice. To the denatured probe the following was added; 2 µl each of dATP, dGTP and dTTP solutions, 1 µl Random Primers Buffer Mixture, 5 µl (approximately 50 µCi) [α-32P]dCTP, 3000 Ci/mmol, 10 µCi/µl and 1 µl Klenow Fragment. The synthesis reaction was incubated for 2 hours at room temperature, before being denatured by heating to 95°C for 5 minutes, then cooled on ice. Radioactively labelled probe was hybridised to membranes in fresh modified Church and Gilbert buffer overnight at 65°C. To wash the blots, the membranes were incubated at 65°C in low, medium and high stringency buffers for 30, 15 and 10 minutes, respectively. After washing, blots were exposed to X-ray film overnight at - 80°C to visualise bands.

Smad3 exon 1 deletion in wild type CCEs as well as *Smad2*$^{-/-}$ KT15 cells (Tremblay et al. 2000) was screened using *XbaI* digest with a 3' external probe (see Table 14 for used primers). Four different probes were screened on wildtype CCE DNA and the best probe selected for experiments. Cre-mediated excision in *Smad1*^{RobPC} ES cells was screened using *BamHI* and *EcoRI* digests with a 5' and 3' external probes, which were generated by Kim Tremblay (Tremblay et al. 2001).

5.2.7 Flow cytometry

Embryos were collected from timed matings of *Eomes.GFP* males and wild type (*CD1*) females at E6.5 and E7.5, dissected in cold PBS (1% FCS). Ectoplacental cones were removed and embryos genotyped by fluorescence. For embryo dissociation at E7.5, 45 wild type or 35 *Eomes.GFP*$^{-/+}$ embryos were pooled in M2 medium, washed twice in PBS (-Mg_2Cl_2) (2%FCS) and trypsinized in 300 µl 0.25 % trypsin-EDTA (37°C, 5 minutes) followed by blocking with 600µl M2 medium (33 % FCS) and gentle dissociation by pipetting. Counting revealed ~1.45 x 10^5 (wild type) and 1.78 x 10^5 cells (*Eomes.GFP*$^{-/+}$) per pool, i.e. ~4000 cells/embryo). Cells were washed in PBS (+Mg_2Cl_2) and counterstained with 7-aminoactinomycin D (7AAD) (BD Pharmingen™) following the manufacturer's instructions prior to imaging. ~60 000 cells were used for each experiment shown in Figure 30, from which ~20 000 cells were gated and analyzed.

5.3 Protein Biochemistry

5.3.1 Antibodies

Table 15 Antibodies.

Protein	Antibody	Catalog and #Lot number	Additional information
Blimp1	monoclonal rat-a-mouse raised against aa255-395	sc-130917 (5E7) Lot: GO913	0.4 µg/ml (#524)
Nanog	polyclonal rabbit-a-mouse	ab80892 Lot: GR40243-12	2 ng/ml (#618)
Oct4	polyclonal goat-a-mouse raised against peptide near N-terminus	sc-8628 Lot: F1815	2 ng/ml (#448)
Ap2γ	polyclonal rabbit-a-human raised against aa145-221	sc-8977 Lot: G1112	2 µg/ml (#625)
p-Smad1/5/8 (Ser463/465)	monolonal Goat-a-human raised against residues surrounding Ser463/465 of Smad5	Cell signalling 9516 (41D10) Lot: 6	1:500 (#740) (conc not given)
Smad2	monoclonal mouse-a-mouse raised against aa142-263	BD Transduction 610843 Lot: 3288899	0.25 ng/ml (#110)

Smad3	Monoclonal rabbit-a-human raised against aa200-300	ab40854 Lot: GR16548-6	0.266 µg/ml (#718)
Smad3 (used for validation)	Polyclonal rabbit-a-human raised against 20aa peptide in linker region	Zymed 51-1500 Lot: 40789435	0.5µg/ml (#111)
Stella	polyclonal rabbit-a-mouse raise against aa1-150	sc-67249 Lot: H1809	1 µg/ml (#727)
Tubulin	rabbit polyclonal anti-human raised against aa210-444	sc-9104 Lot: I1009	0.2 µg/ml (#130)
Secondary anti-bodies	donkey-a-rabbit Alexa 488	Molecular Probes A21206 Lot: 1480470	5 µg/ml (#670)
	donkey-a-goat Alexa 594	Molecular Probes A11058 Lot: 1445994	5 µg/ml (#671)
	rabbit anti-rat IgG	Vector Laboratories AI-4001	5 µg/ml (#652)
	goat-a-rabbit Alexa 594	Invitrogen A11037	5 µg/ml (#186)
	goat-a-rabbit Alexa 555	Invitrogen A21429	5 µg/ml (#431)
	donkey-a-rabbit HRP	GE Heathcare NA934VS	1:2000 (conc not given) (#159)

5.3.2 Protein extraction and quantification

Protein from cultured cells or tissues was prepared using RIPA lysis buffer (e.g. 300 µl for a 6 cm dish) containing phosphatase (100 µl in 1ml RIPA) and proteinase inhibitors (Protease-Inhibitor Complex (Roche®), 10 µl in 1ml RIPA lysis). Cells were slightly agitated for 20 minutes at 4°C and then scraped off plates and transferred to eppendorf tubes, pipetted up and down a few times and centrifuged at 14,000 rpm for 20 minutes at 4°C. The supernatant was transferred to a fresh microcentrifuge tube on ice. Protein was quantified using Bradford reagent (BioRad) and assessed by photometry (λ=750nm) using a BSA (NEB) standard curve at 5, 2.5, 1.25, 0.625 and 0.3125 mg/ml. Samples were

aliquoted and stored at - 80°C. Thomas Clague prepared tissue lysates from mice and control lysates for the Western blots shown in Figure 8c.

5.3.3 Western blotting

30 µg protein samples were diluted to a total volume of 15 µl in RIPA buffer and mixed with 5 µl 4x sample buffer containing 10 % β-ME. Samples were denatured at 98°C for 10 minutes and loaded onto 10 % SDS-PAGE gels and run for 2h at 90 volts in loading buffer. Protein was blotted onto MeOH-activated PVDF membrane for 75 minutes at 90V and 400 mA on ice in transfer buffer. Afterwards, the membrane was rinsed with Ponceau stain for 2 min to assess protein transfer and subsequently rinsed with H_2O. After washing in TBST (0.1%) the membrane was blocked in 5% non-fat milk powder/TBST (0.1%) for 1h at RT and incubated in Smad3 antibody over night at 4°C (see Table 15). TBST (0.1%)-washed membranes were subsequently incubated with secondary antibody in block for 1h at RT, washed in TBST (0.1%) and visualized using ECL primer kit at RT for 5 minutes followed by autoradiography. Membranes were stripped with mild stripping buffer at RT for 3 x 20 minutes, washed with TBST (0.1%), blocked for 1h at RT and incubated with Smad2 antibody overnight at 4°C and detected as described above. Blots were subsequently re-stripped and stained with tubulin antibody and processed in an identical fashion.

5.3.4 Immunohistochemistry and Immunofluorescence on paraffin sections

For immunohistochemistry, dewaxed sections subjected to antigen retrieval by boiling for 1h in Tris/EDTA (pH 9.0) and gradually cooled down for 1h, were permeabilized for 10 min in 0.1% Triton X-100 in TBS. Sections were subsequently blocked with 10% normal donkey serum (Stella) or 10% normal goat serum (Blimp1) in TBS.

For Blimp1 immunohistochemistry, sections incubated in primary antibodies (see Table 15) in block overnight were signal-amplified with biotinylated secondary antibody for 45min at RT followed by peroxidase blocking (K4011, DAKO) for 20 minutes at RT and AP-conjugated biotin/streptavidin (ABC-AP, Vector Laboratories) and Vector Red substrate (Vector Laboratories). Sections were lightly counterstained with haematoxylin, co-

versliped and imaged. For p-Smad1/5/8 immuohistochemistry, slides were processed as for Blimp1 except that the secondary antibody was left out.

For Stella immunofluorescence, sections were incubated in primary antibodies (see Table 15) in block over night, incubated with secondary antibody followed by mounting in vectashield containing DAPI. Slides were imaged on a fluorescent slide microscope.

5.3.5 Immunofluorescence on ES cells, EpiLCs, PGCLCs and embryos

ES cells

For Oct4/Nanog staining of ES cells, 2 x 10^4 ES cells (grown in 2i +LIF or serum +LIF) were plated on fibronectin-coated (341635; Merck Millipore, 10 µg/cm² in PBS (-$MgCl_2$), 1 h 37°C) 8-well chamber glass slides and cultured for 1 or 2 days in EpiLC medium or for 2 days in 2i + LIF or FF ES medium. Samples were washed twice with PBS (+ $MgCl_2$) and fixed in 4% PFA (10 min, RT). After three washes in PBS (+ $MgCl_2$), cells were permeabilized in PBSTr (0.2 %) followed by two washes in PBST (0.05 %). Cells were blocked (10% donkey serum, 1% BSA in PBST (0.05 %)) for 1 h at RT, washed once with PBS (- $MgCl_2$) and incubated with Oct4 and Nanog antibodies in block (#448 and #618, see Table 15) for 1h at RT in a humid chamber. Subsequently, cells were washed twice in PBST (0.05 %) and secondary antibodies (#671 and # 670, see Table 15) in block for 1 h at RT in a humid chamber in the dark. Cells were washed twice in PBST (0.05 %) containing 2 µg/ml DAPI (Biotium®, Cat: 40043) and subsequently mounted on coverslips using Vectashield containing DAPI (Vector Laboratories, Cat: H-1200). Images were taken on a Leica epifluorescence microscope.

PGCLCs

For Ap2γ staining of d2 PGCLCs, d2 PGCLC aggregates were transferred to 9-well glass dishes and washed once with PBS (-$MgCl_2$), fixed in 1 % PFA (in PBS (-$MgCl_2$)) for 30 min at RT. Cells were permeabilized by three washes à 5 min in PBSTr (0.1 %) followed by one wash in PBSTr (0.5 %) for 15 min followed by three washes à 5 min in PBSTr (0.1 %). Block was for 2 h in 5 % goat serum, 0.2 % BSA in PBSTr (0.1 %) and was followed by incubation in AP2γ antibody (#625, see Table 15) at 4°C over night. PGCLCs

were washed three times for 5 min in PBSTr (0.1 %) followed by one wash in PBSTr (0.5 %) for 15 min followed by incubation in secondary antibodies (#186, see Table 15) for 2 h at RT in a humid chamber the dark. After five washes à 5 min in PBSTr (0.1 %), PGCLCs were washed once in PBSTr (0.5 %) containing 2 µg/ml DAPI (Biotium®, Cat: 40043) for 15 min, mounted in Vectashield containing DAPI (Vector Laboratories, Cat: H-1200) in chamber slides, left to penetrate for > 4 h and imaged on a Olympus FV1000 confocal microscope.

E7.5 embryos

E7.5 isolated embryos (without Reichert's membrane) in PBS (-$MgCl_2$)/1 % FCS were transferred to 9-well glass dishes with a P20 pipet, fixed in 4 % PFA for 30 min at RT followed by three washes à 5 min in PBSTr (0.1 %) followed by one wash in PBSTr (0.5 %) for 15 min followed by three washes à 5 min in PBSTr (0.1 %). Block was for 2 h in 10 % goat serum, 0.2 % BSA in PBSTr (0.1 %) and was followed by incubation in Blimp1 antibody (#176, see Table 15) at 4°C for 2 days. Embryos were subsequently washed three times for 5 min in PBSTr (0.1 %) followed by one wash in PBSTr (0.1 %) for 15 min followed by incubation in secondary antibody (#652, see Table 15) for 2 h at RT in a humid chamber in the dark. After five washes à 5 min in PBSTr (0.1 %) and three 15 min washes in PBSTr (0.1 %), embryos were incubated in tertiary antibody (#431, see Table 15) for 2 h at RT in the dark in a humid chamber. After five washes à 5 min in PBSTr (0.1 %) embryos were washed three times in PBSTr (0.1 %) containing 2 µg/ml DAPI (Biotium®, Cat: 40043) for 15 min, mounted in Vectashield containing DAPI (Vector Laboratories, Cat: H-1200) in chamber slides, left to penetrate overnight and imaged on a Olympus FV1000 confocal microscope.

5.4 Tissue Culture

5.4.1 Derivation of embryonic stem cells from blastocysts

Isolated blastocysts in drops of FF medium under mineral oil (see section 5.1.4) were incubated in the tissue culture incubator for 24 h and then transferred to individual drops of FF ES medium under mineral oil and left to hatch/attach over night. The next day, FF

ES medium was changed to 2i medium and the blastocysts fed every 2-3 days until the ICM overgrew the trophectoderm cells (~7-10 days). Medium was changed to PBS (-Mg_2Cl_2) and ICM clumps picked and expanded as for normal ES cell colonies. Cells were frozen from 10 cm plates at passage 5 in 2i.

5.4.2 ES cell maintenance

Feeder-Free ES cells were maintained in FF ES medium or 2i medium on gelatin-coated plates (0.1% gelatin for >20 minutes) in an incubator (37°C, 6% CO_2). Cells were passaged 1:2 - 1:6 when confluent (wash with PBS (-Mg_2Cl_2) followed by trypsinization with 0.25% Trypsin-EDTA for 5 minutes at 37°C, resuspension in 5 ml ES medium, pelleted (1000g, 3 minutes) followed by replating in FF ES medium or 2i medium). Since I noted low attachment of 2i cells to gelatin plates, I plated cells in 2i medium supplemented with 25% FF ES medium over night before replacing the medium with pure 2i medium. For freezing, cells were trypsinized, washed in ES medium and spun down prior to resuspension in pre-cooled 1x freezing medium. Vials were immediately transferred to pre-cooled Styrofoam boxes at - 80°C and left over night. For long-term storage, vials were subsequently transferred to liquid nitrogen. Frozen cells were reactivated by incubating frozen vials for a few minutes in a 37°C water bath followed by resuspension in ES medium, pelleting and plating in FF ES medium or 2i medium (see above). Feeder-dependent ES cell were maintained on a feeder-layer of inactivated SNH fibroblasts.

5.4.3 ES cell transfection

For introducing Smad3 deletion CRISPR/Cas9n constructs into mouse ES cells (either wild type CCE or *Smad2*$^{-/-}$ KT15, see Tremblay et al. 2000), 1 x 10^6 cells were transfected with 5 µg total DNA (in < 10µl volume) consisting of 1 µg of each of the four sgRNA plasmids and 1 µg of a puromycin selection plasmid (internal code #1224) diluted in H_2O using the Neon™ Transfection system (MPK10025; Invitrogen®, 3 pulses à 1400 V, 10 ms) and released into antibiotic-free FF ES medium to recover for 24 h. Subsequently, cells were selected for 48 h in complete FF ES medium containing 1 µg/ml puromycin. After two more days of culture in FF ES medium without selection, cells were low-density plated and ~200 individual clones picked after 7 - 10 days.

For Cre-excision of the *Smad1*^{RobPC} allele (Tremblay et al. 2001), 2 x 10^7 cells grown in serum + LIF on feeders were transfected with 20 µg pMC1Cre (Araki et al. 1997) at 200 volts, 950 µF. Cells were subsequently plated onto four 10 cm feeder plates in FD ES medium. Transfected ES cells were grown for 7 - 10 days. Transfected colonies were picked after 7 – 10 days in a 96 well format for Southern blot screening.

5.4.4 Culture and generation of feeder cells

SNH were maintained in STO medium. For preparation of mitotically-inactivated feeder-plates, STOs were treated with 20 µg/ml Mitomycin C (M0503; Sigma) in STO medium for 3 h in the incubator. Afterwards, cells were washed three times with PBS (-Mg_2Cl_2), trypsinized with 0.25 % trypsin-EDTA and suspended in STO or FD ES medium at a density of 3 x 10^5 cells/ml. Gelatinized plates were seeded with 5 x 10^4 cells/cm^2 to generate a monolayer of SNH cells.

5.4.5 Feeder-depletion of feeder-dependent ES cells

To deplete feeder cells from ES cell cultures, total suspensions were plated and feeders left to attach for 40 minutes, after which free-floating cells (mainly ES cells) were transferred to new gelatinized plates. This procedure was repeated at every passage until cells were depleted of residual fibroblasts.

5.4.6 Adapting 2i ES cells to serum + LIF conditions

In order to adapt cells grown in 2i+LIF to serum+ LIF conditions, cells were fed with FF ES medium, and kept at high density by splitting at a ratio of 1:1 - 1:4 when confluent. ES cells grown in 2i needed a substantial phase of adaptation accompanied by cell death for approximately ten passages to adapt to FF ES medium.

5.4.7 Embryoid body differentiation

ES cells in FF ES medium were trypsinized, resuspended in EB medium, pelleted, washed in PBS and counted. A single-cell solution of 1x10^4 cells/ml of feeder-free ES cells in EB medium was pipetted in 20 - 22 rows of twelve 10 µl drops onto square 12cm

plates. The plates were carefully inverted to produce hanging drops and placed onto lids containing a 3 cm plate filled with 2 ml of sterile PBS (-Mg_2Cl_2) to maintain high humidity. EBs in hanging drops were incubated for two days without disturbing. On day 2, 5 plates were inverted and carefully flushed off with 8ml EB medium per plate, pooled, spun for 1 minute at 1000 rpm, and transferred as a suspension in 8ml EB medium on non-gelatinized 10 cm EB dishes, and left to grow for a further 1 - 2 days. To harvest EBs, d2 EBs from 5 (wild type, *Smad3*$^{-/-}$) or 10 (*Smad2*$^{-/-}$, *Smad2/3*$^{-/-}$) 12 cm plates were pooled, spun and washed with PBS (-Mg_2Cl_2). Cell pellets in polypropylene 15ml Falcon tubes were snap-frozen in liquid nitrogen and stored at -80C. For d3 EBs, 2 (wild type, *Smad3*$^{-/-}$) or 4 (*Smad2*$^{-/-}$, *Smad2/3*$^{-/-}$) pooled EB plates were processed in identical fashion. d4 EBs for OneStep analysis were harvested the same way.

5.4.8 Definitive endoderm differentiation

To induce endoderm-enriched EBs, d2 hanging drop EBs were processed as described above but plated in 8 ml definitive endoderm differentiation medium (adopted from Morrison et al. 2008) and were cultured in suspension for one or three more days prior to harvest, which was performed as for EBs (see above).

5.4.9 EpiLC differentiation

EpiLCs were induced from feeder-free ES cells in 2i+LIF medium following the protocol outlined in Hayashi et al. 2011. In brief, 1 x 10^5 cells were resuspended in EpiLC differentiation medium and plated on 12-well plates coated with fibronectin (10 µg/cm^2, coat diluted in PBS (-Mg_2Cl_2) for >30 minutes at 37°C). Cells were fed the next day and harvested at d1 and d2 for RNA isolation (as for EBs, but with trypsinizing cells before pelleting). D0 cells were plated in 2i medium on fibronectin and cultured for two days prior to harvest.

5.4.10 PGCLC differentiation

PGCLCs were induced following the protocol outlined in Hayashi et al. 2011. In brief, 2000 d2 EpiLCs (see above) were cultured in floating condition in wells of ultra-low binding U-bottom 96-well plates in 100 µl of PGCLC differentiation medium for two

days. 24 PGCLC aggregates were used to isolate RNA. Inactivation of trypsin was done with GMEM (+5%FBS).

5.4.11 Alkaline Phosphatase Staining of ES cell colonies

Alkaline Phosphatase staining was performed using the AP staining kit (Millipore®) following the manufacturers conditions. In brief, 600 cells (in 2i + LIF or serum + LIF) were plated on gelatinized 6-well dishes in respective medium. The next day, medium was exchanged to FF ES, EB, 2i + LIF or N2B27 medium. Cells were fed every day, washed in PBS and fixed with 4%PFA/PBS for 1 minute at RT on day 5. After a TBST wash, colonies were stained with 1.7 ml AP staining solution on d5 for 15min at RT and then washed with TBST. Representative colonies were imaged in PBS (-Mg_2Cl_2) and total red, mixed and white colonies on each plate scored.

5.4.12 Giemsa Staining

675 cells in serum + LIF condition in FF ES medium were plated on gelatinized 6 cm plates and fed daily. On day 7, colonies were washed with PBS (-MG_2Cl_2) and fixed with 2.5 ml 70% EtOH for 10 minutes at RT. Colonies were subsequently stained with Giemsa stain (10092-013; Gibco) for 15min at RT. Giemsa stain was washed off extensively with tap water. Plates were inverted to dry and imaged.

5.5 Histology

5.5.1 Paraffin embedding and sectioning

For immunohistochemistry, tissue was fixed overnight in 4% paraformaldehyde (PFA), dehydrated in ethanol (1h each in 25%, 50%, 70%, 90%, 100% followed by 1.5h each in 100% (2x), histoclear (2x) then 2h each in 50%histoclear/50%paraffin, paraffin (2x)) and embedded in paraffin wax, and sectioned (6 μm).

5.5.2 Whole-mount in situ hybridization

Confirmatory WISH of Eomes expression in wild type embryos was performed following standard protocols with an Eomes probe from Arnold et al. 2008 (see Manipulating the mouse embryo 4th ed. p.735-740).

5.5.3 Alkaline Phosphatase Staining of embryos

E8.25 embryos were dissected from the deciduae and Reichert's membrane. Pieces of extra-embryonic ectoplacental cone tissue were kept for genotyping. Alkaline phosphatase staining was performed as described previously (Labosky and Hogan 1999, Lawson et al. 1999).

5.6 Solutions and media

Table 16 Solutions and media.

Solution	Formula
Crude lysis buffer	50 mM KCl, 10 mM Tris-HCl pH 8.3, 1.5 mM, $MgCl_2$, 0.45 % NP40, 0.45 % Tween-20, 0.5 mg/ml Proteinase K
Modified Church and Gilbert buffer	500 mM sodium phosphate, pH 7.2, 1mM EDTA, 250 mM NaCl, 5 % SDS, 1 % BSA, 100 µg/ml denatured fish sperm DNA
Southern blot DNA lysis buffer	100 mM Tris, pH7.5, 50 mM Na_2EDTA, 0.5 % SDS, 1 mg/ml Proteinase K
Southern blot denaturation solution	1.5 M NaCl, 500 mM NaOH
Southern blot depurination solution	120 mM HCl
Southern blot low stringency buffer	2x SSC, 1 % SDS
Southern blot medium stringency buffer	0.5x SSC, 0.1 % SDS
Southern blot high stringency buffer	0.3x SSC, 0.1 % SDS
RIPA lysis buffer	50 mM Tris-HCl pH8.0; 150 mM NaCl; % NP-40; 0.1 % SDS; 0.5 % NaDeOxC

FF ES medium	EB medium supplemented with 1000 U/ml LIF (ESG1107; ESGRO)
FD ES medium	DMEM (11960-085; Invitrogen) supplemented with 15 % FCS (10500-062, Gibco: Lot: 07Q3446K), 1 % Penicillin/ Streptomycin (15140-163; Invitrogen), 0.1 mM 2-mercaptoethanol (M-7522; Sigma), 1 % glutamine (25030-13; Invitrogen)
Defintive endoderm differentiation medium	N2B27 medium supplemented with 50 ng/ml Activin A (Peprotech) and 20 ng/ml EGF (AF-100-15, Peprotech)
EB medium	DMEM supplemented with 15 % FCS, 1 % Penicillin/Streptomycin, 0.1 mM 2-mercaptoethanol, 1 % glutamine, 1 % non-essential amino acids (11140-035; Gibco), 1mM Sodium Pyruvate (S86636; Sigma)
2i medium	N2B27 (NDiff 227, Takara) supplemented with 1 μM PD0325091, 3 μM CHIR99021 and 1000 U/ml LIF
1x freezing medium	90 % FCS, 10 % DMSO
EpiLC differentiation medium	N2B27 supplemented with 20 ng/ml Activin A (Reprotech) and 12 ng/ml bFGF (13256-029; Invitrogen) and 1 % KSR (10828-010; Gibco, Lot: 1508151)
GK15 medium	GMEM (11710-035; Gibco) supplemented with with 15 % KSR, 0.1 mM NEAA, 1 mM sodium pyruvate, 0.1 mM 2-mercaptoethanol, 100 U/ml penicillin, 0.1 mg/ml streptomycin, and 2 mM L-glutamine, LIF (1000 U/ml; Invitrogen).
PGCLC differentiation medium	GK15 medium supplemented with 500 ng/ml of recombinant human BMP4 (Q53XC5; R&D Systems)
STO medium	DMEM supplemented with 10 % bovine calf serum (SH0072.03; Hyclone), 1 % glutamine and 1 % Penicillin/Streptomycin
0.1% gelatine solution	*In sterile MQ*

6

References

Abranches E, Silva M, Pradier L, Schulz H, Hummel O, Henrique D, Bekman E. Neural differentiation of embryonic stem cells in vitro: a road map to neurogenesis in the embryo. PLoS One. 4(7):e6286. (2009)
Acampora D, Mazan S, Lallemand Y, Avantaggiato V, Maury M, Simeone A, Brûlet P. Forebrain and midbrain regions are deleted in Otx2-/- mutants due to a defective anterior neuroectoderm specification during gastrulation. Development. 121(10):3279-90. (1995)
Acampora D, Di Giovannantonio LG, Di Salvio M, Mancuso P, Simeone A. Selective inactivation of Otx2 mRNA isoforms reveals isoform-specific requirement for visceral endoderm anteriorization and head morphogenesis and highlights cell diversity in the visceral endoderm. Mech Dev. 126(10):882-97. (2009)
Acampora D, Di Giovannantonio LG, Simeone A. Otx2 is an intrinsic determinant of the embryonic stem cell state and is required for transition to a stable epiblast stem cell condition. Development. 140(1):43-55. (2013)
Adachi H, Saijoh Y, Mochida K, Ohishi S, Hashiguchi H, Hirao A, Hamada H. Determination of left/right asymmetric expression of nodal by a left side-specific enhancer with sequence similarity to a lefty-2 enhancer. Genes Dev. 13(12):1589-600. (1999)
Agricola E1, Randall RA, Gaarenstroom T, Dupont S, Hill CS. Recruitment of TIF1γ to chromatin via its PHD finger-bromodomain activates its ubiquitin ligase and transcriptional repressor activities. Mol Cell. 43(1):85-96. (2011)
Alarcón C, Zaromytidou AI, Xi Q, Gao S, Yu J, Fujisawa S, Barlas A, Miller AN, Manova-Todorova K, Macias MJ, Sapkota G, Pan D, Massagué J. Nuclear CDKs drive Smad transcriptional activation and turnover in BMP and TGF-beta pathways. Cell. 139(4):757-69. (2009)
Amthor H, Christ B, Rashid-Doubell F, Kemp CF, Lang E, Patel K. Follistatin regulates bone morphogenetic protein-7 (BMP-7) activity to stimulate embryonic muscle growth. Dev Biol. 243(1):115-27. (2002)
Ancelin K, Lange UC, Hajkova P, Schneider R, Bannister AJ, Kouzarides T, Surani MA. Blimp1 associates with Prmt5 and directs histone arginine methylation in mouse germ cells. Nat Cell Biol. 8(6):623-30. (2006)
Andersson O, Reissmann E, Jörnvall H, Ibáñez CF. Synergistic interaction between Gdf1 and Nodal during anterior axis development. Dev Biol. 293(2):370-81. (2006)
Anderson R, Fässler R, Georges-Labouesse E, Hynes RO, Bader BL, Kreidberg JA, Schaible K, Heasman J, Wylie C. Mouse primordial germ cells lacking beta1 integrins enter the germline but fail to migrate normally to the gonads. Development. 126(8):1655-64. (1999)
Ang SL, Rossant J. HNF-3 beta is essential for node and notochord formation in mouse development. Cell. 78(4):561-74. (1994) (1994a in main text)
Ang SL, Conlon RA, Jin O, Rossant J. Positive and negative signals from mesoderm regulate the expression of mouse Otx2 in ectoderm explants. Development. 120(10):2979-89. (1994) (1994b in main text)
Ang SL, Jin O, Rhinn M, Daigle N, Stevenson L, Rossant J. A targeted mouse Otx2 mutation leads to severe defects in gastrulation and formation of axial mesoderm and to deletion of rostral brain. Development. 122(1):243-52. (1996)
Aoki M, Mieda M, Ikeda T, Hamada Y, Nakamura H, Okamoto H. R-spondin3 is required for mouse placental development. Dev Biol. 301(1):218-26. (2007)
Araki K, Imaizumi T, Okuyama K, Oike Y, Yamamura K. Efficiency of recombination by Cre transient expression in embryonic stem cells: comparison of various promoters. J Biochem. 122(5):977-82. (1997)
Aramaki S, Hayashi K, Kurimoto K, Ohta H, Yabuta Y, Iwanari H, Mochizuki Y, Hamakubo T, Kato Y, Shirahige K, Saitou M. A mesodermal factor, T, specifies mouse germ cell fate by directly activating germline determinants. Dev Cell. 27(5):516-29. (2013)
Arima T, Hata K, Tanaka S, Kusumi M, Li E, Kato K, Shiota K, Sasaki H, Wake N. Loss of the maternal imprint in Dnmt3Lmat-/- mice leads to a differentiation defect in the extraembryonic tissue. Dev Biol. 297(2):361-73. (2006)
Arnold SJ, Stappert J, Bauer A, Kispert A, Herrmann BG, Kemler R. Brachyury is a target gene of the Wnt/beta-catenin signaling pathway. Mech Dev. 91(1-2):249-58. (2000)
Arnold SJ, Maretto S, Islam A, Bikoff EK, Robertson EJ. Dose-dependent Smad1, Smad5 and Smad8 signaling in the early mouse embryo. Dev Biol. 96(1):104-18. (2006)
Arnold SJ, Hofmann UK, Bikoff EK, Robertson EJ. Pivotal roles for eomesodermin during axis formation, epithelium-to-mesenchyme transition and endoderm specification in the mouse. Development. 135(3):501-11. (2008)

Arnold SJ, Robertson EJ. Making a commitment: cell lineage allocation and axis patterning in the early mouse embryo. Nat Rev Mol Cell Biol. 10(2):91-103. (2009) Review.
Arnold SJ, Sugnaseelan J, Groszer M, Srinivas S, Robertson EJ. Generation and analysis of a mouse line harboring GFP in the Eomes/Tbr2 locus. Genesis. 47(11):775-81. (2009)
Artus J, Piliszek A, Hadjantonakis AK. The primitive endoderm lineage of the mouse blastocyst: sequential transcription factor activation and regulation of differentiation by Sox17. Dev Biol. 350(2):393-404. (2011)
Attisano L, Wrana JL. Signal integration in TGF-β, WNT, and Hippo pathways. F1000Prime Rep. 5:17. (2013)
BabuRajendran N, Palasingam P, Narasimhan K, Sun W, Prabhakar S, Jauch R, Kolatkar PR. Structure of Smad1 MH1/DNA complex reveals distinctive rearrangements of BMP and TGF-beta effectors. Nucleic Acids Res. 38(10):3477-88. (2010)
Baburajendran N, Jauch R, Tan CY, Narasimhan K, Kolatkar PR. Structural basis for the cooperative DNA recognition by Smad4 MH1 dimers. Nucleic Acids Res. 39(18):8213-22. (2011)
Barak Y, Nelson MC, Ong ES, Jones YZ, Ruiz-Lozano P, Chien KR, Koder A, Evans RM. PPAR gamma is required for placental, cardiac, and adipose tissue development. Mol Cell. (4):585-95. (1999)
Barnes JD, Crosby JL, Jones CM, Wright CV, Hogan BL. Embryonic expression of Lim-1, the mouse homolog of Xenopus Xlim-1, suggests a role in lateral mesoderm differentiation and neurogenesis. Dev Biol. 161(1):168-78. (1994)
Barrow JR, Howell WD, Rule M, Hayashi S, Thomas KR, Capecchi MR, McMahon AP. Wnt3 signaling in the epiblast is required for proper orientation of the anteroposterior axis. Dev Biol. 312(1):312-20. (2007)
Beck F, Erler T, Russell A, James R. Expression of Cdx-2 in the mouse embryo and placenta: possible role in patterning of the extra-embryonic membranes. Dev Dyn. 204(3):219-27. (1995)
Beck S, Le Good JA, Guzman M, Ben Haim N, Roy K, Beermann F, Constam DB. Extraembryonic proteases regulate Nodal signalling during gastrulation. Nat Cell Biol. 4(12):981-5. (2002)
Beddington RS, Robertson EJ. An assessment of the developmental potential of embryonic stem cells in the midgestation mouse embryo. Development. 105(4):733-7. (1989)
Beddington RS, Robertson EJ. Axis development and early asymmetry in mammals. Cell. 96(2):195-209. (1999)
Bell CC, Amaral PP, Kalsbeek A, Magor GW, Gillinder KR, Tangermann P, di Lisio L, Cheetham SW, Gruhl F, Frith J, Tallack MR, Ru KL, Crawford J, Mattick JS, Dinger ME, Perkins AC. The Evx1/Evx1as gene locus regulates anterior-posterior patterning during gastrulation. Sci Rep. 6:26657. (2016)
Belo JA, Bouwmeester T, Leyns L, Kertesz N, Gallo M, Follettie M, De Robertis EM. Cerberus-like is a secreted factor with neutralizing activity expressed in the anterior primitive endoderm of the mouse gastrula. Mech Dev. 68(1-2):45-57. (1997)
Ben-Haim N, Lu C, Guzman-Ayala M, Pescatore L, Mesnard D, Bischofberger M, Naef F, Robertson EJ, Constam DB. The nodal precursor acting via activin receptors induces mesoderm by maintaining a source of its convertases and BMP4. Dev Cell. 11(3):313-23. (2006)
Beyer TA, Weiss A, Khomchuk Y, Huang K, Ogunjimi AA, Varelas X, Wrana JL. Switch enhancers interpret TGF-β and Hippo signaling to control cell fate in human embryonic stem cells. Cell Rep. 5(6):1611-24. (2013)
Biondi CA, Das D, Howell M, Islam A, Bikoff EK, Hill CS, Robertson EJ. Mice develop normally in the absence of Smad4 nucleocytoplasmic shuttling. Biochem J. 404(2):235-45. (2007)
Blum M, Gaunt SJ, Cho KW, Steinbeisser H, Blumberg B, Bittner D, De Robertis EM. Gastrulation in the mouse: the role of the homeobox gene goosecoid. Cell. 69(7):1097-106. (1992)
Bogani D, Morgan MA, Nelson AC, Costello I, McGouran JF, Kessler BM, Robertson EJ, Bikoff EK. The PR/SET domain zinc finger protein Prdm4 regulates gene expression in embryonic stem cells but plays a nonessential role in the developing mouse embryo. Mol Cell Biol. 33(19):3936-50. (2013)
Boroviak T, Loos R, Bertone P, Smith A, Nichols J. The ability of inner-cell-mass cells to self-renew as embryonic stem cells is acquired following epiblast specification. Nat Cell Biol. 16(6):516-28. (2014)

Boroviak T, Loos R, Lombard P, Okahara J, Behr R, Sasaki E, Nichols J, Smith A, Bertone P. Lineage-Specific Profiling Delineates the Emergence and Progression of Naive Pluripotency in Mammalian Embryogenesis. Dev Cell. 35(3):366-82. (2015)
Bortvin A, Eggan K, Skaletsky H, Akutsu H, Berry DL, Yanagimachi R, Page DC, Jaenisch R. Incomplete reactivation of Oct4-related genes in mouse embryos cloned from somatic nuclei. Development. 130(8):1673-80. (2003)
Bourc'his D, Xu GL, Lin CS, Bollman B, Bestor TH. Dnmt3L and the establishment of maternal genomic imprints. Science. 294(5551):2536-9. (2001)
Bradley A, Evans M, Kaufman MH, Robertson E. Formation of germ-line chimaeras from embryo-derived teratocarcinoma cell lines. Nature. 309(5965):255-6. (1984)
Brennan J, Lu CC, Norris DP, Rodriguez TA, Beddington RS, Robertson EJ. Nodal signalling in the epiblast patterns the early mouse embryo. Nature. 411(6840):965-9. (2001)
Brons IG, Smithers LE, Trotter MW, Rugg-Gunn P, Sun B, Chuva de Sousa Lopes SM, Howlett SK, Clarkson A, Ahrlund-Richter L, Pedersen RA, Vallier L. Derivation of pluripotent epiblast stem cells from mammalian embryos. Nature. 448(7150):191-5. (2007)
Brown S, Teo A, Pauklin S, Hannan N, Cho CH, Lim B, Vardy L, Dunn NR, Trotter M, Pedersen R, Vallier L. Activin/Nodal signaling controls divergent transcriptional networks in human embryonic stem cells and in endoderm progenitors. Stem Cells. (8):1176-85. (2011)
Buecker C, Srinivasan R, Wu Z, Calo E, Acampora D, Faial T, Simeone A, Tan M, Swigut T, Wysocka J. Reorganization of enhancer patterns in transition from naive to primed pluripotency. Cell Stem Cell. 14(6):838-53. (2014)
Camus A, Perea-Gomez A, Moreau A, Collignon J. Absence of Nodal signaling promotes precocious neural differentiation in the mouse embryo. Dev Biol. 295(2):743-55. (2006)
Chacko BM, Qin B, Correia JJ, Lam SS, de Caestecker MP, Lin K. The L3 loop and C-terminal phosphorylation jointly define Smad protein trimerization. Nat Struct Biol. 8(3):248-53. (2001)
Chambers I, Colby D, Robertson M, Nichols J, Lee S, Tweedie S, Smith A. Functional expression cloning of Nanog, a pluripotency sustaining factor in embryonic stem cells. Cell. 113(5):643-55. (2003)
Chambers I, Silva J, Colby D, Nichols J, Nijmeijer B, Robertson M, Vrana J, Jones K, Grotewold L, Smith A. Nanog safeguards pluripotency and mediates germline development. Nature. 450(7173):1230-4. (2007)
Chang H, Huylebroeck D, Verschueren K, Guo Q, Matzuk MM, Zwijsen A. Smad5 knockout mice die at mid-gestation due to multiple embryonic and extraembryonic defects. Development. 126(8):1631-42. (1999)
Chang H, Matzuk MM. Smad5 is required for mouse primordial germ cell development. Mech Dev. 104(1-2):61-7. (2001)
Chazaud C, Yamanaka Y, Pawson T, Rossant J. Early lineage segregation between epiblast and primitive endoderm in mouse blastocysts through the Grb2-MAPK pathway. Dev Cell. 10(5):615-24. (2006)
Chen C, Shen MM. Two modes by which Lefty proteins inhibit nodal signaling. Curr Biol. 14(7):618-24. (2004)
Chen SR, Zheng QS, Zhang Y, Gao F, Liu YX. Disruption of genital ridge development causes aberrant primordial germ cell proliferation but does not affect their directional migration. BMC Biol. 11:22. (2013)
Chen X, Weisberg E, Fridmacher V, Watanabe M, Naco G, Whitman M. Smad4 and FAST-1 in the assembly of activin-responsive factor. Nature. 389(6646):85-9. (1997)
Chen X, Xu H, Yuan P, Fang F, Huss M, Vega VB, Wong E, Orlov YL, Zhang W, Jiang J, Loh YH, Yeo HC, Yeo ZX, Narang V, Govindarajan KR, Leong B, Shahab A, Ruan Y, Bourque G, Sung WK, Clarke ND, Wei CL, Ng HH. Integration of external signaling pathways with the core transcriptional network in embryonic stem cells. Cell. 133(6):1106-17. (2008)
Chu GC, Dunn NR, Anderson DC, Oxburgh L, Robertson EJ. Differential requirements for Smad4 in TGFbeta-dependent patterning of the early mouse embryo. Development. 131(15):3501-12. (2004)
Chu J, Shen MM. Functional redundancy of EGF-CFC genes in epiblast and extraembryonic patterning during early mouse embryogenesis. Dev Biol. 342(1):63-73. (2010)
Chun JY, Han YJ, Ahn KY. Psx homeobox gene is X-linked and specifically expressed in trophoblast cells of mouse placenta. Dev Dyn. 216(3):257-66. (1999)

Conlon FL, Barth KS, Robertson EJ. A novel retrovirally induced embryonic lethal mutation in the mouse: assessment of the developmental fate of embryonic stem cells homozygous for the 413.d proviral integration. Development. 111(4):969-81. (1991)

Conlon FL, Lyons KM, Takaesu N, Barth KS, Kispert A, Herrmann B, Robertson EJ. A primary requirement for nodal in the formation and maintenance of the primitive streak in the mouse. Development. 120(7):1919-28. (1994)

Constam DB, Robertson EJ. Regulation of bone morphogenetic protein activity by pro domains and proprotein convertases. J Cell Biol. 144(1):139-49. (1999)

Constam DB. Regulation of TGFβ and related signals by precursor processing. Semin Cell Dev Biol. 32:85-97. (2014) Review.

Costello I, Biondi CA, Taylor JM, Bikoff EK, Robertson EJ. Smad4-dependent pathways control basement membrane deposition and endodermal cell migration at early stages of mouse development. BMC Dev Biol. 9:54. (2009)

Costello I, Pimeisl IM, Dräger S, Bikoff EK, Robertson EJ, Arnold SJ. The T-box transcription factor Eomesodermin acts upstream of Mesp1 to specify cardiac mesoderm during mouse gastrulation. Nat Cell Biol. 13(9):1084-91. (2011)

Costello I, Nowotschin S, Sun X, Mould AW, Hadjantonakis AK, Bikoff EK, Robertson EJ. Lhx1 functions together with Otx2, Foxa2, and Ldb1 to govern anterior mesendoderm, node, and midline development. Genes Dev. 29(20):2108-22. (2015)

Coucouvanis E, Martin GR. Signals for death and survival: a two-step mechanism for cavitation in the vertebrate embryo. Cell. 83(2):279-87. (1995)

Coucouvanis E, Martin GR. BMP signaling plays a role in visceral endoderm differentiation and cavitation in the early mouse embryo. Development. 26(3):535-46. (1999)

Coultas L, Terzano S, Thomas T, Voss A, Reid K, Stanley EG, Scott CL, Bouillet P, Bartlett P, Ham J, Adams JM, Strasser A. Hrk/DP5 contributes to the apoptosis of select neuronal populations but is dispensable for haematopoietic cell apoptosis. J Cell Sci. 120:2044-52. (2007)

Cross JC, Flannery ML, Blanar MA, Steingrimsson E, Jenkins NA, Copeland NG, Rutter WJ, Werb Z. Hxt encodes a basic helix-loop-helix transcription factor that regulates trophoblast cell development. Development. 121(8):2513-23. (1995)

Crossley PH, Martin GR. The mouse Fgf8 gene encodes a family of polypeptides and is expressed in regions that direct outgrowth and patterning in the developing embryo. Development. 121(2):439-51. (1995)

D'Aniello C, Lonardo E, Iaconis S, Guardiola O, Liguoro AM, Liguori GL, Autiero M, Carmeliet P, Minchiotti G. G protein-coupled receptor APJ and its ligand apelin act downstream of Cripto to specify embryonic stem cells toward the cardiac lineage through extracellular signal-regulated kinase/p70S6 kinase signaling pathway. Circ Res. 105(3):231-8. (2009)

D'Aniello C, Fiorenzano A, Iaconis S, Liguori GL, Andolfi G, Cobellis G, Fico A, Minchiotti G. The G-protein-coupled receptor APJ is expressed in the second heart field and regulates Cerberus-Baf60c axis in embryonic stem cell cardiomyogenesis. Cardiovasc Res. 100(1):95-104. (2013)

Datto MB, Frederick JP, Pan L, Borton AJ, Zhuang Y, Wang XF. Targeted disruption of Smad3 reveals an essential role in transforming growth factor beta-mediated signal transduction. Mol Cell Biol. 19(4):2495-504. (1999)

Dehal P et al. The draft genome of Ciona intestinalis: insights into chordate and vertebrate origins. Science. 298(5601):2157-67. (2002)

Dennler S, Huet S, Gauthier JM. A short amino-acid sequence in MH1 domain is responsible for functional differences between Smad2 and Smad3. Oncogene. 18(8):1643-8. (1999)

Derynck R, Zhang YE. Smad-dependent and Smad-independent pathways in TGF-beta family signalling. Nature. 425(6958):577-84. (2003)

Deshwar AR, Chng SC, Ho L, Reversade B, Scott IC. The Apelin receptor enhances Nodal/TGFβ signaling to ensure proper cardiac development. Elife. 5:e13758. (2016)

Dietrich JE, Hiiragi T. Stochastic patterning in the mouse pre-implantation embryo. Development. 134(23):4219-31. (2007)

Ding J, Yang L, Yan YT, Chen A, Desai N, Wynshaw-Boris A, Shen MM. Cripto is required for correct orientation of the anterior-posterior axis in the mouse embryo. Nature. 395(6703):702-7. (1998)

Doetschman TC, Eistetter H, Katz M, Schmidt W, Kemler R. The in vitro development of blastocyst-derived embryonic stem cell lines: formation of visceral yolk sac, blood islands and myocardium. J Embryol Exp Morphol. 87:27-45. (1985)

Doherty AS, Mann MR, Tremblay KD, Bartolomei MS, Schultz RM. Differential effects of culture on imprinted H19 expression in the preimplantation mouse embryo. Biol Reprod. 62(6):1526-35. (2000)

Dufort D, Schwartz L, Harpal K, Rossant J. The transcription factor HNF3beta is required in visceral endoderm for normal primitive streak morphogenesis. Development. 125:3015-25. (1998)

Duncan SA, Manova K, Chen WS, Hoodless P, Weinstein DC, Bachvarova RF, Darnell JE Jr. Expression of transcription factor HNF-4 in the extraembryonic endoderm, gut, and nephrogenic tissue of the developing mouse embryo: HNF-4 is a marker for primary endoderm in the implanting blastocyst. Proc Natl Acad Sci USA. 91(16):7598-602. (1994)

Dunn NR, Vincent SD, Oxburgh L, Robertson EJ, Bikoff EK. Combinatorial activities of Smad2 and Smad3 regulate mesoderm formation and patterning in the mouse embryo. Development. 131(8):1717-28. (2004)

Dunn NR, Koonce CH, Anderson DC, Islam A, Bikoff EK, Robertson EJ. Mice exclusively expressing the short isoform of Smad2 develop normally and are viable and fertile. Genes Dev. 19(1):152-63. (2005)

Dunwoodie SL, Rodriguez TA, Beddington RS. Msg1 and Mrg1, founding members of a gene family, show distinct patterns of gene expression during mouse embryogenesis. Mech Dev. 72(1-2):27-40. (1998)

Dupont S, Mamidi A, Cordenonsi M, Montagner M, Zacchigna L, Adorno M, Martello G, Stinchfield MJ, Soligo S, Morsut L, Inui M, Moro S, Modena N, Argenton F, Newfeld SJ, Piccolo S. FAM/USP9x, a deubiquitinating enzyme essential for TGFbeta signaling, controls Smad4 monoubiquitination. Cell. 136(1):123-35. (2009)

Dush MK, Martin GR. Analysis of mouse Evx genes: Evx-1 displays graded expression in the primitive streak. Dev Biol. 151(1):273-87. (1992)

Dziadek M, Adamson E. Localization and synthesis of alphafoetoprotein in post-implantation mouse embryos. J Embryol Exp Morphol. 43:289-313. (1978)

Elias S, McGuire JR, Yu H, Humbert S. Huntingtin is required for epithelial polarity through RAB11A-mediated apical trafficking of PAR3-aPKC. PLoS Biol. 13(5):e1002142. (2015)

Ema M, Mori D, Niwa H, Hasegawa Y, Yamanaka Y, Hitoshi S, Mimura J, Kawabe Y, Hosoya T, Morita M, Shimosato D, Uchida K, Suzuki N, Yanagisawa J, Sogawa K, Rossant J, Yamamoto M, Takahashi S, Fujii-Kuriyama Y. Krüppel-like factor 5 is essential for blastocyst development and the normal self-renewal of mouse ESCs. Cell Stem Cell. 3(5):555-67. (2008)

Evans MJ, Kaufman MH. Establishment in culture of pluripotential cells from mouse embryos. Nature. 292(5819):154-6. (1981)

Factor DC, Corradin O, Zentner GE, Saiakhova A, Song L, Chenoweth JG, McKay RD, Crawford GE, Scacheri PC, Tesar PJ. Epigenomic comparison reveals activation of "seed" enhancers during transition from naive to primed pluripotency. Cell Stem Cell. 14(6):854-63. (2014)

Faial T, Bernardo AS, Mendjan S, Diamanti E, Ortmann D, Gentsch GE, Mascetti VL, Trotter MW, Smith JC, Pedersen RA. Brachyury and SMAD signalling collaboratively orchestrate distinct mesoderm and endoderm gene regulatory networks in differentiating human embryonic stem cells. Development. 142(12):2121-35. (2015)

Fainsod A, Deissler K, Yelin R, Marom K, Epstein M, Pillemer G, Steinbeisser H, Blum M. The dorsalizing and neural inducing gene follistatin is an antagonist of BMP-4. Mech Dev. 63(1):39-50. (1997)

Fuentealba LC, Eivers E, Ikeda A, Hurtado C, Kuroda H, Pera EM, De Robertis EM. Integrating patterning signals: Wnt/GSK3 regulates the duration of the BMP/Smad1 signal. Cell. 131(5):980-93. (2007)

Fuerer C, Nostro MC, Constam DB. Nodal·Gdf1 heterodimers with bound prodomains enable serum-independent nodal signaling and endoderm differentiation. J Biol Chem. 289(25):17854-71. (2014)

Fujimori H, Mukai H, Murakami Y, Hemberger M, Hippo Y, Masutani M. The H19 induction triggers trophoblast lineage commitment in mouse ES cells. Biochem Biophys Res Commun. 436(2):313-8. (2013)

Fujiwara T, Dunn NR, Hogan BL. Bone morphogenetic protein 4 in the extraembryonic mesoderm is required for allantois development and the localization and survival of primordial germ cells in the mouse. Proc Natl Acad Sci USA. 98(24):13739-44. (2001)

Fujiwara T, Dehart DB, Sulik KK, Hogan BL. Distinct requirements for extra-embryonic and embryonic bone morphogenetic protein 4 in the formation of the node and primitive streak and coordination of left-right asymmetry in the mouse. Development. 129(20):4685-96. (2002)

Fujiwara Y, Komiya T, Kawabata H, Sato M, Fujimoto H, Furusawa M, Noce T. Isolation of a DEAD-family protein gene that encodes a murine homolog of Drosophila vasa and its specific expression in germ cell lineage. Proc Natl Acad Sci USA. 91(25):12258-62. (1994)

Gaio U, Schweickert A, Fischer A, Garratt AN, Müller T, Ozcelik C, Lankes W, Strehle M, Britsch S, Blum M, Birchmeier C. A role of the cryptic gene in the correct establishment of the left-right axis. Curr Biol. 9(22):1339-42. (1999)

Galvin-Burgess KE, Travis ED, Pierson KE, Vivian JL. TGF-β-superfamily signaling regulates embryonic stem cell heterogeneity: self-renewal as a dynamic and regulated equilibrium. Stem Cells. (1):48-58. (2013)

Galvin KE, Travis ED, Yee D, Magnuson T, Vivian JL. Nodal signaling regulates the bone morphogenic protein pluripotency pathway in mouse embryonic stem cells. J Biol Chem. 285(26):19747-56. (2010)

Gao, S. et al. Ubiquitin ligase Nedd4L targets activated Smad2/3 to limit TGF-β signaling. Mol Cell 36, 457–468. (2009)

Gardner RL. Mouse chimeras obtained by the injection of cells into the blastocyst. Nature. 220(5167):596-7. (1968)

Gardner RL, Cockroft DL. Complete dissipation of coherent clonal growth occurs before gastrulation in mouse epiblast. Development. 125(13):2397-402. (1998)

Ginsburg M, Snow MH, McLaren A. Primordial germ cells in the mouse embryo during gastrulation. Development. 110(2):521-8. (1990)

Gomes Fernandes M, Dries R, Roost MS, Semrau S, de Melo Bernardo A, Davis RP, Ramakrishnan R, Szuhai K, Maas E, Umans L, Abon Escalona V, Salvatori D, Deforce D, Van Criekinge W, Huylebroeck D, Mummery C, Zwijsen A, de Sousa Lopes SM. BMP-SMAD signaling regulates lineage priming, but is dispensable for self-renewal in mouse embryonic stem cells. Stem Cell Reports. 6(1):85-94. (2016)

Gray PA, Fu H, Luo P, Zhao Q, Yu J, Ferrari A, Tenzen T, Yuk DI, Tsung EF, Cai Z, Alberta JA, Cheng LP, Liu Y, Stenman JM, Valerius MT, Billings N, Kim HA, Greenberg ME, McMahon AP, Rowitch DH, Stiles CD, Ma Q. Mouse brain organization revealed through direct genome-scale TF expression analysis. Science. 306(5705):2255-7. (2004)

Gu Z, Reynolds EM, Song J, Lei H, Feijen A, Yu L, He W, MacLaughlin DT, van den Eijnden-van Raaij J, Donahoe PK, Li E. The type I serine/threonine kinase receptor ActRIA (ALK2) is required for gastrulation of the mouse embryo. Development. 126(11):2551-61. (1999)

Guillemot F, Caspary T, Tilghman SM, Copeland NG, Gilbert DJ, Jenkins NA, Anderson DJ, Joyner AL, Rossant J, Nagy A. Genomic imprinting of Mash2, a mouse gene required for trophoblast development. Nat Genet. (3):235-42. (1995)

Guo G, Yang J, Nichols J, Hall JS, Eyres I, Mansfield W, Smith A. Klf4 reverts developmentally programmed restriction of ground state pluripotency. Development. 136(7):1063-9. (2009)

Guo G, Huss M, Tong GQ, Wang C, Li Sun L, Clarke ND, Robson P. Resolution of cell fate decisions revealed by single-cell gene expression analysis from zygote to blastocyst. Dev Cell. 18(4):675-85. (2010)

Guzman-Ayala M, Lee KL, Mavrakis KJ, Goggolidou P, Norris DP, Episkopou V. Graded Smad2/3 activation is converted directly into levels of target gene expression in embryonic stem cells. PLoS One. 4(1):e4268. (2009)

Habibi E, Brinkman AB, Arand J, Kroeze LI, Kerstens HH, Matarese F, Lepikhov K, Gut M, Brun-Heath I, Hubner NC, Benedetti R, Altucci L, Jansen JH, Walter J, Gut IG, Marks H, Stunnenberg HG. Whole-genome bisulfite sequencing of two distinct interconvertible DNA methylomes of mouse embryonic stem cells. Cell Stem Cell. 13(3):360-9. (2013)

Hackett JA, Surani MA. Beyond DNA: programming and inheritance of parental methylomes. Cell. 153(4):737-9. (2013)

Haffner-Krausz R, Gorivodsky M, Chen Y, Lonai P. Expression of Fgfr2 in the early mouse embryo indicates its involvement in preimplantation development. Mech Dev. 85(1-2):167-72. (1999)

Han DW, Tapia N, Joo JY, Greber B, Araúzo-Bravo MJ, Bernemann C, Ko K, Wu G, Stehling M, Do JT, Schöler HR. Epiblast stem cell subpopulations represent mouse embryos of distinct pregastrulation stages. Cell. 143(4):617-27. (2010)

Han YJ, Lee YH, Chun JY. Identification and characterization of Psx-2, a novel member of the Psx (placenta-specific homeobox) family. Gene. 241(1):149-55. (2000)
Hara K, Kanai-Azuma M, Uemura M, Shitara H, Taya C, Yonekawa H, Kawakami H, Tsunekawa N, Kurohmaru M, Kanai Y. Evidence for crucial role of hindgut expansion in directing proper migration of primordial germ cells in mouse early embryogenesis. Dev Biol. 330(2):427-39. (2009)
Harper J, Mould A, Andrews RM, Bikoff EK, Robertson EJ. The transcriptional repressor Blimp1/Prdm1 regulates postnatal reprogramming of intestinal enterocytes. Proc Natl Acad Sci USA. 108(26):10585-90. (2011)
Harrison SM, Houzelstein D, Dunwoodie SL, Beddington RS. Sp5, a new member of the Sp1 family, is dynamically expressed during development and genetically interacts with Brachyury. Dev Biol. 227(2):358-72. (2000)
Hart AH, Hartley L, Ibrahim M, Robb L Identification, cloning and expression analysis of the pluripotency promoting Nanog genes in mouse and human. Dev Dyn. 230(1):187-98. (2004)
Hart AH, Willson TA, Wong M, Parker K, Robb L. Transcriptional regulation of the homeobox gene Mixl1 by TGF-beta and FoxH1. Biochem Biophys Res Commun. 333(4):1361-9. (2005)
Hata K, Okano M, Lei H, Li E. Dnmt3L cooperates with the Dnmt3 family of de novo DNA methyltransferases to establish maternal imprints in mice. Development. 129(8):1983-93. (2002)
Hay DC, Sutherland L, Clark J, Burdon T. Oct-4 knockdown induces similar patterns of endoderm and trophoblast differentiation markers in human and mouse embryonic stem cells. Stem Cells. 22(2):225-35. (2004)
Hayashi K, Kobayashi T, Umino T, Goitsuka R, Matsui Y, Kitamura D. SMAD1 signaling is critical for initial commitment of germ cell lineage from mouse epiblast. Mech Dev. 118(1-2):99-109. (2002) (2002a in main text)
Hayashi K, Surani MA. Self-renewing epiblast stem cells exhibit continual delineation of germ cells with epigenetic reprogramming in vitro. Development. 136(21):3549-56. (2009)
Hayashi S, Lewis P, Pevny L, McMahon AP. Efficient gene modulation in mouse epiblast using a Sox2Cre transgenic mouse strain. Mech Dev. 119 Suppl. 1:97-101. (2002) (2002b in main text)
Hayashi K, Ohta H, Kurimoto K, Aramaki S, Saitou M. Reconstitution of the mouse germ cell specification pathway in culture by pluripotent stem cells. Cell. 146(4):519-32. (2011)
Hayashi K, Ogushi S, Kurimoto K, Shimamoto S, Ohta H, Saitou M. Offspring from oocytes derived from in vitro primordial germ cell-like cells in mice. Science. 338(6109):971-5. (2012)
He W, Dorn DC, Erdjument-Bromage H, Tempst P, Moore MA, Massagué J. Hematopoiesis controlled by distinct TIF1gamma and Smad4 branches of the TGFbeta pathway. Cell. 125(5):929-41. (2006)
Hébert JM, Boyle M, Martin GR. mRNA localization studies suggest that murine FGF-5 plays a role in gastrulation. Development. 112(2):407-15. (1991)
Hébert JM, Rosenquist T, Götz J, Martin GR. FGF5 as a regulator of the hair growth cycle: evidence from targeted and spontaneous mutations. Cell. 78(6):1017-25. (1994)
Hemberger M, Dean W, Reik W. Epigenetic dynamics of stem cells and cell lineage commitment: digging Waddington's canal. Nat Rev Mol Cell Biol. 10(8):526-37. (2009) Review.
Herrmann BG, Labeit S, Poustka A, King TR, Lehrach H. Cloning of the T gene required in mesoderm formation in the mouse. Nature. 343(6259):617-22. (1990)
Hill CS. Transcriptional Control by the SMADs. Cold Spring Harb Perspect Biol. 8:a022079 (2016)
Hirate Y, Hirahara S, Inoue K, Suzuki A, Alarcon VB, Akimoto K, Hirai T, Hara T, Adachi M, Chida K, Ohno S, Marikawa Y, Nakao K, Shimono A, Sasaki H. Polarity-dependent distribution of angiomotin localizes Hippo signaling in preimplantation embryos. Curr Biol. 23(13):1181-94. (2013)
Hirate Y, Hirahara S, Inoue K, Kiyonari H, Niwa H, Sasaki H. Par-aPKC-dependent and -independent mechanisms cooperatively control cell polarity, Hippo signaling, and cell positioning in 16-cell stage mouse embryos. Dev Growth Differ. 57(8):544-56. (2015)
Hoffman JA, Wu CI, Merrill BJ. Tcf7l1 prepares epiblast cells in the gastrulating mouse embryo for lineage specification. Development. 140(8):1665-75. (2013)
Holland PW, Harper SJ, McVey JH, Hogan BL. In vivo expression of mRNA for the Ca++-binding protein SPARC (osteonectin) revealed by in situ hybridization. J Cell Biol. 105:473-82. (1987)

Hoodless PA, Haerry T, Abdollah S, Stapleton M, O'Connor MB, Attisano L, Wrana JL. MADR1, a MAD-related protein that functions in BMP2 signaling pathways. Cell. 85(4):489-500. (1996)

Hoodless PA, Pye M, Chazaud C, Labbé E, Attisano L, Rossant J, Wrana JL. FoxH1 (Fast) functions to specify the anterior primitive streak in the mouse. Genes Dev. 15(10):1257-71. (2001)

http://www.arrayanalysis.org/ accessed on 18/09/2016 1pm

http://www.webgestalt.org/ accessed on 18/09/2016 1pm

http://crispr.mit.edu accessed on 18/09/2016 1pm

http://www.addgene.org/48140/ accessed on 18/09/2016 1pm

http://www.cmbi.ru.nl/cdd/biovenn/ accessed on 18/09/2016 1pm

http://www.informatics.jax.org/ accessed on 18/09/2016 1pm

Hu YC, Nicholls PK, Soh YQ, Daniele JR, Junker JP, van Oudenaarden A, Page DC. Licensing of primordial germ cells for gametogenesis depends on genital ridge signaling. PLoS Genet. 11(3):e1005019. (2015)

Huminiecki L, Goldovsky L, Freilich S, Moustakas A, Ouzounis C, Heldin CH. Emergence, development and diversification of the TGF-beta signalling pathway within the animal kingdom. BMC Evol Biol. 9:28. (2009)

Hurlin PJ, Steingrìmsson E, Copeland NG, Jenkins NA, Eisenman RN. Mga, a dual-specificity transcription factor that interacts with Max and contains a T-domain DNA-binding motif. EMBO J. 18(24):7019-28. Erratum in: EMBO J. 19(14):3841. (1999)

Inman GJ, Nicolás FJ, Callahan JF, Harling JD, Gaster LM, Reith AD, Laping NJ, Hill CS. SB-431542 is a potent and specific inhibitor of transforming growth factor-beta superfamily type I activin receptor-like kinase (ALK) receptors ALK4, ALK5, and ALK7. Mol Pharmacol. 62(1):65-74. (2002)

Inman GJ, Hill CS. Stoichiometry of active smad-transcription factor complexes on DNA. J Biol Chem. 277(52):51008-16. Erratum in: J Biol Chem. 278(19):17580. (2003)

Ishiuchi T, Enriquez-Gasca R, Mizutani E, Bošković A, Ziegler-Birling C, Rodriguez-Terrones D, Wakayama T, Vaquerizas JM, Torres-Padilla ME. Early embryonic-like cells are induced by downregulating replication-dependent chromatin assembly. Nat Struct Mol Biol. 22(9):662-71. (2015)

Iwafuchi-Doi M, Matsuda K, Murakami K, Niwa H, Tesar PJ, Aruga J, Matsuo I, Kondoh H. Transcriptional regulatory networks in epiblast cells and during anterior neural plate development as modeled in epiblast stem cells. Development. 139(21):3926-37. (2012)

Izumi N, Era T, Akimaru H, Yasunaga M, Nishikawa S. Dissecting the molecular hierarchy for mesendoderm differentiation through a combination of embryonic stem cell culture and RNA interference. Stem Cells. 25(7):1664-74. (2007)

Jackman SM, Kong X, Fant ME. Plac1 (placenta-specific 1) is essential for normal placental and embryonic development. Mol Reprod Dev. 79(8):564-72. (2012)

James D, Levine AJ, Besser D, Hemmati-Brivanlou A. TGFbeta/activin/nodal signaling is necessary for the maintenance of pluripotency in human embryonic stem cells. Development. 132(6):1273-82. (2005)

Kaivo-oja N, Jeffery LA, Ritvos O, Mottershead DG. Smad signalling in the ovary. Reprod Biol Endocrinol. 4:21. (2006)

Kanai-Azuma M, Kanai Y, Gad JM, Tajima Y, Taya C, Kurohmaru M, Sanai Y, Yonekawa H, Yazaki K, Tam PP, Hayashi Y. Depletion of definitive gut endoderm in Sox17-null mutant mice. Development. 129(10):2367-79. (2002)

Kang Y, Kim J, Anderson JP, Wu J, Gleim SR, Kundu RK, McLean DL, Kim JD, Park H, Jin SW, Hwa J, Quertermous T, Chun HJ. Apelin-APJ signaling is a critical regulator of endothelial MEF2 activation in cardiovascular development. Circ Res. 113(1):22-31. (2013)

Karwacki-Neisius V, Göke J, Osorno R, Halbritter F, Ng JH, Weiße AY, Wong FC, Gagliardi A, Mullin NP, Festuccia N, Colby D, Tomlinson SR, Ng HH, Chambers I. Reduced Oct4 expression directs a robust pluripotent state with distinct signaling activity and increased enhancer occupancy by Oct4 and Nanog. Cell Stem Cell. 12(5):531-45. (2013)

Kaufmann LT, Gierl MS, Niehrs C. Gadd45a, Gadd45b and Gadd45g expression during mouse embryonic development. Gene Expr Patterns. 11(8):465-70. (2011)

Kazanskaya O, Ohkawara B, Heroult M, Wu W, Maltry N, Augustin HG, Niehrs C. The Wnt signaling regulator R-spondin 3 promotes angioblast and vascular development. Development. 135(22):3655-64. (2008)

Kehler J, Tolkunova E, Koschorz B, Pesce M, Gentile L, Boiani M, Lomelí H, Nagy A, McLaughlin KJ, Schöler HR, Tomilin A. Oct4 is required for primordial germ cell survival. EMBO Rep. 5(11):1078-83. (2004)
Kemp CR, Willems E, Wawrzak D, Hendrickx M, Agbor Agbor T, Leyns L. Expression of Frizzled5, Frizzled7, and Frizzled10 during early mouse development and interactions with canonical Wnt signaling. Dev Dyn. 236:2011-19. (2007)
Kent LN, Konno T, Soares MJ. Phosphatidylinositol 3 kinase modulation of trophoblast cell differentiation. BMC Dev Biol. 10:97. (2010)
Kim SW, Yoon SJ, Chuong E, Oyolu C, Wills AE, Gupta R, Baker J. Chromatin and transcriptional signatures for Nodal signaling during endoderm formation in hESCs. Dev Biol. 357(2):492-504. (2011)
Kispert A, Herrmann BG. The Brachyury gene encodes a novel DNA binding protein. EMBO J. 12(8):3211-20. Erratum in: EMBO J. 12(12):4898-9. (1993)
Kispert A, Koschorz B, Herrmann BG. The T protein encoded by Brachyury is a tissue-specific transcription factor. EMBO J. 14(19):4763-72. (1995)
Kitajima S, Takagi A, Inoue T, Saga Y. MesP1 and MesP2 are essential for the development of cardiac mesoderm. Development. 127(15):3215-26. (2000)
Kojima Y, Kaufman-Francis K, Studdert JB, Steiner KA, Power MD, Loebel DA, Jones V, Hor A, de Alencastro G, Logan GJ, Teber ET, Tam OH, Stutz MD, Alexander IE, Pickett HA, Tam PP. The transcriptional and functional properties of mouse epiblast stem cells resemble the anterior primitive streak. Cell Stem Cell. 14(1):107-20. (2014)
Kolodziejczyk AA, Kim JK, Tsang JC, Ilicic T, Henriksson J, Natarajan KN, Tuck AC, Gao X, Bühler M, Liu P, Marioni JC, Teichmann SA. Single Cell RNA-Sequencing of Pluripotent States Unlocks Modular Transcriptional Variation. Cell Stem Cell. 17(4):471-85. (2015)
Kretzschmar M, Doody J, Timokhina I, Massagué J. A mechanism of repression of TGFbeta/ Smad signaling by oncogenic Ras. Genes Dev. 13(7):804-16. (1999)
Kroll J, Shi X, Caprioli A, Liu HH, Waskow C, Lin KM, Miyazaki T, Rodewald HR, Sato TN. The BTB-kelch protein KLHL6 is involved in B-lymphocyte antigen receptor signaling and germinal center formation. Mol Cell Biol. 25(19):8531-40. (2005)
Kuales G, Weiss M, Sedelmeier O, Pfeifer D, Arnold SJ. A Resource for the transcriptional signature of bona fide trophoblast stem cells and analysis of their embryonic persistence. Stem Cells Int. 218518. (2015)
Kumar A, Lualdi M, Lyozin GT, Sharma P, Loncarek J, Fu XY, Kuehn MR. Nodal signaling from the visceral endoderm is required to maintain Nodal gene expression in the epiblast and drive DVE/AVE migration. Dev Biol. 400(1):1-9. (2015)
Kurimoto K, Yabuta Y, Ohinata Y, Shigeta M, Yamanaka K, Saitou M. Complex genome-wide transcription dynamics orchestrated by Blimp1 for the specification of the germ cell lineage in mice. Genes Dev. 22(12):1617-35. (2008)
Kurimoto K, Yabuta Y, Hayashi K, Ohta H, Kiyonari H, Mitani T, Moritoki Y, Kohri K, Kimura H, Yamamoto T, Katou Y, Shirahige K, Saitou M. Quantitative dynamics of chromatin remodeling during germ cell specification from mouse embryonic stem cells. Cell Stem Cell. 16(5):517-32. (2015)
Kwon GS, Viotti M, Hadjantonakis AK. The endoderm of the mouse embryo arises by dynamic widespread intercalation of embryonic and extraembryonic lineages. Dev Cell. 15(4):509-20. (2008)
Kwon GS, Hadjantonakis AK. Transthyretin mouse transgenes direct RFP expression or Cre-mediated recombination throughout the visceral endoderm. Genesis. 47(7):447-55. (2009)
Labbé E, Silvestri C, Hoodless PA, Wrana JL, Attisano L. Smad2 and Smad3 positively and negatively regulate TGF beta-dependent transcription through the forkhead DNA-binding protein FAST2. Mol Cell. 2(1):109-20. (1998)
Labosky PA, Hogan BL. Mouse primordial germ cells. Isolation and in vitro culture. Methods Mol Biol. 97:201-12. (1999)
Latos PA, Sienerth AR, Murray A, Senner CE, Muto M, Ikawa M, Oxley D, Burge S, Cox BJ, Hemberger M. Elf5-centered transcription factor hub controls trophoblast stem cell self-renewal and differentiation through stoichiometry-sensitive shifts in target gene networks. Genes Dev. 29(23):2435-48. (2015)
Lawson KA, Meneses JJ, Pedersen RA. Clonal analysis of epiblast fate during germ layer formation in the mouse embryo. Development. 113(3):891-911. (1991)
Lawson KA, Hage WJ. Clonal analysis of the origin of primordial germ cells in the mouse. Ciba Found Symp. 182:68-84; discussion 84-91. (1994)

Lawson KA, Dunn NR, Roelen BA, Zeinstra LM, Davis AM, Wright CV, Korving JP, Hogan BL. Bmp4 is required for the generation of primordial germ cells in the mouse embryo. Genes Dev. 13(4):424-36. (1999)
Le Good JA, Joubin K, Giraldez AJ, Ben-Haim N, Beck S, Chen Y, Schier AF, Constam DB. Nodal stability determines signaling range. Curr Biol. 15(1):31-6. (2005)
Lebrun JJ, Takabe K, Chen Y, Vale W. Roles of pathway-specific and inhibitory Smads in activin receptor signaling. Mol Endocrinol. 13(1):15-23. (1999)
Lee KL, Lim SK, Orlov YL, Yit le Y, Yang H, Ang LT, Poellinger L, Lim B. Graded Nodal/Activin signaling titrates conversion of quantitative phospho-Smad2 levels into qualitative embryonic stem cell fate decisions. PLoS Genet. 7(6):e1002130. (2011)
Levine AJ, Brivanlou AH. GDF3, a BMP inhibitor, regulates cell fate in stem cells and early embryos. Development. 133(2):209-16. (2006)
Levine AJ, Levine ZJ, Brivanlou AH. GDF3 is a BMP inhibitor that can activate Nodal signaling only at very high doses. Dev Biol. 325(1):43-8. (2009)
Li C, Li YP, Fu XY, Deng CX. Anterior visceral endoderm SMAD4 signaling specifies anterior embryonic patterning and head induction in mice. Int J Biol Sci. 6(6):569-83. (2010)
Li L, Liu C, Biechele S, Zhu Q, Song L, Lanner F, Jing N, Rossant J. Location of transient ectodermal progenitor potential in mouse development. Development. 140(22):4533-43. (2013) (2013a in main text)
Li P, Chen Y, Meng X, Kwok KY, Huang X, Choy KW, Wang CC, Lan H, Yuan P. Suppression of malignancy by Smad3 in mouse embryonic stem cell formed teratoma. Stem Cell Rev. 9(5):709-20. (2013) (2013b in main text)
Lin SC, Wani MA, Whitsett JA, Wells JM. Klf5 regulates lineage formation in the pre-implantation mouse embryo. Development. 137(23):3953-63. (2010)
Lin TP, Labosky PA, Grabel LB, Kozak CA, Pitman JL, Kleeman J, MacLeod CL. The Pem homeobox gene is X-linked and exclusively expressed in extraembryonic tissues during early murine development. Dev Biol. 166(1):170-9. (1994)
Liu P, Wakamiya M, Shea MJ, Albrecht U, Behringer RR, Bradley A. Requirement for Wnt3 in vertebrate axis formation. Nat Genet. 22(4):361-5. (1999)
López-Rovira T, Chalaux E, Massagué J, Rosa JL, Ventura F. Direct binding of Smad1 and Smad4 to two distinct motifs mediates bone morphogenetic protein-specific transcriptional activation of Id1 gene. J Biol Chem. 277(5):3176-85. (2002)
Lorthongpanich C, Doris TP, Limviphuvadh V, Knowles BB, Solter D. Developmental fate and lineage commitment of singled mouse blastomeres. Development. 139(20):3722-31. (2012)
Lu CC, Robertson EJ. Multiple roles for Nodal in the epiblast of the mouse embryo in the establishment of anterior-posterior patterning. Dev Biol. 273(1):149-59. (2004)
MacGregor GR, Zambrowicz BP, Soriano P. Tissue non-specific alkaline phosphatase is expressed in both embryonic and extraembryonic lineages during mouse embryogenesis but is not required for migration of primordial germ cells. Development. 121(5):1487-96. (1995)
Macias MJ, Martin-Malpartida P, Massagué J. Structural determinants of Smad function in TGF-β signaling. Trends Biochem Sci. 40(6):296-308. (2015)
Madan B, Madan V, Weber O, Tropel P, Blum C, Kieffer E, Viville S, Fehling HJ. The pluripotency-associated gene Dppa4 is dispensable for embryonic stem cell identity and germ cell development but essential for embryogenesis. Mol Cell Biol. 29(11):3186-203. (2009)
Maeda I, Okamura D, Tokitake Y, Ikeda M, Kawaguchi H, Mise N, Abe K, Noce T, Okuda A, Matsui Y. Max is a repressor of germ cell-related gene expression in mouse embryonic stem cells. Nat Commun. 4:1754. (2013)
Magnúsdóttir E, Dietmann S, Murakami K, Günesdogan U, Tang F, Bao S, Diamanti E, Lao K, Gottgens B, Azim Surani M. A tripartite transcription factor network regulates primordial germ cell specification in mice. Nat Cell Biol. 15(8):905-15. (2013)
Maître JL, Turlier H, Illukkumbura R, Eismann B, Niwayama R, Nédélec F, Hiiragi T. Asymmetric division of contractile domains couples cell positioning and fate specification. Nature. 536(7616):344-8. (2016)
Malaguti M, Nistor PA, Blin G, Pegg A, Zhou X, Lowell S. Bone morphogenic protein signalling suppresses differentiation of pluripotent cells by maintaining expression of E-Cadherin. Elife. 2:e01197. (2013)
Manipulating the Mouse Embryo: A Laboratory Manual, fourth edition (ed. Behringer R, Gertsenstein M, Nagy K, Nagy A), CSH Press (2014)
Mao X, Fujiwara Y, Chapdelaine A, Yang H, Orkin SH. Activation of EGFP expression by Cre-mediated excision in a new ROSA26 reporter mouse strain. Blood. 97(1):324-6. (2001)

Marchand M, Horcajadas JA, Esteban FJ, McElroy SL, Fisher SJ, Giudice LC. Transcriptomic signature of trophoblast differentiation in a human embryonic stem cell model. Biol Reprod. 84(6):1258-71. (2011)
Marikawa Y, Alarcon VB. Creation of trophectoderm, the first epithelium, in mouse preimplantation development. Results Probl Cell Differ. 55:165-84. (2012)
el Marjou F, Janssen KP, Chang BH, Li M, Hindie V, Chan L, Louvard D, Chambon P, Metzger D, Robine S. Tissue-specific and inducible Cre-mediated recombination in the gut epithelium. Genesis. 39(3):186-93. (2004)
Marks H, Kalkan T, Menafra R, Denissov S, Jones K, Hofemeister H, Nichols J, Kranz A, Stewart AF, Smith A, Stunnenberg HG. The transcriptional and epigenomic foundations of ground state pluripotency. Cell. 149(3):590-604. (2012)
Martello G, Bertone P, Smith A. Identification of the missing pluripotency mediator downstream of leukaemia inhibitory factor. EMBO J. 32(19):2561-74. (2013)
Martin GR. Isolation of a pluripotent cell line from early mouse embryos cultured in medium conditioned by teratocarcinoma stem cells. Proc Natl Acad Sci USA. 78(12):7634-8. (1981)
Massagué J, Seoane J, Wotton D. Smad transcription factors. Genes Dev. 19(23):2783-810. (2005) Review.
Massagué J. TGFβ signalling in context. Nat Rev Mol Cell Biol. 13(10):616-30. (2012) Review.
Masui S, Ohtsuka S, Yagi R, Takahashi K, Ko MS, Niwa H. Rex1/Zfp42 is dispensable for pluripotency in mouse ES cells. BMC Dev Biol. 8:45. (2008)
Matsuo I, Kuratani S, Kimura C, Takeda N, Aizawa S. Mouse Otx2 functions in the formation and patterning of rostral head. Genes Dev. 9(21):2646-58. (1995)
Mesnard D, Guzman-Ayala M, Constam DB. Nodal specifies embryonic visceral endoderm and sustains pluripotent cells in the epiblast before overt axial patterning. Development. 133(13):2497-505. (2006)
Meno C, Shimono A, Saijoh Y, Yashiro K, Mochida K, Ohishi S, Noji S, Kondoh H, Hamada H. lefty-1 is required for left-right determination as a regulator of lefty-2 and nodal. Cell. 94(3):287-97. (1998)
Menon S, Chi H, Zhang H, Deng XW, Flavell RA, Wei N. COP9 signalosome subunit 8 is essential for peripheral T cell homeostasis and antigen receptor-induced entry into the cell cycle from quiescence. Nat Immunol. 8(11):1236-45. (2007)
Mi Y, Shapiro SD, Baenziger JU. Regulation of lutropin circulatory half-life by the mannose/N-acetylgalactosamine-4-SO4 receptor is critical for implantation in vivo. J Clin Invest. 109(2):269-76. (2002)
Mikedis MM, Downs KM. Mouse primordial germ cells: a reappraisal. Int Rev Cell Mol Biol. 309:1-57. (2014) Review.
Mishina Y, Hanks MC, Miura S, Tallquist MD, Behringer RR. Generation of Bmpr/Alk3 conditional knockout mice. Genesis. 32(2):69-72. (2002)
Mitsui K, Tokuzawa Y, Itoh H, Segawa K, Murakami M, Takahashi K, Marauyama M, Maeda M, Yamanaka S. The homeoprotein Nanog is required for maintenance of pluripotency in mouse epiblast and ES cells. Cell. 113:631–642. (2003)
Miura S, Singh AP, Mishina Y. Bmpr1a is required for proper migration of the AVE through regulation of Dkk1 expression in the pre-streak mouse. Dev Biol. 341(1):246-54. (2010)
Miyazawa K, Shinozaki M, Hara T, Furuya T, Miyazono K. 2002. Two major Smad pathways in TGF-beta superfamily signalling. Genes Cells. 7(12):1191-204. (2002) Review.
Molyneaux K, Wylie C. Primordial germ cell migration. Int J Dev Biol. 48(5-6):537-44. (2004) Review.
Monteiro RM, de Sousa Lopes SM, Korchynskyi O, ten Dijke P, Mummery CL. Spatio-temporal activation of Smad1 and Smad5 in vivo: monitoring transcriptional activity of Smad proteins. J Cell Sci. 117(20):4653-63. (2004)
Morasso MI, Grinberg A, Robinson G, Sargent TD, Mahon KA. Placental failure in mice lacking the homeobox gene Dlx3. Proc Natl Acad Sci USA. 96(1):162-7. (1999)
Moriwaki K, Tsukita S, Furuse M. Tight junctions containing claudin 4 and 6 are essential for blastocyst formation in preimplantation mouse embryos. Dev Biol. 312(2):509-22. (2007)
Morkel M, Huelsken J, Wakamiya M, Ding J, van de Wetering M, Clevers H, Taketo MM, Behringer RR, Shen MM, Birchmeier W. Beta-catenin regulates Cripto- and Wnt3-dependent gene expression programs in mouse axis and mesoderm formation. Development. 130(25):6283-94. (2003)
Morris SM, Tallquist MD, Rock CO, Cooper JA. Dual roles for the Dab2 adaptor protein in embryonic development and kidney transport. EMBO J. 21(7):1555-64. (2002)

Morrisey EE, Musco S, Chen MY, Lu MM, Leiden JM, Parmacek MS. The gene encoding the mitogen-responsive phosphoprotein Dab2 is differentially regulated by GATA-6 and GATA-4 in the visceral endoderm. J Biol Chem. 275(26):19949-54. (2000)

Morrison GM, Oikonomopoulou I, Migueles RP, Soneji S, Livigni A, Enver T, Brickman JM. Anterior definitive endoderm from ESCs reveals a role for FGF signaling. Cell Stem Cell. 3(4):402-15. (2008)

Morsut L, Yan KP, Enzo E, Aragona M, Soligo SM, Wendling O, Mark M, Khetchoumian K, Bressan G, Chambon P, Dupont S, Losson R, Piccolo S. Negative control of Smad activity by ectodermin/Tif1gamma patterns the mammalian embryo. Development. 137(15):2571-8. (2010)

Mould A, Morgan MA, Li L, Bikoff EK, Robertson EJ. Blimp1/Prdm1 governs terminal differentiation of endovascular trophoblast giant cells and defines multipotent progenitors in the developing placenta. Genes Dev. 26(18):2063-74. (2012)

Mould AW, Morgan MA, Nelson AC, Bikoff EK, Robertson EJ. Blimp1/Prdm1 Functions in Opposition to Irf1 to Maintain Neonatal Tolerance during Postnatal Intestinal Maturation. PLoS Genet. 11(7):e1005375. (2015)

Moustakas A, Heldin CH. The regulation of TGFbeta signal transduction. Development. 136(22):3699-714. (2009) Review.

Mullen AC, Orlando DA, Newman JJ, Lovén J, Kumar RM, Bilodeau S, Reddy J, Guenther MG, DeKoter RP, Young RA. Master transcription factors determine cell-type-specific responses to TGF-β signaling. Cell. 147(3):565-76. (2011)

Murakami K, Günesdogan U, Zylicz JJ, Tang WW, Sengupta R, Kobayashi T, Kim S, Butler R, Dietmann S, Surani MA. NANOG alone induces germ cells in primed epiblast in vitro by activation of enhancers. Nature. 529(7586):403-7. (2016)

Nakaki F, Hayashi K, Ohta H, Kurimoto K, Yabuta Y, Saitou M. Induction of mouse germ-cell fate by transcription factors in vitro. Nature. 501(7466):222-6. (2013)

Nakamura T, Takio K, Eto Y, Shibai H, Titani K, Sugino H. Activin-binding protein from rat ovary is follistatin. Science. 247(4944):836-8. (1990)

Nelson AC, Mould AW, Bikoff EK, Robertson EJ. Single-cell RNA-seq reveals cell type-specific transcriptional signatures at the maternal-foetal interface during pregnancy. Nat Commun. 7:11414. (2016)

Ng YK, George KM, Engel JD, Linzer DI. GATA factor activity is required for the trophoblast-specific transcriptional regulation of the mouse placental lactogen I gene. Development. 120(11):3257-66. (1994)

Ng RK, Dean W, Dawson C, Lucifero D, Madeja Z, Reik W, Hemberger M. Epigenetic restriction of embryonic cell lineage fate by methylation of Elf5. Nat Cell Biol. 10(11):1280-90. (2008)

Nichols J, Evans EP, Smith AG. Establishment of germ-line-competent embryonic stem (ES) cells using differentiation inhibiting activity. Development. 110(4):1341-8. (1990)

Nichols J, Zevnik B, Anastassiadis K, Niwa H, Klewe-Nebenius D, Chambers I, Schöler H, Smith A. Formation of pluripotent stem cells in the mammalian embryo depends on the POU transcription factor Oct4. Cell. 95(3):379-91. (1998)

Nichols J, Smith A. Naive and primed pluripotent states. Cell Stem Cell. 4(6):487-92. (2009) Review.

Nichols J, Smith A. Pluripotency in the embryo and in culture. CSH Perspect Biol. 4(8):a008128. (2012) Review.

Nishioka N, Yamamoto S, Kiyonari H, Sato H, Sawada A, Ota M, Nakao K, Sasaki H. Tead4 is required for specification of trophectoderm in pre-implantation mouse embryos. Mech Dev. 125(3-4):270-83. (2008)

Nishioka N, Inoue K, Adachi K, Kiyonari H, Ota M, Ralston A, Yabuta N, Hirahara S, Stephenson RO, Ogonuki N, Makita R, Kurihara H, Morin-Kensicki EM, Nojima H, Rossant J, Nakao K, Niwa H, Sasaki H. The Hippo signaling pathway components Lats and Yap pattern Tead4 activity to distinguish mouse trophectoderm from inner cell mass. Dev Cell. 16(3):398-410. (2009)

Niwa H, Burdon T, Chambers I, Smith A. Self-renewal of pluripotent embryonic stem cells is mediated via activation of STAT3. Genes Dev. 12(13):2048-60. (1998)

Niwa H, Miyazaki J, Smith AG. Quantitative expression of Oct-3/4 defines differentiation, dedifferentiation or self-renewal of ES cells. Nat Genet. 24(4):372-6. (2000)

Niwa H, Masui S, Chambers I, Smith AG, Miyazaki J. Phenotypic complementation establishes requirements for specific POU domain and generic transactivation function of Oct-3/4 in embryonic stem cells. Mol Cell Biol. 22(5):1526-36. (2002)

Niwa H, Toyooka Y, Shimosato D, Strumpf D, Takahashi K, Yagi R, Rossant J. Interaction between Oct3/4 and Cdx2 determines trophectoderm differentiation. Cell. 123(5):917-29. (2005)
Norris DP, Robertson EJ. Asymmetric and node-specific nodal expression patterns are controlled by two distinct cis-acting regulatory elements. Genes Dev. 13(12):1575-88. (1999)
Norris DP, Brennan J, Bikoff EK, Robertson EJ. The Foxh1-dependent autoregulatory enhancer controls the level of Nodal signals in the mouse embryo. Development. 129(14):3455-68. (2002)
Nowotschin S, Costello I, Piliszek A, Kwon GS, Mao CA, Klein WH, Robertson EJ, Hadjantonakis AK. The T-box transcription factor Eomesodermin is essential for AVE induction in the mouse embryo. Genes Dev. 27(9):997-1002. (2013).
Ohinata Y, Payer B, O'Carroll D, Ancelin K, Ono Y, Sano M, Barton SC, Obukhanych T, Nussenzweig M, Tarakhovsky A, Saitou M, Surani MA. Blimp1 is a critical determinant of the germ cell lineage in mice. Nature. 436(7048):207-13. (2005)
Ohinata Y, Sano M, Shigeta M, Yamanaka K, Saitou M. A comprehensive, non-invasive visualization of primordial germ cell development in mice by the Prdm1-mVenus and Dppa3-ECFP double transgenic reporter. Reproduction. 136(4):503-14. (2008)
Ohinata Y, Ohta H, Shigeta M, Yamanaka K, Wakayama T, Saitou M. A signaling principle for the specification of the germ cell lineage in mice. Cell. 137(3):571-84. (2009)
Ohlsson R, Falck P, Hellström M, Lindahl P, Boström H, Franklin G, Ahrlund-Richter L, Pollard J, Soriano P, Betsholtz C. PDGFB regulates the development of the labyrinthine layer of the mouse fetal placenta. Dev Biol. 212(1):124-36. (1999)
Okamura D, Kimura T, Nakano T, Matsui Y. Cadherin-mediated cell interaction regulates germ cell determination in mice. Development. 130(26):6423-30. (2003)
Okamura D, Tokitake Y, Niwa H, Matsui Y. Requirement of Oct3/4 function for germ cell specification. Dev Biol. 317(2):576-84. (2008)
Okano M, Bell DW, Haber DA, Li E. DNA methyltransferases Dnmt3a and Dnmt3b are essential for de novo methylation and mammalian development. Cell. 99(3):247-57. (1999)
Oliver G, Mailhos A, Wehr R, Copeland NG, Jenkins NA, Gruss P. Six3, a murine homologue of the sine oculis gene, demarcates the most anterior border of the developing neural plate and is expressed during eye development. Development. 121(12):4045-55. (1995)
Osorno R, Tsakiridis A, Wong F, Cambray N, Economou C, Wilkie R, Blin G, Scotting PJ, Chambers I, Wilson V. The developmental dismantling of pluripotency is reversed by ectopic Oct4 expression. Development. 139(13):2288-98. (2012)
Palmieri SL, Peter W, Hess H, Schöler HR. Oct-4 transcription factor is differentially expressed in the mouse embryo during establishment of the first two extraembryonic cell lineages involved in implantation. Dev Biol. 166(1):259-67. (1994)
Pan H, Schultz RM. Sox2 modulates reprogramming of gene expression in two-cell mouse embryos. Biol Reprod. 85(2):409-16. (2011)
Papaioannou VE. The T-box gene family: emerging roles in development, stem cells and cancer. Development. 141(20):3819-33. (2014)
Papanayotou C, Collignon J. Activin/Nodal signalling before implantation: setting the stage for embryo patterning. Philos Trans R Soc Lond B Biol Sci. 369(1657):20130539. (2014) Review.
Papanayotou C, Benhaddou A, Camus A, Perea-Gomez A, Jouneau A, Mezger V, Langa F, Ott S, Sabéran-Djoneidi D, Collignon J. A novel nodal enhancer dependent on pluripotency factors and smad2/3 signaling conditions a regulatory switch during epiblast maturation. PLoS Biol. 12(6):e1001890. (2014)
Parast MM, Yu H, Ciric A, Salata MW, Davis V, Milstone DS. PPARgamma regulates trophoblast proliferation and promotes labyrinthine trilineage differentiation. PLoS One. 4(11):e8055. (2009)
Parr BA, Cornish VA, Cybulsky MI, McMahon AP. Wnt7b regulates placental development in mice. Dev Biol. 237(2):324-32. (2001)
Pauklin S, Vallier L. Activin/Nodal signalling in stem cells. Development. 142(4):607-19. (2015) Review.
Pauli A, Norris ML, Valen E, Chew GL, Gagnon JA, Zimmerman S, Mitchell A, Ma J, Dubrulle J, Reyon D, Tsai SQ, Joung JK, Saghatelian A, Schier AF. Toddler: an embryonic signal that promotes cell movement via Apelin receptors. Science. 343(6172):1248636. (2014)
Pearce JJ, Evans MJ. Mml, a mouse Mix-like gene expressed in the primitive streak. Mech Dev. 87(1-2):189-92. (1999)

Pease S, Braghetta P, Gearing D, Grail D, Williams RL. Isolation of embryonic stem (ES) cells in media supplemented with recombinant leukemia inhibitory factor (LIF). Dev Biol. 141(2):344-52. (1990)

Pelton TA, Sharma S, Schulz TC, Rathjen J, Rathjen PD. Transient pluripotent cell populations during primitive ectoderm formation: correlation of in vivo and in vitro pluripotent cell development. J Cell Sci. 115(2):329-39. (2002)

Perea-Gómez A, Shawlot W, Sasaki H, Behringer RR, Ang S. HNF3beta and Lim1 interact in the visceral endoderm to regulate primitive streak formation and anterior-posterior polarity in the mouse embryo. Development. 126(20):4499-511. (1999)

Perea-Gomez A, Vella FD, Shawlot W, Oulad-Abdelghani M, Chazaud C, Meno C, Pfister V, Chen L, Robertson E, Hamada H, Behringer RR, Ang SL. Nodal antagonists in the anterior visceral endoderm prevent the formation of multiple primitive streaks. Dev Cell. 3(5):745-56. (2002)

Pereira PN, Dobreva MP, Graham L, Huylebroeck D, Lawson KA, Zwijsen AN. Amnion formation in the mouse embryo: the single amniochorionic fold model. BMC Dev Biol. 11:48. (2011)

Pfendler KC, Catuar CS, Meneses JJ, Pedersen RA. Overexpression of Nodal promotes differentiation of mouse embryonic stem cells into mesoderm and endoderm at the expense of neuroectoderm formation. Stem Cells Dev. 14(2):162-72. (2005)

Piccolo S, Agius E, Leyns L, Bhattacharyya S, Grunz H, Bouwmeester T, De Robertis EM. The head inducer Cerberus is a multifunctional antagonist of Nodal, BMP and Wnt signals. Nature. 397(6721):707-10. (1999)

Qin BY, Chacko BM, Lam SS, de Caestecker MP, Correia JJ, Lin K. Structural basis of Smad1 activation by receptor kinase phosphorylation. Mol Cell. 8(6):1303-12. (2001)

Radzisheuskaya A, Chia Gle B, dos Santos RL, Theunissen TW, Castro LF, Nichols J, Silva JC. A defined Oct4 level governs cell state transitions of pluripotency entry and differentiation into all embryonic lineages. Nat Cell Biol. 15(6):579-90. (2013)

Ralston A, Rossant J. Cdx2 acts downstream of cell polarization to cell-autonomously promote trophectoderm fate in the early mouse embryo. Dev Biol. 313(2):614-29. (2008)

Ralston A, Cox BJ, Nishioka N, Sasaki H, Chea E, Rugg-Gunn P, Guo G, Robson P, Draper JS, Rossant J. Gata3 regulates trophoblast development downstream of Tead4 and in parallel to Cdx2. Development. 137(3):395-403. (2010)

Ran FA, Hsu PD, Lin CY, Gootenberg JS, Konermann S, Trevino AE, Scott DA, Inoue A, Matoba S, Zhang Y, Zhang F. Double nicking by RNA-guided CRISPR Cas9 for enhanced genome editing specificity. Cell. 154(6):1380-9. Erratum in: Cell. 155(2):479-80. (2013)

Redshaw N, Camps C, Sharma V, Motallebipour M, Guzman-Ayala M, Oikonomopoulos S, Thymiakou E, Ragoussis J, Episkopou V. TGF-β/Smad2/3 signaling directly regulates several miRNAs in mouse ES cells and early embryos. PLoS One. 8(1):e55186. (2013)

Rhinn M, Dierich A, Shawlot W, Behringer RR, Le Meur M, Ang SL. Sequential roles for Otx2 in visceral endoderm and neuroectoderm for forebrain and midbrain induction and specification. Development. 125(5):845-56. (1998)

Ribes V, Briscoe J. Establishing and interpreting graded Sonic Hedgehog signaling during vertebrate neural tube patterning: the role of negative feedback. CSH Perspect Biol. 1(2):a002014. (2009)

Roberts RM, Fisher SJ. Trophoblast stem cells. Biol Reprod. 84(3):412-21. (2011) Review.

Robertson E, Bradley A, Kuehn M, Evans M. Germ-line transmission of genes introduced into cultured pluripotential cells by retroviral vector. Nature. 323(6087):445-8. (1986)

Robertson, EJ. Teratocarcinomas and embryonic stem cells: a practical approach. IRL Press, Washington, D.C. (1987)

Robertson EJ, Charatsi I, Joyner CJ, Koonce CH, Morgan M, Islam A, Paterson C, Lejsek E, Arnold SJ, Kallies A, Nutt SL, Bikoff EK. Blimp1 regulates development of the posterior forelimb, caudal pharyngeal arches, heart and sensory vibrissae in mice. Development. 134(24):4335-45. (2007)

Robertson EJ. Dose-dependent Nodal/Smad signals pattern the early mouse embryo. Semin Cell Dev Biol. 32:73-9. (2014) Review.

Roelen BA, Lin HY, Knezević V, Freund E, Mummery CL. Expression of TGF-betas and their receptors during implantation and organogenesis of the mouse embryo. Dev Biol. 166(2):716-28. (1994)

Rogers MB, Hosler BA and Gudas, LJ. Specific expression of a retinoic acid-regulated, zinc-finger gene, Rex-1, in preimplantation embryos, trophoblast and spermatocytes. Development. 113(3):815-824. (1991)

Rosendahl A, Speletas M, Leandersson K, Ivars F, Sideras P. Transforming growth factor-beta- and Activin-Smad signaling pathways are activated at distinct maturation stages of the thymopoeisis. Int Immunol 15(12):1401-14. (2003)
Rossant J, Guillemot F, Tanaka M, Latham K, Gertenstein M, Nagy A. Mash2 is expressed in oogenesis and preimplantation development but is not required for blastocyst formation. Mech Dev. 73(2):183-91. (1998)
Rossant J. Stem cells and early lineage development. Cell. 132(4):527-31. (2008)
Runyan C, Schaible K, Molyneaux K, Wang Z, Levin L, Wylie C. Steel factor controls midline cell death of primordial germ cells and is essential for their normal proliferation and migration. Development. 133(24):4861-9. (2006)
Runyan C, Gu Y, Shoemaker A, Looijenga L, Wylie C. The distribution and behavior of extragonadal primordial germ cells in Bax mutant mice suggest a novel origin for acrococcygeal germ cell tumors. Int J Dev Biol. 52(4):333-44. (2008)
Russ AP, Wattler S, Colledge WH, Aparicio SA, Carlton MB, Pearce JJ, Barton SC, Surani MA, Ryan K, Nehls MC, Wilson V, Evans MJ. Eomesodermin is required for mouse trophoblast development and mesoderm formation. Nature. 404(6773):95-9. (2000)
Saga Y, Miyagawa-Tomita S, Takagi A, Kitajima S, Miyazaki Ji, Inoue T. MesP1 is expressed in the heart precursor cells and required for the formation of a single heart tube. Development. 126(15):3437-47. (1999)
Saijoh Y, Oki S, Tanaka C, Nakamura T, Adachi H, Yan YT, Shen MM, Hamada H. Two nodal-responsive enhancers control left-right asymmetric expression of Nodal. Dev Dyn. 232(4):1031-6. (2005)
Saitou M, Payer B, O'Carroll D, Ohinata Y, Surani MA. Blimp1 and the emergence of the germ line during development in the mouse. Cell Cycle. 4(12):1736-40. (2005)
Saitou M, Yamaji M. Primordial germ cells in mice. CSH Perspect Biol. 4(11):a008375. (2012) Review.
Sajini AA, Greder LV, Dutton JR, Slack JM. Loss of Oct4 expression during the development of murine embryoid bodies. Dev Biol. 371(2):170-9. (2012)
Sakai Y, et al., The retinoic acid-inactivating enzyme CYP26 is essential for establishing an uneven distribution of retinoic acid along the anterio-posterior axis within the mouse embryo. Genes Dev. 15(2):213-25. (2001)
Sato M, Kimura T, Kurokawa K, Fujita Y, Abe K, Masuhara M, Yasunaga T, Ryo A, Yamamoto M, Nakano T. Identification of PGC7, a new gene expressed specifically in preimplantation embryos and germ cells. Mech Dev. 113(1):91-4. (2002)
Schmierer B, Hill CS. TGFbeta-SMAD signal transduction: molecular specificity and functional flexibility. Nat Rev Mol Cell Biol. 8(12):970-82. (2007)
Schöler HR, Dressler GR, Balling R, Rohdewohld H, Gruss P. Oct-4: a germline-specific transcription factor mapping to the mouse t-complex. EMBO J. 9(7):2185-95. (1990)
Seki Y, Hayashi K, Itoh K, Mizugaki M, Saitou M, Matsui Y. Extensive and orderly reprogramming of genome-wide chromatin modifications associated with specification and early development of germ cells in mice. Dev Biol. 278(2):440-58. (2005)
Shapiro-Shelef M, Lin KI, McHeyzer-Williams LJ, Liao J, McHeyzer-Williams MG, Calame K. Blimp-1 is required for the formation of immunoglobulin secreting plasma cells and pre-plasma memory B cells. Immunity. 19(4):607-20. (2003)
Shi Y, Wang YF, Jayaraman L, Yang H, Massagué J, Pavletich NP. Crystal structure of a Smad MH1 domain bound to DNA: insights on DNA binding in TGF-beta signaling. Cell. 94(5):585-94. (1998)
Shi Y, Massagué J. Mechanisms of TGF-beta signaling from cell membrane to the nucleus. Cell. 113(6):685-700. (2003) Review.
Shiratori H, Sakuma R, Watanabe M, Hashiguchi H, Mochida K, Sakai Y, Nishino J, Saijoh Y, Whitman M, Hamada H. Two-step regulation of left-right asymmetric expression of Pitx2: initiation by nodal signaling and maintenance by Nkx2. Mol Cell. 7(1):137-49. (2001)
Silva J, Nichols J, Theunissen TW, Guo G, van Oosten AL, Barrandon O, Wray J, Yamanaka S, Chambers I, Smith A. Nanog is the gateway to the pluripotent ground state. Cell. 138(4):722-37. (2009)
Simmons DG, Cross JC. Determinants of trophoblast lineage and cell subtype specification in the mouse placenta. Dev Biol. 284(1):12-24. (2005)
Simon CS, Downes DJ, Gosden ME, Telenius J, Higgs DR, Hughes JR, Costello I, Bikoff EK, Robertson EJ. Functional characterisation of cis-regulatory elements governing dynamic Eomes expression in the early mouse embryo. Development. 201
7 Feb 7. pii: dev.147322. [Epub ahead of print]

Sirard C, de la Pompa JL, Elia A, Itie A, Mirtsos C, Cheung A, Hahn S, Wakeham A, Schwartz L, Kern SE, Rossant J, Mak TW. The tumor suppressor gene Smad4/Dpc4 is required for gastrulation and later for anterior development of the mouse embryo. Genes Dev. 12(1):107-19. (1998)

Skarnes WC, Rosen B, West AP, Koutsourakis M, Bushell W, Iyer V, Mujica AO, Thomas M, Harrow J, Cox T, Jackson D, Severin J, Biggs P, Fu J, Nefedov M, de Jong PJ, Stewart AF, Bradley A. A conditional knockout resource for the genome-wide study of mouse gene function. Nature. 474(7351):337-42. (2011)

Smallwood SA, Lee HJ, Angermueller C, Krueger F, Saadeh H, Peat J, Andrews SR, Stegle O, Reik W, Kelsey G. Single-cell genome-wide bisulfite sequencing for assessing epigenetic heterogeneity. Nat Methods. 11(8):817-20. (2014)

Smith AG, Heath JK, Donaldson DD, Wong GG, Moreau J, Stahl M, Rogers D. Inhibition of pluripotential embryonic stem cell differentiation by purified polypeptides. Nature. 336(6200):688-90. (1988)

Smith ZD, Chan MM, Mikkelsen TS, Gu H, Gnirke A, Regev A, Meissner A. A unique regulatory phase of DNA methylation in the early mammalian embryo. Nature. 484(7394):339-44. (2012)

Snow MHL. Gastrulation in the mouse: Growth and regionalization of the epiblast, Development. 42:293-303. (1977)

Solter D, Skreb N, Damjanov I. Extrauterine growth of mouse egg-cylinders results in malignant teratoma. Nature. 227(5257):503-4. (1970)

de Sousa Lopes SM, Roelen BA, Monteiro RM, Emmens R, Lin HY, Li E, Lawson KA, Mummery CL. BMP signaling mediated by ALK2 in the visceral endoderm is necessary for the generation of primordial germ cells in the mouse embryo. Genes Dev. 18(15):1838-49. (2004)

de Sousa Lopes SM, Hayashi K, Surani MA. Proximal visceral endoderm and extraembryonic ectoderm regulate the formation of primordial germ cell precursors. BMC Dev Biol. 7:140. (2007)

Soriano P. Generalized lacZ expression with the ROSA26 Cre reporter strain. Nat Genet. 21(1):70-1. (1999)

Stevens LC. The development of transplantable teratocarcinomas from intratesticular grafts of pre- and postimplantation mouse embryos. Dev Biol. 21(3):364-82. (1970)

Stower MJ, Srinivas S. Heading forwards: anterior visceral endoderm migration in patterning the mouse embryo. Philos Trans R Soc Lond B Biol Sci. 369(1657):20130546. (2014). Review.

Strumpf D, Mao CA, Yamanaka Y, Ralston A, Chawengsaksophak K, Beck F, Rossant J. Cdx2 is required for correct cell fate specification and differentiation of trophectoderm in the mouse blastocyst. Development. 132(9):2093-102. (2005)

Sugimoto M, Kondo M, Koga Y, Shiura H, Ikeda R, Hirose M, Ogura A, Murakami A, Yoshiki A, Chuva de Sousa Lopes SM, Abe K. A simple and robust method for establishing homogeneous mouse epiblast stem cell lines by wnt inhibition. Stem Cell Reports. 4(4):744-57. (2015)

Sumi T, Oki S, Kitajima K, Meno C. Epiblast ground state is controlled by canonical Wnt/β-catenin signaling in the postimplantation mouse embryo and epiblast stem cells. PLoS One. 8(5):e63378. (2013)

Sun J, Ting MC, Ishii M, Maxson R. Msx1 and Msx2 function together in the regulation of primordial germ cell migration in the mouse. Dev Biol. 417(1):11-24. (2016)

Sun LT, Yamaguchi S, Hirano K, Ichisaka T, Kuroda T, Tada T. Nanog co-regulated by Nodal/Smad2 and Oct4 is required for pluripotency in developing mouse epiblast. Dev Biol. 392(2):182-92. (2014)

Takaoka K, Hamada H. Cell fate decisions and axis determination in the early mouse embryo. Development. 139(1):3-14. (2012) Review.

Takasaki N, Rankin T, Dean J. Normal gonadal development in mice lacking GPBOX, a homeobox protein expressed in germ cells at the onset of sexual dimorphism. Mol Cell Biol. 21(23):8197-202. (2001)

Tam PP, Zhou SX. The allocation of epiblast cells to ectodermal and germ-line lineages is influenced by the position of the cells in the gastrulating mouse embryo. Dev Biol. 178(1):124-32. (1996)

Tam PP and Gad JM. Gastrulation in the Mouse Embryo, Chapter 16 in: Gastrulation: from cells to embryo (ed. Stern, CD), CSH Press, New York (2004)

Tam PP, Loebel DA. Gene function in mouse embryogenesis: get set for gastrulation. Nat Rev Genet. 8(5):368-81. (2007)

Tamai Y, Ishikawa T, Bösl MR, Mori M, Nozaki M, Baribault H, Oshima RG, Taketo MM. Cytokeratins 8 and 19 in the mouse placental development. J Cell Biol. 151(3):563-72. (2000)
Tamplin OJ, Kinzel D, Cox BJ, Bell CE, Rossant J, Lickert H. Microarray analysis of Foxa2 mutant mouse embryos reveals novel gene expression and inductive roles for the gastrula organizer and its derivatives. BMC Genomics. 9:511. (2008)
Tamplin OJ, Cox BJ, Rossant J. Integrated microarray and ChIP analysis identifies multiple Foxa2 dependent target genes in the notochord. Dev Biol. 360(2):415-25. (2011)
Tanaka M, Gertsenstein M, Rossant J, Nagy A. Mash2 acts cell autonomously in mouse spongiotrophoblast development. Dev Biol. 190(1):55-65. (1997)
Tanaka M, Puchyr M, Gertsenstein M, Harpal K, Jaenisch R, Rossant J, Nagy A. Parental origin-specific expression of Mash2 is established at the time of implantation with its imprinting mechanism highly resistant to genome-wide demethylation. Mech Dev. 87(1-2):129-42. (1999)
Tanaka SS, Yamaguchi YL, Steiner KA, Nakano T, Nishinakamura R, Kwan KM, Behringer RR, Tam PP. Loss of Lhx1 activity impacts on the localization of primordial germ cells in the mouse. Dev Dyn. 239(11):2851-9. (2010)
Tang WW, Kobayashi T, Irie N, Dietmann S, Surani MA. Specification and epigenetic programming of the human germ line. Nat Rev Genet. 17(10):585-600. (2016)
Teo AK, Arnold SJ, Trotter MW, Brown S, Ang LT, Chng Z, Robertson EJ, Dunn NR, Vallier L. Pluripotency factors regulate definitive endoderm specification through eomesodermin. Genes Dev. 25(3):238-50. (2011)
Tesar PJ, Chenoweth JG, Brook FA, Davies TJ, Evans EP, Mack DL, Gardner RL, McKay RD. New cell lines from mouse epiblast share defining features with human embryonic stem cells. Nature. 448(7150):196-9. (2007)
Thomas P, Beddington R. Anterior primitive endoderm may be responsible for patterning the anterior neural plate in the mouse embryo. Curr Biol. 6(11):1487-96. (1996)
Thomas PQ, Brown A, Beddington RS. Hex: a homeobox gene revealing peri-implantation asymmetry in the mouse embryo and an early transient marker of endothelial cell precursors. Development. 125(1):85-94. (1998)
Tokuzawa Y, Kaiho E, Maruyama M, Takahashi K, Mitsui K, Maeda M, Niwa H, Yamanaka S. Fbx15 is a novel target of Oct3/4 but is dispensable for embryonic stem cell self-renewal and mouse development. Mol Cell Biol. 23(8):2699-708. (2003)
Tortelote GG, Hernández-Hernández JM, Quaresma AJ, Nickerson JA, Imbalzano AN, Rivera-Pérez JA. Wnt3 function in the epiblast is required for the maintenance but not the initiation of gastrulation in mice. Dev Biol. 374(1):164-73. (2013)
Treichel D, Becker MB, Gruss P. The novel transcription factor gene Sp5 exhibits a dynamic and highly restricted expression pattern during mouse embryogenesis. Mech Dev. 101(1-2):175-9. (2001)
Tremblay KD, Hoodless PA, Bikoff EK, Robertson EJ. Formation of the definitive endoderm in mouse is a Smad2-dependent process. Development. 127(14):3079-90. (2000)
Tremblay KD, Dunn NR, Robertson EJ. Mouse embryos lacking Smad1 signals display defects in extra-embryonic tissues and germ cell formation. Development. 128(18):3609-21. (2001)
Tripathi R, Saini HK, Rad R, Abreu-Goodger C, van Dongen S, Enright AJ. Messenger RNA and microRNA profiling during early mouse EB formation. Gene Expr Patterns. 11(5-6):334-44. (2011)
Tsakiridis A, Huang Y, Blin G, Skylaki S, Wymeersch F, Osorno R, Economou C, Karagianni E, Zhao S, Lowell S, Wilson V. Distinct Wnt-driven primitive streak-like populations reflect in vivo lineage precursors. Development. 2014 141(6):1209-21. Erratum in: Development. 142(4):809. (2015)
Tsankov AM, Gu H, Akopian V, Ziller MJ, Donaghey J, Amit I, Gnirke A, Meissner A. Transcription factor binding dynamics during human ES cell differentiation. Nature. 518(7539):344-9. (2015)
Vallier L, Mendjan S, Brown S, Chng Z, Teo A, Smithers LE, Trotter MW, Cho CH, Martinez A, Rugg-Gunn P, Brons G, Pedersen RA. Activin/Nodal signalling maintains pluripotency by controlling Nanog expression. Development. 136(8):1339-49. (2009)
Varlet I, Collignon J, Norris DP, Robertson EJ. Nodal signaling and axis formation in the mouse. CSH Symp Quant Biol. 62:105-13. (1997)
Vincent SD, Dunn NR, Hayashi S, Norris DP, Robertson EJ. Cell fate decisions within the mouse organizer are governed by graded Nodal signals. Genes Dev. 17(13):1646-62. (2003) (2003a in main text)

Vincent SD, Robertson EJ. Highly efficient transgene-independent recombination directed by a maternally derived SOX2CRE transgene. Genesis. 37(2):54-6. (2003) (2003b in main text)
Vincent SD, Norris DP, Le Good JA, Constam DB, Robertson EJ. Asymmetric Nodal expression in the mouse is governed by the combinatorial activities of two distinct regulatory elements. Mech Dev. 121(11):1403-15. (2004)
Vincent SD, Dunn NR, Sciammas R, Shapiro-Shalef M, Davis MM, Calame K, Bikoff EK, Robertson EJ. The zinc finger transcriptional repressor Blimp1/Prdm1 is dispensable for early axis formation but is required for specification of primordial germ cells in the mouse. Development. 132(6):1315-25. (2005)
Waldrip WR, Bikoff EK, Hoodless PA, Wrana JL, Robertson EJ. Smad2 signaling in extraembryonic tissues determines anterior-posterior polarity of the early mouse embryo. Cell. 92(6):797-808. (1998)
Warr N, Siggers P, Bogani D, Brixey R, Pastorelli L, et al. Sfrp1 and Sfrp2 are required for normal male sexual development in mice. Dev Biol 326(2):273–284. (2009)
Washkowitz AJ, Schall C, Zhang K, Wurst W, Floss T, Mager J, Papaioannou VE. Mga is essential for the survival of pluripotent cells during peri-implantation development. Development. 142(1):31-40. (2015)
Weber S, Eckert D, Nettersheim D, Gillis AJ, Schäfer S, Kuckenberg P, Ehlermann J, Werling U, Biermann K, Looijenga LH, Schorle H. Critical function of AP-2 gamma/TCFAP2C in mouse embryonic germ cell maintenance. Biol Reprod. 82(1):214-23. (2010)
West JA, Park IH, Daley GQ, Geijsen N. In vitro generation of germ cells from murine embryonic stem cells. Nat Protoc. 1(4):2026-36. (2006)
Wiles MV, Keller G. Multiple hematopoietic lineages develop from embryonic stem (ES) cells in culture. Development. 111(2):259-67. (1991)
Wiles MV, Johansson BM. Embryonic stem cell development in a chemically defined medium. Exp Cell Res. 247(1):241-8. (1999)
Wilkinson DG, Bhatt S, Herrmann BG. Expression pattern of the mouse T gene and its role in mesoderm formation. Nature. 343(6259):657-9. (1990)
Winger Q, Huang J, Auman HJ, Lewandoski M, Williams T. Analysis of transcription factor AP-2 expression and function during mouse preimplantation development. Biol Reprod. 75(3):324-33. (2006)
Winnier G, Blessing M, Labosky PA, Hogan BL. Bone morphogenetic protein-4 is required for mesoderm formation and patterning in the mouse. Genes Dev. 9(17):2105-16. (1995)
Wrana, JL, Ozdama B., Le Roy, C. and Benchabane, H. Signaling receptors of the TGF-β family. In: The TGF-β Family (ed. Derynck R and Miyazono K), CSH Press, New York. 179-202. (2008)
Xi Q, Wang Z, Zaromytidou AI, Zhang XH, Chow-Tsang LF, Liu JX, Kim H, Barlas A, Manova-Todorova K, Kaartinen V, Studer L, Mark W, Patel DJ, Massagué J. A poised chromatin platform for TGF-β access to master regulators. Cell. 147(7):1511-24. (2011)
Yabuta Y, Kurimoto K, Ohinata Y, Seki Y, Saitou M. Gene expression dynamics during germline specification in mice identified by quantitative single-cell gene expression profiling. Biol Reprod. 75(5):705-16. (2006)
Yagi K, Goto D, Hamamoto T, Takenoshita S, Kato M, Miyazono K. Alternatively spliced variant of Smad2 lacking exon 3. Comparison with wild-type Smad2 and Smad3. J Biol Chem. 274(2):703-9. (1999)
Yamaguchi TP, Takada S, Yoshikawa Y, Wu N, McMahon AP. T (Brachyury) is a direct target of Wnt3a during paraxial mesoderm specification. Genes Dev. 13(24):3185-90. (1999)
Yamaguchi S, Kimura H, Tada M, Nakatsuji N, Tada T. Nanog expression in mouse germ cell development. Gene Expr Patterns. 5(5):639-46. (2005)
Yamaji M, Seki Y, Kurimoto K, Yabuta Y, Yuasa M, Shigeta M, Yamanaka K, Ohinata Y, Saitou M. Critical function of Prdm14 for the establishment of the germ cell lineage in mice. Nat Genet. 40(8):1016-22. (2008)
Yamamoto M, Beppu H, Takaoka K, Meno C, Li E, Miyazono K, Hamada H. Antagonism between Smad1 and Smad2 signaling determines the site of distal visceral endoderm formation in the mouse embryo. J Cell Biol. 184(2):323-34. (2009)
Yang DH, Smith ER, Roland IH, Sheng Z, He J, Martin WD, Hamilton TC, Lambeth JD, Xu XX. Disabled-2 is essential for endodermal cell positioning and structure formation during mouse embryogenesis. Dev. Biol. 251(1):27-44. (2002)
Yang X, Li C, Xu X, Deng C. The tumor suppressor SMAD4/DPC4 is essential for epiblast proliferation and mesoderm induction in mice. Proc Natl Acad Sci USA. 95(7):3667-72. (1998)

Yang X, Letterio JJ, Lechleider RJ, Chen L, Hayman R, Gu H, Roberts AB, Deng C. Targeted disruption of SMAD3 results in impaired mucosal immunity and diminished T cell responsiveness to TGF-beta. EMBO J. 18(5):1280-91. (1999)

Yasunaga M, Tada S, Torikai-Nishikawa S, Nakano Y, Okada M, Jakt LM, Nishikawa S, Chiba T, Era T, Nishikawa S. Induction and monitoring of definitive and visceral endoderm differentiation of mouse ES cells. Nat Biotechnol. 23(12):1542-50. (2005)

Yeom YI, Fuhrmann G, Ovitt CE, Brehm A, Ohbo K, Gross M, Hübner K, Schöler HR. Germline regulatory element of Oct-4 specific for the totipotent cycle of embryonal cells. Development. 122(3):881-94. (1996)

Ying QL, Stavridis M, Griffiths D, Li M, Smith A. Conversion of embryonic stem cells into neuroectodermal precursors in adherent monoculture. Nat Biotechnol. 21(2):183-6. (2003)

Ying QL, Wray J, Nichols J, Batlle-Morera L, Doble B, Woodgett J, Cohen P, Smith A. The ground state of embryonic stem cell self-renewal. Nature. 453(7194):519-23. (2008)

Ying Y, Zhao GQ. Cooperation of endoderm-derived BMP2 and extraembryonic ectoderm-derived BMP4 in primordial germ cell generation in the mouse. Dev Biol. 232(2):484-92. (2001)

Ying Y, Liu XM, Marble A, Lawson KA, Zhao GQ. Requirement of Bmp8b for the generation of primordial germ cells in the mouse. Mol Endocrinol. 14(7):1053-63. (2000)

Yoon SJ, Wills AE, Chuong E, Gupta R, Baker JC. HEB and E2A function as SMAD/FOXH1 cofactors. Genes Dev. 25(15):1654-61. (2011)

Yoon SJ, Foley JW, Baker JC. HEB associates with PRC2 and SMAD2/3 to regulate developmental fates. Nat Commun. 6:6546. (2015)

Zakin L, Reversade B, Virlon B, Rusniok C, Glaser P, Elalouf JM, Brulet P. Gene expression profiles in normal and Otx2-/- early gastrulating mouse embryos. Proc Natl Acad Sci USA. 97(26):14388-93. (2000)

Zemel S, Bartolomei MS, Tilghman SM. Physical linkage of two mammalian imprinted genes, H19 and insulin-like growth factor 2. Nat Genet. 2(1):61-5. (1992)

Zhang K, Li L, Huang C, Shen C, Tan F, Xia C, Liu P, Rossant J, Jing N. Distinct functions of BMP4 during different stages of mouse ES cell neural commitment. Development. 137(13):2095-105. (2010)

Zheng-Fischhöfer Q, Kibschull M, Schnichels M, Kretz M, Petrasch-Parwez E, Strotmann J, Reucher H, Lynn BD, Nagy JI, Lye SJ, Winterhager E, Willecke K. Characterization of connexin31.1-deficient mice reveals impaired placental development. Dev Biol. 312(1):258-71. (2007)

Zhu Y, Richardson JA, Parada LF, Graff JM. Smad3 mutant mice develop metastatic colorectal cancer. Cell. 94(6):703-14. (1998)